



UNIVERSITÀ DEGLI STUDI DI MILANO
FACOLTÀ DI SCIENZE E TECNOLOGIE

DEPARTMENT OF CHEMISTRY

DOCTORATE SCHOOL IN INDUSTRIAL CHEMISTRY (XIXX CYCLE)

**PURINE NUCLEOSIDE PHOSPHORYLASES AS
BIOCATALYSTS AND PHARMACOLOGICAL TARGETS**

MARCO RABUFFETTI

R10601

Tutor: Prof. Giovanna SPERANZA

Co-Tutor: Prof. Gabriella MASSOLINI (University of Pavia)

Coordinator: Prof. Maddalena Pizzotti

Academic Year 2015/2016

TABLE OF CONTENTS

Abbreviations	VI
1 INTRODUCTION	1
1.1. General introduction	1
1.1.1. General remarks on nucleosides, nucleotides and their analogues	1
1.1.2. 6-Substituted purine nucleosides	2
1.2. Synthesis of purine and pyrimidine nucleosides	3
1.2.1. Chemical synthesis of purine and pyrimidine nucleosides	3
1.2.2. Chemoenzymatic synthesis of nucleosides	9
1.3. Nucleoside phosphorylases (NPs, EC 2.4.2)	10
1.3.1. Classifications	10
1.3.2. Active sites	13
1.3.3. Catalytic mechanism	14
1.3.4. Transition state	16
1.3.5. Chemoenzymatic synthesis of nucleosides by transglycosylation catalyzed by NPs	17
1.3.6. PNP from <i>Aeromonas hydrophila</i> (AhPNP, EC 2.4.2.1)	18
1.3.7. UP from <i>Clostridium perfringens</i> (CpUP, EC 2.4.2.3)	19
1.4. Purine nucleoside phosphorylase from <i>Mycobacterium tuberculosis</i> (MtPNP)	20
1.4.1. Tuberculosis (TB)	20
1.4.2. PNP from <i>Mycobacterium tuberculosis</i> (MtPNP) as a potential drug target	21
1.4.3. Similarities and differences between HsPNP and MtPNP	21
1.4.4. Analogues of ground and transition states as inhibitors of PNPs	22
1.4.5. Conformation of 8-substituted purine ribonucleosides	24
1.5. Immobilized Enzyme Reactors (IMERs)	25
1.5.1. Immobilized Enzyme Reactors (IMERs)	25
1.5.2. Enzyme immobilization	27
1.6. Background studies on the purine nucleoside phosphorylase from <i>Aeromonas hydrophila</i> (AhPNP)	29
1.6.1. Characterization and synthetic applications of AhPNP	29
1.6.2. AhPNP as an on-line Immobilized Enzyme Reactor (AhPNP-IMER)	31
2 AIMS	34
3 PURINE NUCLEOSIDE PHOSPHORYLASES AS BIOCATALYSTS AND PHARMACOLOGICAL TARGETS	35
3.1. Chemical synthesis of structurally modified purine nucleobases and nucleosides	35
3.1.1. Synthesis of 6-substituted purines (2-10 , 12-24)	35
3.1.2. Synthesis of 2-amino-6-methoxypurine (26)	38
3.1.3. Synthesis of 6-substituted inosines (28-36 , 38-48)	38
3.1.4. Synthesis of 6-O-methylguanosine (58)	41
3.1.5. Synthesis of arabinosylguanine (59)	42
3.1.6. Synthesis of 7-methylpurine and 7-methylguanine nucleoside iodides (64-67)	44
3.1.7. Synthesis of 8-substituted inosines, guanosines and adenosines (69-80)	45
3.2. Chemoenzymatic synthesis of nucleosides catalyzed by the PNP from <i>Aeromonas hydrophila</i> (AhPNP)	49
3.2.1. Chemoenzymatic synthesis of 6-substituted purine ribonucleosides catalyzed by AhPNP (“in batch” reaction)	49

3.2.2. Chemoenzymatic synthesis of 6-substituted purine ribonucleosides catalyzed by <i>Ahp</i> PNP-IMER (“in flow” reaction)	52
3.2.2.1. Covalent immobilization of <i>Ahp</i> PNP and IMER preparation	52
3.2.2.2. Activity and stability of <i>Ahp</i> PNP-IMER	53
3.2.2.3. Analytical apparatus and optimization of the reaction conditions	53
3.2.2.4. Enzymatic synthesis, on-line monitoring and purification of 6-substituted purine ribonucleosides	55
3.2.3. Chemoenzymatic synthesis of 6-substituted purine 2'-deoxyribo- and arabinonucleosides catalyzed by <i>Ahp</i> PNP	58
3.2.4. Chemoenzymatic synthesis of adenosine, 2'-deoxyadenosine and arabinosyladenine catalyzed by a <i>Cp</i> UP-IMER coupled with a <i>Ahp</i> PNP-IMER (“in flow” reaction)	61
3.2.4.1. Development, activity and stability of <i>Cp</i> UP/ <i>Ahp</i> PNP-IMER and <i>Cp</i> UP-IMER	61
3.2.4.2. <i>Cp</i> UP-IMER/ <i>Ahp</i> PNP-IMER apparatus and optimization of the reaction conditions	62
3.2.4.3. Synthesis of 2'-deoxyadenosine, adenosine and arabinosyladenine	63
3.3. Evaluation of the inhibitory activity of 8-substituted purine ribonucleosides against the PNP from <i>Mycobacterium tuberculosis</i> (<i>Mt</i> PNP)	65
3.3.1. LC-ESI-MS/MS enzymatic assay	65
3.3.2. Kinetic parameters of <i>Ah</i> , <i>Hs</i> and <i>Mt</i> PNP	66
3.3.3. Inhibition screening assays	68
4 SYNTHESIS OF POTENTIAL LIGANDS OF THE HUMAN GPR17 RECEPTOR	71
4.1. Role of GPR17 in neurodegenerative disorders	71
4.1.1. Neurodegenerative disorders	71
4.1.2. G Protein-Coupled Receptors (GPCRs)	71
4.1.3. GPR17 as a potential target against neurodegeneration	72
4.2. <i>In silico</i> screening and synthesis of potential GPR17 ligands	73
4.2.1. <i>In silico</i> screening of potential GPR17 ligands	73
4.2.2. <i>N</i> ² -Alkylation, <i>N</i> ² -acylation and 2-halogenation of guanosine	77
4.2.3. Synthesis of potential GPR17 ligands	81
4.2.3.1. 8-Alkylamino-, <i>N</i> ² -alkyl- and <i>N</i> ² -acyl-purine 5'-ribonucleotides (94-97)	81
4.2.3.2. Synthesis of 8-methylaminoinosinic acid (94)	82
4.2.3.3. Synthesis of <i>N</i> ² - <i>n</i> -octyl-2',3'- <i>O</i> -isopropylidene-guanylic acid (95)	82
4.2.3.4. Synthesis of <i>N</i> ² -acyl-2',3'- <i>O</i> -isopropylidene-guanylic acids (96-97)	86
5 CONCLUSIONS	88
6 APPENDIX	90
6.1. Mechanisms of selected reactions	90
6.1.1. Carbonyl thionation with P ₄ S ₁₀ and Lawesson's reagent	90
6.1.2. 8-Oxygenation of 8-bromopurine nucleosides	91
6.1.3. Negishi cross-coupling	92
6.1.4. Bromination by Sandmeyer-type reaction	94
6.1.5. Phosphorylation of <i>N</i> ² -alkyl- and <i>N</i> ² -acyl-guanosines with POCl ₃ /TEP	94
6.2. General synthetic schemes	97
6.3. Semi-preparative chromatograms, ¹ H-NMR, ¹³ C-NMR and UV-Vis spectra of 6-substituted ribonucleosides synthesized by <i>Ahp</i> PNP-IMER	103
6.3.1. Semi-preparative chromatograms	103
6.3.2. ¹ H-NMR and ¹³ C-NMR spectra	105

6.3.3. Uv-Vis spectra	110
7 EXPERIMENTAL SECTION	111
7.1. Materials and methods	111
7.2. Synthesis of structurally modified nucleobases and nucleosides	113
7.2.1. Synthesis of 6-substituted purines and guanines (2-10, 12-24)	113
7.2.2. Synthesis of 6-substituted inosines and guanosines (28-36, 38-48, 58)	133
7.2.3. Synthesis of arabinosylguanine (59)	159
7.2.4. Synthesis of 7-methylpurine and 7-methylguanine nucleoside iodides (64-67)	164
7.2.5. Synthesis of 8-substituted inosines, guanosines and adenosines (69-80)	168
7.2.6. Synthesis of 8- and N^2 -substituted inosinic and guanylic acids (94-97)	183
7.2.7. Batch and flow synthesis of ribonucleosides	197
Collaborations and acknowledgements	202
References	203

Abbreviations

'	Minutes	NAD(P)H	Nicotinamide adenine dinucleotide (phosphate)
2,2-DMP	2,2-Dimethoxypropane	NBS	<i>N</i> -Bromosuccinimide
AcOEt	Ethyl acetate	NMR	Nuclear Magnetic Resonance
AcOH	Acetic acid	NP	Nucleoside phosphorylase
Ala	Alanine	OAc	Acetate
Arg	Arginine	OTC	Open Tubular Capillary
Asp	Aspartic acid	PDB	Protein Data Bank
ATP	Adenosine triphosphate	<i>Pf</i>	<i>Plasmodium falciparum</i>
BSA	<i>N,O</i> -bis-(trimethylsilyl)acetamide	Phe	Phenylalanine
cAMP	Cyclic adenosine 5'-monophosphate	P _i	Inorganic phosphate
CNS	Central nervous system	PNP	Purine nucleoside phosphorylase
<i>Cp</i>	<i>Clostridium perfringens</i>	<i>p</i> -TsOH	<i>p</i> -Toluenesulfonic acid
DMF	Dimethylformamide	Py	Pyridine
DMSO	Dimethylsulfoxide	PyNP	Pyrimidine nucleoside phosphorylase
DNA	Deoxyribonucleic acid	<i>R_f</i>	Retention factor
<i>Ec</i>	<i>Escherichia coli</i>	RNA	Ribonucleic acid
ESI	ElectroSpray Ionization	RP	Reverse phase
Et ₂ O	Diethyl ether	RT	Room temperature
FDA	Food and Drug Administration	SD	Standard deviation
Gln	Glutamine	Ser	Serine
Glu	Glutamic acid	S _N	Nucleophilic substitution
Gly	Glycine	TB	Tuberculosis
GPCR	G Protein-Coupled Receptor	TBAF	Tetra- <i>n</i> -butylammonium fluoride
h	Hours	TEA	Triethylamine
His	Histidine	TEP	Triethylphosphate
HIV	Human Immunodeficiency Virus	Tf	Trifluoromethanesulfonyl
HPLC	High Performance Liquid Chromatography	THF	Tetrahydrofuran
<i>Hs</i>	<i>Homo sapiens</i>	Thr	Threonine
Ile	Isoleucine	TIPDSCl ₂	1,3-Dichloro-1,1,3,3-tetra- <i>i</i> -propylidisiloxane
IMER	Immobilized Enzyme Reactor	TLC	Thin Layer Chromatography
IR	Infrared	TMSBr	Trimethylsilyl bromide
<i>k</i>	Capacity factor	TP	Thymidine phosphorylase
LC	Liquid Chromatography	t _R	Retention time
Leu	Leucine	TS	Transition state
Lys	Lysine	Tyr	Tyrosine
Met	Methionine	UP	Uridine phosphorylase
MM	Molecular mass	UV-Vis	Ultraviolet-visible
MS	Mass spectrum	Val	Valine
<i>Mt</i>	<i>Mycobacterium tuberculosis</i>	WHO	World Health Organization
MW	Molar weight / Microwave	XRD	X-Rays Diffraction
MWCO	Molar weight cut-off		
<i>N,N</i> -DMA	<i>N,N</i> -Dimethylaniline		

1 | INTRODUCTION

1.1. General introduction

1.1.1. General remarks on nucleosides, nucleotides and their analogues

Nucleosides, nucleotides and their analogues have always attracted a significant interest owing to their crucial implication in several biological processes.¹ These molecules, that can be synthesized *in vivo* either by the *de novo* or the salvage pathways, act as intracellular mediators, coenzymes and energy carriers (cAMP, ATP, NAD(P)H, ...). Needless to say, the most important role of natural nucleosides and nucleotides is the constitution of nucleic acids (DNA and RNA) which convey all the necessary information for cell life.

From the chemist's viewpoint, a boost in nucleic acid chemistry was registered in the 1950-1960s. A great synthetic effort has led to a huge number of modified nucleosides designed with the goal to impair nucleic acid synthesis in specific pathological conditions.

Most nucleoside analogues are used against viral infections (*e.g.* HIV²) or specific cancers^{1,3} (**Figure 1.1**). Upon *in vivo* activation by phosphorylation, either nucleosides are incorporated in the viral/cellular nucleic acid or they inhibit specific enzymes of nucleic acid biosynthesis. They may indeed act as antimetabolites to arrest DNA and/or RNA replication (*e.g.* inhibitors of reverse transcriptase, chain terminators, ...).⁴ Drugs such as Capecitabine and Azacitidine (antitumors) or Abacavir, Tenofovir Disoproxil, Adefovir, Adefovir Dipivoxil, Emtricitabine and Entecavir (antivirals) are only some examples of nucleoside-based molecules approved by the FDA (Food and Drug Administration) in the last twenty years. Some nucleoside and nucleotide analogues have also been used as immunosuppressive drugs, phosphodiesterase inhibitors, epigenetic modulators and neuroprotective agent.⁵ Moreover, natural purine ribonucleoside 5'-monophosphates are employed as building blocks for the preparation of oligonucleotides as well as food additives and flavor enhancers. In particular, the disodium salts of guanylic and inosinic acid (disodium guanylate, Na₂GMP, and inosinate, Na₂IMP) are known for their ability to enhance the taste intensity of monosodium glutamate and play a crucial role in the perception of the so-called *umami* taste ("fifth taste").⁶

Many nucleoside and nucleotide analogues contain simple chemical modifications if compared to their natural counterparts (*e.g.* Capecitabine, Zidovudine, Puromycin...), while others are remarkably different from them (*e.g.* Adefovir, Tenofovir, Abacavir, Neplanocin A...).

Nucleoside chemistry still represents a very active research area, as the effectiveness of such analogues in blocking viral infections and treating solid tumors has further encouraged synthetic attempts to achieve new structurally-related molecules. The prodrug Sofosbuvir, marketed as Sovaldi[®] from 2013, is a paradigmatic example of this trend. In combination with other drugs (*e.g.* Ribavirin⁷ and Daclatasvir, Ledipasvir or Simeprevir⁸), it is used in the treatment of hepatitis C as an alternative to currently rooted

peginterferon-combined therapies.⁹ However, considerable concerns and debates have been raised due its high cost.

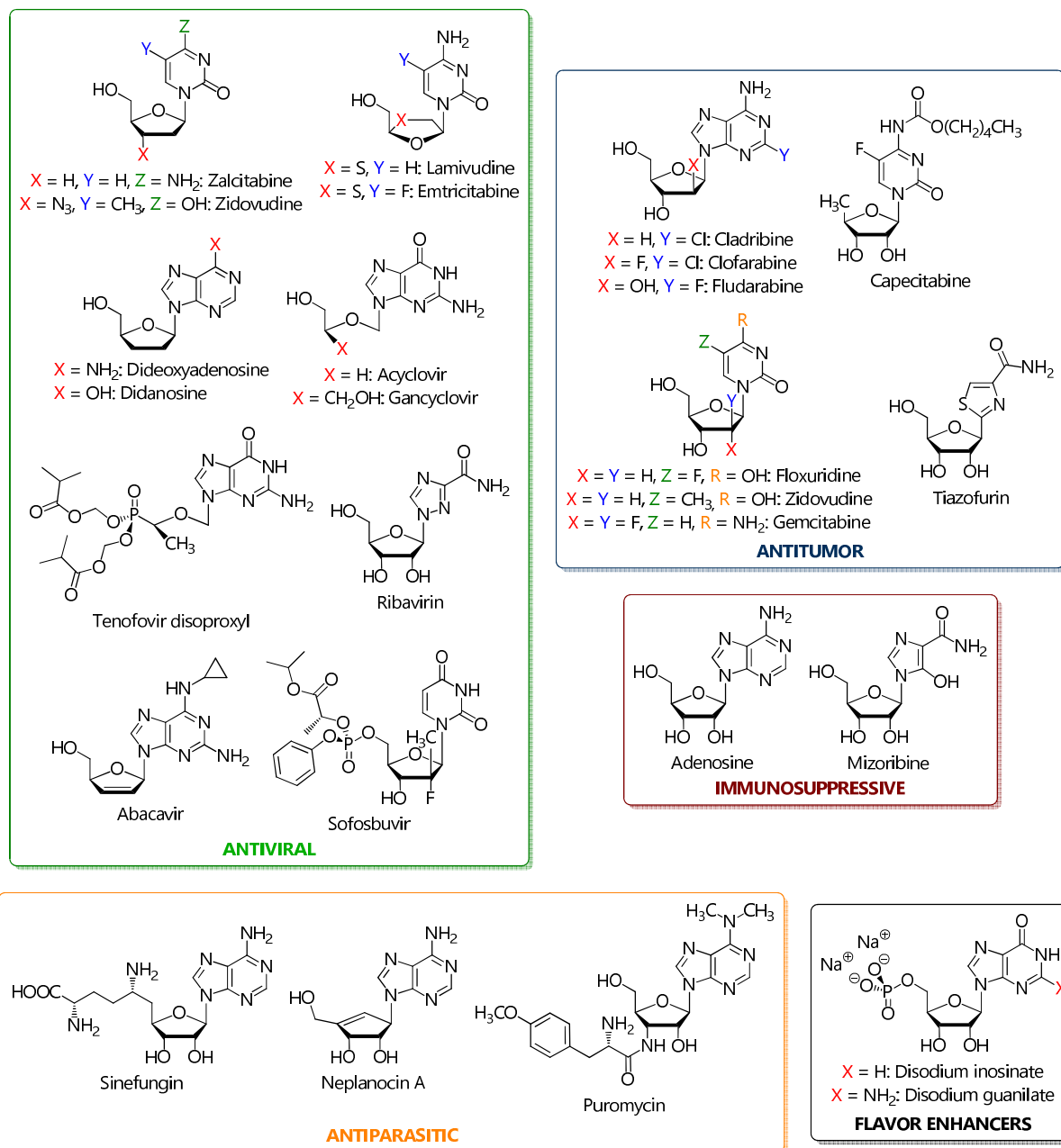


Figure 1.1. Examples of biologically active nucleoside analogues

1.1.2. 6-Substituted purine nucleosides

Among modified nucleosides, ribo-, 2'-deoxyribo- and arabinonucleosides containing purine bases substituted in 6-position (**Figure 1.2**) are characterized by different biological activities:

- cytotoxicity and cytostaticity: 6-aryl-, 6-ethylaryl- and 6-benzyl-, 6-hydroxymethyl-, 6-fluoromethyl-, 6-difluoromethyl-, 6-trifluoromethyl- and a number of 6-amino- and 6-alkoxypurine nucleosides¹⁰;
- antiviral activity: nucleosides bearing 5-membered heterocycles in position 6 (anti-hepatitis C)¹¹;
- antitumor effect: 6-alkyl, 6-amino-, 6-thio-, 6-oxo- and 6-chloropurine nucleosides.¹² A few of them, in combination with proper enzymes such as purine nucleoside phosphorylases (PNPs) have been tested as substrates in the so-called "suicide gene therapy" for the treatment of solid tumors.¹³

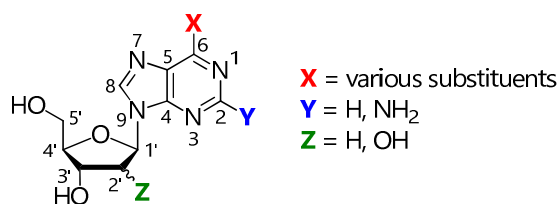


Figure 1.2. General structure of 6-substituted ribo-, 2'-deoxyribo- and arabinonucleosides

1.2. Synthesis of purine and pyrimidine nucleosides

1.2.1. Chemical synthesis of purine and pyrimidine nucleosides

Nucleosides have been synthesized by various chemical methods since the beginning of the last century, with a boost between the 1960s and 1990s.¹⁴ It soon turned out that the crucial issue of nucleoside synthesis is the formation and preservation of the C-N glycosidic bond. The glycosylation reaction is indeed still challenging.

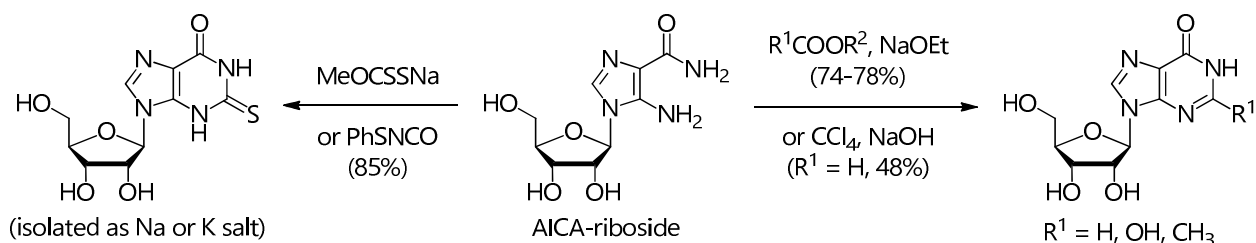
Among the current strategies, two main routes are of wide applicability:

- the modification of preformed nucleoside substrates, in which the glycosidic bond is already a part of the structure;
- glycosylation procedures, that are *convergent approaches* proceeding *via* the condensation of properly protected and/or activated heterocycles and sugar moieties, under conditions suitable to ensure regio- and stereoselectivity.

Both methodologies may be useful for five- and six-membered sugars (*e.g.* ribose, arabinose, glucose, xylose...), as well as for purine and pyrimidine nucleobases.

Concerning the first strategy, which can be defined as a *functionalization approach*, commercially available substrates are usually chosen as starting materials. Examples of this method are reported in literature with or without the proper protections on either the nucleobase or the sugar. Purine nucleosides are generally obtained by this strategy, whereas pyrimidine ones are frequently used as reagents. Yields are extremely variable depending on the specific reaction.

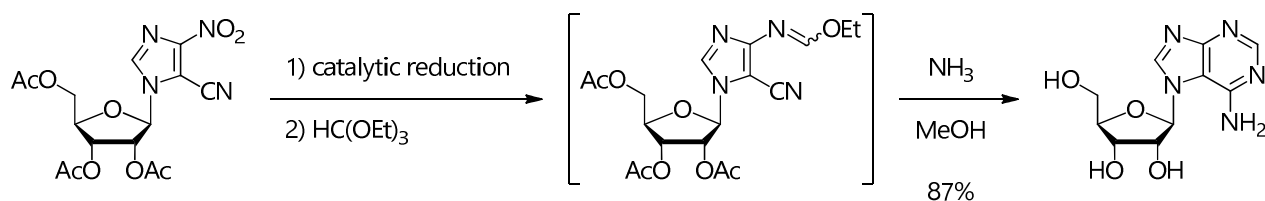
A pivotal role is played by 5-aminoimidazole-4-carboxamide-1- β -D-ribofuranoside (AICA-ribose, Acadesine), often converted into purine ribonucleosides and their analogues by ring annulations with reagents such as carboxylic esters¹⁵, dichlorocarbene (*via* a 5-dichloromethylamino intermediate)¹⁶ or sodium methylxanthate and phenylthioisocyanate¹⁷ (**Scheme 1.1**).



Scheme 1.1. Examples of the synthesis of 2-substituted inosines and 2-thioinosine from AICA-ribose

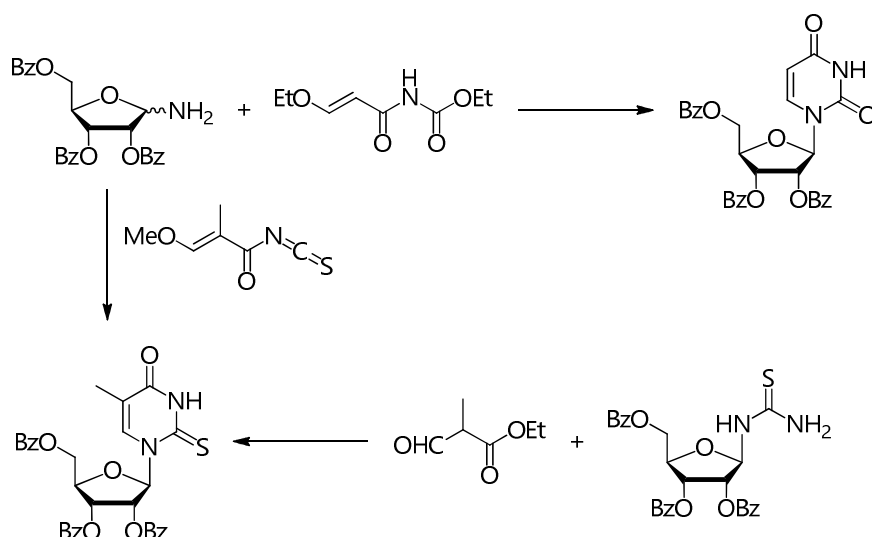
In order to obtain nucleosides with atypical structural features, such as 7-glycosylated purines, glycosylated imidazoles similar to AICA-ribose can be used. Purine bases tend indeed to react easily at N⁹ except for

theophylline. Imidazole elongation and diazine ring closing are performed with simple reagents such as orthoformates and amines (**Scheme 1.2**).¹⁸



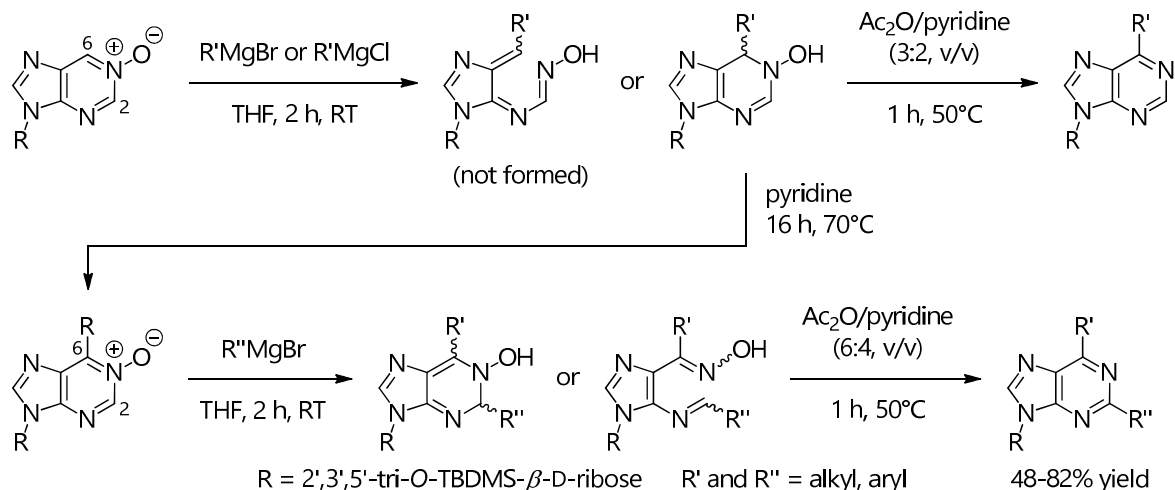
Scheme 1.2. Example of the synthesis of 7-glycosylated purines

One of the most common *functionalization* methods to synthesize pyrimidine ribonucleosides exploits the already present C-N bond of fully protected *N*-substituted ribosylamines or ribosylureas. A significant feature of this strategy is the step-by-step construction of the whole heterocyclic ring, whose formation occurs only at the end of the sequence (**Scheme 1.3**). For instance, protected uridine and 2-thiothymidine can be constructed starting from 2,3,5-tri-*O*-benzoyl-*D*-ribofuranosylamine and β -ethoxy-*N*-ethoxycarbonylacrylamide¹⁹ or α -methyl- β -methoxyacryloyl isothiocyanate²⁰, respectively. The latter product can be obtained by treating 2,3,5-tri-*O*-benzoyl-*D*-ribofuranosylthiourea with ethyl α -formylpropionate.²¹



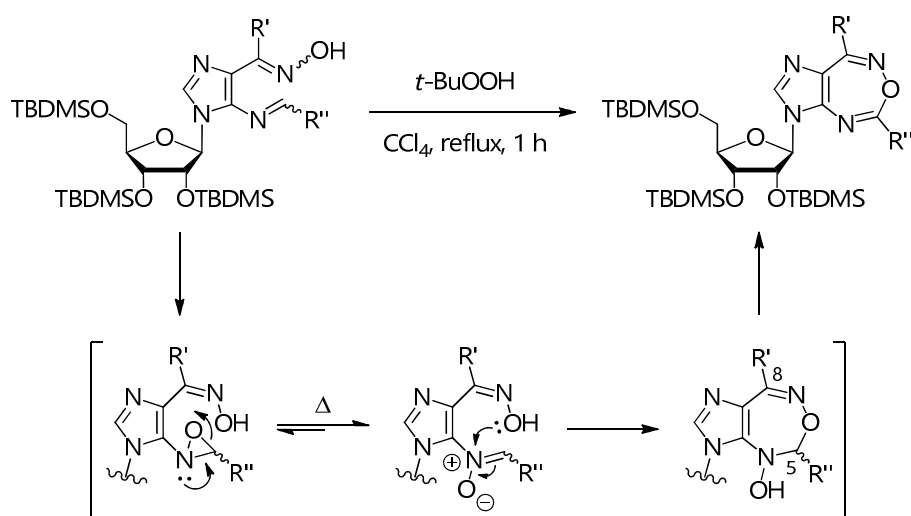
Scheme 1.3. Examples of the synthesis of thymine nucleosides by ring closure of *N*-substituted ribosylamines and their thioureas

A novel procedure for the functionalization of positions 2 and 6 of purine nucleosides was reported by G. Piccialli and co-workers in 2013 (**Scheme 1.4**).²² The protocol exploits the reactivity of the corresponding carbons in the *N*¹-oxide of protected Nebularine (purine-9-riboside), which reacts with Grignard nucleophiles regioselectively on C⁶ and on C² after aromatization. A ring opening to an oximealdimine and a second aromatization complete the sequence in 48-82% yield. This method is particularly useful for the introduction of functionalized 2-pyridyl moieties in position 6.²³



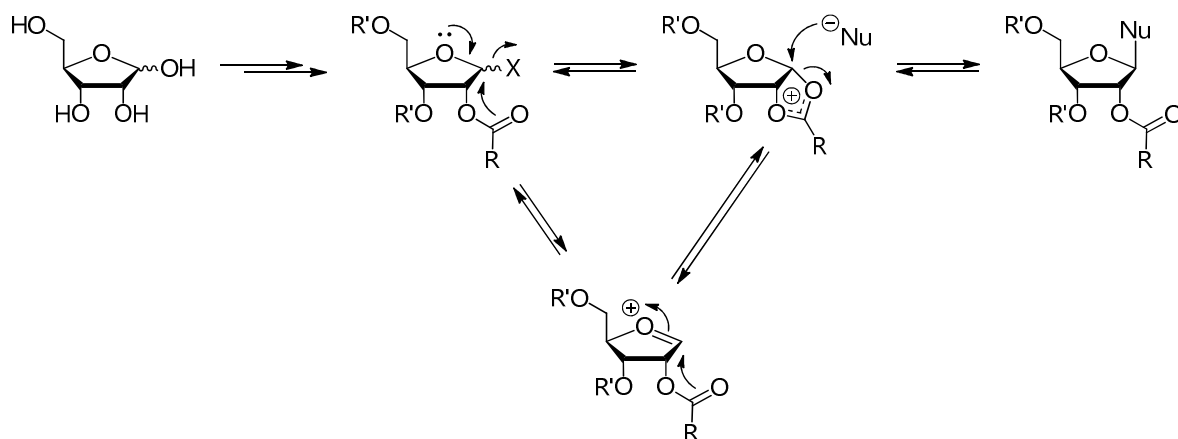
Scheme 1.4. Synthesis of 2,6-alkyl(aryl)purine nucleosides from Nebularine N^1 -oxide

Such a strategy can be used to synthesize a specific class of ring-expanded nucleosides (RENS, biologically relevant mimics of purine derivatives) containing 5:7-fused imidazo[4,5-*d*][1,2,6]oxadiazepine rings (**Scheme 1.5**). The reaction was speculated to proceed through an oxaziridine (formed by treatment of the oximealdimine intermediate with *t*-BuOOH in refluxed CCl_4) which rearranges to a nitrone. Ring closure and dehydration afforded the 5,8-dialkyl(aryl)-REN.²⁴



Scheme 1.5. Synthesis of 5,8-dialkyl(aryl)-RENS (ring-expanded nucleosides)

The alternative strategy to obtain either a purine or a pyrimidine nucleoside is to follow a *convergent approach*, in which a new C-N glycosidic bond is formed between the two structural components of the molecule (**Scheme 1.6**). Both nucleobase and sugar often need protections not only on acid/base-labile moieties but also on potential nucleophilic atoms (especially nitrogens), since all these methods consist of an S_N1 - or S_N2 -type reaction at low to high pH, catalyzed by Lewis acids, if necessary, or promoted under alkaline conditions. The attack of a heterocycle on the activated anomeric carbon in an electrophilic sugar (mostly ribose) gives better yields when the 2'-hydroxyl function is protected by an acyl group, selectively forming the β -nucleoside by virtue of neighbouring group participation. The use of chlorine and bromine is widespread to activate position 1'.



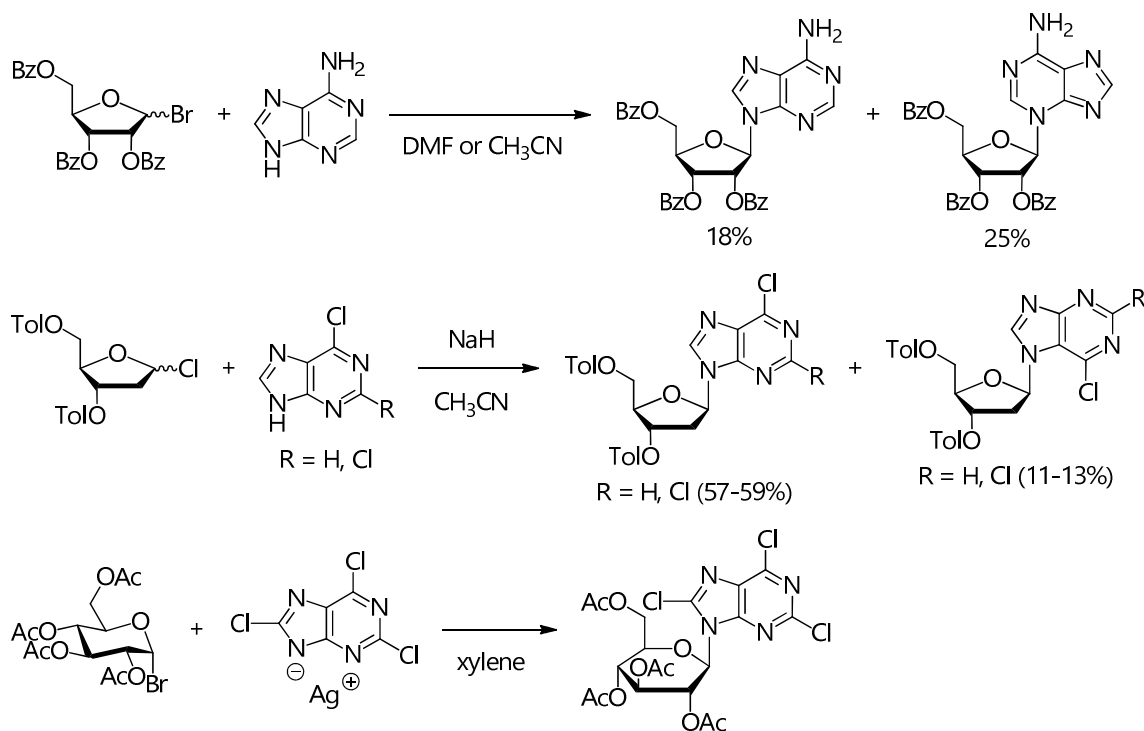
Scheme 1.6. General mechanism of glycosylations by the *convergent approach*

The mechanism suggests that the stereoselective synthesis of 2'-deoxyribonucleosides directly from 1'-chloro- or 1'-bromo-2'-deoxyribose is less efficient due to the absence of any assisting effect by adjacent positions. Experimental data confirm this behavior.²⁵

At least five different variations of such a direct strategy have been reported, depending on the reaction conditions:

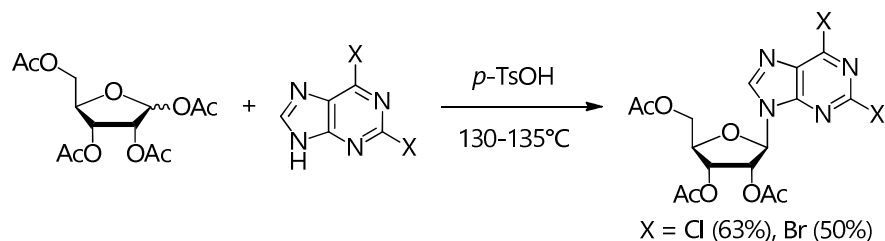
- uncatalyzed glycosylation of nucleobases or their metal salts;
- acid-catalyzed fusion at high temperature;
- classic Hilbert-Johnson reaction;
- Vorbrüggen reaction (Hilbert-Johnson silyl variation);
- Lewis acid-catalyzed chemical transglycosylation.

The first method involves the combination of a nucleobase ring or its metal (Ag, Hg or Na) salt and a protected 1'-halosugar (**Scheme 1.7**).²⁶



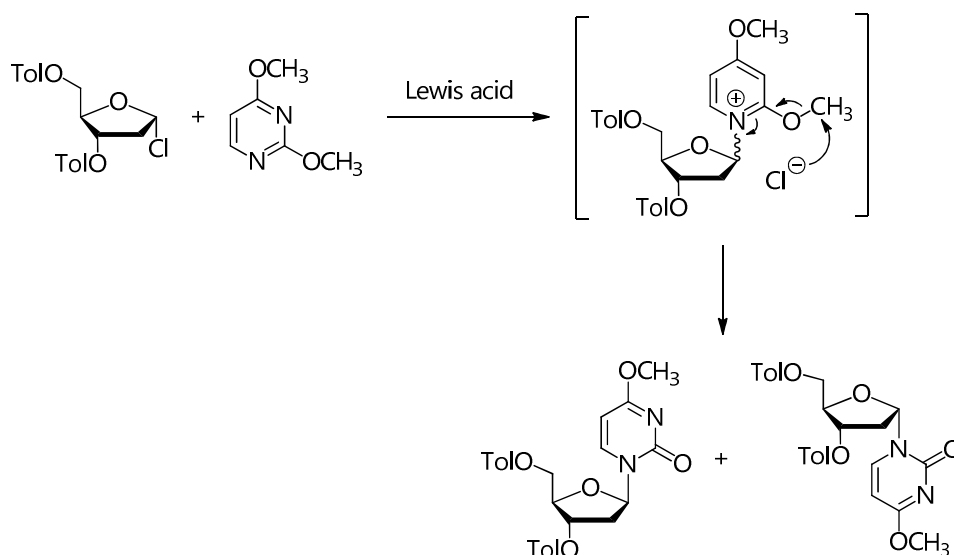
Scheme 1.7. Examples of the uncatalyzed glycosylation of nucleobases and their metal salts

In the acid-catalyzed fusion, high temperatures (up to 150-170°C) allow the direct condensation of a free base with peracetylated ribose in a fuse state in the presence of a Lewis acid (**Scheme 1.8**).²⁷ This simple procedure is incompatible with aliphatic halides and thermolabile moieties. Yields seldom exceed 70% and harsh conditions may also lead to inversion at C^{2'} in the formed nucleoside, as well as to complex mixtures.



Scheme 1.8. Example of acid-catalyzed fusion

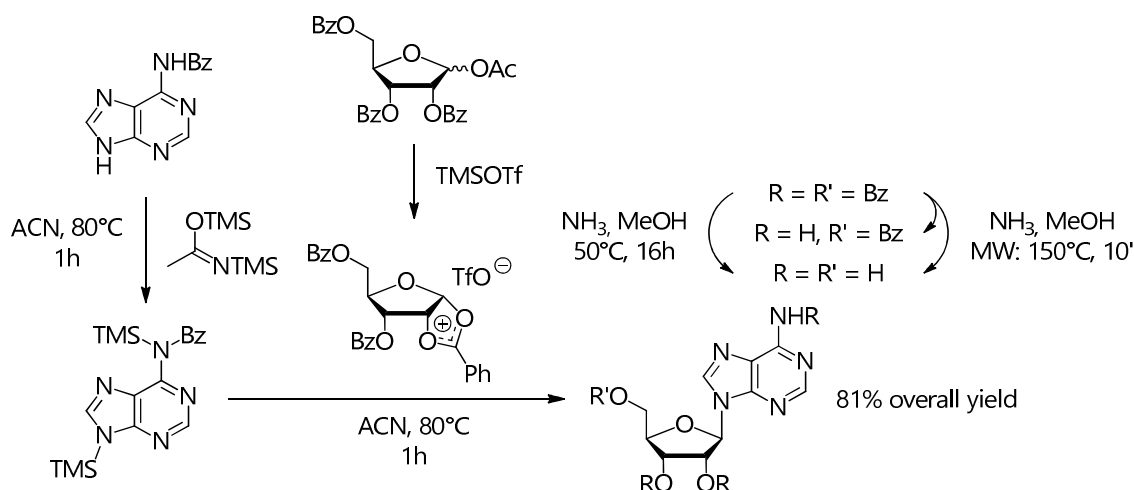
The classic Hilbert-Johnson reaction has found a widespread use in the condensation of acylated furanoses and pyranoses under the influence of a Friedel-Crafts catalyst. For instance, 2,4-diprotected pyrimidines can react with activated 2'-deoxyribose to form a mixture of the α and β anomers, in which the first product predominates (**Scheme 1.9**).^{26d, 28}



Scheme 1.9. Example of the Hilbert-Johnson reaction

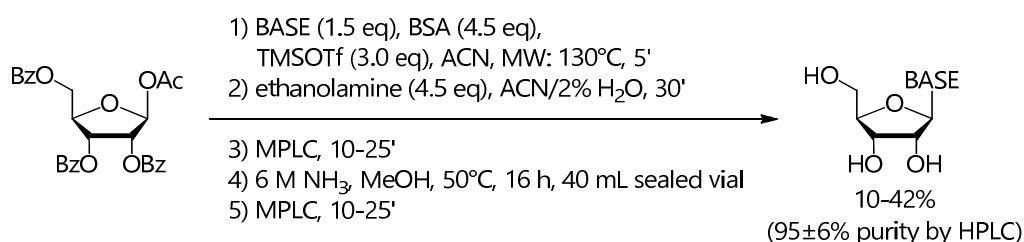
Moreover, this protocol holds a number of drawbacks, first of all moderate yields because of extensive by-products formation. They include undesired α anomers in high proportions with respect to the β ones, as well as *O*-glycosides and *N*-alkylated species.

In order to overcome such shortcomings, in the 1970s Vorbrüggen and co-workers developed a “silyl version” of the Hilbert-Johnson glycosylation, so far one of the mildest general methods for nucleoside formation (**Scheme 1.10**).²⁹ In this alternative, a Sn or Ti Lewis acid (such as SnCl₄ or TiCl₄) catalyzes the condensation of a sugar tetra-*O*-acetate and a silylated base, both more soluble than their parent compounds. Despite the evident improvements, regioselectivity is still often challenging since a nucleobase contains multiple basic sites and the reaction is seldom irreversible.



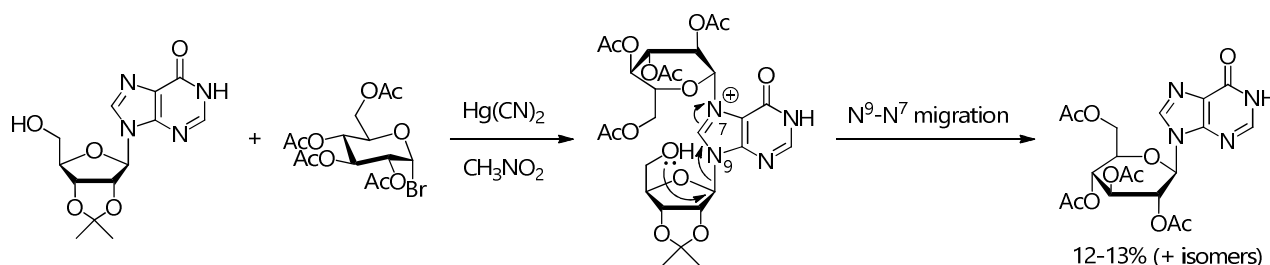
Scheme 1.10. Example of the Vorbrüggen glycosylation

In 2007 the Vorbrüggen glycosylation was adapted by Bookser and Raffaele into a one-step 5'/130°C microwave assisted reaction (**Scheme 1.11**). After quenching by neutralization and direct MPLC (Medium Pressure Liquid Chromatography) purification, deprotection was performed with NH₃/MeOH. This procedure was applied to the coupling of numerous bases with various sugars for the high-throughput preparation of nucleosides containing heterocyclic bases which would have required more effort according to previously published methods.³⁰



Scheme 1.11 Adapted Vorbrüggen glycosylation

Finally, the idea to synthesize nucleosides by chemical transglycosylation came from the observation of the intramolecular migrations of glycosyl moieties from N¹ or N³ to N⁹ in purines under acidic conditions (**Scheme 1.12**). In the presence of a suitable Lewis acid, this approach is unique and often useful, especially for the preparation of functionalized products unavailable through conventional methods.³¹



Scheme 1.12. Example of chemical transglycosylation

Nevertheless, all these *convergent approaches* are characterized by a number of drawbacks:

- they all require multistep syntheses, frequently associated with protection/deprotection reactions and anomeric activation;

- synthetic schemes are complex and isolation of intermediates and products, as well as their purification, is tedious;
- high/low temperatures are often necessary, as well as the use of organic solvents and metal catalysts, in syntheses frequently characterized by a high environmental impact and raising problems of waste disposal;
- the formation of several undesired by-products from concurring side-reactions is often regular;
- regio- and stereoselectivity in the C-N bond formation can be not satisfactory:
 - ♦ since heterocyclic bases are multidentate nucleophiles, glycosidic bond generation is inefficient on the desired nitrogen atom, leading to multiple products;
 - ♦ control of the anomeric configuration is low, especially for 2'-deoxyribonucleosides due to the lack of assistance by OH^{2'};

For such reasons, the chemoenzymatic synthesis may be a complementary strategy.

1.2.2. Chemoenzymatic synthesis of nucleosides

Enzymatic syntheses based on glycosyl-transferring enzymes have been shown to be an advantageous alternative to chemical methods due to the high selectivity of biocatalysts, mild reaction conditions and the overall simplicity of the approach.³² Generally speaking, the use of one or more enzymatic steps in chemical synthetic routes has become very popular, showing that enzymes are considered powerful tools by chemists.³³

For synthetic purposes, enzymatic reactions can be performed using:

- 1) whole cells³⁴ or cell-free extracts;
- 2) isolated and purified enzymes;
- 3) immobilized enzymes.

The use of whole cells or enzyme extracts requires the control of side-reactions which can result in the co-occurrence of undesirable by-products, as well as possible contaminants in the final target, such as proteins or toxins from the organism that produces the catalyst. Moreover, intra- and extracellular diffusion problems have to be addressed.

Isolated and purified enzymes considerably reduce some of the above mentioned drawbacks. However, the instability of the protein under non-physiological conditions (temperature, pH, ionic strength, co-solvents, ...), a difficult biocatalyst recovery from the reaction medium and high production costs may represent significant limitations.

Enzymes immobilized on proper matrixes by either adsorption or covalent interactions are extremely attractive to overcome such problems, as well as their variants entrapped in soluble form inside devices (*e.g.* membranes and microcapsules). In the latter case, impermeability to the enzyme is necessary to ensure a continuous and efficient exchange of substrates and products.³⁵

A solid-supported enzyme can be separated from the reaction medium by filtration and is thus available for reuse. Depending on the immobilization technique, properties of the biocatalyst such as stability, selectivity and K_M may be significantly affected.^{33, 36} Indeed, the design of a tailor-made immobilization plays a pivotal role to take full advantage from this technology. In the view of preparative applications, it is mandatory to simplify the downstream process: the availability of an immobilized and stabilized enzyme meets this need both by virtue of its easy handling and operational stability for a repeated use.

A range of drawbacks associated with soluble enzymes can be circumvented by switching from homogeneous to heterogeneous biocatalysis:

- short and long term stability should be higher against a wide variety of conditions. In fact, harsh temperatures and pH are frequently essential to achieve the solubilization of substrates and products

at the high concentrations required by a preparative process, whereas native enzymes usually show narrow stability windows and shelf life;

- denaturation is hardly an issue;
- simple filtration can be relied on for enzyme removal from the reaction mixture;
- recycle and reuse are highly feasible.

Activity loss is one of the possible outcomes upon immobilization on solid supports, often due to conformational changes. However, it is frequently compensated by long-term stability.

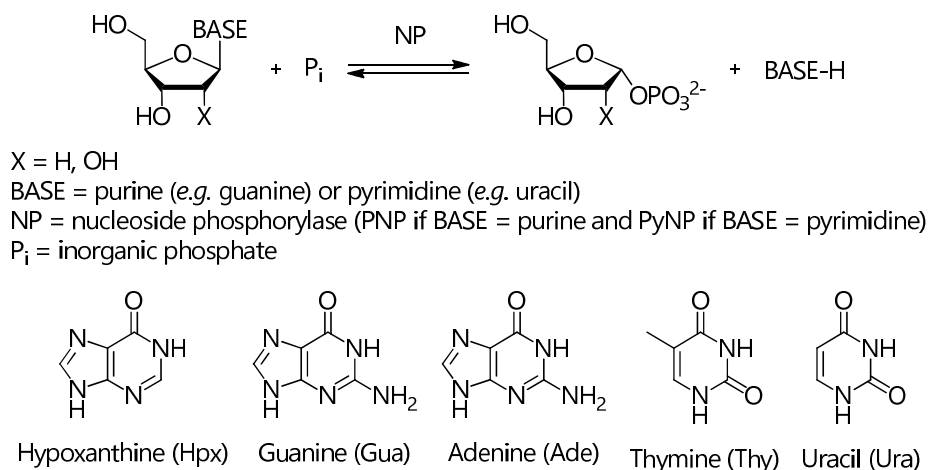
The idea to use enzymes as biocatalysts in the preparation of nucleosides was envisaged and carried out by Krenitsky and co-workers in the late 1960s, with the goal to overcome the typical drawbacks encountered in the chemical synthesis of these molecules.³⁷

To date, two main classes of enzymes have been employed in nucleoside synthesis: nucleoside phosphorylases (NPs, EC 2.4.2) and *N*-2'-deoxyribosyltransferases (DRTs, EC 2.4.2.6). Although by a different mechanism, they both catalyze the formation of the C-N glycosidic bond through the transfer of a carbohydrate residue to a nucleobase.^{32a}

1.3. Nucleoside phosphorylases (NPs, EC 2.4.2)

1.3.1. Classifications

Nucleoside phosphorylases (NPs, EC 2.4.2) are enzymes which catalyze the phosphorolysis of purine and pyrimidine ribo- and 2'-deoxyribonucleosides. This reversible cleavage of the C-N β -glycosidic bond occurs in the presence of an inorganic phosphate ion (P_i) as co-substrate to generate the corresponding α -D-pentose-1-phosphate and the conjugated nucleobase (**Scheme 1.13**).



Scheme 1.13. General reaction catalyzed by nucleoside phosphorylases (NPs) and common nucleobases

As for thermodynamics, the reaction is shifted toward nucleoside synthesis, being the equilibrium constant for mammalian NPs about 50.³⁸ However, *in vivo* phosphorolysis is often coupled with an enzymatic sequence based on oxidation and 5'-phosphoribosylation of the released nucleobase, favoring the glycosidic cleavage. The latter reactions are catalyzed by xanthine oxidase (XO) and hypoxanthine-guanine phosphoribosyl transferase (HGPRT).^{12a}

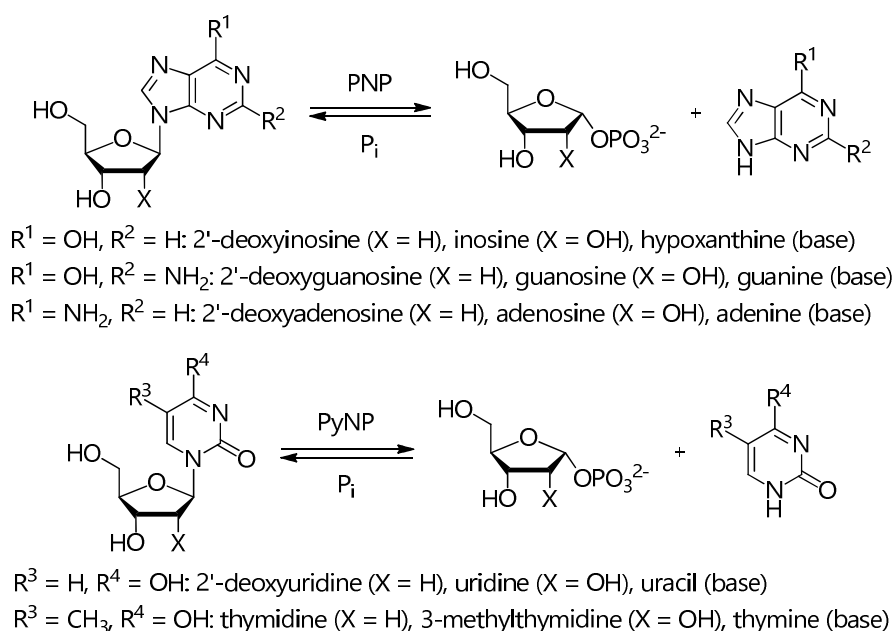
NPs from various organisms are fundamental biocatalysts in the so-called "salvage pathway", in which purine and pyrimidine nucleosides can be synthesized by recycling intermediates belonging to degradative

mechanisms of nucleic acids. The recycled materials can therefore be converted back into ribo- and 2'-deoxyribonucleotides. The role of recycling alternatives is fundamental in most organisms, in that the *de novo* construction is not available for all tissues, especially because of its energy-costly nature.^{12a, 39}

Many attempts on different classifications of NPs have been tried over the last decades, yet none of them has resulted inclusive of all possible cases. Among the characteristics that can be assumed as classification elements, three are of particular importance:

- nucleobase or nucleoside substrate specificity (purine or pyrimidine);
- quaternary structure (dimeric, trimeric or hexameric);
- molecular mass (low-MM or high-MM) only for PNPs.

The first and simplest distinction between NPs depends on their substrate specificity and divides them into purine nucleoside phosphorylases (PNPs, EC 2.4.2.1) and pyrimidine nucleoside phosphorylases (PyNPs, EC 2.4.2.2), the first ones specific for purine nucleosides (*e.g.* inosine, guanosine, adenosine, ...) and the latter for pyrimidine derivatives (*e.g.* uridine, thymidine, ...) (**Scheme 1.14**).



Scheme 1.14. General phosphorolysis catalyzed by PNPs and PyNPs

Another possible classification of NPs introduced by Pugmire and Ealick started from the analysis of the protein structure along with their ability to process specific substrates.^{13a} The first class, nucleoside phosphorylases-I (NPs-I), includes enzymes with a common single-domain subunit and an either trimeric or hexameric quaternary structure, able to recognize a broad variety of purine nucleosides (PNPs) and uridine analogues (UPs) as substrates. Examples are human (*Hs*), *Escherichia coli* (*Ec*) and *Bacillus subtilis* (*Bs*) PNPs, as well uridine phosphorylase from *E. coli* (*EcUP*). Enzymes belonging to the second family, nucleoside phosphorylases-II (NPs-II), show a dimeric quaternary structure, contain a two-domain recurring in their subunit fold and accept only pyrimidine substrates (PyNPs). Thymidine and uridine nucleosides are recognized by these enzymes in lower organisms, while in higher ones only thymidine substrates are. Among them uridine and thymidine phosphorylases (for instance, TPs from *E. coli* and *Lactobacillus casei*) are worth mentioning.

In 2000, Shugar and co-workers reported a tentative classification of PNPs based on their molecular mass (MM), ranging from ~ 80 and ~ 180 kDa.^{12a} PNPs were divided into low- and high-MM enzymes. Interestingly, members belonging to the same group shared not only equal quaternary structure but also subunit

composition and definite activity toward specific substrates. A third class was composed of PNPs from bacteria, parasites and mammals which were not ascribed to either groups.

The first two classes (**Table 1.1**) were defined as follows:

- low-MM homotrimers (~ 80-100 kDa), specific for 6-oxopurines and their related nucleosides, often referred to as “Ino-Guo phosphorylases”;
- high-MM homohexamers (~ 110-160 kDa) with a broader substrate specificity extended to both 6-oxo- and 6-aminonucleosides, being adenosine a much better substrate than inosine and guanosine (*e.g.* in *B. subtilis*).

	PNP class		
	Low-MM	High-MM	Others
Molecular mass	~ 80-100 kDa	~ 110-160 kDa	~ 60-180 kDa
Quaternary structure	homotrimers	homohexamers	homodimers, -trimers, -tetramers, -pentamers and -hexamers
Specificity	6-oxopurines, their nucleosides and some analogues	very broad (6-oxo and 6-aminopurines, their nucleosides and many analogues)	<ul style="list-style-type: none"> • 1ST group: specificity as for low-MM PNPs, but not homotrimers • 2ND group: specificity as high-MM PNPs, but not homohexamers
Natural substrates	Ino, Guo	Ino, Guo, Ado	various
Sources	mainly mammals (human, calf) and some bacteria (<i>B. subtilis</i> PNPI, <i>Cellulomonas</i>)	mainly bacteria (<i>E. coli</i> , <i>S. typhi</i> , <i>S. sulfataricum</i>) and <i>Mycoplasma</i> (<i>M. pneumoniae</i>)	some bacteria (<i>P. vulgaris</i>), mammals (bovine liver mitochondria) and parasites (<i>P. falciparum</i>)

Table 1.1. Classification of PNPs by Shugar and co-workers

Typical models of trimeric PNPs are the ones from *Homo sapiens* and *Mycobacterium tuberculosis*⁴⁰, while hexameric structures can be represented by PNPs from *E. coli* (*EcPNP*), *Salmonella typhimurium* (*StPNP*), *Plasmodium falciparum* (*PfPNP*), *B. subtilis* (*BsPNP*) and *Proteus vulgaris* (*PvPNP*)^{12a}. *Hs* and *EcPNP* are depicted in **Figure 1.3a** and **1.3b**, respectively.

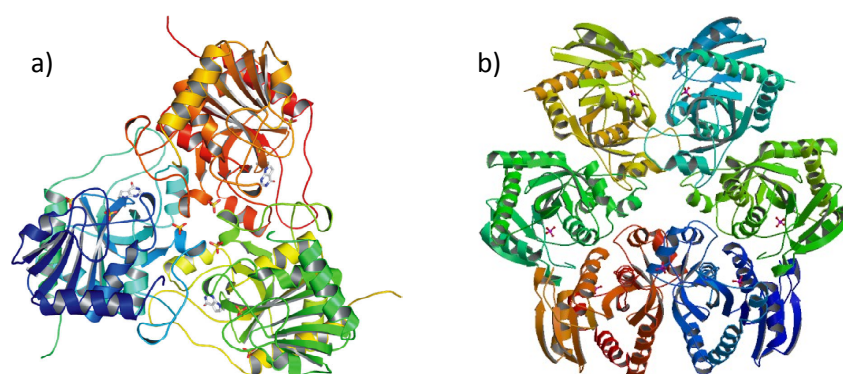


Figure 1.3. Structures of: **a)** *HsPNP* (Reprinted with permission from *J. Struct. Biol.* **2010**, *169*, 379-388)⁴¹; **b)** *EcPNP*⁴².

1.3.2. Active sites

As for all PNPs, each active site can be divided into three parts:

- phosphate ion binding site;
- sugar binding site;
- purine binding site.

The active site of the *Hs*PNP complex with Immucillin-H (a transition state analogue inhibitor, see 1.3.4) and a phosphate ion is represented in **Figure 1.4**.^{12a, 43}

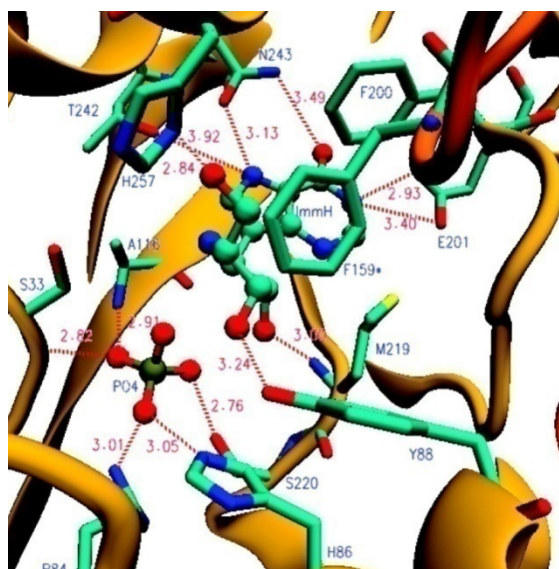


Figure 1.4. Active site of the *Hs*PNP complex with Immucillin-H and a phosphate ion (Adapted from *Biochemistry* **2010**, 49, 2058-2067. Copyright 2013 American Chemical Society)⁴⁴

Each subunit of this trimeric PNP is constituted by a distorted β -barrel made of a five- and an eight-stranded mixed β -sheet and flanked by seven α -helices. The active site is located near the boundaries between subunits and protected by Phe₁₅₉ acting as a lid from the nearest neighboring portion.

The least profound part of the site is localized near to a Gly-rich loop and hosts the co-substrate phosphate in a largely hydrophilic environment with Ser₃₃, Arg₈₄, His₈₆ and Ser₂₂₀.

The sugar moiety binds to *Hs*PNP in a rather hydrophobic pocket that allows an optimal alignment of the anomeric centre with the phosphate ion. Tyr₈₈, the backbone amide nitrogen of Met₂₁₉ and His₈₆ are notable exceptions, interacting by hydrogen bonds with the polar part of the pentose ring (OH^{3'} specifically points toward Tyr₈₈). Several aromatic residues, such as Phe₁₅₉ (from the adjacent subunit), Phe₂₀₀, His₈₆ and Tyr₈₈, are placed very close to the rear part of ribose or 2'-deoxyribose and assist the ones interfaced with the other sugar portion.

The purine binding site is buried deeply inside the core of the active one and its distinguishing residues are partly polar and partly hydrophobic. The first group allows the strong selectivity of *Hs*PNP for 6-oxonucleosides and bases, driven by a compact series of hydrogen bonds of Glu₂₀₁, Lys₂₄₄, Thr₂₄₂ and Asn₂₄₃ with N¹H, N²H₂, O⁶ and N⁷. The ability of Asn₂₄₃ to block the CO group in position 6 is assured by a polarization in the γ -amide through another similar interaction with OH of Thr₂₄₂. As for apolar residues, the core of the purine ring is involved in a series of hydrophobic touches with Ala₁₁₆, Phe₂₀₀, Val₂₁₇, Met₂₁₉, Gly₂₁₈ and Thr₂₄₂.

The hexameric PNP from *E. coli* was studied by XRD at a 2.0 Å resolution by Mao *et al.* in 1997.⁴⁵ Although its crystal structure showed an overall similarity with the human PNP in terms of subunit and active site

geometry (especially the secondary structure around substrates), it also contained a series of residues remarkably dissimilar from the ones in trimeric enzymes. *EcPNP* is a disc-shaped hexamer that may be viewed as a trimer of dimers, each containing two active sites.

The active site of the *EcPNP* complex with Formycin B (a weak inhibitor of PNPs) and a phosphate ion is depicted in **Figure 1.5**. Its higher openness may account for the wider substrate acceptance of hexameric PNPs, if compared with trimers.

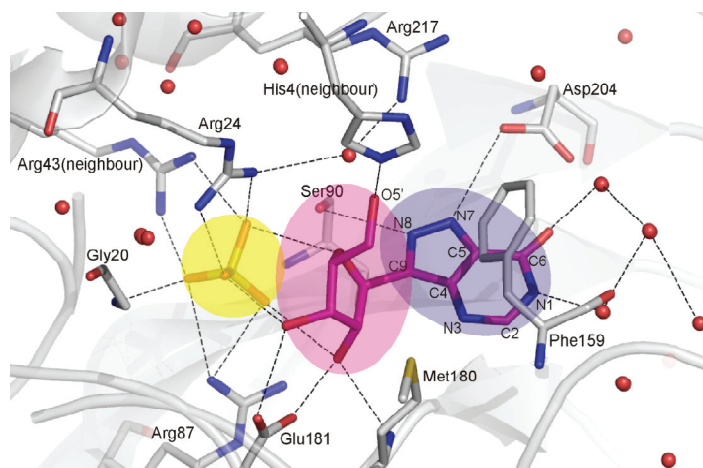


Figure 1.5. Active site of the *EcPNP* complex with Formycin B and a phosphate ion (Adapted from *Croat. Chem. Acta* **2013**, *86*, 117-127)⁴⁶

The polar interactions with the inorganic ion involving Arg₈₄, His₈₆ and Ser₂₂₀ in the human enzyme are reproduced by Arg₂₄, Arg₈₇ and Arg₄₃ in the bacterial one. A few additional hydrogen bonds are generated with both the backbone amide and side chain of Gly₂₀ and Ser₉₀.

Van der Waals contacts are generated by Val₁₇₈, Glu₁₇₉ and Met₁₈₀ and exploited by *EcPNP* to anchor the ribose moiety and align its anomeric carbon against the phosphate ion oxygens. These hydrophobic bonds are assisted by a supplementary electron-rich interaction involving Phe₁₅₉ and the pentose apolar side containing O^{4'}. The role of this residue is both as a lid-like fragment and a hydrophobic contributor. Upon substrate binding, a large loop is subjected to movements shifting His₄ and His₄₇ near to the ribose moiety allowing them to interact with OH^{3'} and OH^{4'}, respectively.

As in the *HsPNP*, the purine binding pocket is neither entirely hydrophobic nor hydrophilic. Phe₁₆₇ and Ile₂₀₆ are added to Val₁₇₈, Met₁₈₀ and Phe₁₅₉, the latter from a second subunit, strengthening the apolar interactions. As for polar residues, once again Glu₂₀₁ and Lys₂₄₄ cooperate in binding to N¹H, N²H₂ and the 6-carbonyl group. However, the hydrogen bonding pattern between Glu₂₀₁, Asn₂₄₃ and the base, typical of mammalian PNPs, is not retained since the latter residue is shifted with Asp₂₀₄. This catalytically relevant residue lies very close to N⁷.

1.3.3. Catalytic mechanism

Despite the presence of different PNP classes with specific activities toward nucleosides, the catalytic mechanism of these enzymes has been generalized since the late 1990s. All literature sources agree with the formation of a transition state (TS) characterized by a strong oxacarbenium ion character. The ribosyl electrophile then migrates from the nucleobase, which acts as a leaving group, to the deprotonated phosphate nucleophile through either a concerted or a stepwise mechanism.

More in details, two similar models have been proposed by Canduri *et al.*⁴⁷, Bennett *et al.*⁴⁸ and Koellner *et al.*⁴⁹ for *Hs* and *Ec*PNP, respectively, to explain the catalytic mechanism of both enzyme classes (I and II) (Figure 1.6). Crystallographic information and functional analysis were carried out to support them.

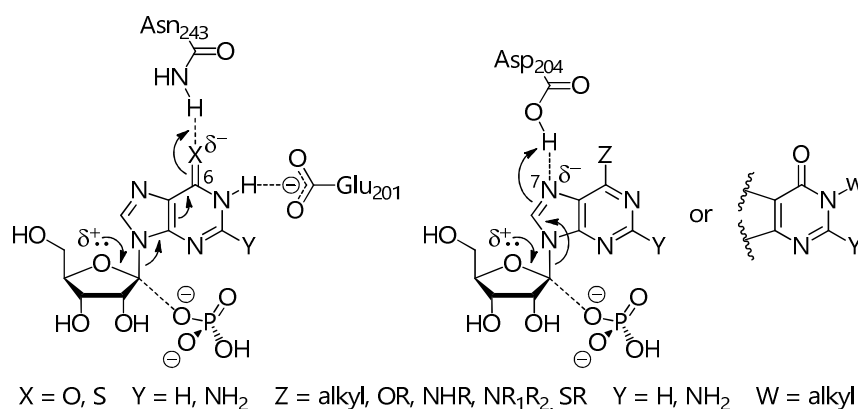


Figure 1.6. Proposed TSs and catalytic mechanisms for class I and II PNPs (e.g. *Hs* and *Ec*PNP, respectively)

The analysis of several PNP-substrate complexes suggests that the binding pose of the β -D-nucleoside presents a high-energy *anticlinal* torsion angle of the C-N bond and the ribose group in an uncommon C⁴ *endo* sugar pucker. Such an unstable conformation should induce a weakening of the glycosidic bond. Cleavage at position 1' is also promoted by an electronic flow from the endocyclic oxygen, triggered by the deprotonation of the phosphate co-substrate. As a result, the lone pair on O^{4'} is forced closer enough to the glycosidic bond to disrupt its stability. An oxocarbenium ion stabilized by the phosphate ion is formed as a transient intermediate and is captured by one of the nucleophile oxygens in a S_N1-type attack. The nucleobase is released after protonation.⁵⁰

As for class I enzymes (low-MM, trimeric or tetrameric), a carbonyl or thiocarbonyl moiety in position 6 is necessary to form a key hydrogen bond with an Asn residue (Asn₂₄₃ in *Hs*PNP) and to stabilize the partial negative charge delocalized on the purine ring. The wider substrate specificity shown by class II PNPs (high-MM, hexameric), on the contrary, is caused by a relocation of the stabilizing hydrogen bond on N⁷. In this case, an Asp residue (Asp₂₀₄ in *Ec*PNP) is likely to protonate the leaving purine base. This suggests why PNP class II can recognize adenosines and 6-substituted congeners too. Another interesting difference with respect to the first class is a second interaction between N¹H and a Glu residue (Glu₂₀₁ in *Hs*PNP) which alters the keto-enol tautomeric equilibrium, preventing the reconstitution of the carbonyl form.

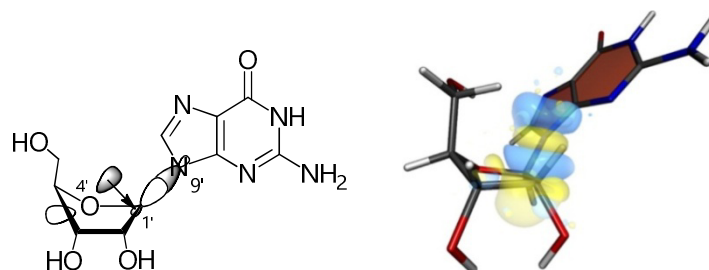


Figure 1.7. Schematic and molecular representations of the electron transition $n_{O4'} \rightarrow \sigma^*_{C1'-N9}$ (Adapted from *J. Phys. Chem. B*, **2013**, *117*, 6019-6026. Copyright 2013 American Chemical Society)⁵¹

According to dynamic simulations reported in 2013 by Barnett and Naidoo, the trimeric bovine PNP (*Bos taurus* PNP, structurally similar to the human one) forces the substrate in an unnatural flattened *endo* conformation anchored by hydrogen bonds between the phosphate dianion and OH^{2'}-OH^{3'}. The additional

interactions of N¹H with Glu₂₀₁ and of the aromatic bicycle with Phe₂₀₀ further increase the restriction of the base movements and therefore the alteration of the sugar pucker preferred conformation. As a result, an elongation of the glycosydic bond is generated by a massive electron migration from the nonbonding orbital of the endocyclic oxygen ($n_{O4'}$) to the antibonding one associated to the C^{1'}-N⁹ bond ($\sigma^*_{C1'-N9}$). The consequent transition ($n_{O4'} \rightarrow \sigma^*_{C1'-N9}$) causes a weakening of the glycosydic bond and a reduction of the activation barrier for the nucleophilic attack by the phosphate ion on C^{1'} (**Figure 1.7**).⁵¹

However, a real understanding of the molecular mechanism of hexameric PNPs is still ahead, with some recent results opening new questions whose complexity is higher than expected.⁴⁶

1.3.4. Transition state

In 2015 Evans, Schramm and Tyler published a review on Immucillins, useful mimics of the transition state of PNPs which can act as strong inhibitors to be used as antibiotics or with other potential clinical applications, such as toward leukemia, gout, autoimmune disorders, solid tumors.⁵² Human and bovine PNPs were studied by the kinetic isotopic effect (KIE) measured in arsenolysis of inosine and compared in terms of their transition state structures (**Figure 1.8**).

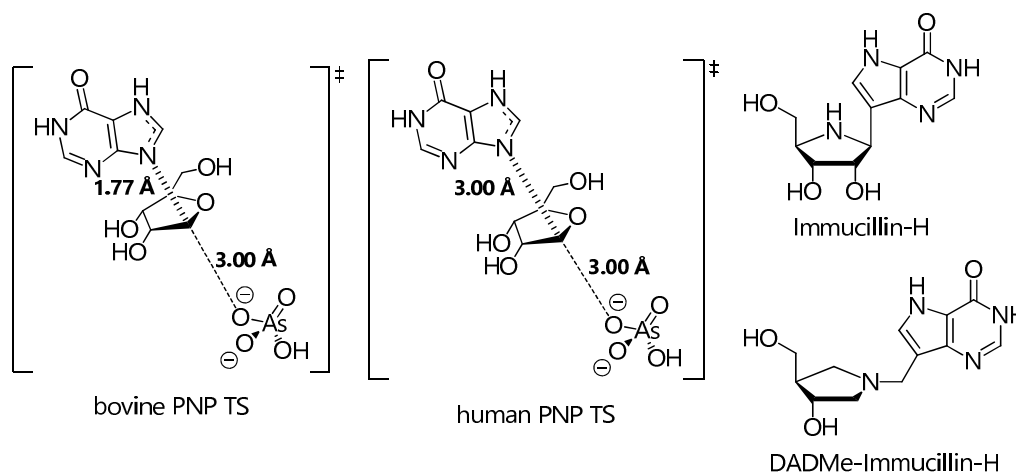
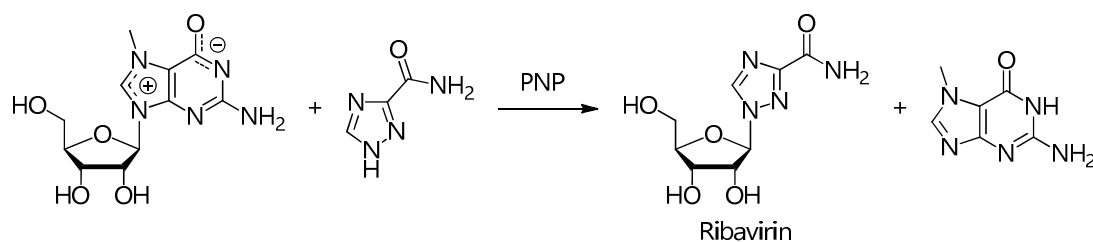


Figure 1.8. Transition states of arsenolysis catalyzed by bovine and human PNP (Adapted from *Curr. Med. Chem.* **2015**, *22*, 3897-3909)⁵²

Experimental data obtained with the bovine PNP allowed to identify an early dissociative TS bearing a significant ribocation character and still a partial bond order associated to the glycosydic bond, elongated to 1.77 Å. The arsenate dianion, however, lies still separated from the sugar unit at a 3.00 Å distance in the active site. This TS was noted to surprisingly differ from the one of the human enzyme, despite the very high sequence alignment match (87% in total and 100% regarding the active site residues which bind to the substrate).⁵³

HsPNP is indeed characterized by a transition state involving an already departed nucleobase and a nucleophile still not attacking the anomeric carbon. In this S_N1-type configuration, a fully developed ribocation is located at about the same 3.00 Å distance from both hypoxanthine and arsenate.⁵⁴

The features of the two TSs are reproduced by Immucillin-H (Forodesine) and DADMe-Immucillin-H (Urodesine), respectively, because of their striking structural similarities to the C^{1'}-N⁹ distance in both of them. Furthermore, they can be employed as models for PNPs belonging to different classes. For example, *PfPNP* is a hexameric structure whose phosphorylase mechanism proceeds through a very similar TS to *HsPNP* (highly dissociative) in spite of different catalytic residues.⁵⁵

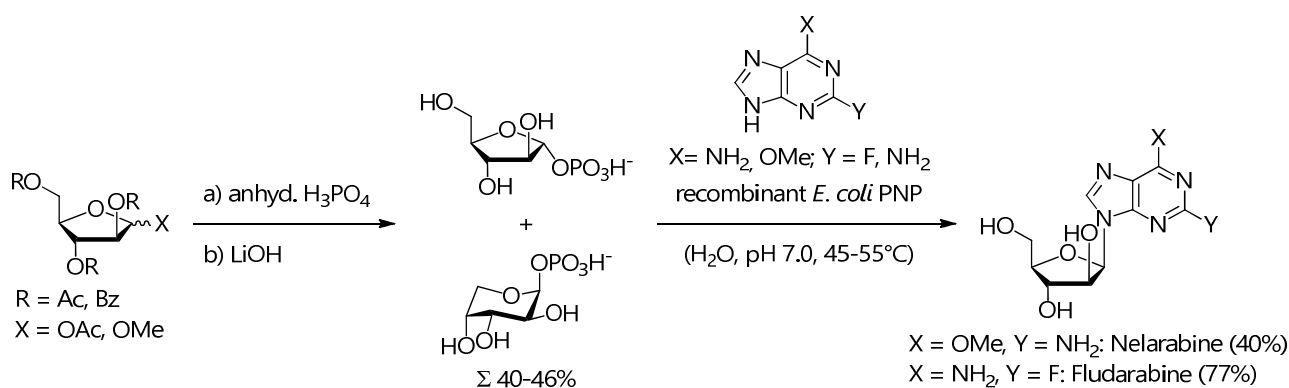


Scheme 1.17. “One-pot, one-enzyme” transglycosylation

Since the reverse transglycosylation is totally interdicted, in that the 7-methylpurine base is not a substrate of PNP, 7-methylated purine nucleosides may be chosen as a convenient pool of sugar *donors*.

Very recent examples of NP-catalyzed transglycosylations have revealed the great potential of enzymatic methods for the production of nucleoside analogues, such as Vidarabine (arabinosyladenine), a second-line antiherpes drug^{10c, 58}, Clofarabine (2-chloro-2'-fluoroarabinosyladenine), a second-generation purine nucleoside analogue used for the treatment of pediatric acute leukemia⁵⁹, and some 2,6-dihalogenated purine nucleosides as precursors for the synthesis of many anti-leukaemia drugs (*e.g.* Cladribine, Clofarabine and Fludarabine)⁶⁰.

Since a pentose-1-phosphate is the key intermediate, its chemical synthesis followed by an enzymatic glycosylation may be preferred. In 2011, Mikhailopulo and co-workers reported the monoenzymatic synthesis of Fludarabine and Vidarabine catalyzed by *Ec*PNP (**Scheme 1.18**).⁶¹ 1,2,3,5-tetra-*O*-acetyl- α -D-arabinofuranose, methyl-2,3,5-tri-*O*-benzoyl- α -D-arabinofuranoside and 1-*O*-acetyl-2,3,5-tri-*O*-benzoyl- α -D-arabinofuranose were chemically phosphorylated with H_3PO_4 to a mixture of the furanose and pyranose forms of α -D-arabinose-1-phosphate, the first of which was processed by the enzyme as glycosylation reagent, yielding Nelarabine and Fludarabine in 40 and 77% yield, respectively. The first reaction was demonstrated to reach the equilibrium at almost 1:1 base/Nelarabine ratio, whereas the second one was shifted toward Fludarabine formation. In addition, the presence of the pyranose-1-phosphate did not interfere with the glycosylation reaction.

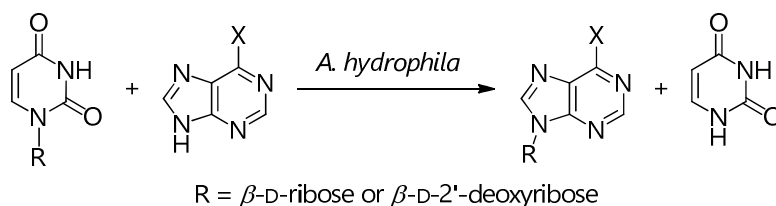


Scheme 1.18. Synthesis of Nelarabine and Fludarabine by the *Ec*PNP-catalyzed glycosylation of an α -D-arabinofuranose/pyranose-1-phosphate mixture

1.3.6. PNP from *Aeromonas hydrophila* (*Ahp*PNP, EC 2.4.2.1)

In 2005 Trelles *et al.* performed an extensive screening of various microorganisms in order to synthesize 6-substituted ribo- and 2'-deoxyribonucleosides by a biocatalyzed transglycosylation. A pyrimidine nucleoside (uridine or thymidine) was exploited as β -D-ribose *donor* and 6-substituted purines as *acceptors*. Among all

the tested microorganisms, the broad substrate specificity of *Aeromonas hydrophila* (*Ah*) resulted quite attractive from a synthetic viewpoint (**Table 1.2**).⁶²



Nucleoside	Product formation (%) ^{a)}	Time (h)
Adenosine	33	4
2'-Deoxyadenosine	89	4
6-Chloroinosine	10	1
6-Methoxyinosine	41	1
6-Thioinosine	-	-
6-Iodoinosine	-	-

^{a)} HPLC conversions

Table 1.2. Synthesis of 6-substituted purine ribonucleosides by transglycosylation catalyzed by *A. hydrophila* cells

In the recent past, from the strain of *A. hydrophila* reported by Trelles *et al.*, the purine nucleoside phosphorylase encoded by the *deoD* gene was cloned, over-expressed in *E. coli* and purified by Ubiali, Speranza and co-workers. From its high MM (155 kDa) and substrate specificity directed to inosine, guanosine and adenosine, *Ah*PNP was assumed to be a PNPII belonging to NP-I family (see **1.3.1**)^{13a}, thus having a hexameric quaternary structure. Purity, assessed by SDS-PAGE (Sodium Dodecyl Sulphate - PolyAcrylamide Gel Electrophoresis), was more than 90% and protein concentration 4.0-6.0 mg·mL⁻¹.⁶³

1.3.7. UP from *Clostridium perfringens* (*CpUP*, EC 2.4.2.3)

The uridine phosphorylase from *Clostridium perfringens* (*CpUP*) belongs to a family of enzymes crucial for the metabolism of pyrimidine nucleosides and nucleotides. They are selective for uridine and 2'-deoxyuridine, spanning from prokariotes to yeasts and higher organisms, and together with thymidine phosphorylases (TPs), they constitute the two major classes of PyNPs.^{13a}

To date, neither any structure has been proposed for *CpUP* nor any sequence alignments have been performed to investigate the arrangement of aminoacidic residues in the catalytic site. The quaternary structures of other UPs have been elucidated both in bacteria and in humans.

Given the high structural conservation of UPs, literature information allows to predict the main features of *CpUP* monomers. Most subunits in known bacterial UPs are arranged in a toroid configuration composed of three dimers with a three-layered $\alpha/\beta/\alpha$ sandwich. Concerning the active site, uridine interacts on its hydroxyl and carbonyl groups with polar residues such as Glu and Arg, which are also catalytically active. Hydrophobic side chains generate an arrangement of apolar contacts with the sugar and the inner nucleobase. The phosphate ion is anchored by hydrogen bonds in a binding site considerably similar to the one in NPs.⁶⁴

The S_N1-type catalytic mechanism shared by most UPs is similar to that of PNPs (**Figure 1.9**). In essence, the usual oxonium ion is formed and the conjugate nucleobase is released upon weakening of the glycosidic

bond. Two hydrogen bonds between the carbonyl moieties and an Arg-Lys couple stabilize the negative charge as a hydroxyl group from Ser prevents tautomerization at N¹H, while the orthophosphate ion forms α -D-ribose-1-phosphate.^{13a}

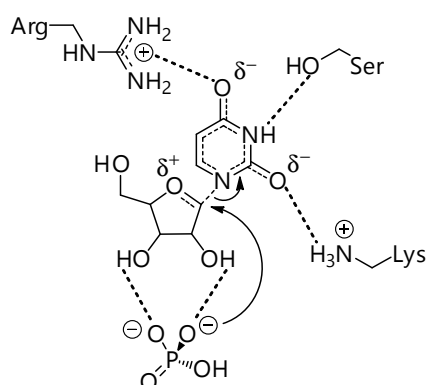


Figure 1.9. General catalytic mechanism of UPs

1.4. Purine nucleoside phosphorylase from *Mycobacterium tuberculosis* (MtPNP)

1.4.1. Tuberculosis (TB)

Tuberculosis (TB), caused by *Mycobacterium tuberculosis* (*Mt*), still represents one of the top ten death causes in emerging parts of the world as well as a resurgent disease in developing countries. As pointed out by the World Health Organization (WHO), which has been publishing annual reports on this subject since 1997, in 2015 there were 10.4 million new TB cases (11.5% of which involved co-infection with the HIV virus in HIV-positive people) and 1.4 million TB deaths to be added to 0.4 million supplementary deceases among HIV-positive patients (Figure 1.10).⁶⁵

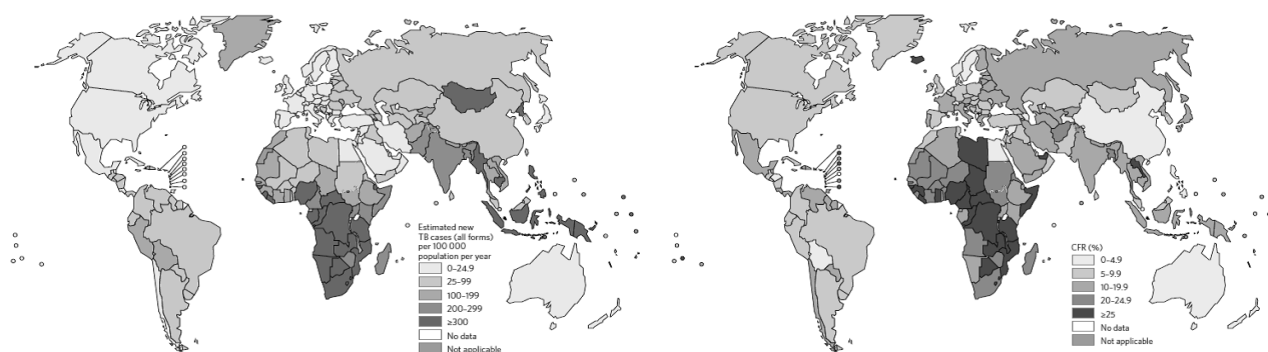


Figure 1.10. TB incidence rate and case fatality ratio for HIV-positive and negative people (2015)⁶⁵

Since efficient vaccines and fast-acting drugs are still being sought, TB is regarded as a global emergency against human health. Drugs such as Rifampicin, Isoniazid, pyrazinamide and Ethambutol generally lead to remission in 95% cases, but at the same time TB relapse and drug resistance can likely occur as consequences of intermittent dosing, patient non-compliance, advanced disease, immunosuppression and co-infection by HIV.⁶⁶

In the last years several multi- and extensively drug resistant (MDR and XDR, respectively) strains of *M. tuberculosis* have been developing, making medical treatments often unsuccessful (Figure 1.11).⁶⁷

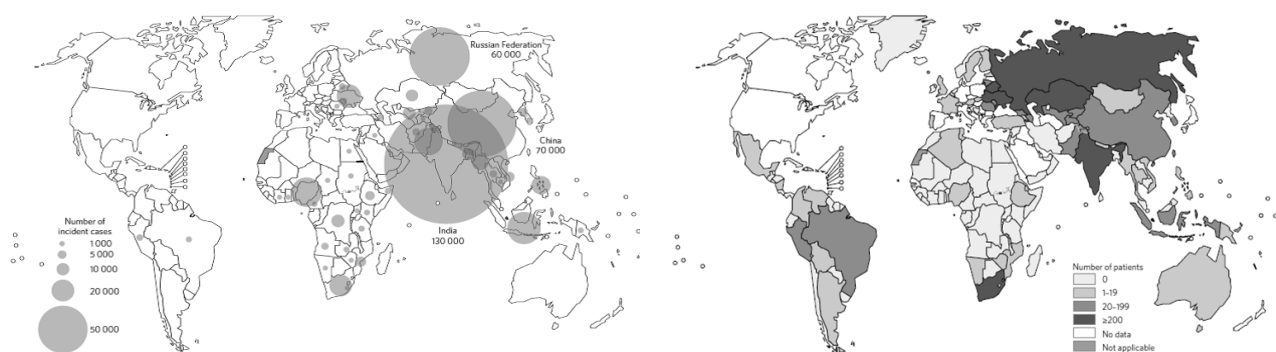


Figure 1.11. MDR-TB incidence and number of patients with laboratory-confirmed XDR-TB (2015)⁶⁵

Programs centered on TB medical treatment are being defied by the ongoing emergence of MDR, XDR and even totally drug-resistant (TRD) *M. tuberculosis* strains, which have evolved into completely irresponsive viruses. Unfortunately, although new drugs are now essential, only a few candidate leads are now being tested in clinical trials against them (e.g. diarylquinolines).⁶⁸

In essence, one of the most relevant goals of WHO is the worldwide eradication of TB by 2050, hence the need for the discovery of new antitubercular agents has become a global priority. In spite of the renewed interest registered in the last 20 years, novel and improved strategies to control this infection are urgently needed.

1.4.2. PNP from *Mycobacterium tuberculosis* (MtPNP) as a potential drug target

Due to their vast presence in organisms, enzymes often represent ideal targets for the action of new chemical entities (NCEs), many of them through selective inhibition.

Briefly, an ideal pharmacological target for TB treatment should answer at least three requisites:

- growth and persistence of *M. tuberculosis* must be strictly dependent on it;
- selectivity must be assured, by either the exclusive presence of the target in the pathogen or the preservation of its host counterpart;
- bacterial barriers must not hamper the physical access of the drug.⁶⁹

Since 2011, enzymes of the purine salvage pathway in *M. tuberculosis* have been suggested as potential targets for the development of new antitubercular agents.⁷⁰ Although it has not been yet clarified when the microorganism sways from the *de novo* to the salvage nucleic acid pathway, it is clear that the latter route is preferred under stressful conditions (i.e. cell replication and lack of energy). In this frame, the PNP from *M. tuberculosis* (MtPNP) might be a potential target for the rational design of analogues that can selectively inhibit *Mtb* replication and survival, thus answering the urgent need of new agents against MDR-XDR-TDR TB strains. Promising results have already been obtained with such an approach targeting the PNP from *P. falciparum*, responsible for malaria.⁷¹

1.4.3. Similarities and differences between HsPNP and MtPNP

In the classification on PNPs proposed by Shugar and co-workers (see 1.3.1)^{12a}, both the human enzyme and the one from *M. tuberculosis* belong to the class of low-MM homotrimers with a weight approaching the superior limit of 100 kDa.

Information gathered in the last decades has demonstrated that the differences in structural features^{41, 72} and transition state⁷³ of MtPNP with respect to the human homologue are modest but potentially useful. The two enzymes have only 40% aminoacidic sequence identity even though their structures and catalytic

mechanisms are similar, as verified by the Basic Local Alignment Search Tool (BLAST) based on the Kegg database.

The active site structure of *Mt*PNP and the main interactions between its residues and inosine are reported in **Figure 1.12a** and **1.12b**, respectively.^{72b, 73, 74}

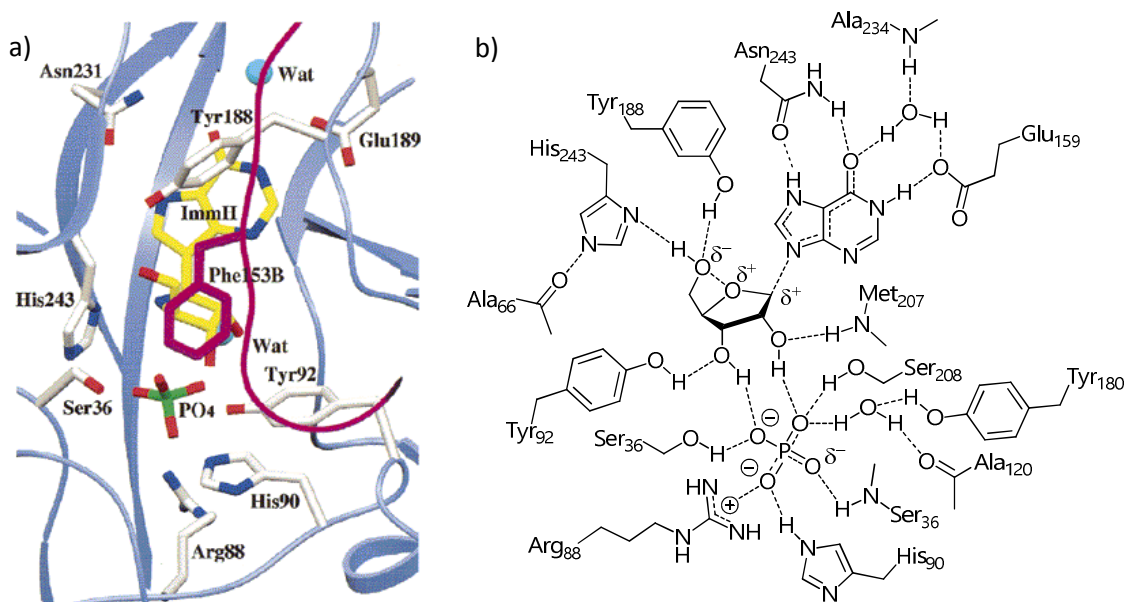


Figure 1.12. *Mt*PNP-Immucillin-H complex: **a)** active site (Phe₁₅₃ from an adjacent subunit is highlighted in violet) (Reprinted from *Biochemistry* **2001**, **40**, 8204-8215. Copyright 2001 American Chemical Society)^{74a}; **b)** interactions of inosine with the active site residues of *Mt*PNP in the TS.

Phe₂₀₀ in *Hs*PNP is replaced by a Tyr₁₈₈ residue, whose phenolic ring, perpendicular to the nucleobase plane, forms a 2.8 Å hydrogen bond with OH^{5'} in nucleoside substrates and other equivalent moieties of analogues (iminoribitol, 2'-deoxyguanosine and inhibitors such as Immucillin-H and DADMe-Immucillin-H (see **1.4.4**)^{54, 76, 77}). As the single binding element not retained in *Mt*PNP, Tyr₁₈₈ may play the role of a discriminating anchor for modified ligands, potentially triggering stronger contacts with the bacterial target. Such a hydrogen bond is clearly prevented in mammalian PNPs by the presence of hydrophobic Phe₂₀₀.^{13a}

Another interesting alteration defined by molecular dynamics (MD) is the role of Phe₁₅₉, which operates as a lid in *Hs*PNP, whereas in *Mt*PNP does not form any π - π contact with the purine ring. This residue appears to intervene in sugar binding instead, lying close to C^{3'} and C^{5'}. Taking into account the diffuse nature of a hydrophobic interaction, this variation is likely less reliable for further inhibitors.⁴⁰

The dissimilar role of some amino acids in PNPs with comparable structures and sequences allows structure-based drug design strategies, as confirmed by the case of the human and bovine PNPs. Although their sequences are 87% superimposable, including all catalytic residues, various inhibitors exhibit different specificity toward them.⁷⁵

1.4.4. Analogues of ground and transition states as inhibitors of PNPs

Inhibitors of trimeric PNPs, with K_i ranging from mM to pM, have been studied and synthesized in the last decades and may be divided into two major categories:

- analogues of the ground state;
- analogues of the transition state, divided into four generations (the first mimicking an early TS and the remaining three a late one, see **1.3.4**).

Nucleosides mimicking the features of the ground state in PNP substrates (**Figure 1.12**) are usually either moderately weak or good inhibitors (IC_{50} in the mM-nM range) and display modifications on the nucleobase, by large 9-deazotation and substitution on C^8 with a limited range of simple groups, as well as on the ribose moiety.⁷⁶ To improve their potency by additional interactions with the polar residues located in the orthophosphate sub-pocket, the β -sugar group can be linked to a phosphate/phosphonate group triggering a double competition against both co-substrates. This choice can be made also in acyclic derivatives.

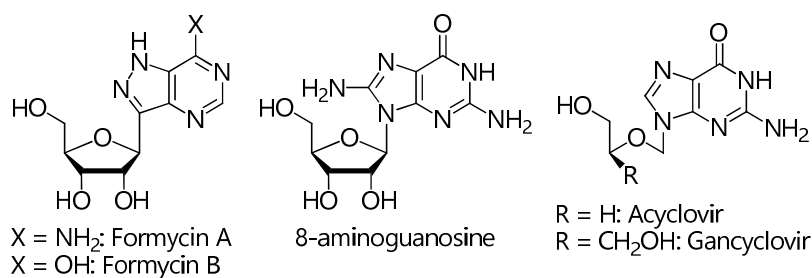


Figure 1.12. Examples of ground state analogues of trimeric PNPs

As outlined above, the three main groups of ground state analogs are 9-deaza-, 8-substituted- and acyclonucleoside analogs. The first class shows a $C^{1'}$ - C^9 bond resistant to phosphorolysis and includes true inhibitors, contrary to molecules as 8-amino and 8-hydroxy derivatives. The latter could be rather defined as slow-reacting substrates. Concerning open-structures, the Acyclovir series plays a major role.

A pivotal innovation in the context of PNP-selective inhibitors has been introduced since the middle 2000s.⁷⁷ Potent inhibitors (K_i in the pM range) mimicking the TS have been proposed, all fulfilling the following requirements:

- a ribocation mimic in an appropriate geometry to allow the formation of an ion pair with the phosphate ion;
- a 6-oxo-9-deazapurine base with elevated pK_a , able to interact with the residues that stabilize the leaving group;
- two or three hydroxyl moieties to reproduce the network of hydrogen bonds with either ribose or 2'-deoxyribose.

Owing to the scarce difference between ground and transition state in terms of the phosphate ion, its mimics are generally not studied. The described strategy has led to potent analogs classified in four generations, the first similar to an early TS and the remaining ones to a late one (**Figure 1.13**). Bovine, malarial, human and tubercular PNPs are successfully affected by them.^{54, 75a}

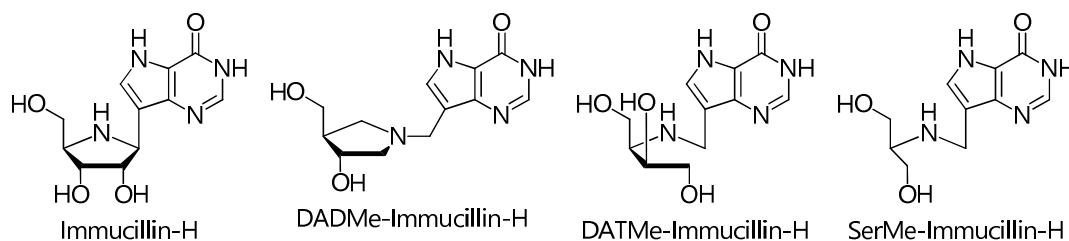


Figure 1.13. Examples of transition state analogues of trimeric PNPs

Immucillin-H ($K_i = 58$ pM) is the lead of the first generation family, containing an iminoribitol portion protonated in the active site to reproduce the oxocarbenium ion. The second generation of TS mimics is associated with DADMe-Immucillin-H ($K_i = 9$ pM), which contains a methylene spacer unifying 9-

deazahypoxanthine and a chiral dihydroxypyrrolidine. By virtue of the CH₂ bridge, the distance between the two portions is similar to that of the leaving nucleobase in a late TS (3.0 Å). The oxonium ion can be replicated once again by protonation of the tertiary nitrogen atom. The two remaining series contain open-chain aminoalcohols and may be rationalized as acyclic Immucillin-H-like compounds, whose simplified structures have been developed in order to reduce the complexity and length of synthetic preparation, as well as to enhance their flexibility. Both DATMe-Immucillin-H (K_i = 9 pM) and SerMe-Immucillin-H (K_i = 5 pM) are among the strongest inhibitors known for PNPs. The main difference between them is the higher stereochemical simplification of the fourth generation, caused by an achiral serinol moiety.

Noticeably, a number of second generation TS mimics have shown activity against not only the human enzyme, but also other ones, such as *Mt*PNP.⁷³

1.4.5. Conformation of 8-substituted purine ribonucleosides

The glycosidic bond in nucleosides is a free rotor which can allow the molecule to adopt different conformations in solution. The torsion angle χ has been chosen as the variable to describe the relative position of the nucleobase with respect to the sugar ring, and in purine nucleosides is defined as the dihedral angle associated to the O^{4'}-C^{1'}-N⁹-C⁴ segment, while it is measured around O^{4'}-C^{1'}-N¹-C² in pyrimidine species (**Figure 1.14**).⁷⁸

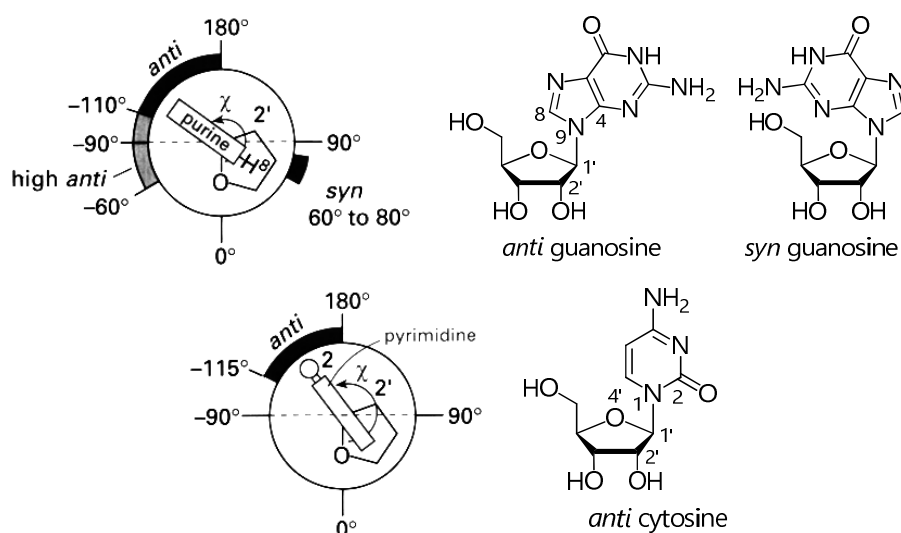


Figure 1.14. Conformations accessible to purine and pyrimidine ribonucleosides by rotation around the glycosidic bond (Adapted from *Nucleic acids in chemistry and biology*, Oxford University Press 1996)⁷⁸

The extreme *syn* (60 to 80°) and *anti* (-110 to -180°) conformations are available for all purine nucleosides in dynamic equilibria, with an additional *high anti* area (-60 to -110°) for molecules with serious steric impediments. Apart from specific cases, pyrimidine nucleosides can exist only as *anti* conformers (-115 to -180°).

However, not all χ values are accessible to every nucleoside, strongly depending on either the sugar or nucleobase substitution. Concerning natural purine nucleosides, most of them notoriously prefer the *anti* conformation both in solution and in crystals. On the other hand, a number of properly functionalized ones are known to exist either as *syn* conformers or as a *syn-anti* equilibrium mixture, whose composition is determined by the nature of substituents.⁷⁹

Substitution at position 8 is a key requirement to obtain the *syn* conformation, and by far the most effective factor eclipsing the base over the sugar ring is the necessity to keep the 8-moiety as far as possible

from steric hindrance and electronic repulsions. As proof of its relevance in terms of biologically active analogues (*e.g.* nucleotides and oligonucleotides, both cyclic and linear⁸⁰), this phenomenon has been extensively studied over the last decades.⁸¹ Some authors have also suggested a possible hydrogen bond between N³ and OH^{5'}, capable of modifying the electronic properties of the aromatic nitrogens. Therefore, the *syn* conformation energy can be lowered, making it accessible even at room temperature. On the other hand, the increase in size of the 8-substituent leads to an enhancement of steric hindrance and, consequently, to a reduction in stability of the *anti* conformer.⁸²

Specific elements in ¹H and ¹³C NMR have been studied to assess the conformation of 8-substituted nucleosides around the glycosidic bond.

In proton spectra, H^{2'} undergoes a distinctive downfield shift up to 0.5 ppm. The corresponding unsubstituted nucleoside must always be taken into account as reference. A possible explanation speculates the existence of a current deshielding effect generated on position 2' by N³, whose lone pair is located closer to the sugar pucker in the *syn* conformation.⁸³

Besides, the use of ¹³C-NMR appears to be more reliable, since carbon shifts span across a larger range and $\Delta\delta$ is easily measurable. Reporting several δ values of 8-substituted adenosines, guanosines and inosines, Uesugi noticed that the effect of the *syn* conformation on ¹³C signals is opposite with respect to ¹H, leading to an upfield shift (1-4 ppm) and, therefore, a shorter distance between C^{2'} and C^{3'}. This phenomenon seems dependent only on the conformational *anti-syn* shift, regardless of the 8-substituent.⁸⁴

In 1987, on the basis of $\Delta\delta$ trends and high-field ¹³C-NMR data, Nair and Young proposed a practical method to argue the conformation of 8-substituted purine ribonucleosides with no need for reference compounds. For candidates with free hydroxyls, the *syn* conformation shows $\Delta\delta_{C^{2'}-C^{3'}} < 0.5$ ppm, whilst in the opposite case of the *anti* structure $\Delta\delta_{C^{2'}-C^{3'}} > 2.8$ ppm (absolute values must be considered). A $\Delta\delta$ ranging in between indicates a dynamic *syn-anti* equilibrium shifted toward either left or right according to the distance from the two extremes.⁸⁵

By using this rule, 8-bromo-, 8-methoxy- and 8-*p*-chlorophenylthioadenosine, 8-bromoguanosine and 8-bromo- and 8-dimethylaminoguanosine have been confirmed as predominant *syn* conformers. 8-Amino and 8-methylaminoguanosine exist in a flexible *syn-anti* mixture. Spectra were recorded in D₂O and DMSO-*d*₆.^{85, 86}

1.5. Immobilized Enzyme Reactors (IMERs)

1.5.1. Immobilized Enzyme Reactors (IMERs)

The very first step in developing a biocatalytic process is to investigate the substrate specificity of any involved enzyme. For instance, in the case of NPs such an evaluation is typically carried out by submitting nucleoside libraries to phosphorolysis and measuring conversion, which can be indicative of the enzymatic ability to catalyze the reverse reaction.

In order to speed up the enzymatic screening of libraries, miniaturized analytical tools are at the center of research interest. In the last decades, the higher availability of bioactive supports obtained by enzyme immobilization has sustained a great expansion in the bioanalysis field.⁸⁷

Enzymes can be immobilized on a suitable chromatographic support to form Immobilized Enzyme Reactors (IMERs), in which the biocatalyzed reaction occurs upon substrates injection during their elution (Figure 1.16).⁸⁸

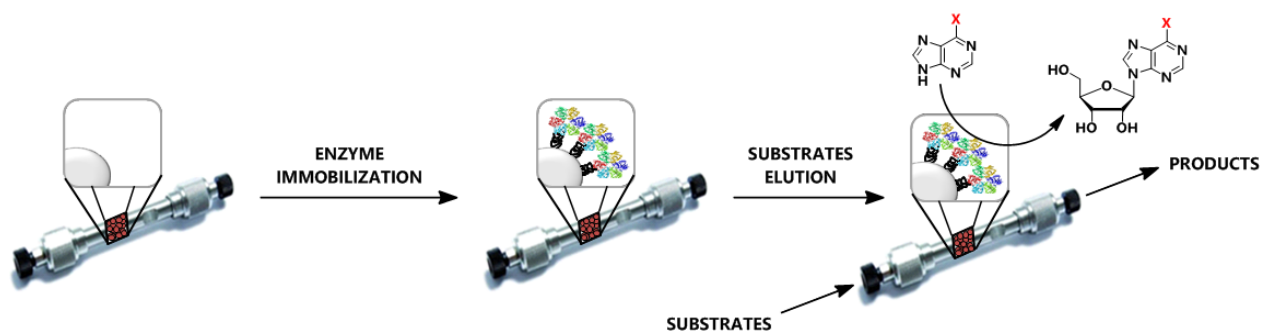


Figure 1.16. Example of the preparation and use of an IMER for the chemoenzymatic synthesis of modified nucleosides

Various benefits can be granted by these devices:

- immobilized enzymes are more stable than their soluble counterparts;
- enzymatic structure and activity are generally conserved, if the binding chemistry and physico-chemical properties of the stationary phase are neutral toward them;
- reusability is assured, allowing simple elution and easy recovery of the enzyme;
- experimental data are more reproducible;
- analysis time and costs can be greatly reduced due to automatization, allowing the sequential screening of extended libraries in a short time;
- miniaturization into columns and capillaries requires very low sample amount in analytical assays (often only a few μL).

The insertion of such tools into systems with an autosampler and an on-line integrated apparatus for reaction monitoring and purification may result in the set-up of bioreactors capable of carry out screening and synthesis (**Figure 1.17**).

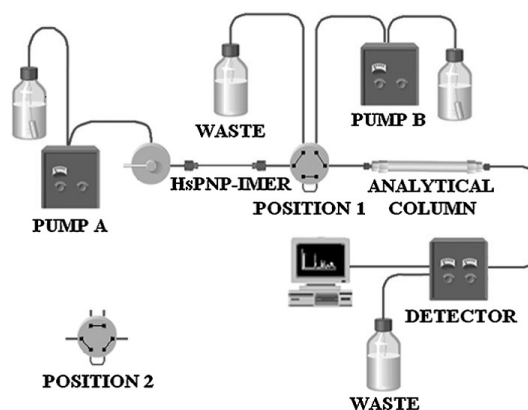


Figure 1.17. Schematic representation of an IMER-based apparatus for screening

From the preparative viewpoint, an ideal arrangement for IMERs is their incorporation in tools for continuous flow synthesis as an alternative to batch reactions. The overall equipment is typically composed by a pump with solvents tanks to generate the flow and transfer reagents from their reservoir to a proper mixing system, the reactor (also broadened to coils, chips and vessels if necessary), a monitoring analytical unit and a vessel to collect products. An upgraded equipped system also presents multiple reactors, recycling coils, supported scavengers to eliminate waste and quench promoters, as well as initiators and a back-pressure regulator to avoid overheating and irregular flows.

Flow equipments like the one reported in **Figure 1.17** allow the following key advantages:

- automation simplifies the precise control of reaction parameters, such as flow rate of reagents and hence their relative ratio, mixing and reaction rate;
- reproducibility, safety and reaction time can be optimized;
- operations concerning sample handling and purification are greatly reduced;
- the minimal scale leads to an improved heat-mass transfer;
- balance issues can be secured due to the regular amount of reagents flowing in the system in each time unit, even at high scale;
- it becomes much simpler to scale up a reaction from mg to g scale with no need to repeat the operation on the whole equipment, since the reaction flow through the IMER is constant and the same effect can result from increased processing times (and therefore volumes).

While flow methods have been developed to aid in synthetic and medicinal chemistry as an alternative to batch processing, on the contrary the use of flow bioprocesses is still in its infancy.⁸⁹ Anyway, the coupling of benefits from biocatalysis and continuous flow synthesis is likely to allow this new technology to grow rapidly, as demonstrated by novel IMER-based applications.⁹⁰

An early significant example of IMERs, reported in 1999 by Sotolongo *et al.*, was based on a horse liver alcohol dehydrogenase (HLADH) non-covalently bonded to an immobilized artificial membrane (IAM)-based HPLC support.⁹¹ In 2012, de Moraes *et al.* described the testing of potential HsPNP ligands through a HsPNP-based IMER obtained by immobilizing the enzyme in a fused silica Open Tubular Capillary (OTC) and using DI4G, a fourth generation Immucillin-like derivative, as reference compound.^{87e}

1.5.2. Enzyme immobilization

Since the second half of the 20TH century, countless efforts have been oriented at developing strategies for enzyme immobilization, which can be carried out either by linking them to solid supports (or carriers) or by entrapping them in a proper matrix. Less explored strategies involve the support-free cross-linking of two or more catalysts with each other.⁹² As of the first category, covalent or noncovalent bonds may be selected, depending on protein, reaction conditions or specific necessities.

The choice of a suitable carrier is pivotal since it impacts on the microenvironment conditions for the desired transformation. Dimension of particles, pores and channels, hydro- or lipophilicity, mechanical and physical resistance against stresses, surface-to-volume ratio, lack of reactivity as substrate of the enzyme, accessibility, inertness toward microbic attack and ease of derivatization are relevant factors. An ideal carrier should obviously display all these properties in the best combination at a reasonable cost.⁹³

Covalent immobilization is the paramount choice in the case of pharmaceutical and food industry applications, as it minimizes product contamination by enzyme leaching.

Depending on the properties of the carrier and of the protein, immobilization can be performed either directly or upon functionalization of the matrix with an activating agent (**Figure 1.18a**). The latter can be a bi-functional reagent such as a dialdehyde (*e.g.* glutaraldehyde), which also acts as spacer to keep the enzyme far from the carrier surface. Such a strategy reduces steric hindrance effects around the enzyme, thereby favouring the catalysis.⁹⁴

Lysines are the most generally useful residues for covalent immobilization of enzymes. In this case the pH of the reacting solution must be controlled, as imines/iminium ions are key intermediates in the binding process. Furthermore, the nucleophilicity of NH₂ groups on the protein changes according to their different pK_a (approximately 9 and 10.5 for the α and γ positions, respectively). This indirect selection can result in the generation of either one covalent bond or a multipoint attachment on the support, increasing the catalyst stability in the latter case.⁹⁵

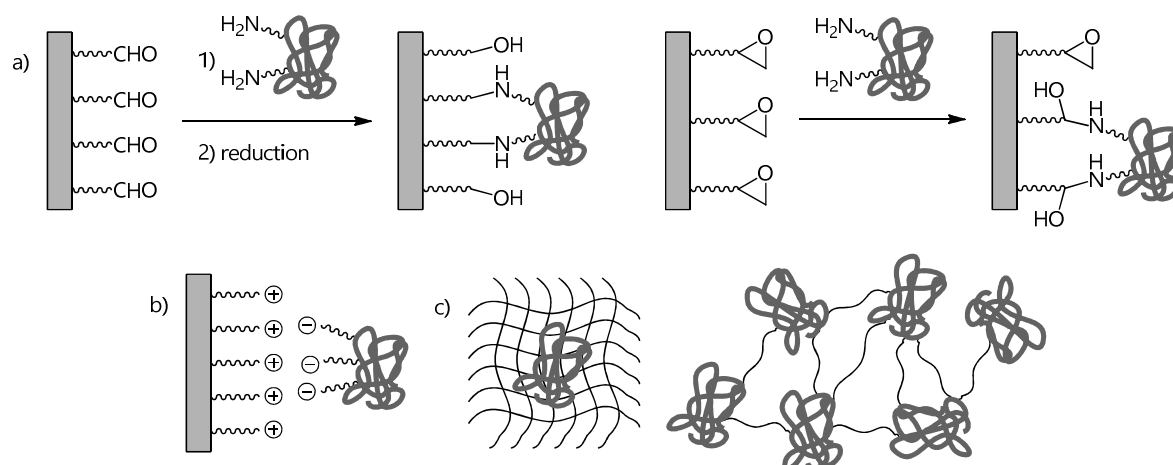


Figure 1.18. Examples of enzyme immobilization: **a)** covalent immobilization; **b)** adsorption by ionic interactions; **c)** entrapment and cross-linking.

Many other carriers functionalized with a variety of electrophiles (*e.g.* epoxides) are currently accessible at reasonable costs. The best combination of enzyme, support and possible linker(s) has to be determined in a “tailor-made” fashion for each protein.

Milder adsorption techniques may also be used, relying on nonspecific interactions based on physical or ionic binding. The first case includes hydrogen bonds (*e.g.* with cellulose), Van der Waals contacts or hydrophobic ones (*i.e.* on acrylamide or carbon surfaces), whereas the other set includes ion pairs (*e.g.* in ion exchange resins) (**Figure 1.18b**).⁹⁶

The need for stronger non-covalent interactions has led to the design of entrapments, in which the catalyst is incorporated in a polymeric network directly produced in the enzyme solution (**Figure 1.18c**). Neither organic polymers (gelatin, alginate, polyacrylamide, ...) nor silica sol-gels, hollow fibers and microcapsules can avoid catalyst detachment, making it necessary to proceed with additional cross-linking using multifunctional assistants (dextran sulfate, polyethylamine, ...).⁹⁷

To date, only a few examples of NPs immobilization on solid supports have been reported for analytical and synthetic purposes. For instance, IMERs containing the PNP from *Schistosoma mansoni*⁹⁸ and the human one^{87e} were exploited for inhibitors screening.

Concerning nucleoside synthesis, some NPs have been immobilized on Sepabeads® coated with polyethylenediamine/imine or on aldehyde-activated agarose (*e.g.* glyoxylagarose). Cross-linking with aldehyde dextran was required in the first case to strengthen the non-covalent interactions between the enzyme and the cationic support. The high activity and stability of the immobilized biocatalysts allowed to synthesize 2'-deoxyguanosine in 92% yield (with a UP and a PNP from *B. subtilis* under strong temperature and pH conditions)⁹⁹, Floxuridine in 62% and 74-76% conversion (with a TP from *E. coli* and a PyNP from *B. subtilis*, respectively)^{95b, 100}, Vidarabine and Didanosine in 74 and 44% conversion respectively (with a UP from either *C. perfringens* or *Streptococcus pyogenes* coupled with a PNP from either *A. hydrophila* or *Citrobacter koseri*)¹⁰¹ and Vidarabine in 53% yield and high purity (98.7%) (with a UP from *C. perfringens* and a PNP from *A. hydrophila*)^{10c}.

A PyNP from *Thermus thermophilus* and a PNP from *Geobacillus thermoglucosidasius* were recently immobilized on epoxide beads to catalyze the bienzymatic trasglycosylation of 2'-substituted ribo- and arabino-like uracils with 2,6-disubstituted purines to the corresponding nucleosides, which are important intermediates in the synthesis of biologically active products. By virtue of the thermostability of both enzymes, the preparation of 6-chloro-2-fluoropurine-9-riboside was run under high substrate concentrations at 60°C and successfully scaled up to multimilligram scale (60% yield).⁶⁰

1.6. Background studies on the purine nucleoside phosphorylase from *Aeromonas hydrophila* (AhPNP)

1.6.1. Characterization and synthetic applications of AhPNP

As already explained, in 2012 a purine nucleoside phosphorylase from *Aeromonas hydrophila* (AhPNP) was over-expressed in *E. coli* and purified by Ubiali, Speranza and co-workers (see 1.3.6).^{63b}

The enzyme was characterized by studying the phosphorolysis of the six natural purine ribo- and 2'-deoxyribonucleosides, which were easily processed with a strong preference for 2'-deoxyinosine (Table 1.3).

Substrate	Specific activity (IU·mg ⁻¹) ^{a)}
Inosine	75
2'-Deoxyinosine	137
Guanosine ^{b)}	26
2'-Deoxyguanosine ^{b)}	28
Adenosine	35
2'-Deoxyadenosine	28

^{a)} IU = $\mu\text{mol}\cdot\text{min}^{-1}$

^{b)} [substrate] = 1 mM

Experimental conditions: 50 mM K₂HPO₄ buffer (pH 7.5), RT, volume = 10 mL, [substrate] = 5 mM

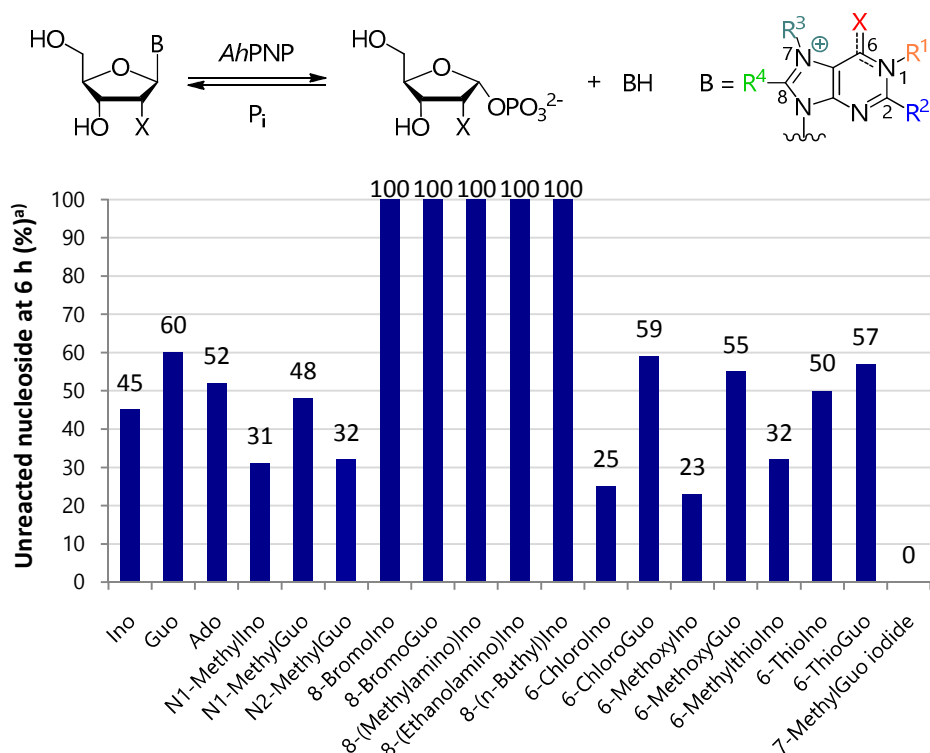
Table 1.3. Activity of AhPNP toward six natural purine ribonucleosides

AhPNP was found to be quite stable, retaining 100% initial activity after a 24 h incubation in 50 mM K₂HPO₄ buffer containing 20% glycerol (v/v) at pH 7.5.

The substrate specificity of AhPNP was further investigated by submitting a series of 1-, 2-, 6-, 7- and 8-substituted purine ribonucleosides to the phosphorolysis reaction (Figure 1.19).

From the inspection of experimental data, some consideration on the substrate specificity of AhPNP can be drawn:

- all 1-, 2-, 6- and 7-substituted nucleosides were recognized by the enzyme. Of course, the phosphorolysis extent depended on the position and nature of the substitution, with the best results for *N*¹-methylinosine, *N*²-methylguanosine, 6-chloroinosine, 6-methoxyinosine and 6-methylthioinosine (30-50% unreacted nucleoside);
- 7-methylguanosine iodide was the only analogue showing a complete phosphorolysis to 7-methylguanine and α -D-ribose-1-phosphate;
- concerning 6-substituted analogues, conversions were in the range 23-59%, pointing out the broad substrate specificity of AhPNP;
- by contrast, 8-substituted ribonucleosides were not tolerated by AhPNP. This lack of recognition may be related to their preferred *syn* conformation in aqueous solution, which should be adopted if the 8-group is bulky enough to generate steric constraints (see 1.4.5).^{81,82} The forced conformational change from *anti* to *syn* may generate a structure incompatible with the active site of AhPNP.



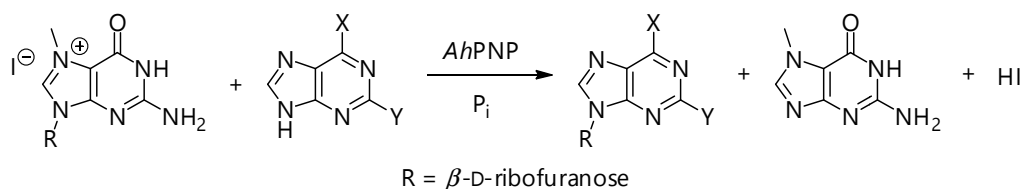
^{a)} Estimated by HPLC

Experimental conditions: 50 mM K_2HPO_4 buffer (pH 7.5) with 20% (v/v) glycerol, RT, volume = 20 mL, [substrate] = 5 mM (Ino = inosine, Guo = guanosine, Ado = adenosine)

Figure 1.19. Unreacted nucleoside at 6 h in the AhPNP-catalyzed phosphorolysis of 1-, 2-, 6-, 7- and 8-substituted purine ribonucleosides

In order to explore the synthetic potential of AhPNP, a few “one-pot, one-enzyme” transglycosylations were carried out. Four 6-substituted purines were used as sugar *acceptors*, whereas 7-methylguanosine iodide was chosen as D-ribose *donor* for several reasons (**Table 1.4**). First of all, its phosphorolysis catalyzed by AhPNP is rapid, complete and irreversible under the selected conditions. Secondly, its conjugated nucleobase is scarcely soluble in aqueous solvents, so it can precipitate thus shifting the equilibrium to product formation. In addition, it is neither a substrate nor an inhibitor of AhPNP. 7-methylguanosine iodide can be synthesized very easily by direct methylation of guanosine in high yield and purity.

On semi-preparative scale, three 6-substituted purine ribonucleosides were prepared and isolated in very high yield (71-93%) and purity.



X	Y	Donor/acceptor ratio	Isolated yield (%)
NH ₂	Cl	3:1	93
H	OCH ₃	4:1	71
NH ₂	SCH ₃	4:1	93
H	CH ₃	4:1	not isolated ^{a)}

^{a)} Synthesized on analytical scale

Experimental conditions: 50 mM K₂HPO₄ buffer (pH 7.5), RT, volume = 20 mL

Table 1.4. Synthesis of 6-substituted ribonucleosides *via* AhPNP-catalyzed transglycosylation

1.6.2. AhPNP as an on-line Immobilized Enzyme Reactor (AhPNP-IMER)

The broad substrate specificity shown by AhPNP toward purine- and sugar-modified nucleosides pushed forward the development of an Immobilized Enzyme Reactor (IMER) based on this enzyme for a rapid and robust screening of modified nucleosides, thus exploring its use in the synthesis of nucleoside analogues by transglycosylation. The resulting AhPNP-IMER was able to assess the same activity ranking order as determined with the soluble enzyme, thus validating the biochromatographic system for a routine use as reported by Speranza, Ubiali and co-workers in 2013.¹⁰²

Specifically, AhPNP was covalently immobilized on the inner surface of a fused silica Open Tubular Capillary (OTC) by following a previously reported protocol used to assay the inhibitory activity of new compounds against HsPNP^{87e} and the one from *Schistosoma mansoni* (SmPNP).⁹⁸

The AhPNP-IMER was introduced into a bi-dimensional column-switching apparatus and connected to an analytical HPLC system by a six-port switching valve (**Figure 1.20**).

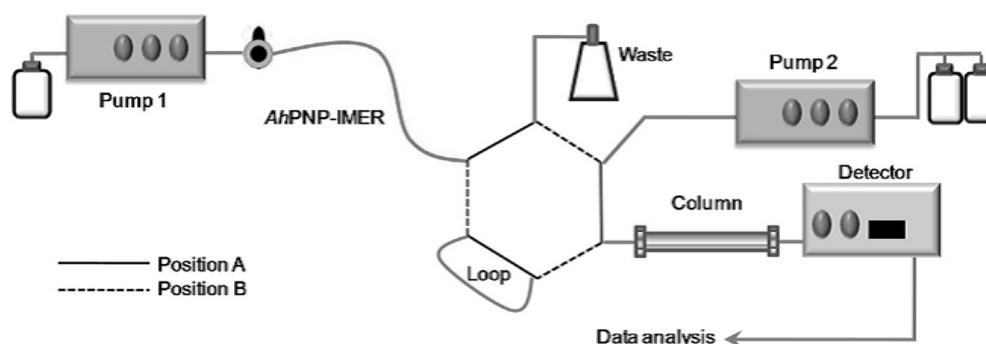


Figure 1.20. Sketch of the AhPNP-IMER connected to the analytical HPLC (Reprinted with permission from *J. Chromatogr. B* **2014**, *968*, 79-86)¹⁰²

The sample was loaded with the valve in position A, directly connected with pump 1 to deliver the eluent in the IMER capillary, where the reaction occurred. The valve was then switched to position B and, as a result, analytes (products and unreacted reagents) were loaded directly in a 20 μ L loop on the head of the analytical HPLC column for subsequent separation, identification and quantification as the original position A was selected again. An example of the resulting chromatogram is presented in **Figure 1.21**.

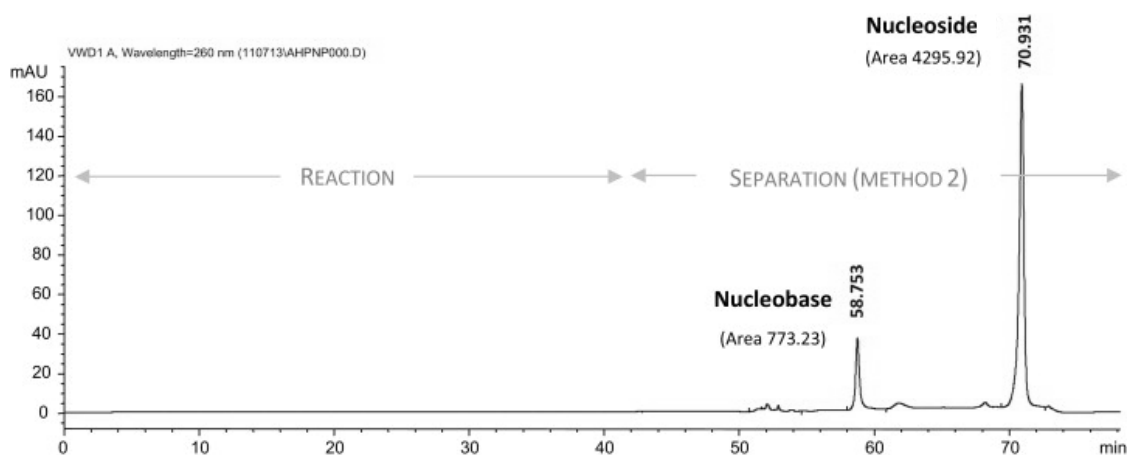


Figure 1.21. Chromatogram obtained from the *AhpNP*-IMER apparatus (Reprinted with permission from *J. Chromatogr. B* **2014**, *968*, 79-86)¹⁰²

The immobilization process was reproducible, as resulted from the comparison of two bioreactors prepared by using ~ 200-300 μg of protein that afforded a yield of 7% and 10% for *AhpNP*-IMER I and *AhpNP*-IMER II, respectively. Kinetic parameters (K_M and V_{max}) were also determined (**Table 1.5**). K_M values were measured by using inosine as substrate of the phosphorolysis reaction.

	Soluble <i>AhpNP</i>	<i>AhpNP</i> -IMER I	<i>AhpNP</i> -IMER II
K_M (μM) ^{a)}	1.8 ± 0.5	10.2 ± 1.4	6.0 ± 2.2
V_{max} ($\mu\text{mol}\cdot\text{min}^{-1}$)	$4.0 \times 10^2 \pm 2.0 \times 10^2$	$9.3 \times 10^{-4} \pm 4.0 \times 10^{-5}$	$1.5 \times 10^{-4} \pm 1.2 \times 10^{-5}$
Enzyme (mg)	0.001	0.030	0.021
Immobilization yield (%)	-	10	7

^{a)} The reaction was stopped after 1'

Table 1.5. Immobilization yields and kinetic parameters of soluble *AhpNP* and *AhpNP*-IMERS

The IMER catalyzed 60 reactions/capillary with no activity loss, thus resulting a reliable tool for repeated screening of nucleoside analogues. Long-term storage was remarkable, with 100% residual activity after 1 month.

A number of natural and modified nucleosides were assayed in phosphorolysis catalyzed by *AhpNP*-IMER (**Figure 1.22**), exploiting the apparatus depicted in **Figure 1.20**. It is worth noting that the *AhpNP*-IMER showed the same activity ranking order as determined with the soluble enzyme, being indeed predictive of the catalytic activity in solution.

N^6 -substituted adenosines (**31-36**) were submitted to phosphorolysis not only to support the IMER validation, but also in order to explore the possibility to prepare them by transglycosylation (according to the substrate specificity of *AhpNP*). Experimental data showed that the IMER was active toward different 6-substituted purine ribonucleosides (**31**, **33** and **34**), with the only exception of **36**, which was not processed neither by the native enzyme, nor by the IMER.

7-Methylguanosine iodide (**65**) deserved a specific comment because of the strikingly different values between the evaluation with the free and the immobilized enzyme. As mentioned before, the phosphorolysis was complete when the reaction was catalyzed by the native catalyst, whereas it did not occur through the IMER. It was hypothesized that the permanent charge of the analyte might generate

repulsive interactions with the positively charged surface of the immobilized PNP, preventing the phosphorolysis from occurring.

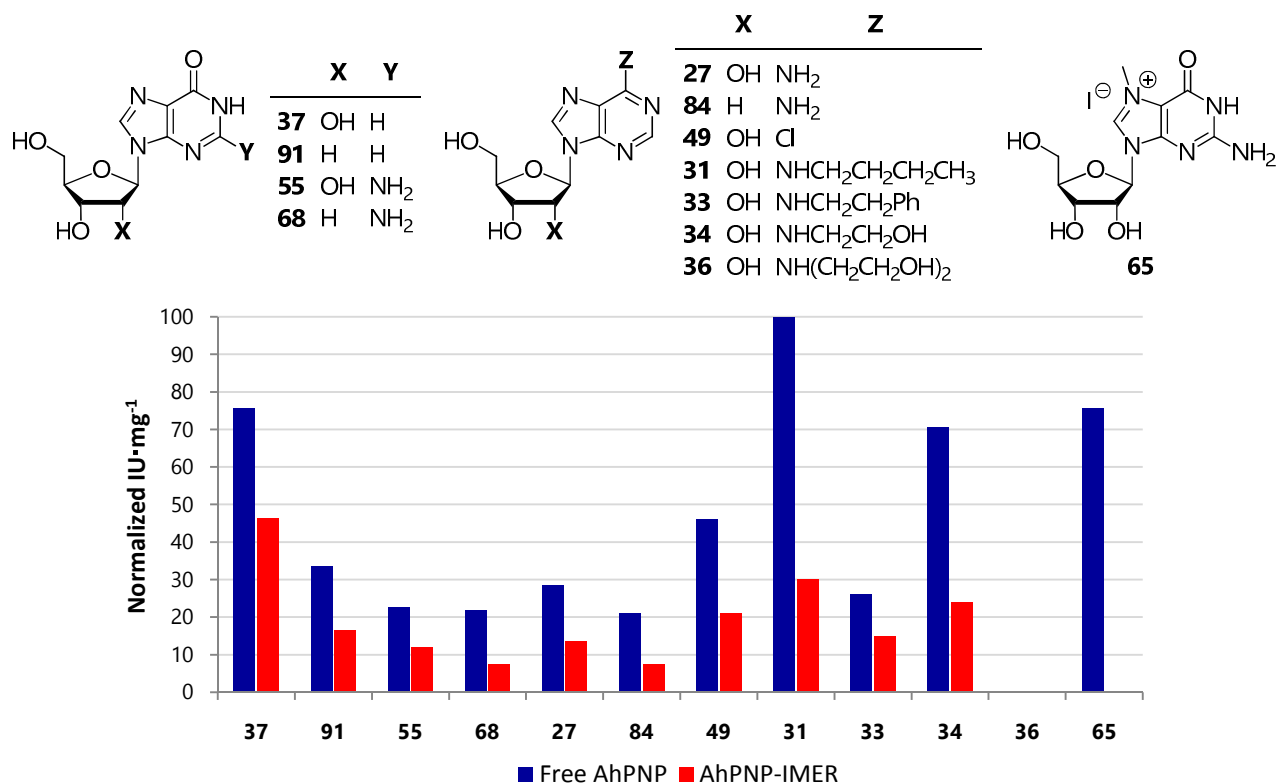


Figure 1.22. Comparison between the activity ranking order of soluble AhPNP and AhPNP-IMER

2 | AIMS

The research work described in this PhD Thesis was developed along three parallel but intertwining lines:

- the exploitation of the purine nucleoside phosphorylase from *Aeromonas hydrophila* (AhPNP) and the uridine phosphorylase from *Clostridium perfringens* (CpUP) as biocatalysts in the chemoenzymatic “one-pot, one-enzyme” or “one-pot, two-enzyme” synthesis of 2- and 6-substituted purine ribo-, 2'-deoxyribo- and arabinonucleosides by “in batch” and “in flow” transglycosylations, starting from a wide array of sugar *donors* and purine *acceptors*, mostly synthesized on purpose;
- the synthesis and screening of the inhibitory activity of some 8-substituted purine ribonucleosides toward the purine nucleoside phosphorylase from *Mycobacterium tuberculosis* (MtPNP) by a medium-throughput LC-ESI-MS/MS assay, also assessing the selectivity of the prepared compounds against the bacterial enzyme with respect to the human one (HsPNP);
- the synthesis of a small library of 8- and N^2 -substituted derivatives of inosinic and guanylic acids on the basis of *in silico* molecular modeling studies and in view of their use as potential ligands of the human GPR17 receptor.

3 | PURINE NUCLEOSIDE PHOSPHORYLASES AS BIOCATALYSTS AND PHARMACOLOGICAL TARGETS

3.1. Chemical synthesis of structurally modified purine nucleobases and nucleosides

3.1.1. Synthesis of 6-substituted purines (2-10, 12-24)

A series of twenty-four 6-substituted purine nucleobases (**1-22**) were used as sugar *acceptors* in transglycosylations catalyzed by the PNP from *Aeromonas hydrophila* (**Figure 3.1**).

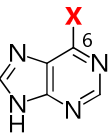
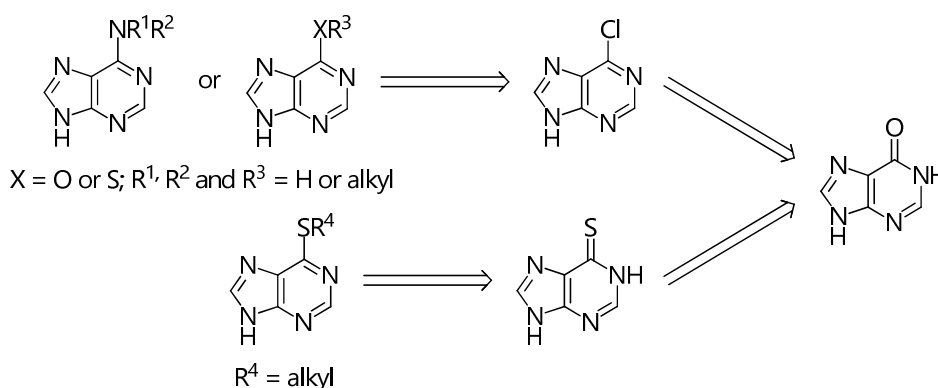
	$X = NR^1R^2$	$X = OR$	$X = SR$
	1 NH ₂	11 OH	17 SH
	2 NHCH ₃	12 OCH ₃	18 SCH ₃
	3 NHCH ₂ CH ₃	13 OCH ₂ CH ₃	19 SCH ₂ CH ₃
	4 NHCH(CH ₃) ₂	14 OCH(CH ₃) ₂	20 SCH(CH ₃) ₂
	5 NHCH ₂ CH ₂ CH ₂ CH ₃	15 OCH ₂ CH ₂ CH ₂ CH ₃	21 SCH ₂ CH ₂ CH ₂ CH ₃
	6 NHCyclohexyl	16 OCH ₂ CH ₂ Ph	22 SCH ₂ CH ₂ Ph
	7 NHCH ₂ CH ₂ Ph		
	8 NHCH ₂ CH ₂ OH	$X = \text{halogen or alkyl}$	
	9 N(CH ₃) ₂	23 Cl	
	10 N(CH ₂ CH ₂ OH) ₂	24 CH ₃	

Figure 3.1. 6-Substituted purines (**1-22**)

Among them, adenine (**1**), hypoxanthine (**11**) and 6-methylpurine (**24**) were purchased from commercial sources. All other substrates were prepared by synthetic procedures either already known in literature or originally developed in the Laboratory of Organic Chemistry (Prof. Giovanna Speranza) at the Department of Chemistry of the University of Milan.

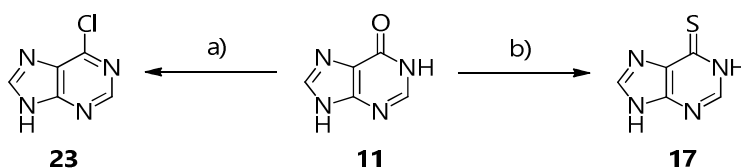
The retrosynthetic strategy is shown in **Scheme 3.1**. 6-Chloro- (**23**) and 6-thiopurine (**17**) were identified as precursors for *N*⁶-monosubstituted and *N*⁶,*N*⁶-disubstituted adenines, 6-alkoxypurines and 6-thiopurines. Both intermediates can be obtained from hypoxanthine (**11**). Alkylamino, alkoxy and alkylthio derivatives were prepared by halogen displacement, while an *S*-alkylation strategy was devised for the remaining substituents.



Scheme 3.1. Retrosynthetic analysis of 6-substituted purines

The main issue of such functionalizations is that the 6-carbonyl group of hypoxanthine (**11**), belonging to an amido moiety, is quite unreactive toward primary or secondary amines, alkoxydes, alkanethiolates and alkyl halides. Therefore, the basic strategy was to convert it into either an effective leaving group or a suitable nucleophile. According to this approach, 6-chloro- (**23**) and 6-thiopurine (**17**) were considered the best choices as intermediates.

A chlorine atom was directly installed on C⁶ of hypoxanthine (**11**) by treatment with POCl₃ in refluxed *N,N*-DMA. Dry reagents and solvents were essential to avoid side reactions and to obtain a clear product. P₂S₅ in refluxed pyridine was exploited to convert the carbonyl group into a thiocarbonyl moiety. Purification of the resulting products proceeded by crystallization from H₂O and EtOH, respectively (**Scheme 3.2**).



Reagents and conditions (yield): a) POCl₃, *N,N*-DMA, reflux (89%); b) P₂S₅, Py, reflux (80%).

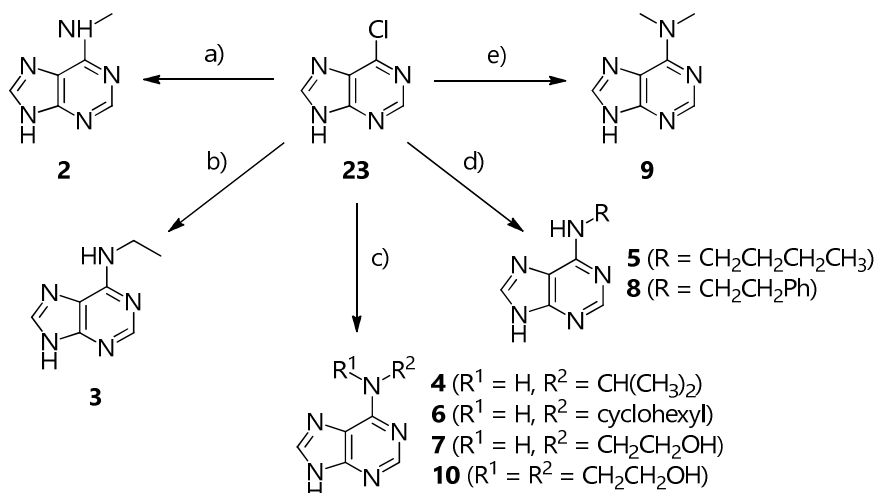
Scheme 3.2. Synthesis of 6-chloro- (**23**) and 6-thiopurine (**17**)

*N*⁶-Substituted (**2-8**) and *N*⁶,*N*⁶-disubstituted (**9** and **10**) adenines were prepared by treatment of **23** with the proper primary or secondary amine or amine solution, choosing an alcohol (EtOH or *n*-BuOH) as solvent under reflux and adding TEA as base, if necessary (**Scheme 3.3**). All products were purified by precipitation, flash column chromatography or semi-preparative HPLC.

The synthesis of aryl ethers by aromatic nucleophilic substitution was performed under reflux to synthesize 6-alkoxy purines **12-16** (**Scheme 3.4**). The necessary sodium alkoxydes were obtained *in situ* by dissolving metallic Na in the corresponding dry alcohols, with dry THF as solvent in the case of **16**, and semi-preparative HPLC was exploited to purify all products in good to high yield, with the only exception of **14**. The lower yield of the latter compound can probably be ascribed to the slow dissolution of Na in the secondary alcohol and to the steric hindrance of the corresponding alkoxyde. Treatment of *i*-PrOH with NaH was therefore selected as an alternative for a faster and more efficient deprotonation, yielding the desired purine in almost quantitative yield.

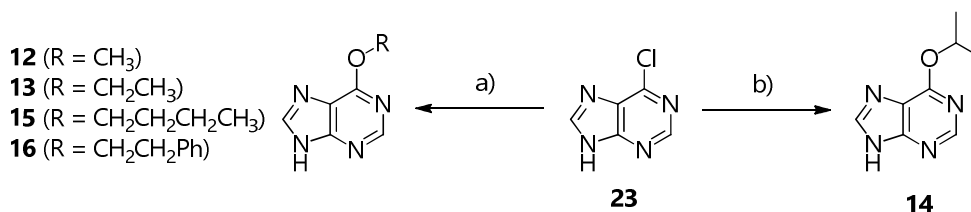
6-Alkylthiopurines (**18-22**) were prepared either by halogen substitution on 6-chloropurine (**23**) with the proper thiol, deprotonated *in situ* by 1 M NaOH as solvent, or by *S*-alkylation of 6-thiopurine (**17**) in the presence of a base (**Scheme 3.5**). In the first case, temperature was always kept 10°C below the boiling point of the thiol in order to prevent its volatilization. In the latter approach, alkyl bromides or iodides were

used. The synthesis of **22** required the use of DMF in place of an aqueous solvent and the substitution of NaOH with K_2CO_3 to achieve better results. Neutralization and precipitation afforded the target products.



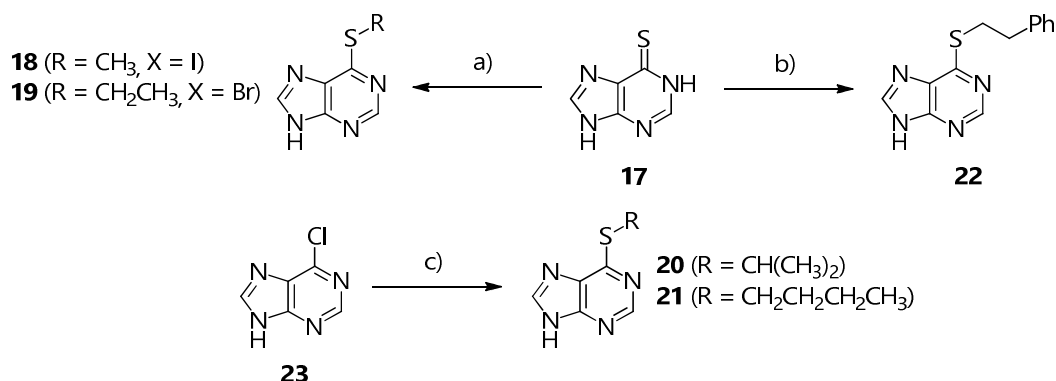
Reagents and conditions (yield): a) 40% aq. CH_3NH_2 , TEA, *n*-BuOH, reflux (64%); b) 70% aq. $CH_3CH_2NH_2$, EtOH, reflux (78%); c) R^1R^2NH , TEA (for **4** and **10**), EtOH, reflux (62-86%); d) RNH_2 , EtOH, reflux (80-88%); e) 2.0 M $(CH_3)_2NH$ in THF, EtOH, reflux (40%).

Scheme 3.3. Synthesis of N^6 -substituted and N^6,N^6 -disubstituted adenines (**2-10**)



Reagents and conditions (yield): a) Na, ROH, THF (for **16**), reflux (50-84%); b) Na, *i*-PrOH, reflux (16%) or NaH, *i*-PrOH, reflux (97%).

Scheme 3.4. Synthesis of 6-alkoxy-purines (**12-16**)

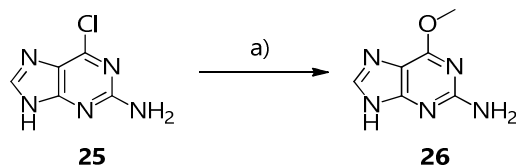


Reagents and conditions (yield): a) RX , 1 M NaOH (59%-73%); b) $PhCH_2CH_2Br$, 1 M NaOH (12%) or $PhCH_2CH_2I$, K_2CO_3 , DMF (66%); c) RSH , 1 M NaOH, $10^\circ C$ below RSH b.p. (50-85%).

Scheme 3.5. Synthesis of 6-alkylthiopurines (**18-22**)

3.1.2. Synthesis of 2-amino-6-methoxypurine (26)

The same protocol used for most 6-alkoxypurines was repeated to convert commercial 2-amino-6-chloropurine (**25**) into 2-amino-6-methoxypurine (**26**) in NaOMe/MeOH under reflux (**Scheme 3.6**).



Reagents and conditions (yield): a) Na, MeOH, reflux (70-94%).

Scheme 3.6. Synthesis of 2-amino-6-methoxyguanine (**26**)

3.1.3. Synthesis of 6-substituted inosines (28-36, 38-48)

In order to proceed with the HPLC analysis of transglycosylation mixtures, the ribonucleoside counterparts of 6-substituted purine *acceptors* (**27-50**) were required as reference compounds (**Figure 3.2**).

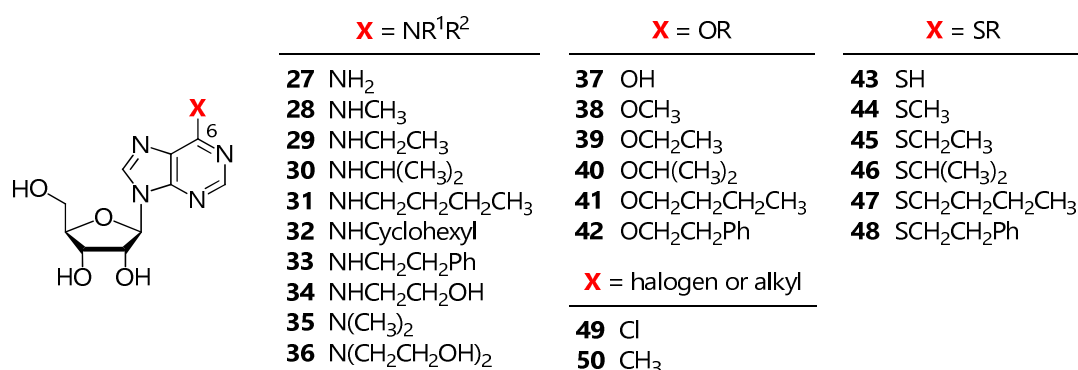
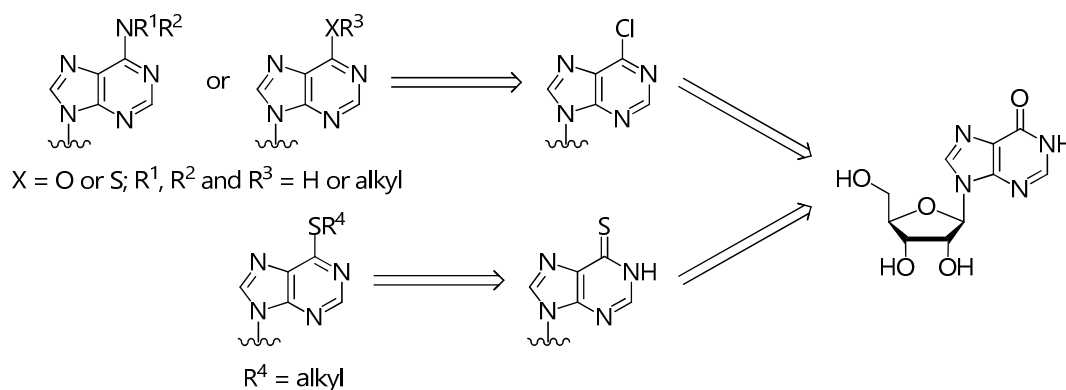


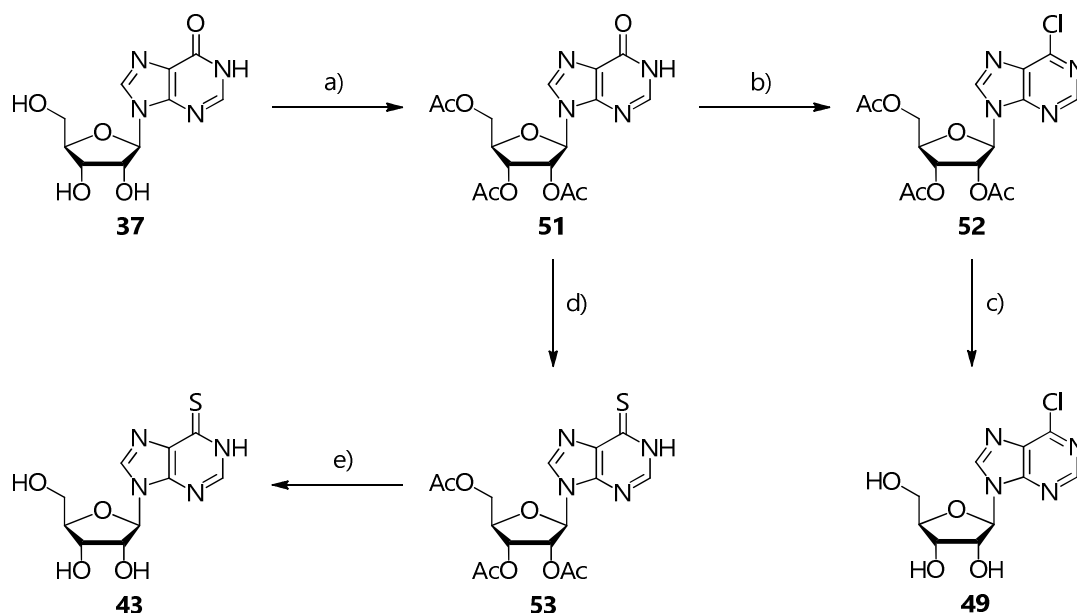
Figure 3.2. 6-substituted inosines (**27-50**)

Only adenosine (**27**), inosine (**37**) and 6-methylthioinosine (**44**) were purchased from commercial sources. The synthesis of the remaining nucleosides was carried out by following a strategy similar to that adopted with the nucleobases (**Scheme 3.7**), starting from the activation of position 6 by either halogenation or thienation. Owing to the very low nucleophilicity of the amino group in adenosine, N^6 -substituted and N^6,N^6 -disubstituted derivatives had to be synthesized starting from 6-chloropurine riboside (**49**) by substitution with the suitable primary or secondary amine. The same strategy was followed to obtain 6-alkoxyinosines and three 6-alkylthio derivatives (**45-47**), whereas *S*-alkylation was repeated for the remaining thionucleosides.



Scheme 3.7. Retrosynthetic analysis of 6-substituted purine ribonucleosides

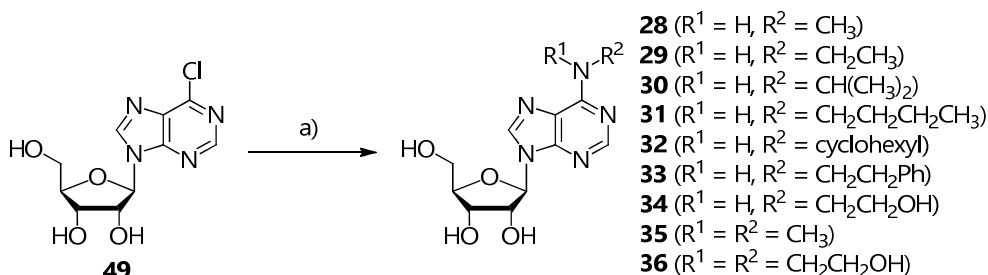
Inosine (**37**) was chosen as starting material in all cases (**Scheme 3.8**). Since both chlorination and introduction of a thiocarbonyl group at position 6 may lead to unwanted side reactions of the hydroxyl moieties, the sugar portion was protected by acetylation with Ac₂O, TEA and a catalytic amount of DMAP (7 mol %) in CH₃CN at room temperature. Chlorination of **51** was performed with SOCl₂ in a refluxed CH₂Cl₂/DMF mixture, whereas thienation was carried out with Lawesson's reagent (2,4-bis-(4-methoxyphenyl)-1,3-dithia-2,4-diphosphetane-2,4-disulfide) in refluxed pyridine (see **6.1.1**).¹⁵² Attempts with POCl₃ in the presence of TEA and *N,N*-DMA or PPh₃/CCl₄ (Appel's protocol)¹⁰³ and with P₂S₅ gave worse results, because of overphosphorylated by-products formation and poor substrate conversion, respectively. Either aminolysis with NH₄OH or alcoholysis with NaOMe on intermediates **52** and **53** allowed the removal of the protecting acetyl moieties, the latter treatment in poorer yield and purity. **49** and **43** were purified by flash column chromatography and recrystallization, respectively.



Reagents and conditions (yield): a) Ac₂O, TEA, 7 mol % DMAP, CH₃CN (95%); b) SOCl₂, CH₂Cl₂/DMF, reflux (98%); c) 33% aq. NH₄OH, MeOH (69%); d) Lawesson's reagent, Py, reflux (77%); e) NaOMe, MeOH (58%) or 28% aq. NH₄OH, MeOH (74%).

Scheme 3.8. Synthesis of 6-chloro- (**49**) and 6-thioinosine (**43**)

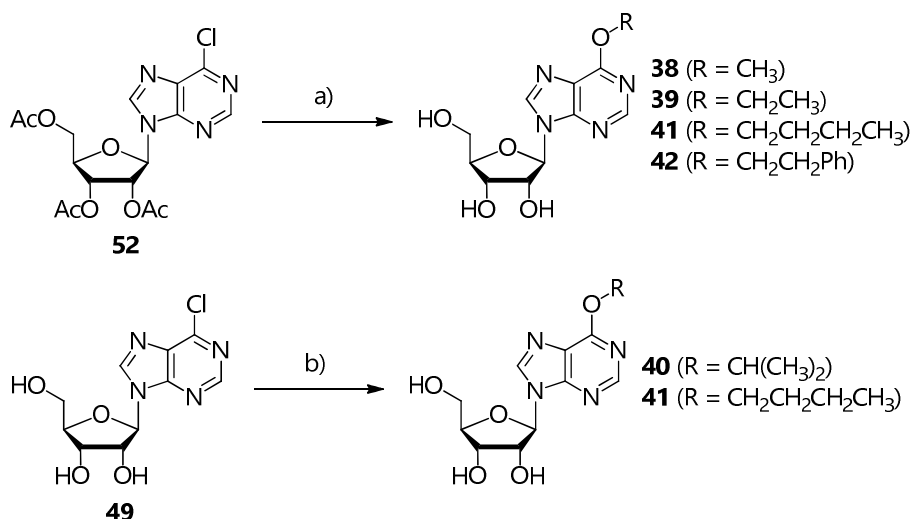
Primary or secondary amines and TEA in refluxed EtOH were used to obtain all N^6 -substituted and N^6,N^6 -disubstituted adenosines (**28-36**) in very good yields (**Scheme 3.9**). Purification was carried out either by flash column chromatography or by precipitation.



Reagents and conditions (yield): a) R^1R^2NH , TEA, EtOH, reflux (65-94%).

Scheme 3.9. Synthesis of N^6 -substituted and N^6,N^6 -disubstituted adenosines (**28-36**)

Since acetyl protecting groups are cleaved by simple alcoholysis to volatile acetate esters, deprotection of the ribose moiety was not necessary in the course of the synthesis of most O^6 -alkyl derivatives of inosine (**38, 39, 41** and **42**) (**Scheme 3.10**). An excess of Na in the suitable refluxed alcohol was used as reagent (for **38, 39** and **41**) and THF was chosen as solvent in the case of the 2-phenylethoxy group (**42**). Neutralization with NH_4Cl and either flash column chromatography or precipitation afforded the products. The alternative synthesis of **41** with $n\text{-BuONa}$, prepared *in situ* from Na in a $n\text{-BuOH/DMSO}$ mixture, gave poorer results in terms of yield (from 86 to 59%) and was plagued by significant drawbacks, such as the residual presence of DMSO after flash column chromatography, which made freeze-drying necessary to purify the product. Once again, $i\text{-PrOH}$ was deprotonated to the corresponding alkoxide by NaH and reacted with the deprotected 6-chloro precursor **49** to form product **40**.

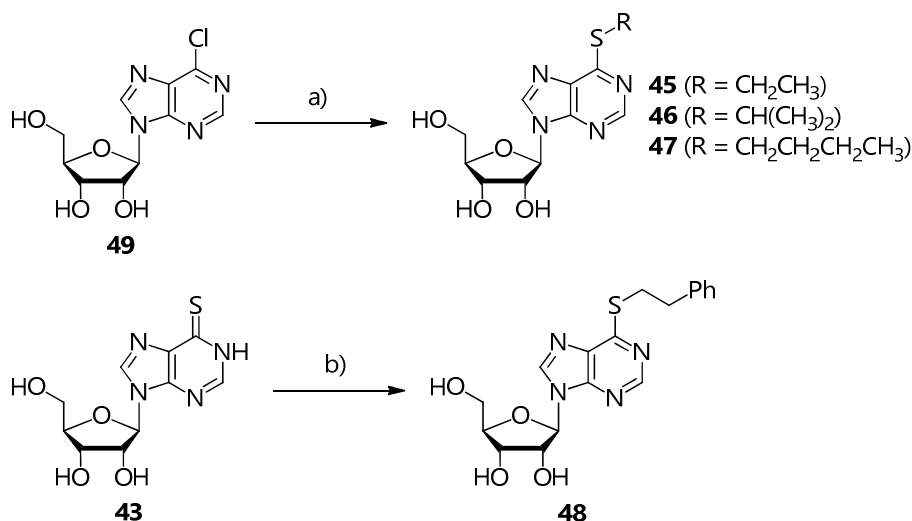


Reagents and conditions (yield): a) Na, ROH, THF (for **42**), reflux (29%-quantitative); b) NaH, $i\text{-PrOH}$, reflux (for **40**, 32%) or Na, $n\text{-BuOH/DMSO}$, reflux (for **41**, 59%).

Scheme 3.10. Synthesis of 6-alkoxyinosines (**38-42**)

Unlike purines (see **3.1.1**), the chlorine displacement strategy was selected for most S -alkyl derivatives of 6-thioinosine (**45-47**), while only **48** was synthesized by the S -alkylation approach (**Scheme 3.11**). The low yield of the latter method with respect to the first one may be ascribed to the extremely high reactivity of

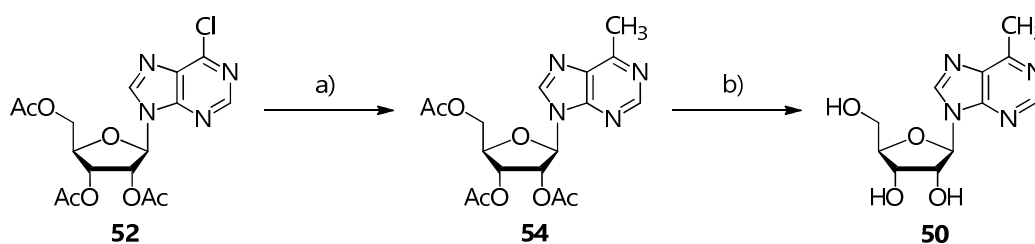
free hydroxyl groups in aqueous NaOH and the subsequent formation of overalkylated by-products. The proper thiol was deprotonated *in situ* by Na₂CO₃ in EtOH. The mixture was always refluxed with the only exception of the one containing CH₃CH₂SH, for which the temperature was kept at 30°C due to its volatility. Once again, purification was obtained by flash column chromatography. **48** was prepared according to a similar procedure to the synthesis of **22**. PhCH₂CH₂Br was added directly to a suspension of **43** and Na₂CO₃ in DMF, premixed in order to allow the quantitative formation of the thiolate anion.



Reagents and conditions (yield): a) RSH, Na₂CO₃, EtOH, 30°C (for **45**) or reflux (for **46** and **47**) (59-88%);
b) PhCH₂CH₂Br, K₂CO₃, DMF (47%).

Scheme 3.11. Synthesis of 6-alkylthioinosines (**45-48**)

The introduction of a methyl group in position 6 of the purine ring was performed by a Pd-mediated Negishi cross-coupling on **52** (see **6.1.3**)¹⁵⁵, followed by acetate removal with NH₄OH in MeOH (**Scheme 3.12**). A 2.0 M solution of (CH₃)₂Zn in toluene, Pd(PPh₃)₄ (15 mol %) and dry THF were chosen as methylating agent, catalyst and solvent for the first reaction, respectively.

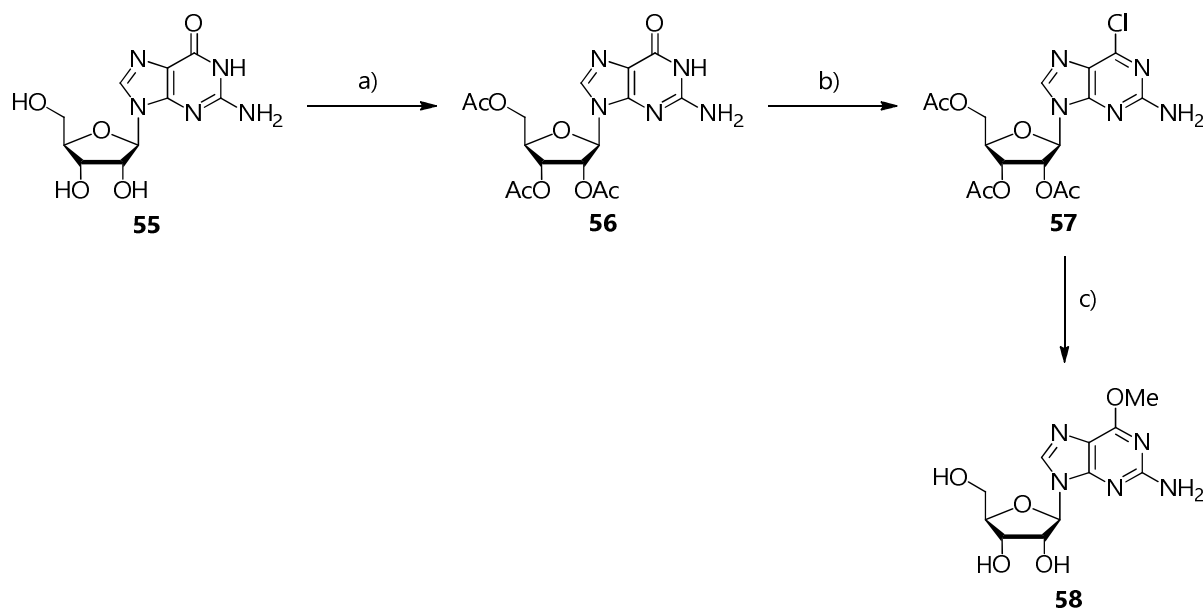


Reagents and conditions (yield): a) 2.0 M (CH₃)₂Zn in toluene, 15 mol % Pd(PPh₃)₄, THF, 55°C → RT (81%);
c) 33% aq. NH₄OH, MeOH (66%).

Scheme 3.12. Synthesis of 6-methylinosine (**50**)

3.1.4. Synthesis of 6-O-methylguanosine (**58**)

To obtain 6-O-methylguanosine (**58**), the 6-carbonyl group of guanosine (**55**) was chlorinated by treatment with POCl₃, *N,N*-DMA and Et₄NCl in refluxed CH₃CN, in analogy with 6-chloropurine (**23**), and subsequent reaction of **56** with NaOMe in dry MeOH at RT (**Scheme 3.13**). As usual, no further hydroxyl transesterification was needed after flash column chromatography.



Reagents and conditions (yield): a) Ac_2O , TEA, 7 mol % DMAP, CH_3CN (94%); b) POCl_3 , *N,N*-DMA, Et_4NCl , CH_3CN , reflux (76%); c) Na, MeOH (57%).

Scheme 3.13. Synthesis of 6-*O*-methylguanosine (**58**)

3.1.5. Synthesis of arabinosylguanine (**59**)

In order to synthesize purine arabinosyl derivatives by a “one-pot, one-enzyme” transglycosylation catalyzed by *AhpNP*, 7-methylarabinosylguanine iodide may be used as a convenient sugar *donor*, following the synthetic scheme developed for the enzymatic synthesis of 6-substituted purine ribonucleosides where 7-methylguanosine iodide was chosen as *D*-ribose source (see **3.2.1**).^{57, 63, 104} The advantage of this approach relies on the formation of 7-methylguanine as by-product that is neither a substrate nor an inhibitor of the enzyme. As a result, the equilibrium-controlled transglycosylation can be completely shifted toward product formation (see **1.6.1**).^{57, 63b}

The synthesis of 7-methylarabinosylguanine (**67**) was undertaken starting from arabinosylguanine (**59**) (**Figure 3.3**).

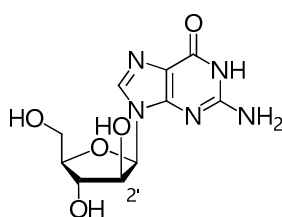
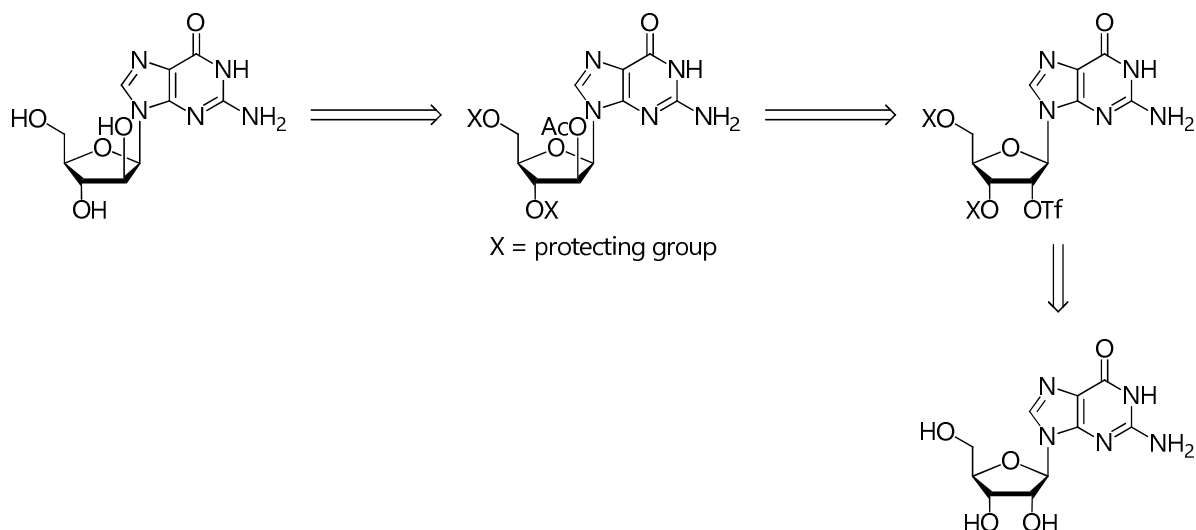


Figure 3.3. Arabinosylguanine (**59**)

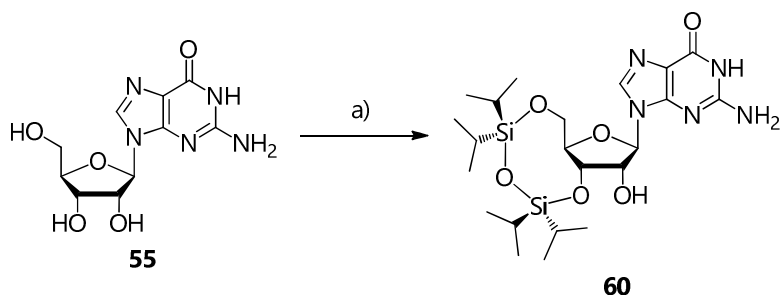
Almost all reported strategies to prepare arabinosylguanine start from guanosine (**55**). Since the two molecules are epimers, differing only in the opposite configuration of $\text{C}^{2'}$, all procedures involve its stereochemical inversion. One of the first protocols described in literature was reported by Hansske *et al.* According to it, the reaction requires a Moffatt oxidation with $\text{DMSO}/\text{Ac}_2\text{O}$ followed by reduction with NaBH_4 . The formal hydride attack occurs specifically on the α side of the sugar largely due to the steric hindrance around the guanine base.¹⁰⁵ In a more recent variant developed by Mehta *et al.* in 2014, the Swern-like reagent couple was substituted by Dess-Martin periodinane.¹⁰⁶ Gruen *et al.* managed to achieve

the same result by an S_N2 strategy (**Scheme 3.14**), according to which $\text{OH}^{2'}$ was converted into a stable leaving group by triflation, followed by displacement with NaOAc and deacetylation. The other two hydroxyl groups needed a non-orthogonal protection to prevent inversion at $\text{C}^{3'}$ and side reactions at the $5'$ -position.¹⁰⁷



Scheme 3.14. Retrosynthetic analysis of arabinosylguanine

The first step of the sequence was the preliminary double protection of ribose in **55** by the use of the well-known Markiewicz reagent (1,3-dichloro-1,1,3,3-tetra-*i*-propyldisiloxane, TIPDSCl₂) on $\text{OH}^{3'}$ and $\text{OH}^{5'}$ (**Scheme 3.15**). An excess of imidazole in dry DMF was necessary to promote the displacement of the two chlorine atoms on the reagent first by $\text{OH}^{5'}$ and then by $\text{OH}^{3'}$, with a consequential eight-membered ring closure. Water addition provided **60** by precipitation in almost quantitative yield.

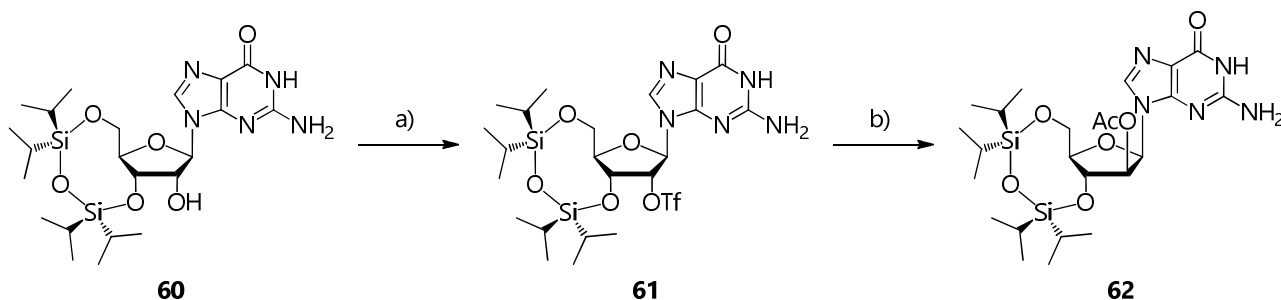


Reagents and conditions (yield): a) TIPDSCl₂, imidazole, DMF (98%).

Scheme 3.15. Protection of $\text{OH}^{3'}$ and $\text{OH}^{5'}$ of **55**

The triflation of **60** was carried out by treatment with TfCl in dry CH_2Cl_2 , DMAP as a catalyst and TEA to neutralize HCl. Control of the reaction temperature was crucial during the addition of the chloride at 0°C , while the reaction was allowed to proceed at RT until completion. The relatively limited reactivity of $\text{C}^{2'}$ toward nucleophiles, likely caused by the detrimental presence of a sterically hindered nucleobase, made it possible to purify **61** by flash column chromatography without decomposition. Nevertheless, the product was reacted as soon as possible with an acetate salt in DMF. Cs^+ was chosen as alkaline ion to maximize the nucleophilicity of the counter anion, which was introduced in position $2'$ by an S_N2 mechanism with concurrent inversion of configuration (**Scheme 3.16**). It was not surprising that this reaction took 24 h,

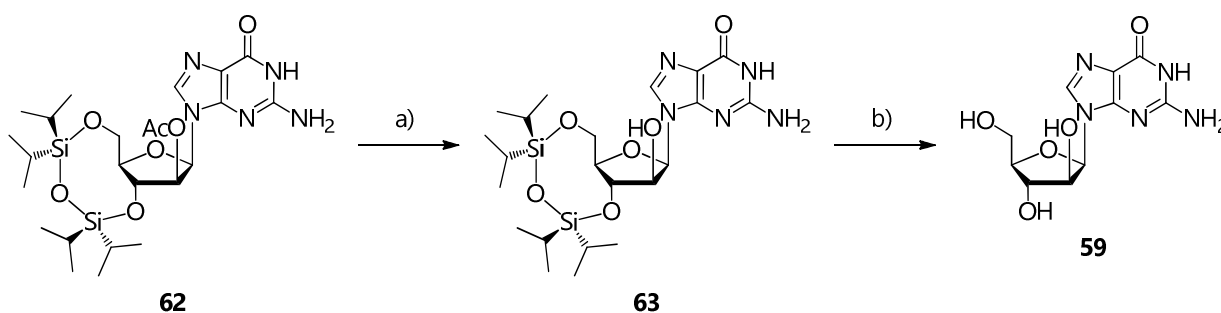
given that the heterocyclic portion shields the reacting carbon. Ester **62** was purified by flash column chromatography.



Reagents and conditions (yield): a) TfCl, TEA, DMAP, CH₂Cl₂ (69%); b) CsOAc, DMF (55%).

Scheme 3.16. Triflation of **60** and S_N2 displacement at C^{2'} of **61**

The remaining acetyl group of **62** was removed by aminolysis with NH₄OH in MeOH/1,4-dioxane. Reaction time was prolonged to 24 h in order to circumvent any detrimental effect of the combined steric hindrances of the nucleobase and the disilyloxane. Finally, double desilylation of **63** with TBAF·3H₂O in THF was performed to cleave the protections on the two ribose hydroxyl groups (**Scheme 3.17**). Semi-preparative HPLC afforded arabinosylguanine (**59**) in good yield.



Reagents and conditions (yield): a) 33% aq. NH₄OH, MeOH/1,4-dioxane (80%); b) TBAF·3H₂O, THF (67%).

Scheme 3.17. Aminolysis of **62** and desilylation of OH^{2'} and OH^{5'} of **63**

3.1.6. Synthesis of 7-methylpurine and 7-methylguanine nucleoside iodides (**64-67**)

7-Methylpurine riboside iodide (**64**) and 7-methylguanine ribo-, 2'-deoxyribo- and arabinonucleoside iodides (**65-67**) were prepared to be used as sugar *donors* in transglycosylation reactions catalyzed by AhPNP, although only **65** and **66** were used (**Figure 3.4**).

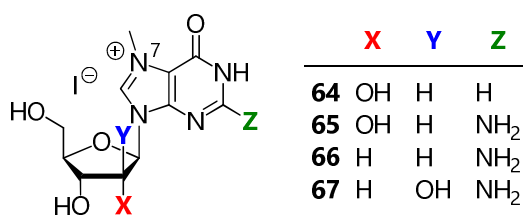
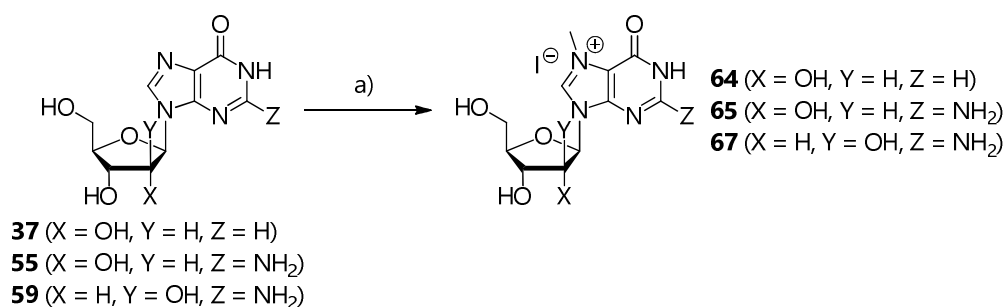


Figure 3.4. 7-Methylpurine and 7-methylguanine nucleoside iodides (**64-67**)

As of **64** and **65**, the choice of MeI as methylating agent and of the proper solvent for S_N2 reactions (DMSO or a DMF/DMSO mixture) led to the regioselective formation of the iodide salts at N⁷ (**Scheme 3.18**). Since

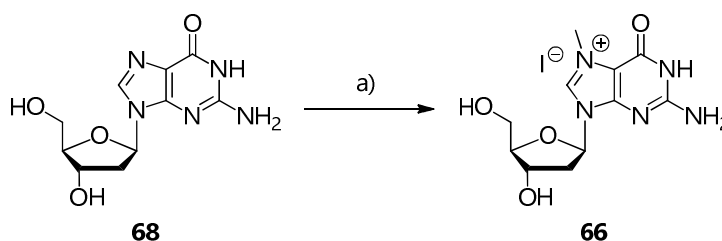
they are too polar to be detected by TLC, the disappearance of the reagent was monitored instead, to assess when the reaction was complete. In addition, light exposure during the reaction at RT was avoided to prevent decomposition of reagents and final products, which had to be stored at -20°C until use. No synthesis of 7-methylarabinosylguanine iodide (**67**) has been reported in literature to date, thus a similar strategy was successfully applied to the methylation of arabinosylguanine (**59**) with MeI in a DMSO/DMF mixture, obtaining a similar yield (83%). After freeze-drying to remove the high-boiling solvent, isolation and purification were carried out in all cases by either precipitation in dry acetone or CHCl_3 , if necessary followed by grinding of the resulting syrup in dry acetone.



Reagents and conditions (yield): a) CH_3I , DMSO (for **64**, 67%) or CH_3I , DMF/DMSO, 30°C (for **65**) or RT (for **67**) (87-89%).

Scheme 3.18. Synthesis of 7-methylinosine, -guanosine and -arabinosylguanine iodides (**64**, **65** and **67**)

The stability of 7-methylated nucleosides in DMSO or DMSO/DMF mixtures varies largely, depending on the nature of the sugar moiety, and was a serious issue in the synthesis of 7-methyl-2'-deoxyguanosine iodide (**66**) (**Scheme 3.19**). The reaction was performed by modifying a previous protocol reported by Voegel *et al.*, under controlled temperature (20°C), short reaction time and excess methyl iodide in order to avoid any decomposition of **66** in DMSO.¹⁰⁸ Attempts under both higher temperatures (25 - 30°C) and longer reaction times did not afford any product, probably because of its low stability in such conditions. The synthesis was therefore controlled by TLC to stop it by adding cold CHCl_3 as soon as reagent consumption was complete and collecting the obtained solid by filtration before other by-products could be formed. The resulting yield was comparable to the one reported in literature (80% vs. 77%).



Reagents and conditions (yield): a) CH_3I , DMSO, 20°C (80%).

Scheme 3.19. Synthesis of 7-methyl-2'-deoxyguanosine iodide (**66**)

3.1.7. Synthesis of 8-substituted inosines, guanosines and adenosines (**69-80**)

With the aim to develop selective inhibitors of the purine nucleoside phosphorylase from *Mycobacterium tuberculosis* (MtPNP), a small library of 8-substituted purine ribonucleosides (**69-80**) was synthesized and assayed, owing to the evidence that some similar analogues had been reported to inhibit PNPs, such as the human enzyme (*e.g.* 8-aminoguanosine, $K_i = 17 \mu\text{M}$) and that from *Plasmodium falciparum* (*e.g.* 8-aryl

substituted inosines, K_i in the μM range). To date, no 8-oxy or 8-thio substituted nucleosides have been proposed as inhibitors of either human or microbial PNPs.

Seven of the obtained molecules (**70**, **71**, **74**, **76**, **77**, **79** and **80**) were screened by a newly developed LC-ESI-MS/MS assay (Figure 3.5).

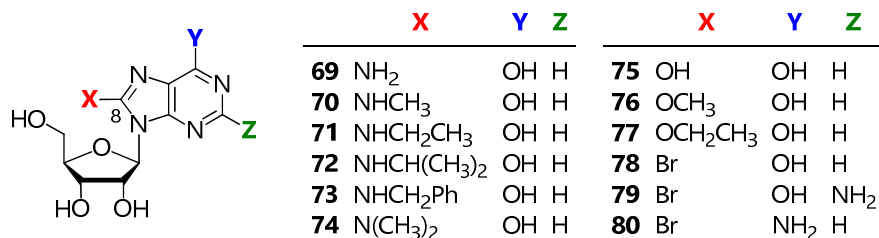
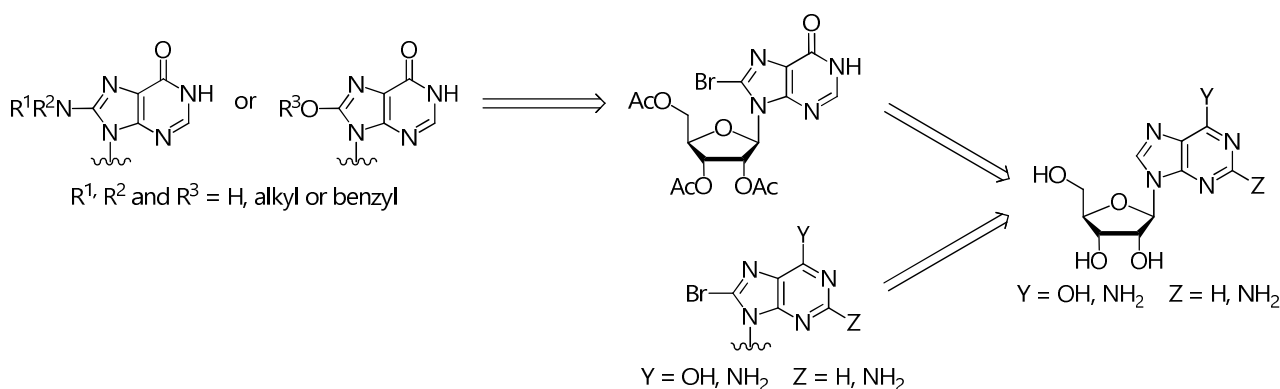


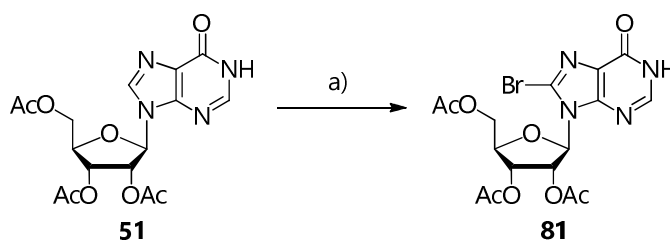
Figure 3.5. 8-Substituted inosines, guanosines and adenosines (**69-80**)

Following an approach similar to that adopted for the functionalization of position 6 of the purine ring, the synthetic strategy consisted of the substitution of H⁸ with a proper halide. Bromination either on the free nucleosides or on the protected ones was followed by treatment with the appropriate nucleophile and successive manipulations, when necessary (Scheme 3.20).



Scheme 3.20. Retrosynthetic analysis of 8-substituted inosines, guanosines and adenosines

To obtain 8-substituted inosines, the triacetylated nucleoside **51** was directly brominated by reaction with Br₂ in a 10% aqueous Na₂HPO₄/1,4-dioxane mixture at moderately basic pH (Scheme 3.21). Since this electrophilic aromatic displacement was found to be exceptionally slow, numerous bromine additions were needed at fixed times and the reaction was stopped after 8 days at more than 90% conversion (roughly evaluated by TLC). Intermediate **81** was obtained after flash column chromatography in 83% yield.

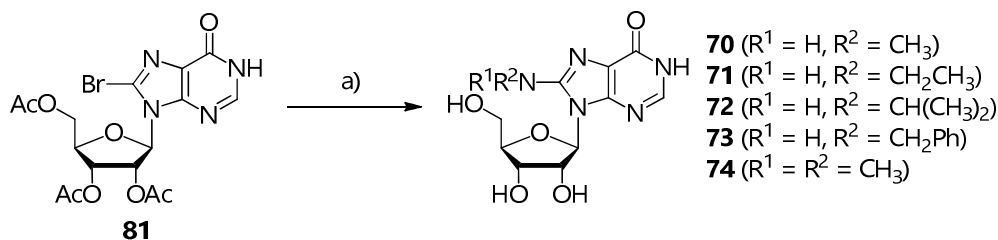


Reagents and conditions (yield): a) Br₂, 10% aq. Na₂HPO₄, 1,4-dioxane (83%).

Scheme 3.21. Synthesis of 8-bromo-2',3',5'-tri-*O*-acetylinosine (**81**)

Most of the following reactions were performed according to similar procedures previously used for other functionalizations.

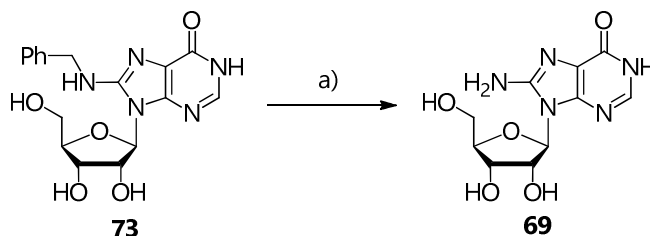
Primary or secondary amines were used on **81** to synthesize 8-alkylamino- and 8-*N,N*-dialkylaminoinosines (**70-74**), respectively, in 1,4-dioxane at 80°C (**Scheme 3.22**). In contrast to previous similar reactions, time had to be extended (between 1 and 3 days) because of the slow reactivity of position 8 in purines, which is generally less prone to nucleophilic attacks than C² and C⁶ and makes it necessary to select longer times, as well as higher reagent concentrations and temperatures. The very low yield of **72** can be attributed to the steric hindrance of *i*-PrNH₂, in sharp contrast even to disubstituted (CH₃)₂NH₂. Because of their low *R_f* in TLC on silica, all products were purified by reverse phase semi-preparative HPLC.



Reagents and conditions (yield): a) R¹R²NH, 1,4-dioxane, 80°C (18-87%).

Scheme 3.22. Synthesis of 8-alkylamino- and 8-*N,N*-dialkylaminoinosines (**70-74**)

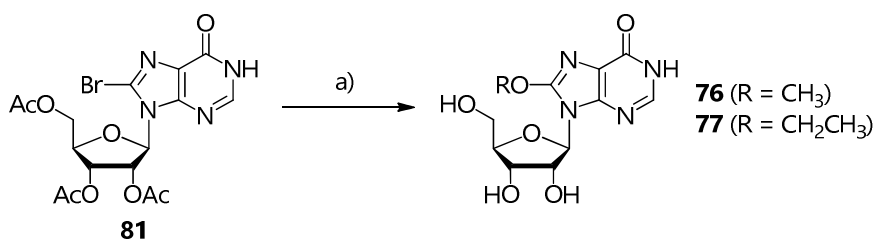
Since the direct reaction of **81** with NH₄OH gave no significant results, 8-aminoinosine (**69**) was obtained by prolonged hydrogenolysis of benzyl derivative **73** with HCOONH₄ in MeOH (**Scheme 3.23**). Pd-C (10 mol %) was chosen as heterogeneous catalyst. Reflux was needed to speed up the reaction, which is slower for benzylamines than for the corresponding ethers.



Reagents and conditions (yield): a) HCOONH₄, 10 mol % Pd-C, MeOH, reflux (96%).

Scheme 3.23. Synthesis of 8-aminoinosine (**69**)

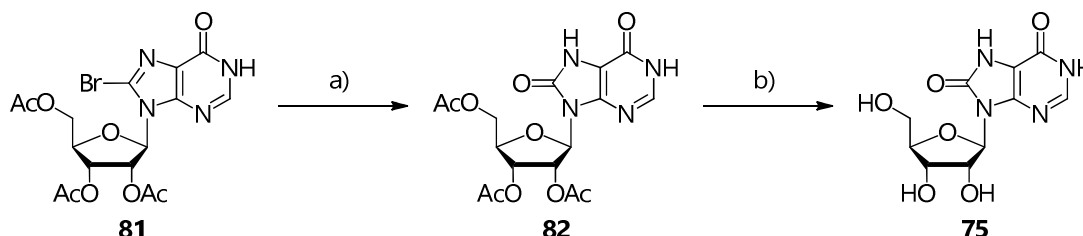
As for 8-alkoxyinosines, sodium alkoxides in the corresponding refluxed alcohols were selected to both displace bromine and the three hydroxyl acetates of **81** (**Scheme 3.24**). Shorter reaction times were allowed by their higher nucleophilic strength. **76** and **77** were both purified by semi-preparative HPLC.



Reagents and conditions (yield): a) Na, ROH, reflux (74-87%).

Scheme 3.24. Synthesis of 8-alkoxyinosines (**76** and **77**)

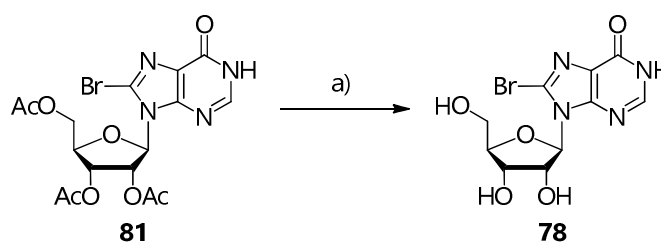
As with **69** regarding NH_4OH , direct hydroxylation of **81** with NaOH and other similar reagents proved to be unsuccessful. The introduction of an 8-oxo moiety was performed by treating **81** with NaOAc in glacial AcOH at $110\text{--}115^\circ\text{C}$ (**Scheme 3.25**). The reaction proceeded through nucleophilic displacement of bromine by the acetate ion followed by hydrolysis of the resulting 2-imidazolyl-like acetate (see **6.1.2**).¹⁵⁴ Usual deprotection of **82** with either NaOMe in dry MeOH or 1.8 M NaOH afforded product **74** after neutralization and precipitation.



Reagents and conditions (yield): a) NaOAc , AcOH , $110\text{--}125^\circ\text{C}$ (93%); b) NaOMe , MeOH (50%) or 1.8 M NaOH (65%).

Scheme 3.25. Synthesis of 8-oxoinosine (**75**)

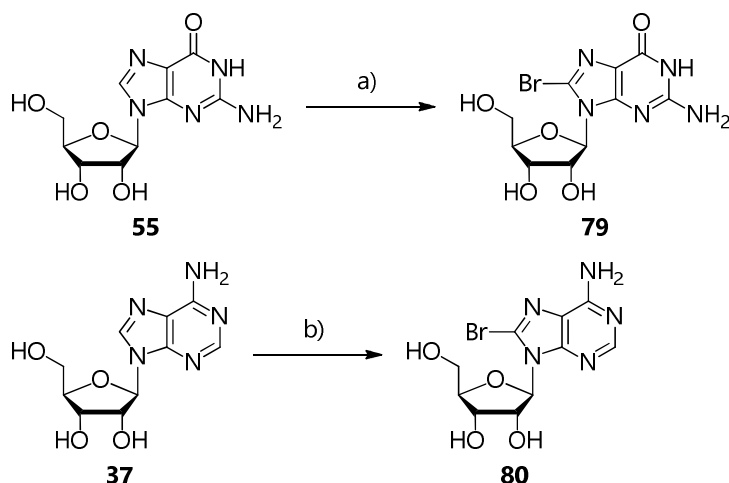
8-Bromoinosine (**78**) was prepared by deprotection of **81** with either NaOMe in MeOH or 1.0 M NaOH and subsequent precipitation by neutralization (**Scheme 3.26**).



Reagents and conditions (yield): a) 1.0 M NaOH (64%) or NaOMe , MeOH (90%).

Scheme 3.26. Synthesis of 8-bromoinosine (**78**)

Unlike inosine, the two 8-bromo derivatives of guanosine and adenosine (**79** and **80**, respectively) could be obtained by direct halogenation with less strong reagents, owing to the greater electronic density delocalized on C^8 , which resulted in increased nucleophilicity and reactivity toward electrophiles (**Scheme 3.27**). The presence of a free amino group at position 2 of guanosine further increases this behavior, allowing the use of NBS in H_2O for the synthesis of **79** in 5 h at RT. A similar strategy was devised for adenosine, despite a lower yield and longer reaction times (4 days). This result led to the choice of bromine water to get **80** much more efficiently in terms of yield (83 vs. 58%) and time (2 days). In order to avoid any oxidation of the sugar moiety, pH of the reaction mixture had to be kept at 4.0 by using 0.5 M aqueous NaOAc as solvent. Either precipitation or recrystallization yielded the desired compound.



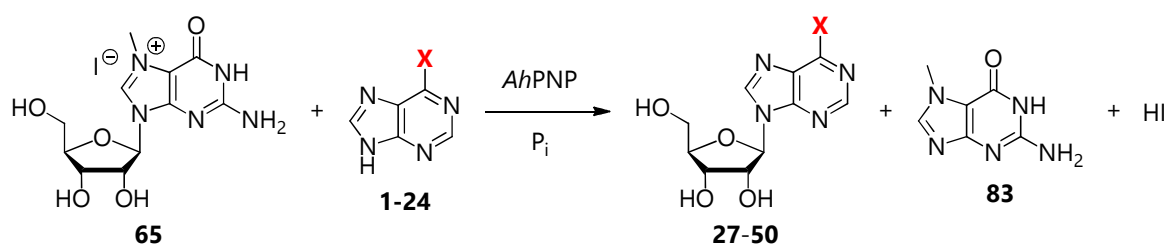
Reagents and conditions (yield): a) NBS, H₂O (89%); b) NBS, H₂O (58%) or bromine water, 0.5 M NaOAc, pH 4.0 (83%).

Scheme 3.27. Synthesis of 8-bromoguanosine (**79**) and 8-bromoadenosine (**80**)

3.2. Chemoenzymatic synthesis of nucleosides catalyzed by the PNP from *Aeromonas hydrophila* (AhPNP)

3.2.1. Chemoenzymatic synthesis of 6-substituted purine ribonucleosides catalyzed by AhPNP (“in batch” reaction)¹⁰⁹

“One-pot, one-enzyme” transglycosylations were performed according to the following conditions (**Scheme 3.28**): 50 mM aqueous K₂HPO₄ buffer containing 20% (v/v) glycerol, room temperature and pH 7.5. 1.15 IU of free AhPNP were added to catalyze both reactions and HI was neutralized by the buffer. Concentrations were 1 mM for both *donor* and *acceptor* (1:1 ratio). In agreement with the previous studies on AhPNP (see **1.6.1**)^{57, 63b}, 7-methylguanosine iodide (**65**) was chosen as a convenient ribose source and the series of synthesized 6-substituted purines (**1-24**) as ribose *acceptors*.



Scheme 3.28. “One-pot, one-enzyme” transglycosylations catalyzed by AhPNP

The use of glycerol was addressed by the need to preserve enzyme activity and to increase substrate solubility. In fact, this co-solvent is routinely used up to 60% for enzyme storage. It was also reported that glycerol can enhance the solubility of nucleoside analogues and nucleobases, which are scarcely soluble in polar solvents such as H₂O.¹⁰⁴

65 was selected because its phosphorolysis catalyzed by AhPNP is rapid, complete and irreversible, leading to 100% conversion to the α -D-ribose-1-phosphate intermediate under optimized conditions. In fact, the generated nucleobase, 7-methylguanine (**83**), is neither a substrate nor an inhibitor due to the presence of

the methyl group which prevents proton extraction from N⁷ and therefore the reverse reaction to the nucleoside iodide. In addition, the nucleobase is poorly soluble in aqueous media and its consequent precipitation shifts the phosphorolysis equilibrium to product formation. In this study, however, the goal was not to maximize the transglycosylation conversion in the view of a preparative synthesis but, under the same “standard” conditions, to assay the substrate specificity of *Ahp*PNP toward a collection of substituted purines.

In this frame, aliquots (200 µL) of transglycosylation mixtures were withdrawn at fixed times (0', 10', 30', 1 h, 3 h, 6 h and 24 h), centrifuged and subsequently analyzed by HPLC. All peaks identities were assigned by comparison of their t_r with those of pure references, either commercially available or synthesized as previously described (see 3.1.3). Analyses were carried out in duplicate.

Base conversion was calculated according to the following equation:

$$\text{Conversion (\%)} = \frac{\text{nucleoside area}}{\text{nucleoside area} + \text{base area}} \cdot 100$$

Conversions at 6 h were chosen as reference values to determine the reaction progress (**Table 3.1**).

From the collected experimental data, it clearly appears that transglycosylation equilibria are shifted to either the base or the corresponding nucleoside to a different extent, depending on the nature of the 6-substituent. Five observations can be drawn:

- twenty-three out of twenty-four 6-monosubstituted purine nucleobases are recognized as substrates by the enzyme;
- within the whole series, the only exception is *N*⁶,*N*⁶-bis-hydroxyethyladenine (**10**) (0% conversion, even when the reaction was carried out for a prolonged time up to 24 h), probably because the bulky and very polar side chains of this compound might be not compatible with the recognition pattern of the enzyme;
- in the adenine series, disubstitution on N⁶ results detrimental for the recognition by *Ahp*PNP, based on the decrease in conversion between **2** and **9** (46 vs. 29%) and **8** and **10** (47 vs. 0%);
- if the base is monosubstituted, bulky and polar groups appear, however, quite well tolerated (**4-8**, **14-16** and **21** span from 38 to 65% conversion);
- the comparison between **23** and **24** (20 and 18% conversion) suggests a very poor influence of the electronic properties associated to the 6-substituent on the transglycosylation extent.

Generally, these results confirm the broad substrate specificity of *Ahp*PNP (see 1.6.1)^{63b}, which can thus be exploited for preparative applications.

Structural and kinetic analyses, which are out of the scope of this Thesis, would be needed for a deeper and more rigorous insight into structural requirements imposed on substrates by the active site of the enzyme, specifically concerning the 6-substitution pattern. These studies will need the available structure of the enzyme or, alternatively, to build up an homology model based on an enzyme of the same class (high-MM PNPs). Indeed, many studies have been and are still being carried out on the PNP from *Escherichia coli* (*Ecp*PNP), which represents the model enzyme for that group and shows a high identity degree at aminoacidic level (> 80%) with *Ahp*PNP (**Figure 3.6**).

In particular, *Ahp*PNP conserves the same four residues involved in the catalytic mechanism of *E. coli* (His₄, Asp₂₀₄, Arg₄₃ and Arg₂₁₇).^{12a}

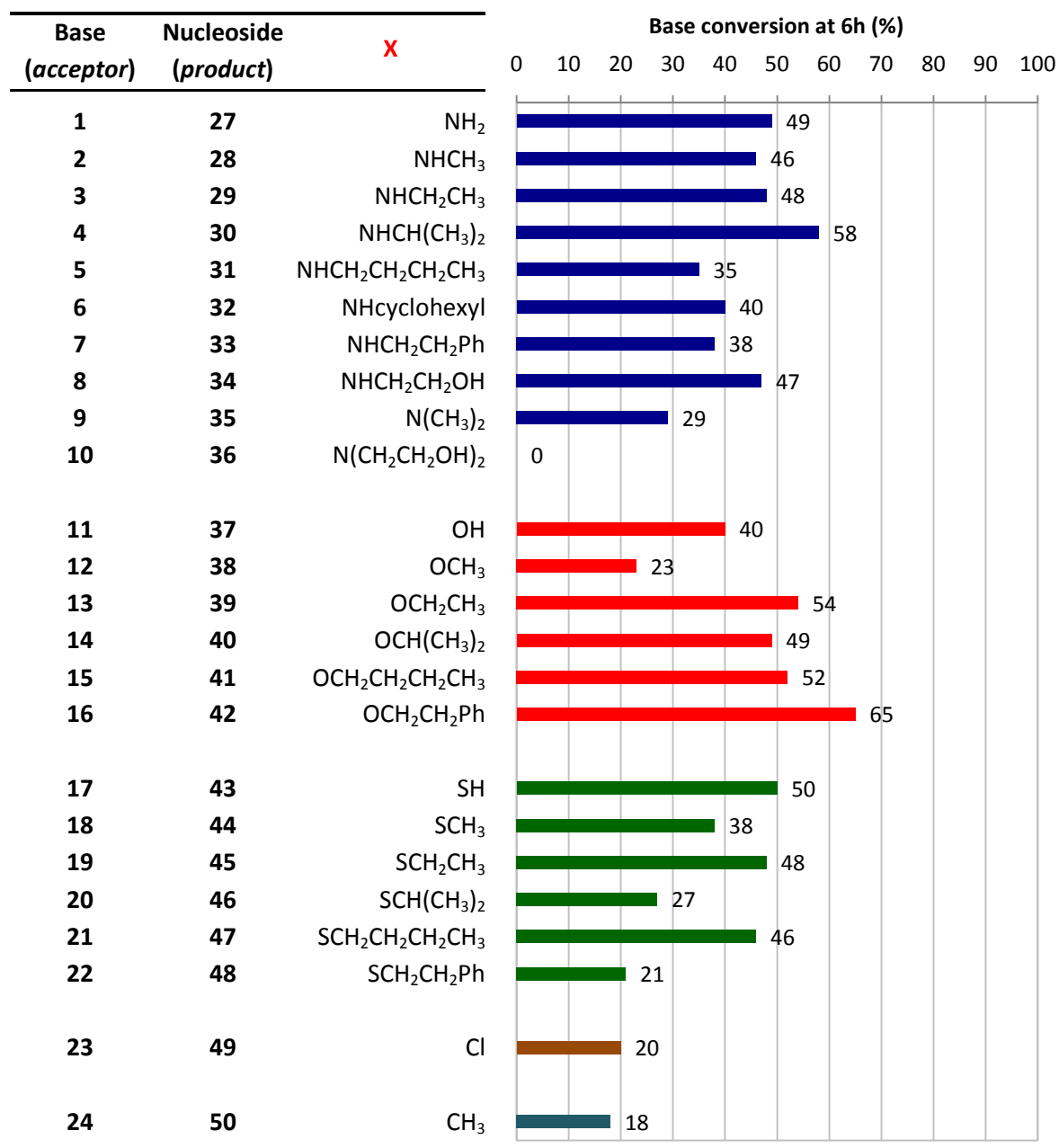

 Table 3.1. Synthesis of 6-substituted ribonucleosides catalyzed by *Ah*PNP and base conversion at 6 h (%)

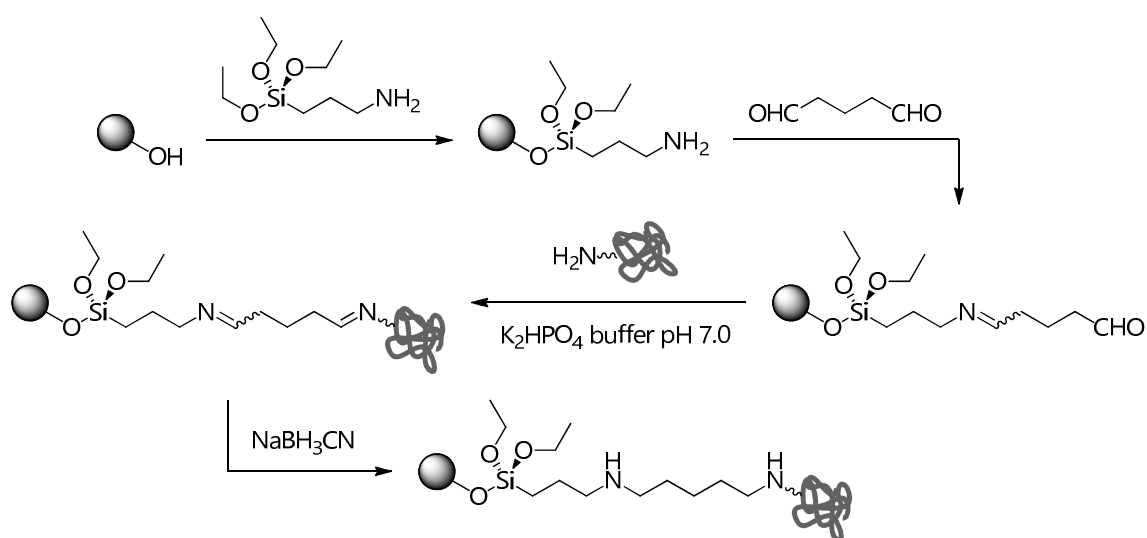
 Figure 3.6. Sequence alignment of *Ah*PNP and *Ec*PNP

3.2.2. Chemoenzymatic synthesis of 6-substituted purine ribonucleosides catalyzed by *Ahp*PNP-IMER (“in flow” reaction)¹¹⁰

3.2.2.1. Covalent immobilization of *Ahp*PNP and IMER preparation

To develop an “*in continuum*” transglycosylation process which might combine biotransformation, reaction monitoring and product isolation, a few reactions described above (see **3.2.1**)¹⁰⁹ were transferred from batch into a flow system. To this aim, the enzyme was immobilized in a pre-packed stainless steel column (50 mm x 4.6 mm) to give an Immobilized Enzyme Reactor (IMER) that was connected to an HPLC apparatus for on-line monitoring and purification of the reaction.

Covalent immobilization was carried out in a column containing aminopropylsilica particles (5 μm , 100 \AA) by following the protocol previously used to bind the same enzyme on the inner surface of a fused silica Open Tubular Capillary (OTC) (**Scheme 3.29**, see **1.6.2**).¹⁰²



Scheme 3.29. Covalent immobilization of *Ahp*PNP on aminopropylsilica particles

First, the aminopropylsilica stationary phase was introduced into a HPLC system and flushed with a 10% (v/v) glutaraldehyde solution in 50 mM K_2HPO_4 (pH 7.5), forming the first transient imine bond. A $2 \text{ mg}\cdot\text{mL}^{-1}$ *Ahp*PNP solution was then recirculated through the whole system overnight at 20°C , in order to allow the superficial amino groups on the enzyme to react with the aldehyde. Lys residues were mostly involved in this interaction with the aldehyde groups provided by the linker. Since imines are prone to hydrolysis, they were reduced in the final step with a 0.1 M NaBH_3CN solution to form stable covalent amine bonds, able to resist hydrolysis.¹¹¹

The amount of immobilized catalyst was calculated by the Bradford assay, that is by measuring the difference in UV absorbance of the enzyme solution between the beginning and the end of the immobilization process.¹¹² Roughly, 25 mg of *Ahp*PNP were successfully immobilized, corresponding to 53% yield. It is important to point out that this satisfactory result was likely due to the higher active surface area of the packed silica bed with respect to the inner surface of the OT capillary used before, which had allowed the immobilization of 30 μg (10% yield).

The *Ahp*PNP-IMER is represented in **Figure 3.7**.

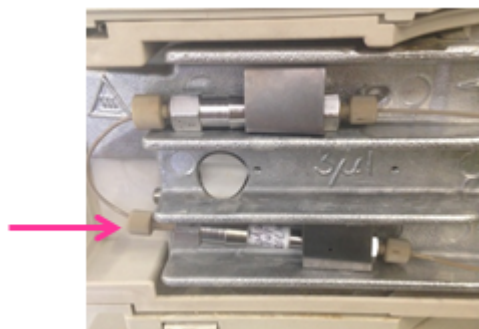


Figure 3.7. *Ah*PNP-IMER (5 μm , 100 \AA , 50 mm x 4 mm)

3.2.2.2. Activity and stability of *Ah*PNP-IMER

The standard activity assay relies on the measurement of the phosphorolysis of inosine (**37**) to hypoxanthine (**11**). This test was carried out periodically on the *Ah*PNP-IMER to evaluate the stability of the bioreactor over time. Activity and stability, the latter calculated as residual activity with respect to the initial one, were assessed from the following equation:

$$\text{Conversion (\%)} = \frac{\text{product area}}{\text{product area} + \text{substrate area}} \cdot 100$$

Stability was measured weekly, demonstrating that the IMER retained its initial activity for more than 50 reactions in 10 months. Whenever not in use, the *Ah*PNP-IMER was stored in 100 mM K_2HPO_4 buffer (pH 7.5) at 4°C.

3.2.2.3. Analytical apparatus and optimization of the reaction conditions

From a general viewpoint, the analytical apparatus containing the *Ah*PNP-IMER was set up by modifying the previously reported one (see 1.6.2)¹⁰², composed of two coupled systems (**Figure 3.8**). The first one contained the IMER and the second one an analytical HPLC column for reaction monitoring. The systems were interfaced by a six-port switching valve (V) containing a 5 μL loop in order to transfer analytes directly from the bioreactor to the HPLC column.

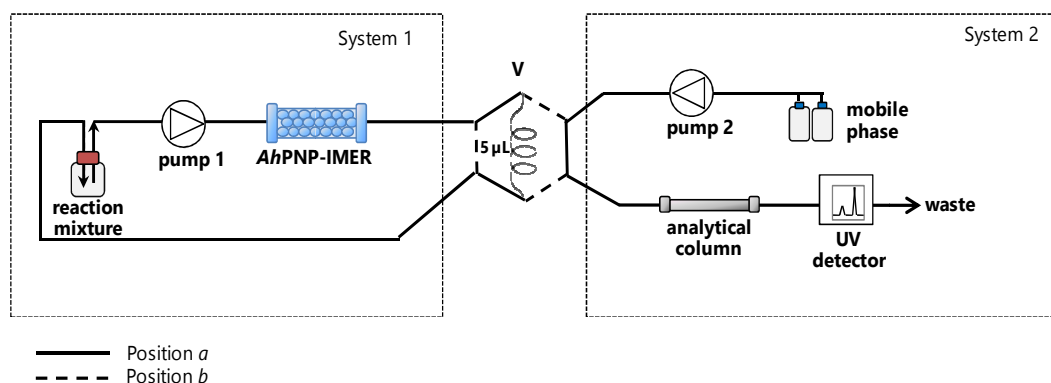
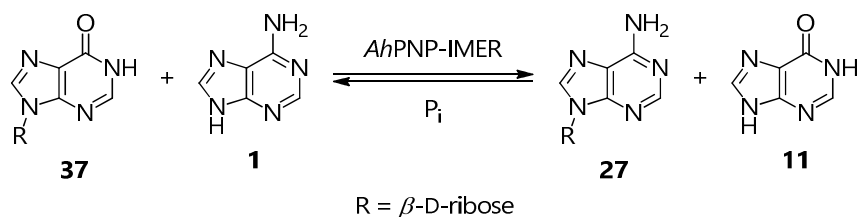


Figure 3.8. IMER-based system (analytical apparatus) (Adapted with permission from *Adv. Synth. Catal.* **2015**, *357*, 2520-2528)¹¹⁰

The system can adopt two different configurations depending on the position (*a* or *b*) of the six-port switching valve (V). As V is in position *a*, the reaction mixture is recirculated continuously through the IMER

to allow the reaction to progress. At fixed times, the valve is automatically switched to position *b* and an aliquot of the mixture is diverted to the analytical apparatus for on-line monitoring, allowing an assessment of the time necessary to reach the equilibrium. This value is crucial for preparative purposes, as purification is performed once the highest conversion has been achieved. The 5 μL aliquot is loaded in the loop and then onto the head of the analytical HPLC column, where substrates (nucleoside *donor* and purine *acceptor*) and products (*donor* conjugated nucleobase and final ribonucleoside) can be separated and identified at 260 nm.

To optimize the reaction conditions, a “two-level, five-factor” fractional factorial design was performed by using the synthesis of adenosine (**27**) as model reaction (**Scheme 3.30**). Conversion was 78%.



Scheme 3.30. Synthesis of adenosine (**27**) by *Ah*PNP-catalyzed transglycosylation

Five factors, whose values were selected on the basis of theoretical considerations and/or preliminary experiments, were taken into consideration:

- inosine (**37**)/adenine (**1**) ratio (x_1);
- K_2HPO_4 buffer concentration (x_2);
- temperature (x_3);
- flow rate (x_4);
- pH (x_5).

Three parameters were chosen as responses:

- phosphorolysis % (y_1);
- transglycosylation % (y_2);
- reaction time (y_3).

The following linear equation was elaborated to fit the mathematical model:

$$y_{1/2/3} = b_0 + b_1x_1 + b_2x_2 + b_3x_3 + b_4x_4 + b_5x_5$$

All regression coefficients were calculated using Matlab[®] 5.2 (The Math Works Inc., Natick Ma, US).

Concerning the three responses (**Figure 3.9**):

- the highest phosphorolysis percentage (y_1) was obtained with the lowest *donor*/base ratio tested (1:1.5 mM) and the highest co-substrate concentration (100 mM K_2HPO_4 buffer). This behavior is justified by the fact that a high phosphate concentration shifts the phosphorolysis equilibrium to the formation of α -D-ribose-1-phosphate;
- on the other hand, opposite conditions (*donor*/base ratio 2:1 and 10 mM K_2HPO_4 buffer) produced the highest transglycosylation percentage (y_2). Since the phosphate ion is a co-substrate in the phosphorolysis reaction and a co-product in the transglycosylation step, a lower buffer concentration and a higher *donor*/base ratio synergistically enhance the equilibrium toward product formation;
- in each reaction set, the equilibrium was reached as soon as the entire volume of the reaction mixture was pumped through the IMER. Any further investigation of the reaction time (y_3) was therefore dropped.

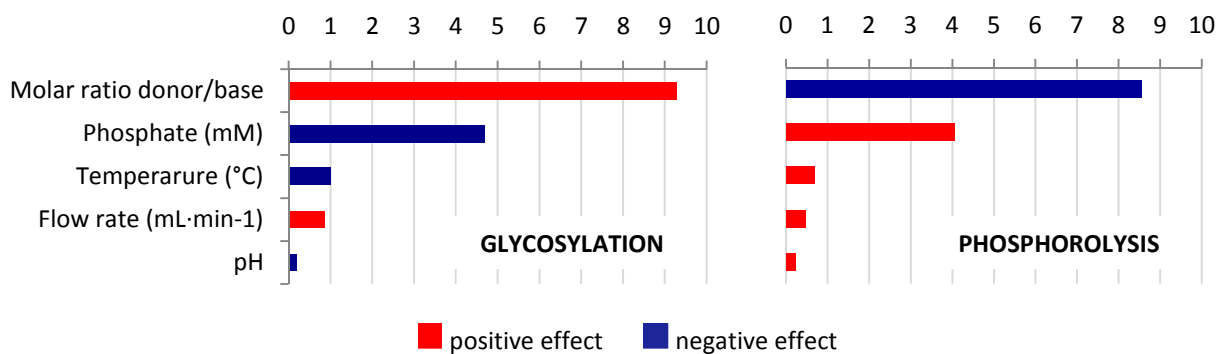
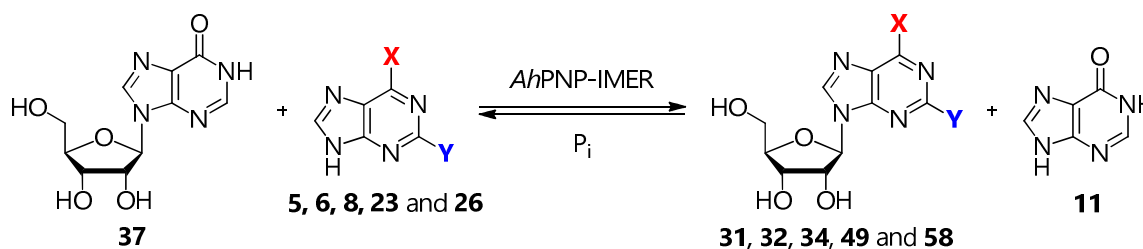


Figure 3.9. Fractional factorial design for the *AhpNP*-IMER

As a result, the flow synthesis of 6-substituted ribonucleosides was performed with a 2:1 *donor/acceptor* ratio (10:5 mM) and in 10 mM K_2HPO_4 buffer as solvent. Other less significant factors were set to enhance substrates solubility (37°C), reduce reaction time ($0.5 \text{ mL}\cdot\text{min}^{-1}$) and preserve long term IMER stability (pH 7.5). Nevertheless, H_2O was found to hardly solubilize purines, which often require the use of co-solvents. As reported, DMSO and glycerol are compatible with *AhpNP*, at least at low concentrations, typically below 10 or 20% (v/v), respectively.¹⁰² DMSO was preferred due to its higher dissolving capacities and added in variable percentages depending on the nature of the nucleobase.

3.2.2.4. Enzymatic synthesis, on-line monitoring and purification of 6-substituted purine ribonucleosides

First of all, a series of five 6-substituted purine ribonucleosides (**31**, **32**, **34**, **49** and **58**) were synthesized on analytical scale in the conditions described below (**Table 3.2**). Each reaction mixture loaded in the IMER system contained inosine (**37**) as ribose *donor* and the appropriate nucleobase (**5**, **6**, **8**, **23** or **26**) in K_2HPO_4 buffer (pH 7.5) with a variable amount of DMSO (0-7.5% (v/v)).



X	Y	Nucleobase (mM)	Nucleoside	Volume (mL)	DMSO (%)	Conversion (%)	Time (min) ^{a)}	Yield (mg) ^{b)}
NHCH ₂ CH ₂ CH ₂ CH ₃	H	2.5 (5)	31	10	7.5	77	20	5.9
NHCyclohexyl	H	2.5 (6)	32	10	0	87	20	7.5
NHCH ₂ CH ₂ OH	H	5.0 (8)	34	5	5.0	81	10	6.1
Cl	H	5.0 (23)	49	5	5.0	52	30	3.8
OCH ₃	NH ₂	5.0 (26)	58	5	0	89	10	6.6

^{a)} Time required to reach the equilibrium

^{b)} Data referred to the semi-preparative synthesis

Table 3.2. Synthesis of 6-substituted purine ribonucleosides catalyzed by the *AhpNP*-IMER

The choice of **37** as D-ribose donor was addressed not only by the fact that it is an inexpensive natural substrate of *Ah*PNP, but also by its relatively good solubility in aqueous media. Furthermore, in contrast with 7-methylguanine (**83**) generated by 7-methylguanosine iodide (**65**), hypoxanthine (**11**) released from **37** is more soluble in H₂O. Substrate/product precipitation would be of course highly detrimental for the flow process.

Each reaction mixture was pumped through the IMER until the equilibrium was reached, in a time depending on the nature of the nucleobase substituents and ranging from 10 to 30'. The sequence of four chromatograms related to the synthesis of **49** at 10', 30', 60' and 90' is reported in **Figure 3.10**, where arrows indicate the start of each run acquired after switching the 6-way valve. The progressive increase of the peak area of **49** can be observed, with the highest conversion reached after only 30'.

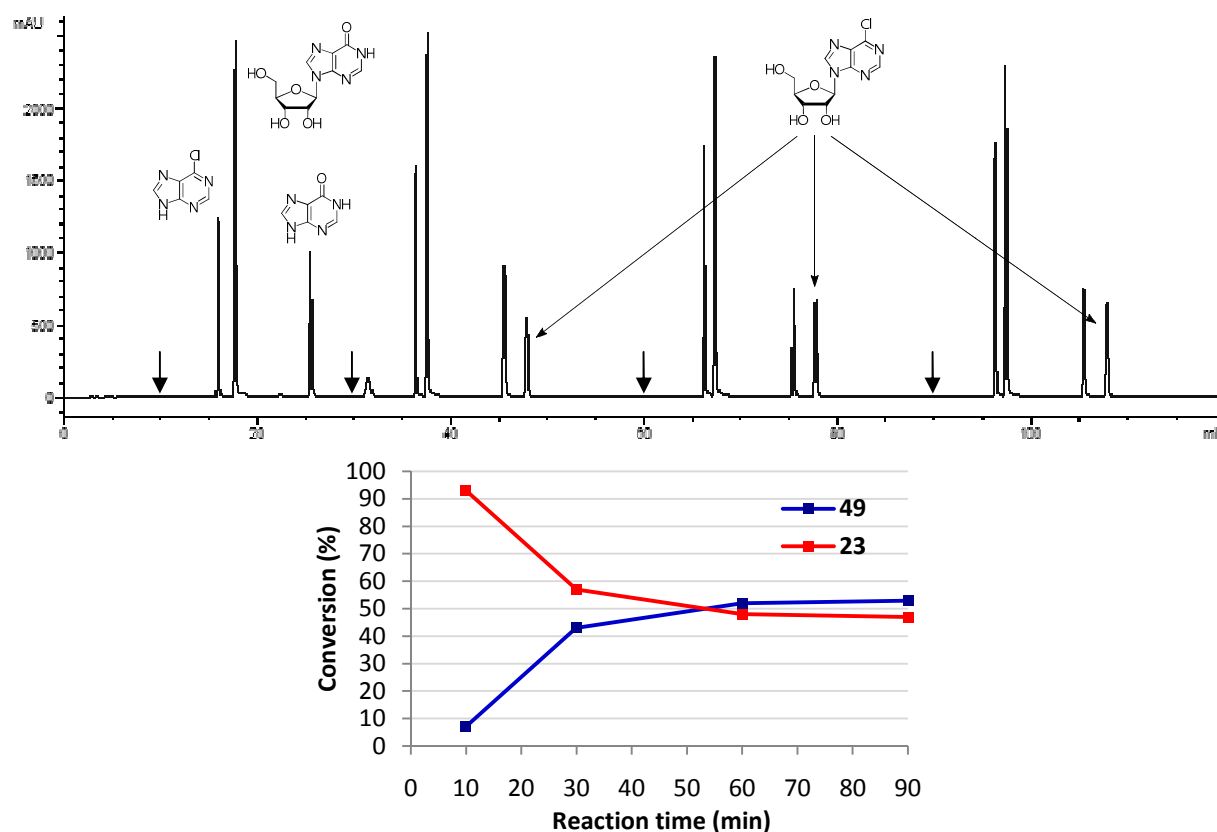


Figure 3.10. Synthesis of **49** by transglycosylation of **23** and **37** catalyzed by *Ah*PNP-IMER (Adapted with permission from *Adv. Synth. Catal.* **2015**, *357*, 2520-2528)¹¹⁰

Conversions were calculated from the depletion of the purine base and the formation of the nucleoside according to the equation previously reported for batch reactions (see **3.2.1**).¹⁰⁹ The advantage of such a flow approach in terms of yield, reaction time, purification and, generally speaking, simplification over the batch synthesis can be drawn from the experimental data presented in **Table 3.2**. The highest conversion for all nucleobases (77-89% with the only exception of 52% for **23**) was achieved after only 30'.

Starting from the conditions optimized on analytical scale, the synthesis of ribonucleosides **31**, **32**, **34**, **49** and **58** was finally repeated on semi-preparative scale (**Figure 3.11**). The on-line monitoring and purification of products was carried out by an apparatus very similar to the one already employed, with two exceptions: a three-way valve (Y) in System 1 and a semi-preparative HPLC column in System 2.

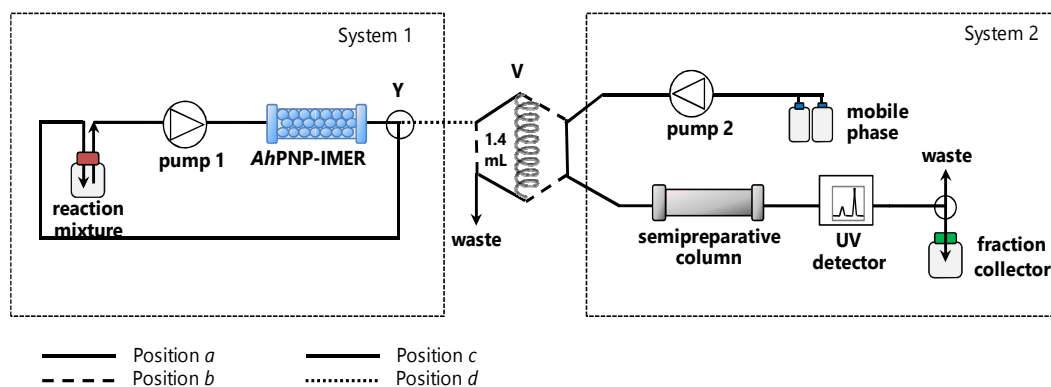


Figure 3.11. IMER-based system (semi-preparative apparatus) (Adapted with permission from *Adv. Synth. Catal.* **2015**, *357*, 2520-2528)¹¹⁰

As V and Y are in position *a* and *c*, respectively, the two systems are disconnected and the reaction is recirculated through the IMER; meanwhile, the column is conditioning. Once again, portions of the mixture can be loaded into the loop (1.4 mL) and transferred to the column as V switches to *b* and Y to *c*. This completely automated procedure was repeated until the whole mixture was consumed, by consecutive on-line sample transfer, to purify the desired product. All reaction mixtures were eluted through the semi-preparative HPLC column. The aliquot corresponding to the product nucleoside was collected, freeze-dried and characterized by $^1\text{H-NMR}$, $^{13}\text{C-NMR}$, MS and UV-Vis spectroscopy (for semi-preparative chromatograms, $^1\text{H-NMR}$, $^{13}\text{C-NMR}$ and Uv-Vis spectra, see **6.3**). The semi-preparative chromatogram and the $^1\text{H-NMR}$ spectrum of **32** are reported, as examples, in **Figures 3.12a** and **3.12b**.

The five products were obtained in high purity and yields, corresponding to their analytical conversions and ranging between 52 and 89% (3.8-7.5 mg), as reported in **Table 3.2**.

Among the assayed purines, **26** represents an interesting substrate because its arabinosyl derivative¹¹³ (Nelarabine) is an anticancer drug currently used in therapy.

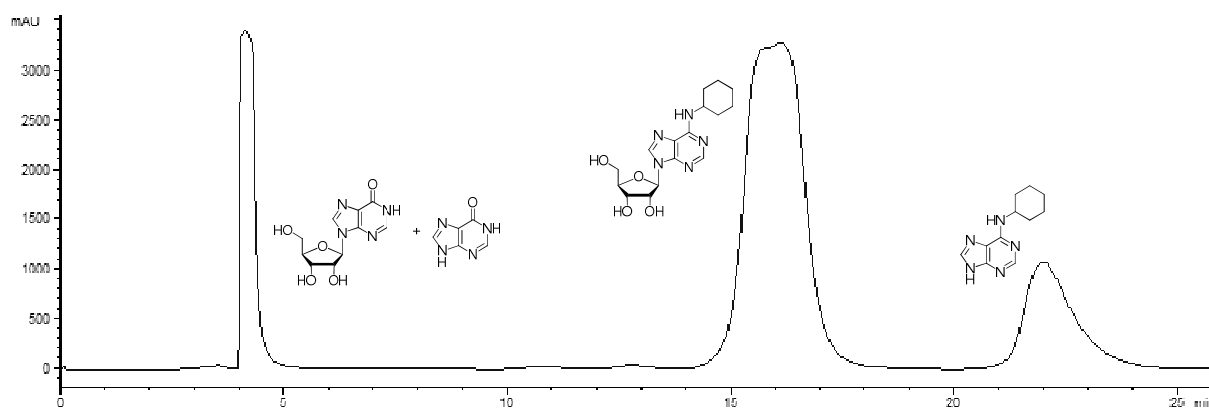


Figure 3.12a. Semi-preparative chromatogram of **32** (Adapted with permission from *Adv. Synth. Catal.* **2015**, *357*, 2520-2528)¹¹⁰

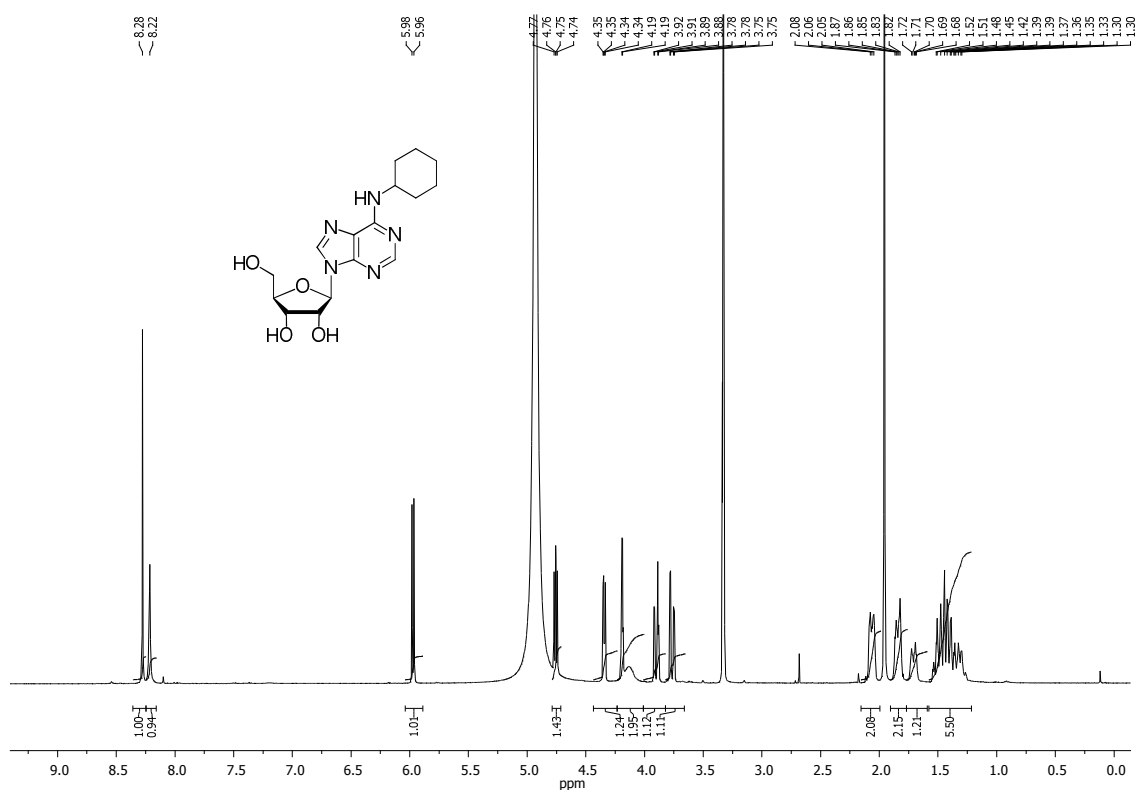


Figure 3.12b. $^1\text{H-NMR}$ spectrum of **32** (CD_3OD) (Adapted with permission from *Adv. Synth. Catal.* **2015**, 357, 2520-2528)¹¹⁰

It must be pointed out that this work was stimulated by the previous phosphorolysis studies that suggested the possibility of synthesizing 6-substituted purine ribonucleosides by a *AhPNP*-catalyzed transglycosylation. Indeed, rather than being aimed at developing a preparative process to obtain the corresponding nucleosides, their goal had been the preliminary definition of substrate specificity for a scaled up process based on that information. In addition, although a direct comparison between a batch and a flow system is not correct because of the different experimental conditions (enzyme amount, ribose *donor*, ...), the advantages of the *AhPNP*-IMER in terms of catalyst reuse, stability, reduced times and circumvention of downstream processing are undeniable.

3.2.3. Chemoenzymatic synthesis of 6-substituted purine 2'-deoxyribo- and arabinonucleosides catalyzed by *AhPNP*

Starting from the encouraging results obtained in the chemoenzymatic synthesis of ribonucleosides by a “one pot, one enzyme” approach, both under batch and flow conditions (see **3.2.1**¹⁰⁹ and **3.2.2**¹¹⁰), the synthesis of other analogues *via* the same strategy was explored. In this case, however, the focus was shifted from base-modified ribonucleosides to sugar-modified purine nucleosides. Indeed, the high promiscuity of *AhPNP* had emerged also toward 2'-deoxyribose and, to a lesser extent, arabinose.^{10c}

2'-Deoxyribo- and arabinonucleosides can be found among relevant molecules endowed with a wide array of pharmacological activities (**Figure 3.13**). In this respect, the chance to access these molecules through innovative and straightforward synthetic routes makes the chemoenzymatic procedures here developed of a wide applicative interest.

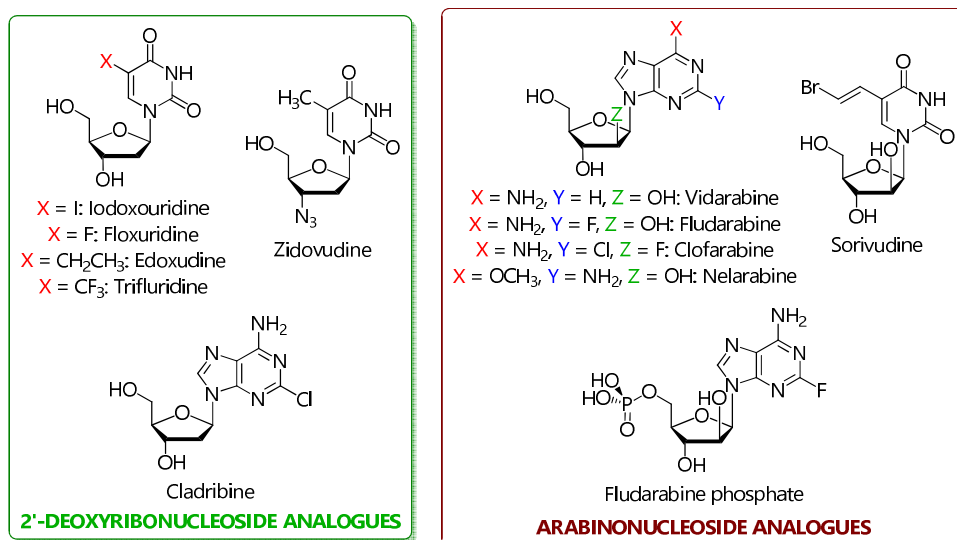


Figure 3.13. Examples of pharmacologically active 2'-deoxyribo- and arabinonucleoside analogues

To obtain a simple and straightforward “one-enzyme” process, 7-methyl-2'-deoxyguanosine and 7-methylarabinosylguanine iodides (**66** and **67**, respectively) were envisaged, and thus prepared and used, as convenient sugar *donors*, according to the previously described strategy.

Before running the enzymatic transglycosylations with **66** and **67**, their stability was assessed (**Figures 3.14a** and **3.14b**).

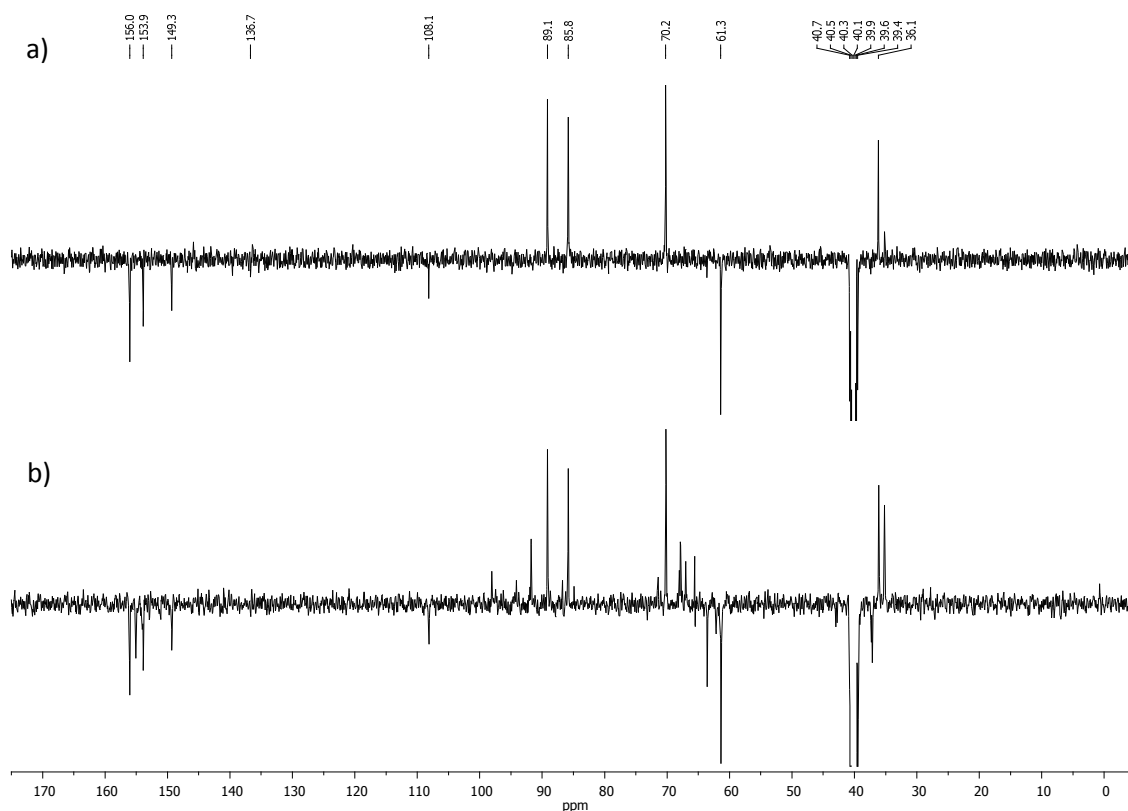
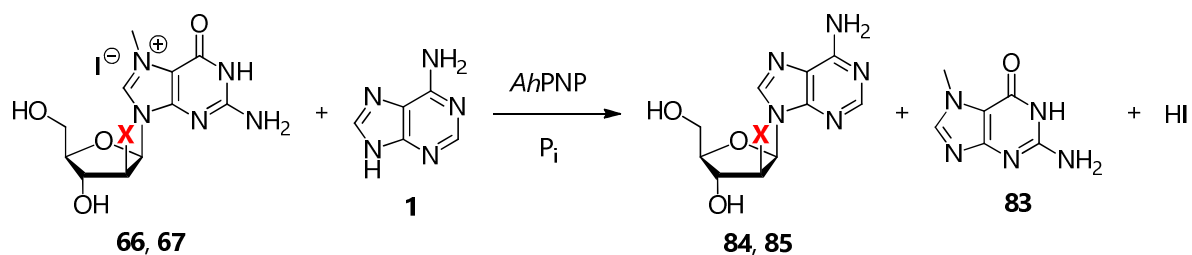


Figure 3.14. Comparison of ¹³C-NMR spectra of **66** in DMSO-*d*₆ (0.05 M): **a**) after 2 h; **b**) after 4 h.

After 48 h, no decomposition/hydrolysis products were detected in batch. However, NMR analysis clearly highlighted the instability of salt **66** in DMSO solution (0.05 M in DMSO-*d*₆) at 25°C. In contrast to **67**, **66**

apparently undergoes a rapid partial decomposition generating new carbon signals after only 4 h (**Figure 3.14b**) and confirming the validity of the precautions taken during its synthesis. The ^{13}C -NMR spectrum of **66** was therefore registered within 2 h at 25°C, showing no sign of decomposition (**Figure 3.14a**).

Transglycosylation reactions were carried out in agreement with the standard protocol (**Table 3.3**), at 25°C in 50 mM K_2HPO_4 buffer (pH 7.5) containing 20% (v/v) glycerol at 1 mM concentration. The nucleoside *donor* and the nucleobase *acceptor* were used in 1:1 molar ratio. Being accepted by *AhpNP*, adenine (**1**) was selected as *acceptor* to assess the feasibility of the approach.



X	Nucleoside	Donor conversion (%) ^{a)}	Nucleoside formation (%) ^{a)}
H	84	> 99	66
OH	85	0	0

^{a)} Determined at 6 h

Table 3.3. Synthesis of **84** and **85** by “one-pot, one-enzyme” transglycosylation catalyzed by *AhpNP*

Reaction progress was monitored by HPLC and conversions were calculated from the sugar *donor* consumption and product formation according to the following equations:

$$\text{Phosphorolysis (\%)} = \frac{\text{sugar donor area}}{\text{initial sugar donor area} + \text{base area}} \cdot f \cdot 100 \quad f = \frac{\text{IS area}}{\text{initial IS area}} \cdot 100$$

$$\text{Transglycosylation (\%)} = \frac{\text{product area}}{\text{product area} + \text{base area}} \cdot 100$$

A conversion factor f was calculated to assess the percentage of phosphorolysis, as the area of 7-methylguanine could not be considered reliable due to its poor water solubility. Uracil (**87**) was added to the reaction mixture as internal standard for this purpose.

Upon the total conversion of **66**, the formation of **84** reached 66% at equilibrium. On the other hand, neither the phosphorolysis of **67** or the formation of **85** were detected (**Figure 3.15**).

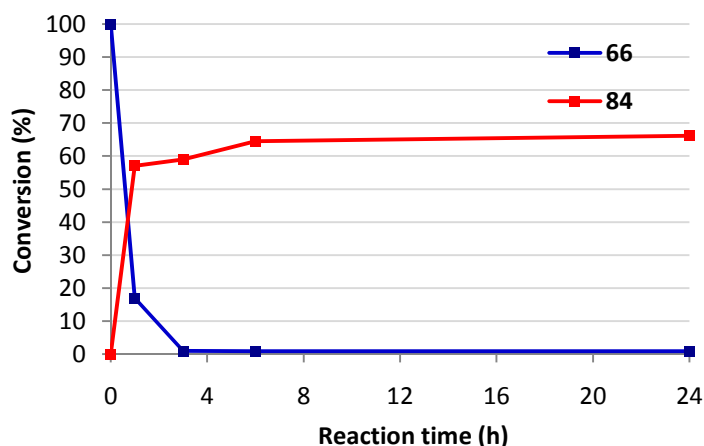


Figure 3.15. Phosphorolysis of **66** and formation of **84** catalyzed by *Ah*PNP

Such preliminary results proved the feasibility of this method for the synthesis of 2'-deoxyadenosine (**84**), but opened the issue of the "lack of fit" between 7-methylarabinosylguanine iodide (**67**) and *Ah*PNP. On one hand, this result appeared consistent with the moderate preference of the enzyme toward arabinosyl derivatives with respect to natural nucleosides.¹⁰¹ On the other hand, however, *Ah*PNP was previously demonstrated to accept α -D-arabinose-1-phosphate as substrate in the synthesis of arabinosyladenine (**85**, Vidarabine), a known antiviral drug.^{10c} In the latter case, the sugar phosphate was produced through the phosphorolysis of arabinosyluracil catalyzed by a uridine phosphorylase from *Clostridium perfringens* (*Cp*UP) in a "two-enzyme, one-pot" reaction. This evidence suggests that, whereas α -D-arabinose-1-phosphate is accepted as substrate, 7-methylarabinosylguanine is not phosphorolyzed by *Ah*PNP. Further experiments are in progress.

3.2.4. Chemoenzymatic synthesis of adenosine, 2'-deoxyadenosine and arabinosyladenine catalyzed by a *Cp*UP-IMER coupled with a *Ah*PNP-IMER ("in flow" reaction)

3.2.4.1. Development, activity and stability of *Cp*UP/*Ah*PNP-IMER and *Cp*UP-IMER

Starting from the flow-based approach for the synthesis and the on-line purification of 6-substituted purine ribonucleosides by transglycosylations catalyzed by the *Ah*PNP-IMER (see 3.2.2)¹¹⁰, the following step was to explore the development of a similar system to perform a bi-enzymatic reaction. This approach, which relies on the coupling of a pyrimidine nucleoside phosphorylase (PyNP) with a purine nucleoside phosphorylase (PNP), is the most frequently exploited scheme, where the pyrimidine nucleoside acts as the *donor* of α -D-pentofuranose-1-phosphate and the purine base as the *acceptor*.^{32e} In this case, the focus was shifted toward the "one-pot, two-enzyme" synthesis of sugar-modified adenine nucleosides, including arabinosyladenine (Vidarabine, **85**), an antiviral drug previously synthesized by the same couple of enzymes but in batch conditions.^{10c}

Since the co-immobilization of both enzymes on the same particle-based support resulted in excessive back-pressures (data not shown), it was decided to explore the use of independent stationary phases for each catalyst to be connected in series. An advantage of this set-up would be the availability of single bioreactors that could be used independently, either for a "one-enzyme" synthesis or in a different sequence. However, the use of two particle bioreactors in series can be critical due to the overall back-pressure of the system. Therefore, an aminopropylsilica monolithic support was selected for *Cp*UP to maintain the same immobilization chemistry used for *Ah*PNP (see 3.2.2.1).¹¹⁴ *Cp*UP (20 mg) was submitted to the immobilization reaction affording a good yield (13 mg, 66%).

When not in use, the *CpUP*-IMER was stored at 4 °C in 100 mM K_2HPO_4 buffer (pH 7.5). It was also completely stable upon 25 reactions in one month.

3.2.4.2. *CpUP*-IMER/*AhPnP*-IMER apparatus and optimization of the reaction conditions

The two IMERs containing *CpUP* and *AhPnP* were connected in series in the usual bidimensional chromatographic apparatus (Figure 3.16).

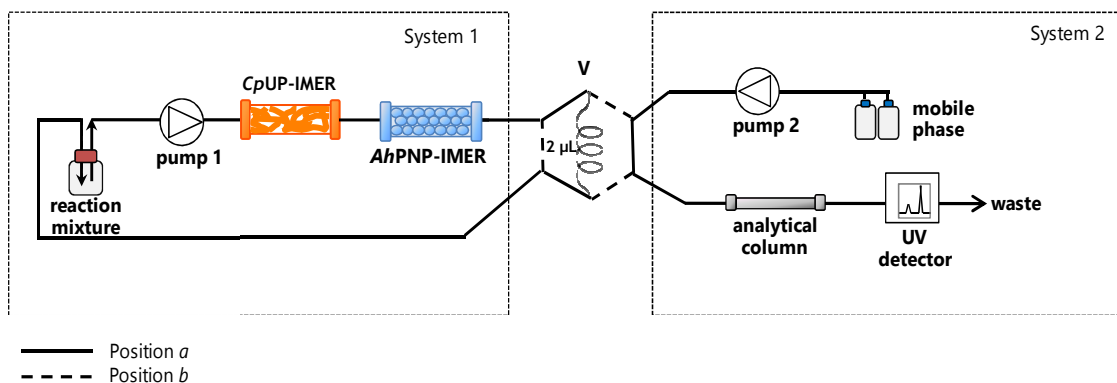
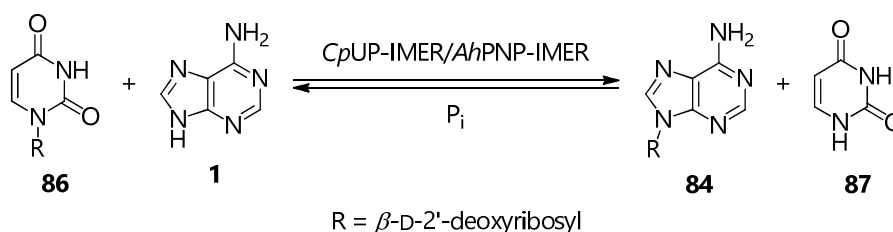


Figure 3.16. Bi-enzymatic IMER-based system (analytical apparatus)

As usual, the biotransformation occurs when the reagents are continuously recirculated through the bioreactors. Conversion is monitored on-line by automatically sampling, at fixed times, the reaction mixture that is analyzed by HPLC.

The system was characterized by using the synthesis of 2'-deoxyadenosine (**84**) as the model transglycosylation reaction (Scheme 3.31).



Scheme 3.31. Synthesis of 2'-deoxyadenosine (**84**) by transglycosylation catalyzed by the *CpUP*-IMER/*AhPnP*-IMER system

A fractional factorial experimental design was performed to optimize the experimental conditions and the same five factors focused upon for the system containing the *AhPnP*-IMER (see 3.2.2.3)¹¹⁰ were included again:

- 2'-deoxyuridine (**86**)/adenine(**1**) ratio (x_1);
- K_2HPO_4 buffer concentration (x_2);
- temperature (x_3);
- flow rate (x_4);
- pH (x_5).

As before, responses were:

- phosphorolysis % (y_1);
- transglycosylation % (y_2);
- reaction time (y_3).

Following the same linear regression model previously assumed to represent the system, all responses were elaborated, clearly showing similar requirements (**Figure 3.17**):

- values associated with both phosphorolysis (y_1) and transglycosylation (y_2) were essentially in agreement with the results for the *AhpNP*-IMER. The two key factors were indeed *donor/base* ratio and K_2HPO_4 buffer concentration;
- a major deviation from the previous model was the role of flow rate, which resulted beneficial for the first time in terms of transglycosylation percentage (y_2) and able to significantly reduce equilibrium time (y_3).

As with the mono-enzymatic apparatus, temperature and pH were set at values compatible with the activity and stability of *AhpNP* and *CpUP*.

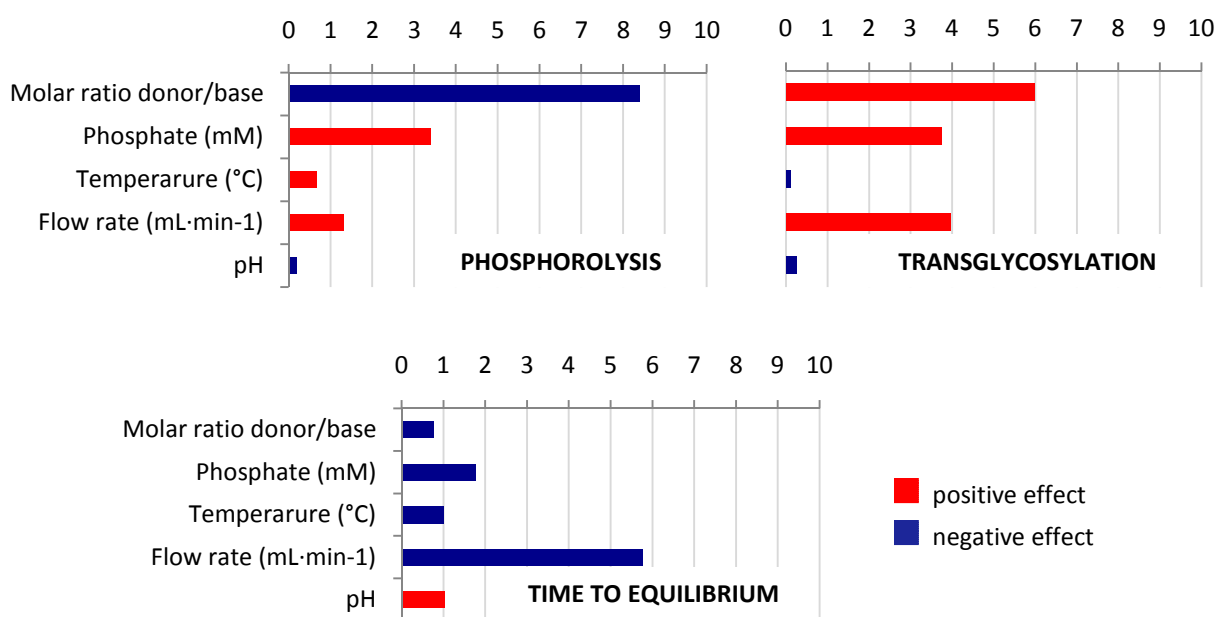


Figure 3.17. Fractional factorial design for the *CpUP*-IMER/*AhpNP*-IMER system

3.2.4.3. Synthesis of 2'-deoxyadenosine, adenosine and arabinosyladenine

The optimized conditions (5 mM **1**, 2:1 *donor/acceptor* ratio, 10 mM (for **86** and **88**) or 2 mM (for **89**) K_2HPO_4 buffer (pH 7.25), 37°C, flow rate 0.5 mL·min⁻¹) were applied to the synthesis of 2'-deoxyadenosine (**84**), adenosine (**27**) and arabinosyladenine (**85**) (**Figure 3.18**). Therefore, 2'-deoxyuridine (**86**), uridine (**88**) and arabinosyluracil (**89**), respectively, were chosen as sugar *donors* for the formation of the corresponding α -D-pentofuranose-1-phosphate by the *CpUP*-IMER-catalyzed phosphorylation, whereas adenine (**1**) was selected as the purine *acceptor* for the glycosylation catalyzed by the *AhpNP*-IMER. The lower concentration used for **89** was addressed by the poor solubility of the corresponding product **85** (~ 2 mM) under experimental conditions.

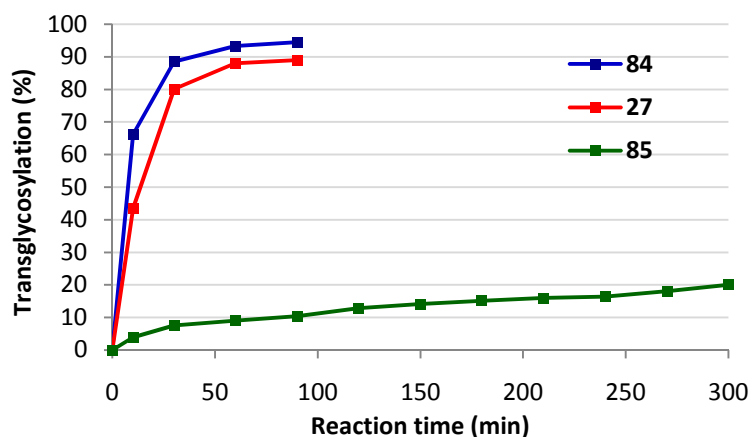
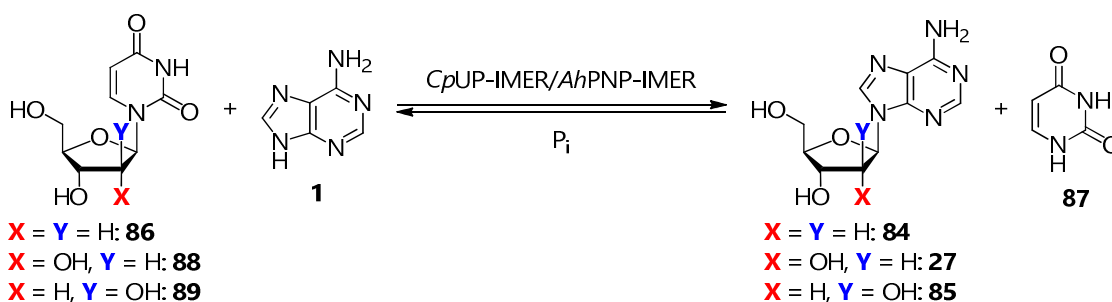


Figure 3.18. Synthesis of **84**, **27** and **85** catalyzed by the *CpUP-IMER/AhpNP-IMER* system

As an example, the sequential chromatogram for the synthesis of **84** is reported in Figure 3.19. By comparing the reaction profile after 30' and 90', it is possible to notice the progressive formation of the target nucleoside **84** and of **87**, as well as the decrease of **86** and **1**.

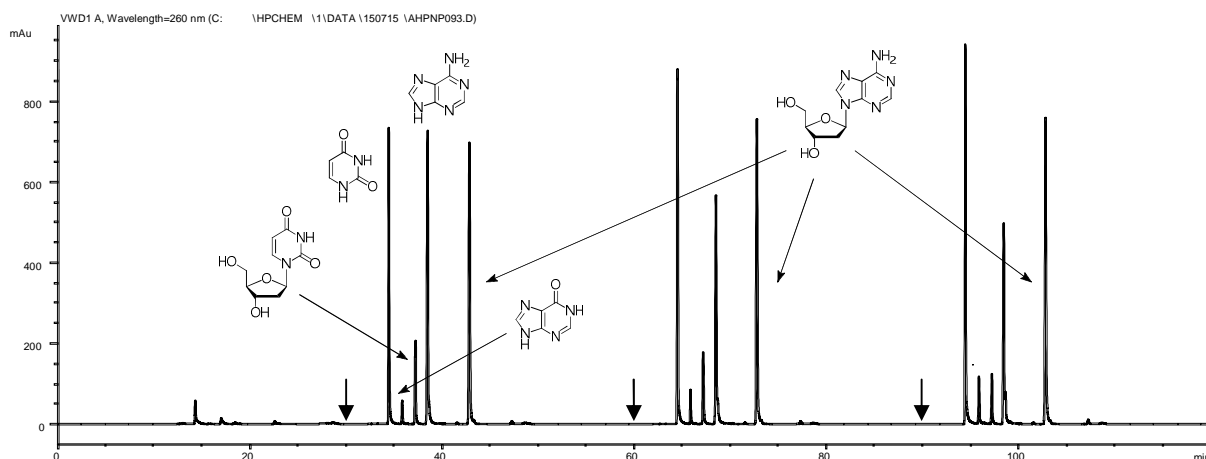


Figure 3.19. Sequential chromatogram for the synthesis of **84**

Moreover, an additional peak between **87** and **89** with a constant area over time was detected. Considering its retention time, it was roughly attributed to hypoxanthine (**11**). In fact, this nucleobase might be a contaminant deriving from the phosphorolysis of inosine (**37**), periodically carried out to test the activity and stability of the *AhpNP-IMER*.

Transglycosylation percentages were calculated as with the *AhpNP-IMER* system. While the synthesis of **84** and **27** reached a plateau corresponding to 95 and 90% conversion (55 and 50% phosphorolysis), respectively, such a trend did not occur in the case of **85**. In fact, after 5 h, the highest obtained conversion

was approximately 20%. These transglycosylation results reflect the substrate specificity of *CpUP* toward **86** ($68 \text{ IU}\cdot\text{mg}^{-1}$), **88** ($60 \text{ IU}\cdot\text{mg}^{-1}$) and **89** ($3 \text{ IU}\cdot\text{mg}^{-1}$), which reveals the higher availability of α -D-ribose- and α -2'-deoxyribose-1-phosphate with respect to their arabinose counterpart for the subsequent transglycosylation.^{10c} For this reason, the synthesis of **85** was run overnight (24 h). Surprisingly, the chromatographic profile was not as expected (**Figure 3.20**).

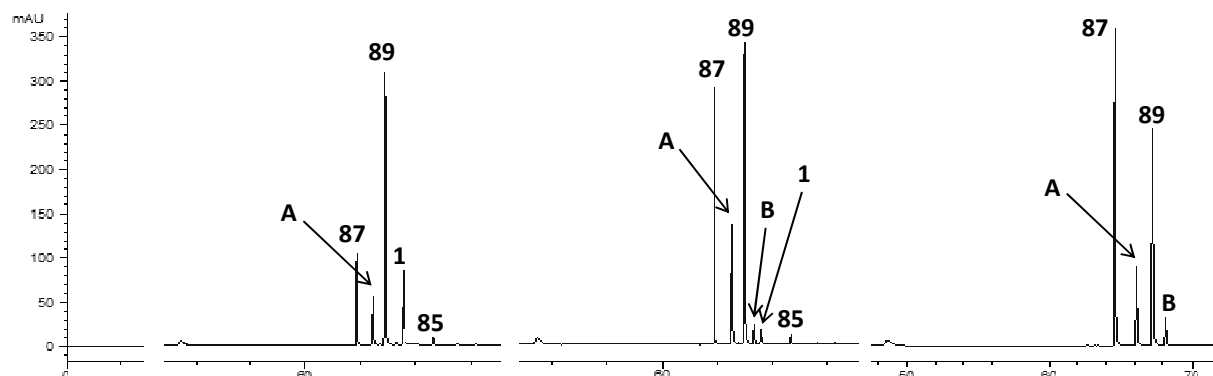


Figure 3.20. Chromatograms for the synthesis of **85** at 60', 180' and 300' (**89**: arabinsyluracyl, **1**: adenine, **85**: arabinsyladenine, **87**: uracyl, **A**: hypoxanthine (1ST unknown peak), **B**: arabinsylhypoxanthine (2ND unknown peak))

In fact, two additional peaks with variable area over time (**A** and **B**) were revealed besides the four expected ones. As the area of **A** decreased while the one of **B** increased proportionally, the analytical method was transferred to an LC-UV-ESI-MS/MS apparatus and **A** was unequivocally attributed to hypoxanthine (**11**), whereas **B** to arabinsylhypoxanthine (**90**), suggesting that a parallel transglycosylation might occur involving **11** as a competitive *acceptor*. On this ground, the results obtained by running the same reaction in batch by using soluble *CpUP* and *AhPNP* under the same experimental conditions were in agreement with this hypothesis, since both the formation of **85** and **90** were observed.

It was speculated that **11** might exclusively derive from the standard activity assay based on the phosphorolysis of inosine (**27**), which was carried out at a very high substrate concentration. Therefore, a contamination of the bioreactor could not be ruled out. It could not be excluded that the same competitive reaction would happen also in the case of **27** and **84**, although both reactions reached the highest conversion in less than 2 h and were stopped immediately after.

This study has paved the way to the transition from an analytical scale device to the development of a meso-scale platform for the preparative synthesis of nucleosides, as well as to the further implementation of such a system with more bioreactors to perform multi-enzymatic reactions.

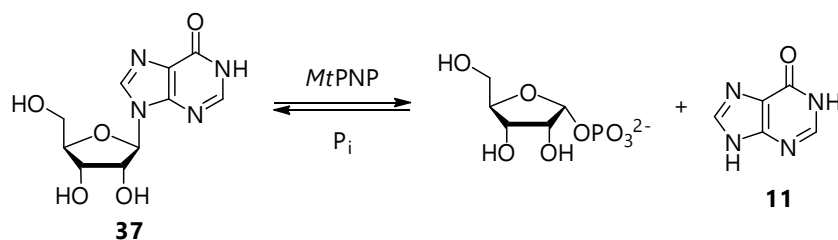
3.3. Evaluation of the inhibitory activity of 8-substituted purine ribonucleosides against the PNP from *Mycobacterium tuberculosis* (*MtPNP*)¹¹⁵

3.3.1. LC-ESI-MS/MS enzymatic assay

One of the goals of the research reported in this Thesis was to prepare modified nucleosides as selective inhibitors of the purine nucleoside phosphorylase from *Mycobacterium tuberculosis* (*MtPNP*). To this aim, a new medium/high throughput LC-ESI-MS/MS method was set up to assess the inhibition activity of a number of 8-substituted purine ribonucleosides (**70**, **71**, **74**, **76**, **77**, **79** and **80**, see 3.1.7) against two

bacterial PNPs (*Ahp*PNP and *Mt*PNP) as well as the human one (*Hsp*PNP). Specifically, *Ahp*PNP was used as the model enzyme, whereas assays with *Hsp*PNP and *Mt*PNP were carried out to determine if the selected compounds might show different selectivities in the inhibition of these enzymes. Indeed, based on the key role of PNPs in the *in vivo* synthesis of nucleosides, they have been identified as a potential therapeutic target to control certain bacterial or parasitic infections.^{70, 98, 116} In the validation of the method, two known inhibitors of PNPs, *i.e.* Acyclovir (**91**) and Formycin A (**92**), were chosen as reference compounds (only the first one being able to inhibit both *Hsp*PNP and *Mt*PNP).

The inhibitory activity was assessed through the phosphorolysis assay of inosine (**37**) to hypoxanthine (**11**), routinely used to test the activity of PNPs, as previously discussed (Scheme 3.32, see 3.2.2.2).



Scheme 3.32. Phosphorolysis of **37** catalyzed by *Mt*PNP

The inhibition assay was performed in a 96-well plate (volume = 0.5 mL, enzyme < 0.2 $\mu\text{g}\cdot\text{well}^{-1}$, 37°C) with an overall time of about 15 min·plate⁻¹ for sample processing and 2 min·sample⁻¹ for analysis (Figure 3.21).

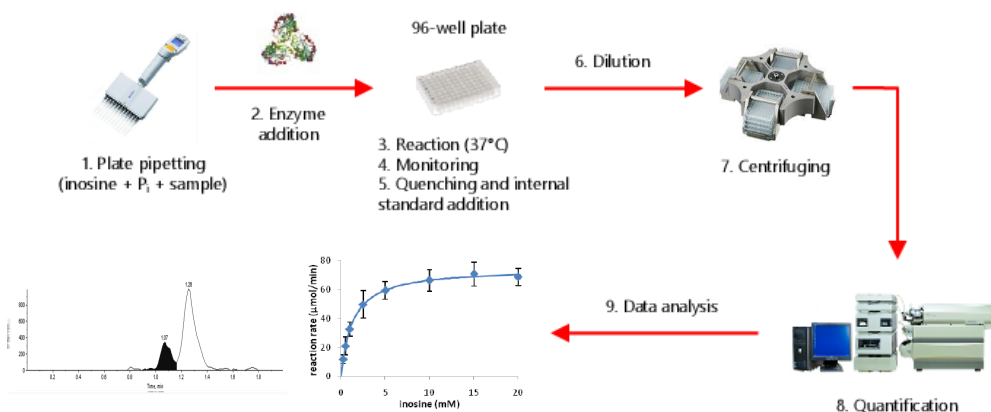


Figure 3.21. Sketch of the LC-ESI-MS/MS analytical apparatus (Adapted with permission from *Anal. Chim. Acta* **2016**, *943*, 89-97)¹¹⁵

A mixture of **37**, K_2HPO_4 buffer and the selected analyte was prepared by pipetting the corresponding solutions in the 96-well plate, and after the addition of the enzyme (*Ahp*PNP, *Hsp*PNP or *Mt*PNP), the reaction was heated at 37°C in a water-shaking bath for the required time. Each mixture was quenched by addition of CH_3CN (1:20) to inactivate the enzyme. Internal standards (ISs) were added as well, then the obtained solution was diluted again for LC separation and ESI-MS/MS quantification.

3.3.2. Kinetic parameters of *Ah*, *Hs* and *Mt*PNP

The Michaelis-Menten curve describes the velocity of an enzymatic reaction (v , $\mu\text{mol}\cdot\text{min}^{-1}$ = μmoles of product produced per minute, also called IU = international unit) under increasing concentrations of substrate ($[\text{S}]$) in a range between 0.1 and 10 times the expected K_M value ($0.1K_M < K_M < 10K_M$).

The following equation describes the classic Michaelis-Menten model:

$$v = \frac{V_{\max} [S]}{K_M + [S]} \quad V_{\max} = k_{\text{cat}} [E]_0$$

K_M is the substrate concentration at which the reaction rate is $\frac{1}{2} V_{\max}$ (maximum reaction rate), while k_{cat} is defined as the maximum number of substrate molecules that an enzyme can convert to product per catalytic site in the unit of time and can be calculated as $k_{\text{cat}} = V_{\max} \cdot [E]_0^{-1}$ ($[E]_0$ = enzyme concentration).

As already mentioned, the phosphorolysis reaction requires inorganic phosphate (P_i) and inosine (**37**). The source of P_i is the assay buffer ($\text{NH}_4\text{H}_2\text{PO}_4$, pH 7.5). The kinetic constants (K_M , V_{\max} and k_{cat}) were determined using increasing concentrations of **37** (0.01-20 mM) under a saturating concentration of P_i and *vice versa* (1 μM -20 mM P_i). The resulting kinetic constants are reported in **Table 3.4**. The kinetic profile of *Ah*PNP is depicted in **Figure 3.22**.

Enzyme	Constant	Substrate			
		Inosine (37)		P_i	
		value	standard error	value	standard error
<i>Ah</i> PNP	K_M (mM)	1.30 [1.8] ^{a)}	$7 \cdot 10^{-2}$	0.19	$2 \cdot 10^{-2}$
	V_{\max} ($\mu\text{mol} \cdot \text{min}^{-1}$)	42	1	49.3	0.9
	K_{cat} (s^{-1})	$3.73 \cdot 10^5$	$9 \cdot 10^3$	$4.43 \cdot 10^5$	$8 \cdot 10^3$
	K_{cat}/K_M ($\text{s}^{-1} \cdot \text{M}^{-1}$)	288	9	2289	8
<i>Hs</i> PNP	K_M (mM)	0.15 [0.133] ^{a)}	$2 \cdot 10^{-2}$	0.66	$5 \cdot 10^{-2}$
	V_{\max} ($\mu\text{mol} \cdot \text{min}^{-1}$)	0.0022	$3 \cdot 10^{-4}$	0.0123	$3 \cdot 10^{-4}$
	K_{cat} (s^{-1})	14	2	76	2
	K_{cat}/K_M ($\text{s}^{-1} \cdot \text{M}^{-1}$)	0.09	$2 \cdot 10^{-3}$	0.11	$2 \cdot 10^{-3}$
<i>Mt</i> PNP	K_M (mM)	0.06 [0.04] ^{a)}	$9 \cdot 10^{-3}$	0.15 [0.583] ^{a)}	$2 \cdot 10^{-2}$
	V_{\max} ($\mu\text{mol} \cdot \text{min}^{-1}$)	0.00908	$9 \cdot 10^{-5}$	0.0026	$1 \cdot 10^{-4}$
	K_{cat} (s^{-1})	15.7 [5.4] ^{a)}	0.2	4.5 [6.9] ^{a)}	0.2
	K_{cat}/K_M ($\text{s}^{-1} \cdot \text{M}^{-1}$)	0.24	$2 \cdot 10^{-4}$	0.03	$2 \cdot 10^{-4}$

^{a)} Values reported in literature

Table 3.4. Kinetic parameters (K_M , V_{\max} and k_{cat}) of **37** and P_i for *Ah*PNP, *Hs*PNP and *Mt*PNP

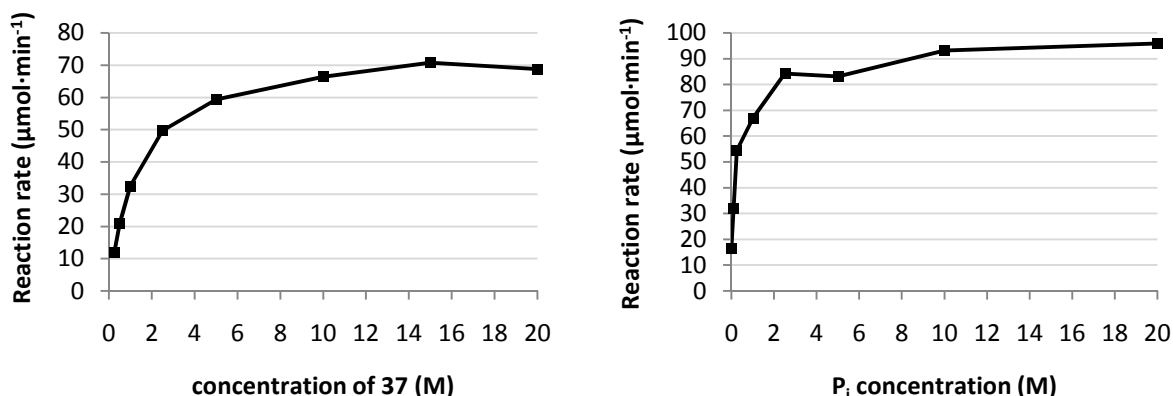


Figure 3.22. Kinetic profile of *Ah*PNP with respect to **37** and P_i

The obtained K_M for *AhpNP* with respect to **37** is in agreement with literature.¹⁰² Indeed, the reported K_M value is 1.8 ± 0.5 mM at 25 °C, therefore a slight difference in the K_M at 37 °C can be expected. The same consideration could be done with *HsPNP* for which the K_M value measured by de Moraes *et al.* (0.133 ± 0.15 mM) was considered as a comparison, since it was assessed by using the same enzymatic preparation.^{87e} Slight differences of *MtPNP* kinetic values reported in literature with respect to the obtained data might be ascribed to the different experimental conditions (temperature and buffer).^{75b}

3.3.3. Inhibition screening assays

A set of nucleoside-based structures (**70**, **71**, **74**, **76**, **77**, **79**, **80**, **91** and **92**) were assayed as potential inhibitors of *MtPNP* (Figure 3.23). Only seven out of the overall pool of the synthesized 8-substituted inosines, guanosines and adenosines (see 3.1.7) were selected for this purpose. Acyclovir (**91**) and Formycin A (**92**) were used as negative and positive controls, being known inhibitors of trimeric PNPs (such as *HsPNP* and *MtPNP*) and hexameric ones, respectively.

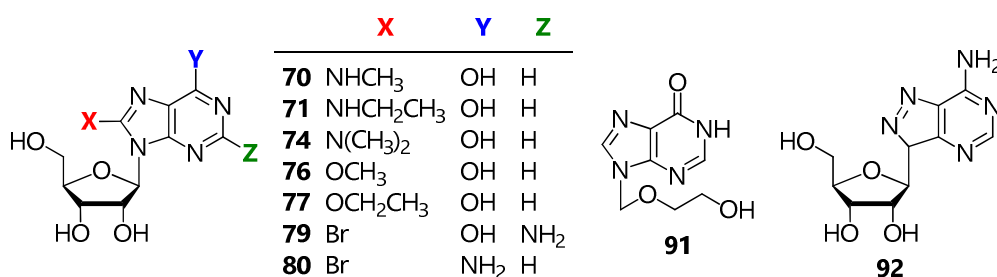


Figure 3.23. Structures of compounds tested as inhibitors (**70-80**, **91** and **92**)

The phosphorolysis reaction was performed by using a concentration of **37** close to the K_M value of the specific enzyme under a saturating concentration of P_i , in the presence of a defined amount of inhibitor (1-0.5 mM).

From the inspection of Figure 3.24 (data about *AhpNP* are not reported), it can be noted that only a few compounds showed an activity toward *HsPNP* and *MtPNP*, namely **70** and **79**, besides the expected inhibition exerted by **91**.

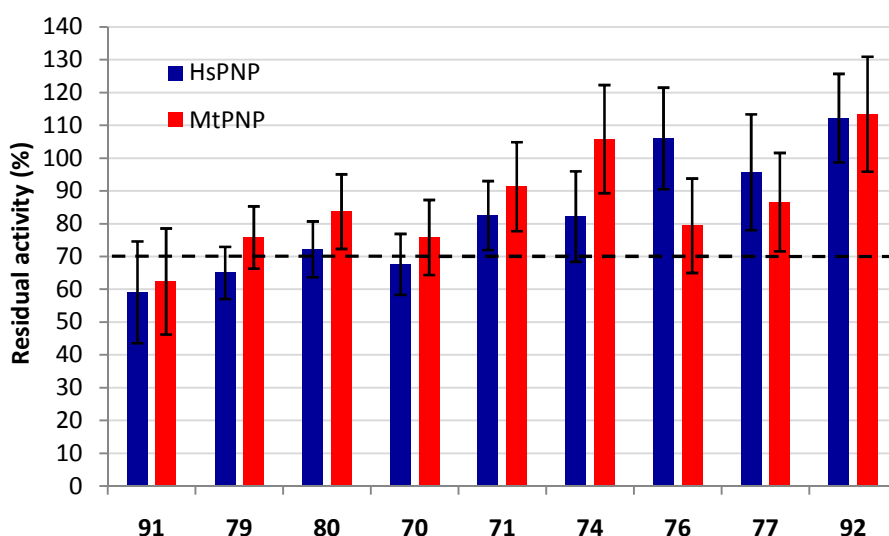


Figure 3.24. Screening of potential inhibitors of *HsPNP* and *MtPNP*

These compounds (**91**, **70** and **79**), which mildly inhibited the target enzymes, were selected for the assessment of their K_i values. The assay was performed at a fixed substrate concentration close to the K_M value for each enzyme, and by increasing the concentration of the inhibitor. All other conditions were the same as in the enzymatic assay. The results, reported in **Table 3.5**, were compared with the activity in absence of inhibitor (100% activity).

Compound	HsPNP		MtPNP	
	-Log(K_i)	SD	-Log(K_i)	SD
91	3.186	0.666	4.511	0.210
70	2.932	1.172	< 3 ^{a)}	-
79	< 3 ^{a)}	-	< 3 ^{a)}	-

^{a)} Not calculated in the selected concentration range (0.1-1 mM)

Table 3.5. K_i values of **91**, **70** and **79** for HsPNP and MtPNP

From these experimental data, the following observations can be drawn:

- the K_i value of **91** for HsPNP, evaluated by Tuttle and Krenitsky *et al.* through a spectrophotometric assay, was found to be 100 μM ¹¹⁷, while the determined one was ~ 600.
- a generally low potency in the studied concentration range was assessed not only for **70** ($K_i = 1.1$ mM for HsPNP) but also for **79**, whose K_i was not even computable for both enzymes, as for **70** with respect to MtPNP.

Such preliminary results might be correlated with the same structural impediments which do not allow AhPNP to phosphorylate 8-substituted ribonucleosides (see **1.4.5**^{81,82} and **1.6.1**^{63b}), since these molecules are likely to adopt a *syn* conformation due to steric constraints at C⁸. As already reported, this probably leads to a lack of recognition by the enzyme.

In order to verify this hypothesis, the empirical method reported by Nair and Young (see **1.4.5**)⁸⁵, which correlates the conformational preference of purine nucleosides to the extent of the ¹³C NMR chemical shift difference between C^{2'} and C^{3'}, was applied to the tested 8-substituted purine nucleosides (**Table 3.6**).

Compound	$\delta_{C^{2'}}$	$\delta_{C^{3'}}$	$\Delta\delta_{C^{2'}.C^{3'}}^{\text{a)}$
70	71.3	71.7	0.4
71	71.0	71.2	0.2
74	71.4	71.1	0.3
76	71.8	71.4	0.4
77	71.7	71.2	0.5
79	70.8	71.0	0.2
80	71.6	71.3	0.3

^{a)} Reported as absolute values

Table 3.6. Calculated $\Delta\delta_{C^{2'}.C^{3'}}$ values for the tested 8-substituted ribonucleosides

The ¹³C-NMR $\Delta\delta_{C^{2'}.C^{3'}}$ values were found to be < 0.5 in all tested compounds, thus hinting a predominant *syn* conformation. These results suggest a relevant role of conformation in all the tested potential inhibitors, which may justify a lack of recognition by not only AhPNP (data not reported) but also at the one from *M. tuberculosis*.

Moreover, although the assayed compounds did not show a relevant inhibitory activity, it is worth pointing out that the developed method is reliable and depends upon on a straightforward and very rapid sample processing and analysis.

4 | SYNTHESIS OF POTENTIAL LIGANDS OF THE HUMAN GPR17 RECEPTOR

4.1. Role of GPR17 in neurodegenerative disorders

4.1.1. Neurodegenerative disorders

Many neurodegenerative disorders are closely linked to metabolic dysregulations of the central nervous system (CNS) caused by the deterioration and malfunction of myelinating cells.¹¹⁸ The myelin sheath is a thin fat layer concentrically convoluted around neuronal axons, whose function is to insulate them to ensure an effective signal transmission in a cell network by protecting its integrity.^{118, 119} Extracellular ATP and uracil nucleosides have been identified as signaling agents. G Protein-Coupled Receptors (GPCRs) play a relevant role in many stages of glial cells development.¹²⁰

Therefore, the demyelination of axons results in exposure toward permanent degeneration, as well as to a number of neurological diseases (multiple sclerosis, ischemia, amyotrophic lateral sclerosis (ALS), Alzheimer's disease and miscellaneous psychiatric disorders such as schizophrenia, depression, autism, dyslexia and bipolar disorder).

For all the reasons described above, remyelination processes may embody an original way to treat disorders of the CNS. Pharmacological treatments can be expected to restore the minimal conditions for myeline production by selectively targeting purinergic receptors (*e.g.* specific GPCRs).

4.1.2. G Protein-Coupled Receptors (GPCRs)

Being the leading group of transmembranal proteins encoded in the human genome, GPCRs represent important drug targets in medicinal chemistry.

As of 2011, six receptors with medium to high resolution crystal structures have been studied with multiple small ligands (rhodopsin, β_1 and β_2 adrenergic receptors, adenosine A_{2A} receptor, chemokine CXCR4 receptor and dopamine D_3 receptor). The first four GPCRs have been isolated in complex with both agonists and antagonists. This protein class is currently vital in drug discovery, as more than 70 new drugs affecting the metabolism of GPCRs have been commercialized in the last fifteen years, representing roughly 24% of all drugs reaching the market during this period.¹²¹

Several common elements can be identified in the structures of GPCRs belonging to various organisms (**Figure 4.1a**). The core of each receptor is an almost perpendicular transmembrane domain (TMD) consisting of seven α -helices (TMs) arranged in a cylindrical fashion and tilted out of plane. Their outer surfaces are largely hydrophobic, confining all binding interactions to the side chains or the intra- and

extracellular domains. The C-terminal region usually resides in the cytosol, while the remaining amino end protrudes from the cellular surface. Ligands can bind by hydrogen bonds to either a deeply hydrophobic cavity or a specific domain, depending on structural features. G Protein likely interacts with extended intracellular loops 2 and 3 (ICL2 and ICL3) connecting TM3-TM4 and TM5-TM6, respectively, thus triggering signal transduction.

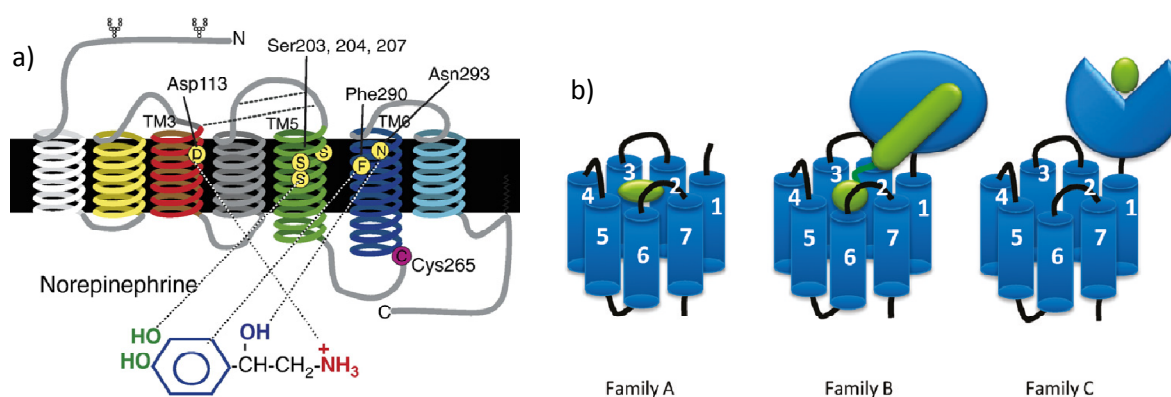


Figure 4.1. GPCR receptors: **a)** general structure (residues interacting with the ligand, in this case norepinephrine, are highlighted) (Adapted with permission from *Biochim. Biophys. Acta* **2007**, *1768*, 794-807)¹²²; **b)** three major families (A, B and C) (Reprinted from *J. Med. Chem.* **2011**, *54*, 4283-4311)¹²¹

The 390 known GPCRs in human organisms can be classified into three major families¹²³ (**Figure 4.1b**):

- family A (rhodopsin family or class I): the most populated and assorted group, especially concerning ligand typologies. Ligands are allocated in the top of the TMD bundle;
- family B (secretin and adhesion families or class II): specific for peptide-based hormones (secretin subfamily) or mostly orphan receptors (adhesion subfamily). Ligand anchoring relies on the cooperation between the TMB pocket and a glycosylated *N*-terminal region;
- family C (glutamate family or class III): specific for Glu and γ -aminobutyric acid (GABA). The binding site is located out of the TMD in a “Venus fly trap” *N*-terminal domain. They are sensitive to Ca^{2+} ions as well as to taste-active molecules.

4.1.3. GPR17 as a potential target against neurodegeneration

Among the GPCR receptors involved in myelin production, GPR17 holds a special position of interest in the eyes of medicinal chemists. Being considered orphan for many years, it has been recently matter of a deeper investigation.¹²⁴

The structure of the human GPR17 maintains all the common features of GPCRs, namely the seven transmembrane R-helices in the main domain, but its 3D structure has not been resolved in details yet, since its isolation has always eluded any effort. The spatial arrangement of GPR17 still remains largely unknown, therefore an aminoacidic sequence comparison with similar receptors is necessary to clarify it. In particular, human P2Y receptors (belonging to family A) show almost 48% sequence identity, especially with conserved motifs essential for ligand recognition and binding such as His-X-X-Arg/Lys in TM6 and Lys-Glu-X-X-Leu in TM7.¹²⁵

The identification of both endogenous and novel synthetic ligands has proceeded through *in silico* analyses based on homology models.¹²⁶ Experimental data generally suggest that GPR17 can interact with a variety of agonist and antagonist agents (**Figure 4.2**).

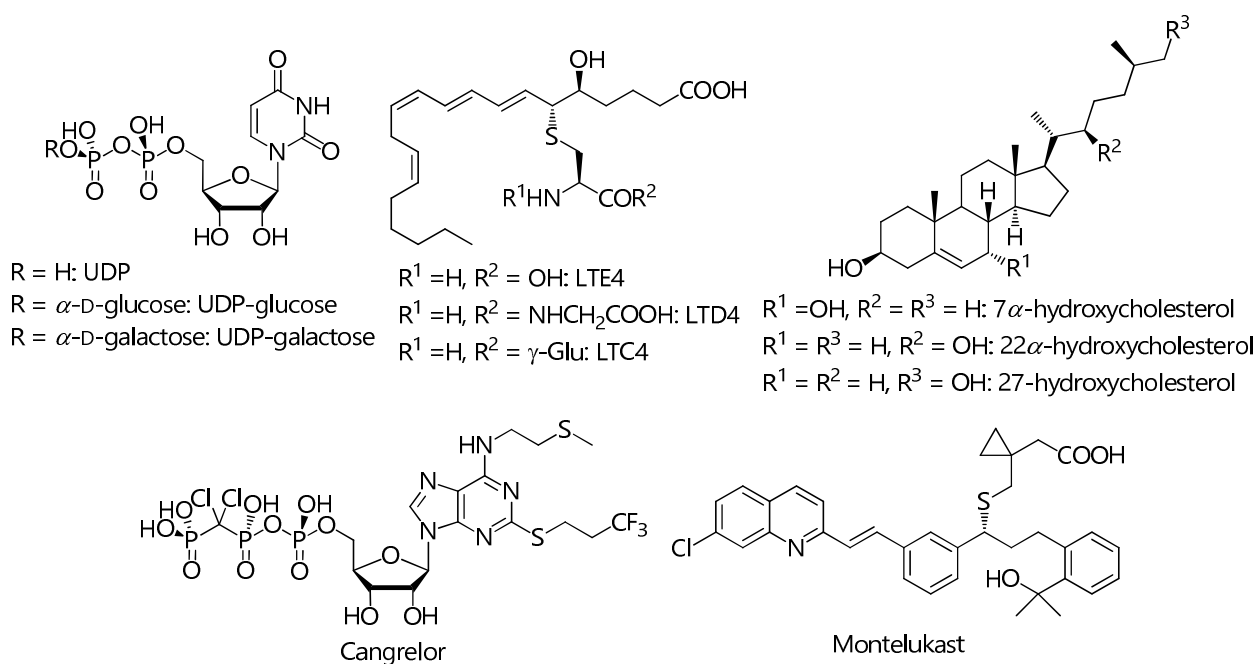


Figure 4.2. Examples of GPR17 agonists and antagonists

GPR17 has been found to be responsive to agonists such as not only nucleotides and their adducts (UDP, UDP-glucose, UDP-galactose), but also radically different messengers, for example cysteinyl leukotrienes (LTE4, LTD4 and LTC4), oxysterols and a wide variety of molecules having quite diverse structures.¹²⁷ This promiscuity largely depends on specific pathologies and physical conditions, as well as emergency situations and association with P2Y receptors.¹²⁸ The extensive diversity in the structures of agonists and antagonists may also be justified by such a potential heterodimerization to adapt and enlarge the substrate pool. Among the antagonists, the antiplatelet drug Cangrelor (Kengreal® or Kengrexal®) and the antiasthmatic Montelukast (Singulair®) are worth mentioning.

Since the late 2000s, research efforts have been focused on studying the involvement of GPR17 in neuronal myelination.^{119e, 129} It appears that the receptor exerts opposed functions depending on the specific stage, enhancing the process in the early steps and exerting a negative control in the following ones, up to total receptor silencing in the final maturation phase.

Since nucleosides and leukotrienes are produced in massive concentrations during brain trauma, GPR17 expression is highly probable. In such occasions, several receptor units are recruited in regions surrounding the damaged area.^{125b, 127b, 129a, 130} Medical observations confirm that myelin disturbance is indeed characterized by an abnormal activity of GPR17, generating a physiological block against cells which prevents the maturation toward tissue regeneration. Therefore, medical treatment with antagonists may reduce the extent of neurodegeneration.

4.2. *In silico* screening and synthesis of potential GPR17 ligands

4.2.1. *In silico* screening of potential GPR17 ligands

As a first approach, a virtual screening was carried out through molecular docking to identify new ligands for GPR17 and to estimate their binding free energy.

This work was performed within a collaboration among the Laboratory of Organic Chemistry (Prof. Giovanna Speranza) and the Laboratory of Molecular and Cellular Pharmacology of Purinergic Transmission (Dr. Stefania Ceruti and Dr. Chiara Parravicini) at the Department of Chemistry and Department of Pharmacological and Biomolecular Sciences, respectively, of the University of Milan, as well as the Laboratory of Pharmaceutical Biocatalysis (Dr. Daniela Ubiali) and the Laboratory of Pharmaceutical Analysis (Prof. Enrica Calleri) at the Department of Drug Sciences of the University of Pavia.

Two main constraints had to be faced:

- the absence of any structural information about the receptor;
- the selection of the pool of candidates from literature and/or from proprietary molecule collections to serve as potential leads.

The first issue was addressed by choosing a homology modeling strategy. Since the human membrane P2Y₁ receptor is known to be phylogenetically related to GPR17 and, among the available GPCR structures, it shares the highest sequence identity with it^{125a,b}, a homology model was built up as template starting from its known structure in the Protein Data Bank (PDB). Indeed, in 2015 Zhang *et al.* isolated and purified a complex of P2Y₁ and its antagonist MRS2500 (**93**, Table 4.1), resolved by XRD (2.7 Å).¹³¹ During the homology modelling procedures, the ligand coordinates were transferred from the template to the homology model to simulate its general position in the binding pocket of GPR17 (Figure 4.3a).

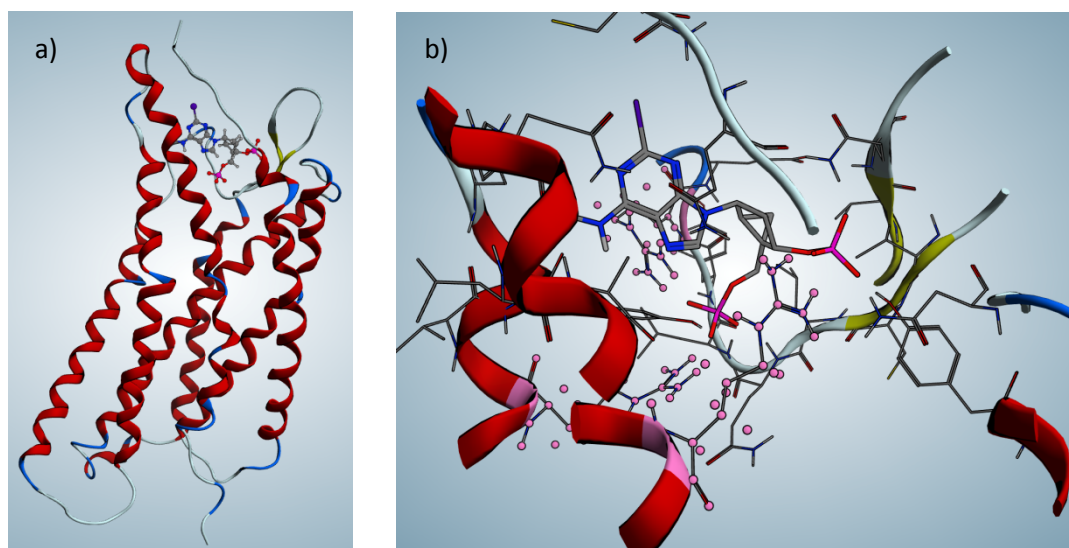


Figure 4.3. Homology model of the GPR17-**93** complex: a) overall structure; b) details of the binding site.

The binding site of GPR17 was identified by an automatic tool and, when compared to the pocket occupied by the reference ligand **93**, resulted to be quite enlarged, spanning across both extracellular regions and transmembrane domains. In terms of the most significant binding residues, the two phosphate groups were found to form electrostatic interactions with the protonated guanidine side chains of Arg₂₅₅ and Arg₂₈₀, while additional hydrogen bonds were detected between the remaining Arg₁₈₆ and the N⁷-N⁶H couple of the purine. Other contacts involved apolar residues and the rest of the heterobicycle, as well as hydrophilic side chains and specific polar anchors on the ligand (Glu and N¹H, Tyr and the secondary phosphate, ...) (Figure 4.3b).

The successful validation of the homology model justified the use of GPR17-**93**.

Given the reported affinity of the receptor for nucleosides and nucleotides, not to mention the striking structure similarity of **93** with such compounds, three distinct databases were generated including the following candidates:

- entries 1-49: 6-, 7- and 8-substituted ribo-, 2'-deoxyribo- and arabinonucleosides whose synthesis is reported in this PhD Thesis (see from **3.1.3** to **3.1.6**);
- entries 50-130: 2-, 6-, 7- and 8-substituted ribo- and 2'-deoxyribonucleosides, as well as 5'-nucleotides, either reported in papers published by the Laboratory of Organic Chemistry (Prof. Giovanna Speranza) at the Department of Chemistry of the University of Milan and the Laboratory of Pharmaceutical Biocatalysis (Dr. Daniela Ubiali) at the Department of Drug Sciences of the University of Pavia since the late 2000s, together with unpublished product/intermediates¹³²;
- entry 131: **93** (MRS2500, reference antagonist).

All 131 compounds were submitted to docking studies to evaluate their relative affinity for the GPR17 model (**Figure 4.4**).

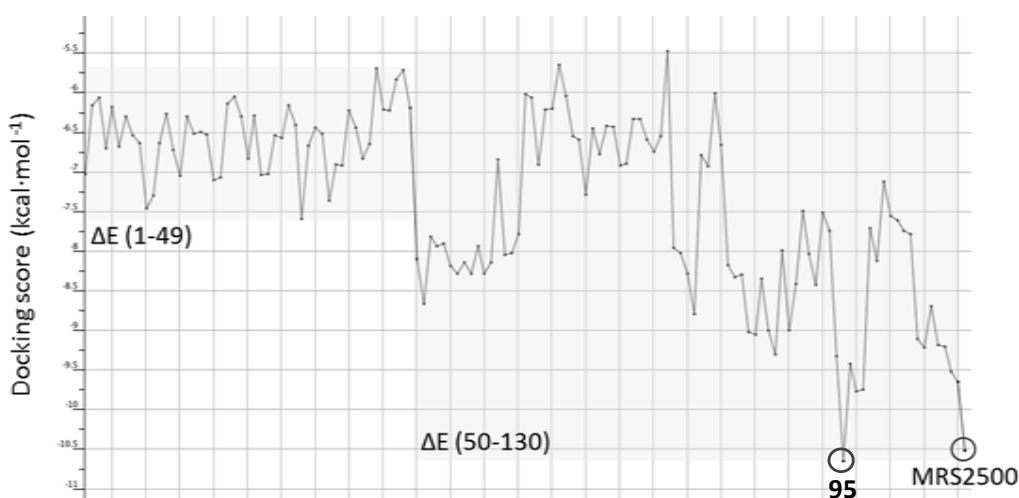


Figure 4.4. Docking scores for entries 1-131

Three observations can be drawn from the coarse analysis of energies:

- MRS2500 (**93**) is one of the best ligands in terms of docking score (binding free energy), second only to one literature molecule (**95**, see **Table 4.1**);
- concerning molecules 1-49, neither docking score values are satisfying nor the difference in score is significant among them ($\Delta E \sim 2 \text{ kcal}\cdot\text{mol}^{-1}$);
- a 5'-phosphate group is present in most candidates with favorable docking energy, remarking the role of Arg₂₅₅ and Arg₂₈₀ in the binding network. Such a connection highlights their probable responsibility in the wide ΔE value ($5 \text{ kcal}\cdot\text{mol}^{-1}$, between ~ -10.5 and $\sim -5.5 \text{ kcal}\cdot\text{mol}^{-1}$ in the second library).

More in details about entries 1-49, four out of the five possible substitution generated results in the interval between -7.5815 and -6.4027. On the contrary, the worst values were found with the 7-methyl iodide salts of inosine, guanosine and their 2'-deoxy analogues, probably because of a repulsive interaction with the receptor binding site containing an array of positive charges. The whole net charge of GPR17 is quite massive (+13, derived from 17 Arg, 8 Lys, 7 Glu and 5 Asp, with 13 additional His which may be protonated depending on pH and chemical environment), hence discouraging any binding of cationic substrates.

Other than **93**, the top scoring candidates were 8-methylaminoinosine (**70**, entry 33) and *N*²-*n*-octyl-2',3'-*O*-isopropylidenedeguanlylic acid (**95**, entry 113) (**Table 4.1**).

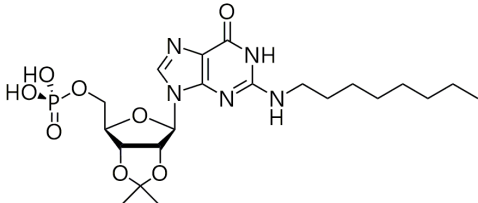
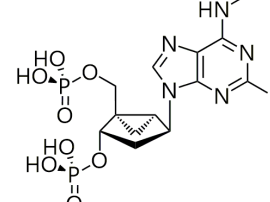
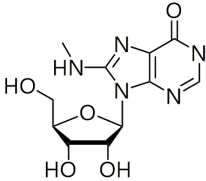
Entry	Code	Structure	Docking score (kcal·mol ⁻¹)
113	95		-10.6441
131	93		-10.5112
33	70		-7.5815

Table 4.1. Best scoring compounds for each library

A noteworthy element was the extreme dissimilarity between the poses of **93** and **95** (**Figure 4.5a**). The *n*-octyl chain of the latter ligand indeed points toward the inner core of the GPR17 model, which is covered with hydrophobic residues able to host alkyl moieties by Van der Waals contacts. This tunnel-like anchor allows the 5'-phosphate group to overlap with that of **93** albeit forcing the purine ring in the opposite direction. To rationalize such a sudden shift, all 17 top scoring entries from the second collection were superimposed (**Figure 4.5b**).

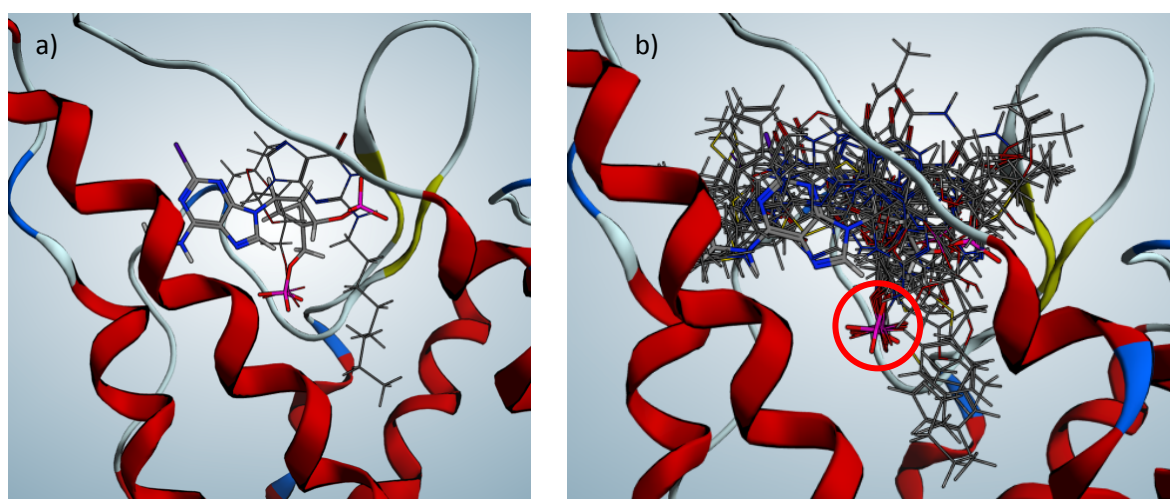


Figure 4.5. Superimposition of ligand poses in GPR17: **a)** **93** and **95**; **b)** 17 top scoring entries in the range 50-130 (superimposed phosphate groups are circled in red).

As poses were rather dispersed in the binding pocket of GPR17, a rational structure-activity relationship could not be defined. The mentioned site is indeed wide and extends also over extracellular loops. Another

evidence is that small ligands tend to occupy the deeper portion of the binding pocket. Anyway, all poses maintain the essential hydrogen bonds with Arg₂₅₅ and Arg₂₈₀.

Despite irregularities, the similarity between a 2',3'-*O*-isopropylidene group and a cyclopropyl ring may justify the small energy difference between **93** and **95**. Furthermore, the addition of long-chain groups especially on N² seems to increase the affinity toward the receptor.

To obtain more accurate data, the docking protocol was modified. New ligands, bearing substituents with different steric hindrance and/or a diverse number of phosphate groups, were included in the dataset, poses sampling was increased and candidates were relocated to a deeper position with respect to the binding region of **93**. Plural binding sites were indirectly confirmed, but no further *in silico* studies have been carried out to date.

Since a long apolar chain in position 2 seems to be essential for stronger energy ties (see **Table 4.1**), the functionalization of N² was explored. Accordingly, N²-acyl groups with increasing chain length were tested, leaving the structure of **95** intact in all other respects. The new molecular modeling computation gave promising results (**Figure 4.6**).

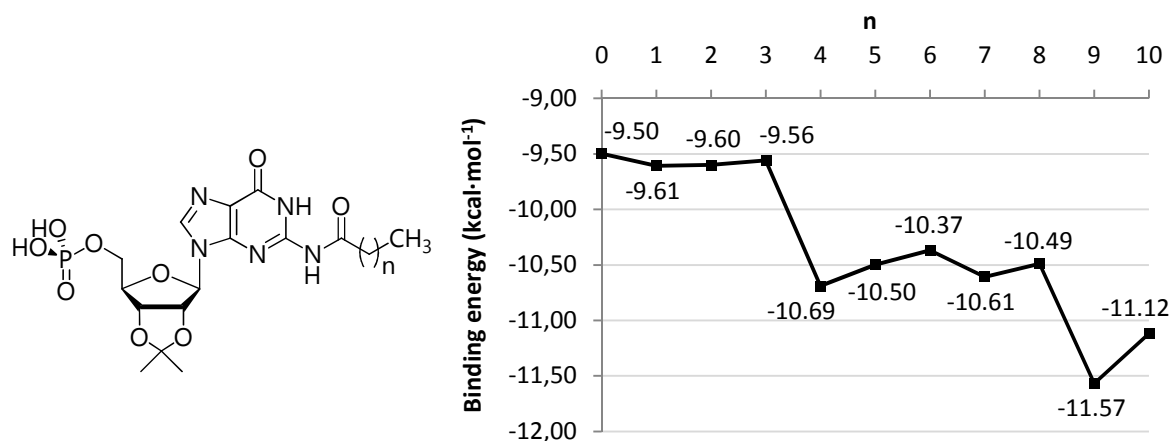


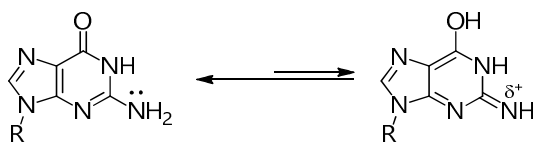
Figure 4.6. Binding free energy of N²-acylguanine 5'-ribonucleotides

Although the even/odd classification does not determine any regular trend, longer chains are definitely preferred by the receptor pocket (*cf.* n = 3, 4 and 9). N²-*n*-undecanoyl-2',3'-*O*-isopropylidene-guanosinic acid (**97**, n = 9) exhibits the topmost affinity.

4.2.2. N²-Alkylation, N²-acylation and 2-halogenation of guanosine

The functionalization of adenine, hypoxanthine and guanine ribonucleosides has been a topic of great interest in the Laboratory of Organic Chemistry (Prof. Giovanna Speranza) at the Department of Chemistry of the University of Milan and therefore has been studied extensively since the first 2000s. This work has been performed as a part of the study on the so-called *umami* taste, specifically to investigate the capacity of 5'-ribonucleotides to enhance the taste intensity of monosodium glutamate (MSG), thus acting as flavor enhancers.^{6, 133}

A number of N²-alkyl and N²-acyl derivatives of guanosine 5'-phosphate (GMP) were prepared by functionalization of the exocyclic 2-amino group of guanosine.¹³⁴ Since the tautomeric keto form of the nucleobase is preferred, the carbonyl oxygen in position 6 withdraws electron density from N², making it considerably less nucleophilic than other amino groups in simple aromatic rings (**Scheme 4.1**).



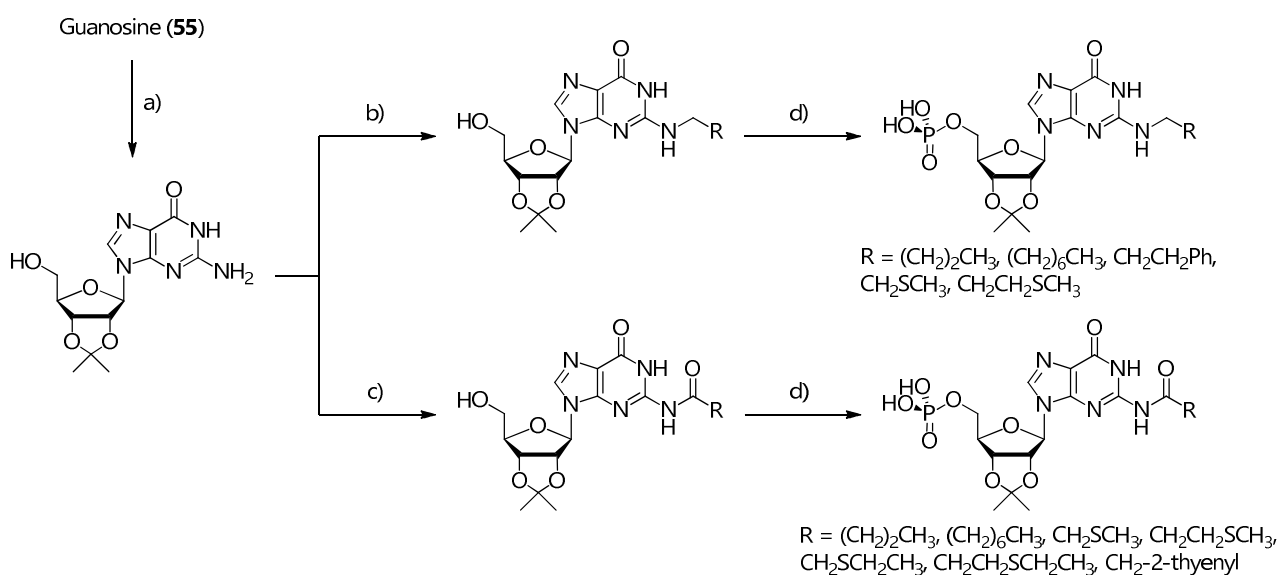
Scheme 4.1. Tautomeric structures of guanine N^9 -derivatives

The prevailing 2-amino-6-keto tautomer provides the exocyclic C-N bond with an additional partial doublet, making it much shorter (1.336 Å) than a typical single one in aromatic rings (1.426 Å) and more similar to an imino one (1.322 Å), as demonstrated by structural measurements (**Table 4.2**).

	Bond type	Observed bond length (Å)	Calculated bond length (Å)	Reference
Guanine	C^2-NH_2	1.336	1.377	135
		1.341		136
		1.330		137
PhNH ₂	$C^{Ar}-NH_2$	1.426		138
AllylNH ₂	$C^{sp^2}-NH_2$	1.340		
AlkylNH ₂	$C^{sp^3}-NH_2$	1.472		
(CH ₃) ₂ C=NH	$C^{sp^2}-NH_2$	1.322		

Table 4.2. Measurement and calculations on different C-N bonds lengths

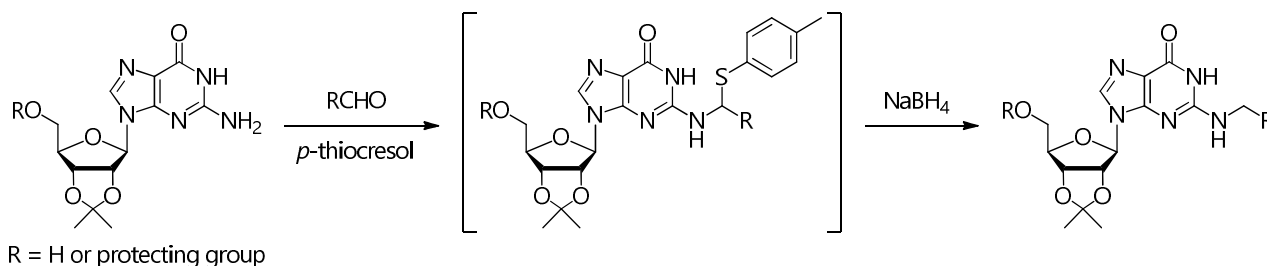
Therefore, the reactivity of N^2H_2 in guanosine as a nucleophile is scarce and no conventional functionalizing methods (e.g. alkylation, reductive amination, azide reduction, ...) can be selected. A number of N^2 -alkyl- and N^2 -acylguanylic acids were prepared by alkylation and acylation (**Scheme 4.2**).^{6a}



Reagents and conditions (yield): a) 2,2-DMP, *p*-TsOH·H₂O, acetone; b) i) RCHO, *p*-thiocresol, EtOH, AcOH, reflux, ii) NaBH₄, EtOH, reflux (43-61%); c) i) TMSCl, Py, CH₂Cl₂, ii) RCOCl, iii) HCl, THF (52-78%); d) POCl₃, H₂O, TEA, 0°C (67-81%).

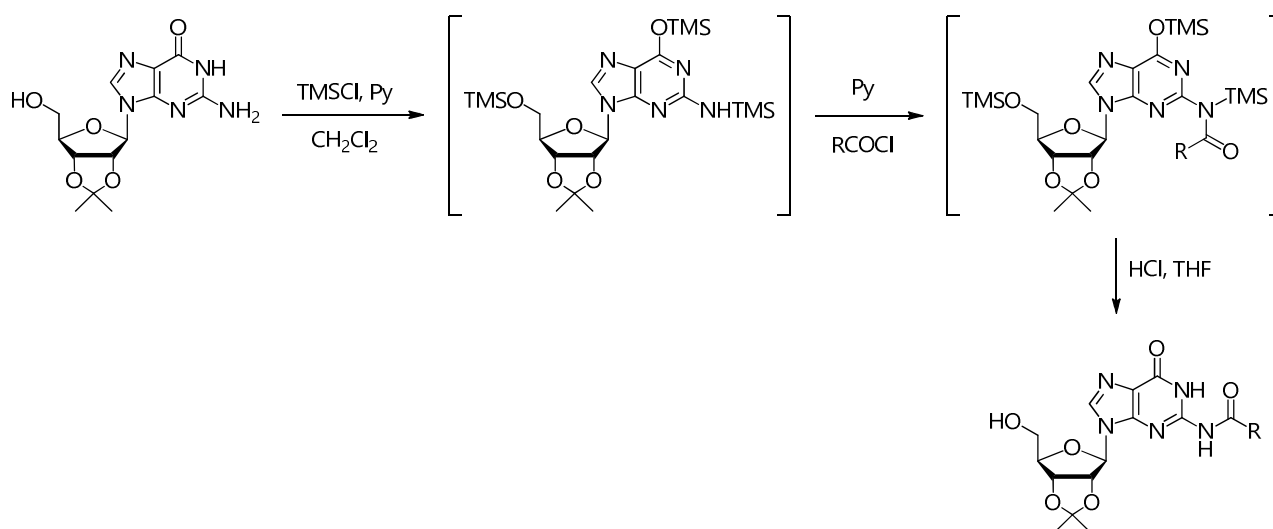
Scheme 4.2. Synthesis of N^2 -alkyl and N^2 -acylguanylic acids as potential *umami* active compounds

The first strategy was followed according to the procedure reported by Kemal and Reese in 1980, properly modified with the use of 2',3'-*O*-isopropylidene-5'-*O*-R-guanosine (**Scheme 4.3**).¹³⁹ The *N*² exocyclic group was indirectly alkylated in a two-step protocol, first forming a thioaminal with excess RCHO and *p*-thiocresol, whose roles were to form a transient iminium ion and trap it by nucleophilic sulfur attack, respectively. Next, NaBH₄ was added to perform a reductive decomposition of the intermediate. Due to the formation of several by-products in the last step, it was sometimes necessary to operate on a temporarily 5'-protected nucleoside.



Scheme 4.3. *N*²-Alkylation of 2',3'-*O*-isopropylidene-5'-*O*-R-guanosines

Similarly, the exocyclic *N*²-acylation proceeded through a non-isolated intermediate temporarily protected with silyl groups. Following the concept of transient protection exploited by Fan *et al.*, excess TMSCl in a CH₂Cl₂/pyridine mixture was selected as protecting mixture, followed by the addition of an acyl chloride under mild conditions to get the desired *N*²-acyl derivative (**Scheme 4.4**). The mechanism of this procedure is characterized by a trisilylated intermediate, protected not only at the 5'-hydroxyl group but also at O⁶ and N²H₂ to prevent the formation of dark impurities and accelerate nitrogen functionalization. A final hydrolysis step could be performed by acidic treatment.¹⁴⁰



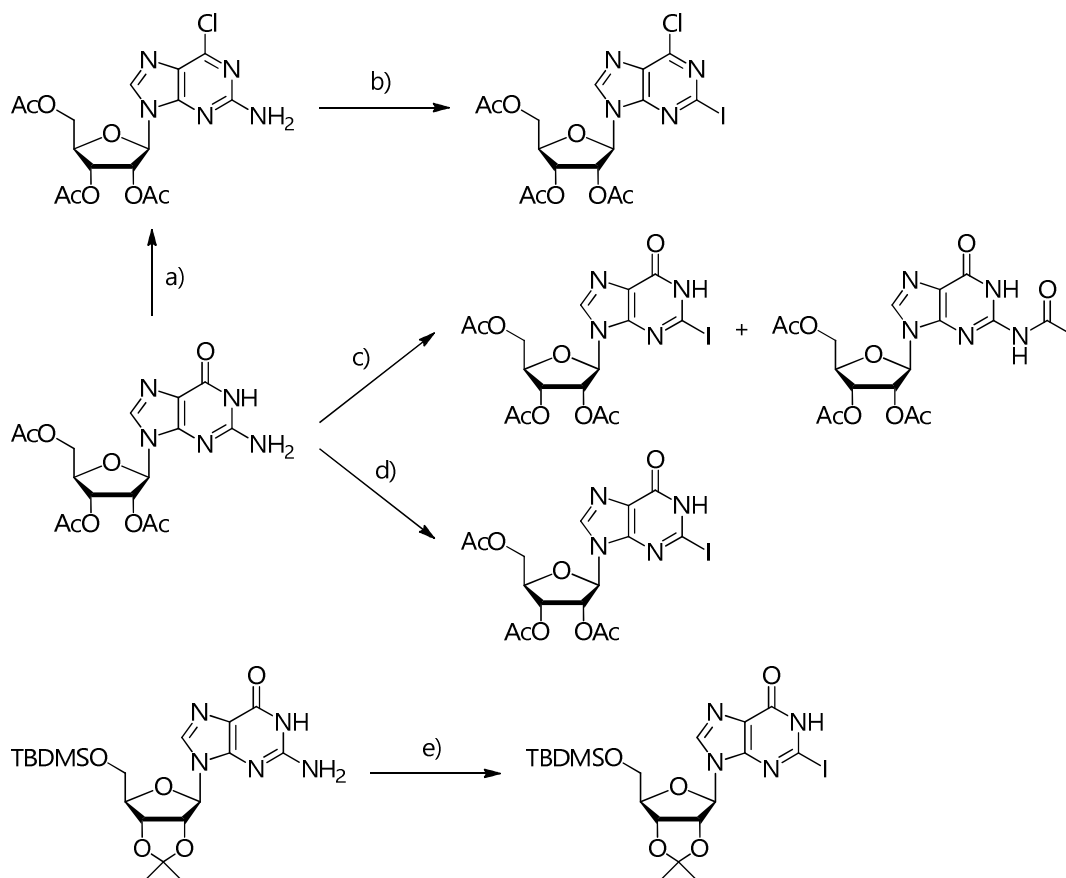
Scheme 4.4. *N*²-Acylation of 2',3'-*O*-isopropylidene-5'-*O*-R-guanosine

All products were subjected to a final phosphorylation reaction with POCl₃ and H₂O in TEP at 0°C. A few sulfoxide moieties in the alkyl or acyl side chain (CH₂CH₂SOCH₃ and CH₂CH₂CH₂SOCH₃) were also introduced by controlled oxidation of the corresponding S-containing analogues.^{6b}

Due to unsatisfactory results in terms of isolation and yields, the preparation of *N*²-alkylguanosine derivatives required a different strategy. Instead of strengthening the nucleophilicity of the exocyclic amine at position C², it was decided to convert it into a proper leaving group, specifically a halogen. In the course

of a research aimed at the synthesis of guanosine 5'-monophosphate (GMP)-MSG conjugates with the two "umami" units linked by a diamine spacer¹⁴¹, numerous variations of the Sandmeyer reaction were investigated.

The first attempts were carried out to introduce an iodine atom (**Scheme 4.5**).

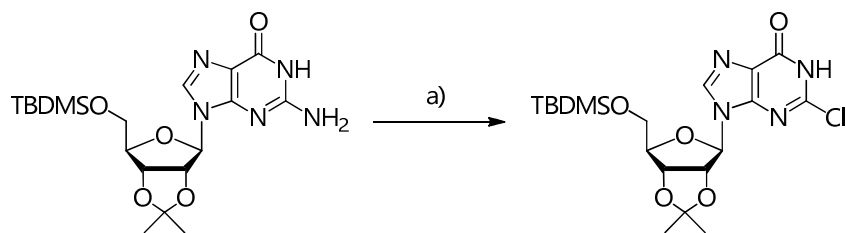


Reagents and conditions (yield): a) POCl_3 , Et_4NCl , N,N -DMA, CH_3CN , reflux (40%); b) $t\text{-BuONO}$, CH_2I_2 , CH_3CN , reflux (75%); c) i -amyl nitrite, CH_3I , CH_3CN , 0-90°C (traces, not isolated); d) i -amyl nitrite, CH_3I , $\text{ClCH}_2\text{CH}_2\text{Cl}$, 65°C (< 30%); e) i -amyl nitrite, CH_3I , $\text{ClCH}_2\text{CH}_2\text{Cl}$, 65°C (not isolated).

Scheme 4.5. Studies on iodination of N^2H_2 in protected guanosines

First of all, the procedure reported by Ohno *et al.* with $t\text{-BuONO}$ and CH_2I_2 in refluxed CH_3CN was repeated on triacetylated 6-chloroguanosine with good results.¹⁴² In order to leave the 6-carbonyl moiety unprotected and simplify the synthetic route, the protocol was modified according to Nair *et al.* by replacing $t\text{-BuONO}$ with i -amyl nitrite and excess CH_3I , and varying the temperature between 0 and 90°C.¹⁴³ Severe drawbacks were encountered in purifying the 2-iodo analogue. In addition, the main product was a triacetylated N^2 -acetylguanosine arising from the radical presumably formed by CH_3CN which had entered the propagation cycle. To avoid solvent reaction, the latter was varied along with the temperature until the desired product was obtained with $\text{ClCH}_2\text{CH}_2\text{Cl}$ at 65°C, in less than 30% yield. The introduction of a 2',3'- O -isopropylidene and a 5'- O -TBDMS group on ribose did not give the desired outcome.

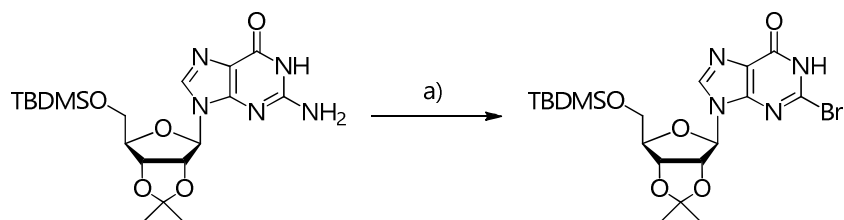
However, since the stability of 2-iodoguanosines was hampered by spontaneous decomposition, the halogen had to be replaced with chlorine. The only successful attempt was made by slightly modifying a procedure reported by Qian and Glaser with SbCl_3 and $t\text{-BuONO}$ in CH_2Cl_2 at -10°C, which led to the 2-chloro derivative in low yield (**Scheme 4.6**).¹⁴⁴



Reagents and conditions (yield): a) SbCl_3 , $t\text{-BuONO}$, CH_2I_2 , -10°C (31%).

Scheme 4.6. Chlorination of N^2H_2 in protected guanosine

Finally bromine was introduced on C^2 in the presence of SbBr_3 and CH_2Br_2 , keeping all other conditions unvaried. With the aim of further increasing the yield and avoiding toxic reagents such as SbX_3 ($\text{X} = \text{F}, \text{Cl}, \text{Br}, \text{I}$), a procedure was developed based on the use at -10°C of $t\text{-BuONO}$ to promote the formation of the necessary diazonium salt and with $\text{TMSBr}/\text{CH}_2\text{Br}_2$ as a halogen source and catalytic system (**Scheme 4.7**) (see **6.1.4**).¹⁴⁵



Reagents and conditions (yield): a) SbBr_3 , $t\text{-BuONO}$, CH_2Br_2 , -10°C (60%) or TMSBr , $t\text{-BuONO}$, CH_2Br_2 , -10°C (70%).

Scheme 4.7. Studies on bromination of N^2H_2 in protected guanosine

This approach is totally unprecedented with respect to known procedures, which always require the modification of O^6 in the purine ring as either chlorine or alkoxyde as a temporary protection (M. Rabuffetti *et al.*, unpublished results).

4.2.3. Synthesis of potential GPR17 ligands

4.2.3.1. 8-Alkylamino-, N^2 -alkyl- and N^2 -acylpurine 5'-ribonucleotides (94-97)

The energy values calculated in docking studies (see **4.2.1**) were exploited to assist the chemical synthesis of potential GPR17 ligands. Four 8-alkylamino-, N^2 -alkyl- and N^2 -acylpurine 5'-ribonucleotides were selected (**Figure 4.8**).

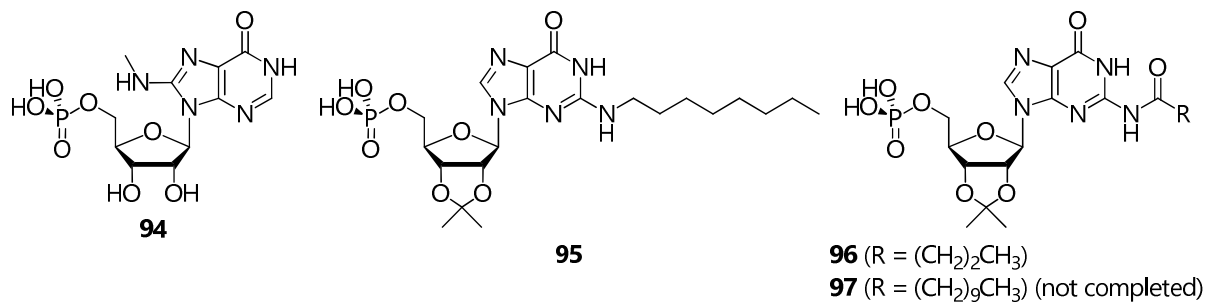
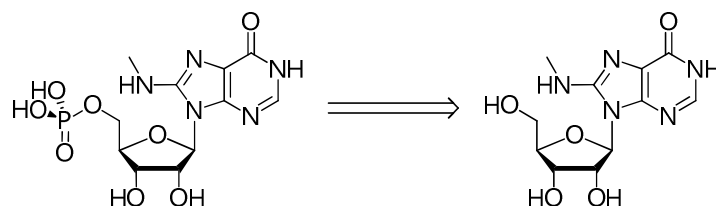


Figure 4.8. Potential ligands of GPR17 (94-97)

97 was selected as the best pose in terms of docking score. Unlike **95** and **96**, **94** was not present in the original pool but was added to the list by phosphorylation of **70**, owing to an assumed beneficial effect of a 5'-phosphate on binding energy. The rationale for the synthesis of **96** was to provide a candidate with worse theoretical affinity, useful as negative control.

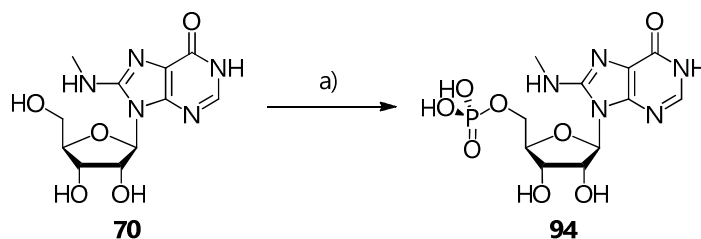
4.2.3.2. Synthesis of 8-methylaminoinosinic acid (**94**)

The synthesis of 8-methylaminoinosinic acid (**94**) is quite simple, consisting of the direct phosphorylation of 8-methylaminoinosine (**70**) on its primary OH group (**Scheme 4.8**).



Scheme 4.8. Retrosynthetic analysis of 8-methylaminoinosinic acid

Phosphorylation was carried out following the procedure already experimented by Ikemoto *et al.* (see **6.1.5**) (**Scheme 4.9**).¹⁴⁶ Under inert atmosphere, the activated **70**-TEP complex was allowed to form at 50-60°C, then excess POCl₃ (6:1) and stoichiometric H₂O were carefully added dropwise at 0°C and the solution was stirred at the same temperature for 6 h, monitoring the disappearance of **70** by TLC until almost quantitative conversion was achieved. Dilution with H₂O, basification to pH 2 and heating at 70°C for 1 h 30' led to the hydrolysis of the intermediate dichlorophosphate, followed by semi-preparative HPCL.

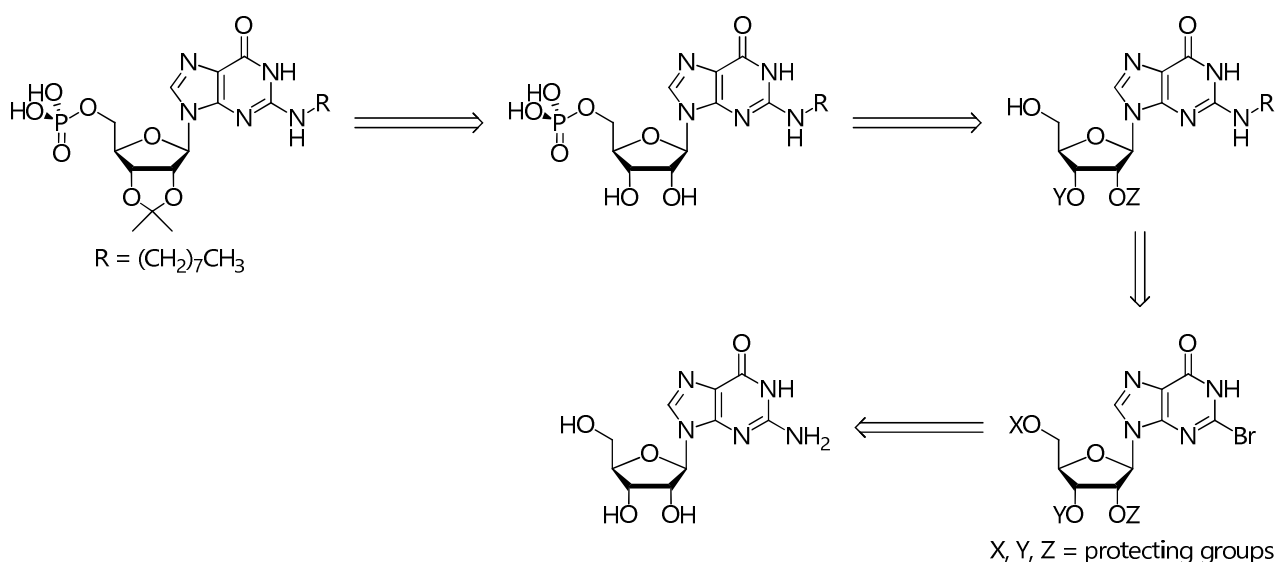


Reagents and conditions (yield): a) i) TEP, 50-60°C; ii) POCl₃, H₂O, 0°C; iii) H₂O, 6 M NaOH (to pH 2); iv) 70°C (75%).

Scheme 4.9. Phosphorylation of **70**

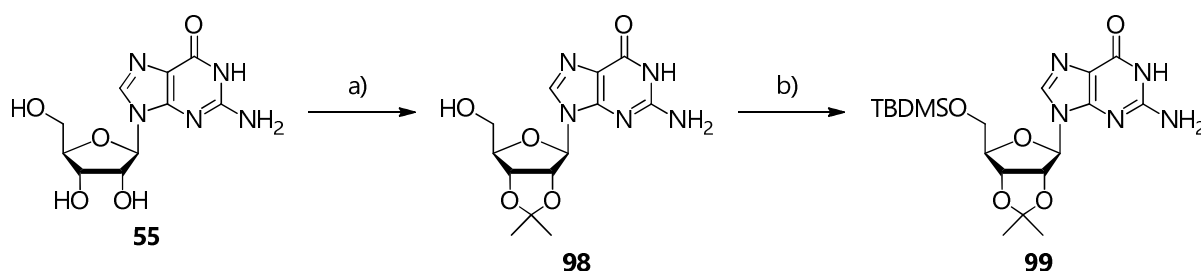
4.2.3.3. Synthesis of *N*²-*n*-octyl-2',3'-*O*-isopropylidene-guanylic acid (**95**)

The retrosynthetic strategy for *N*²-*n*-octyl-2',3'-*O*-isopropylidene-guanylic acid (**95**) required the disconnection of the C-N exocyclic bond. Position 2 of guanosine could be activated by introducing a bromine leaving group (see **4.2.2**) to be displaced by an amine. In order to simplify purifications and preserve the three hydroxyl groups against brominating agents, the ribose moiety had to be protected (**Scheme 4.10**).



Scheme 4.10. Retrosynthetic analysis of *N*²-*n*-octyl-2',3'-*O*-isopropylidene-guanosylic acid

Accordingly, the first synthetic step was the conversion of OH^{2'} and OH^{3'} of guanosine (**55**) to a 2',3'-*O*-isopropylidene with 2,2-dimethoxypropane (2,2-DMP) and a stoichiometric amount of *p*-TsOH·H₂O in acetone. The isolation of **98** proceeded by precipitation and filtration in almost quantitative yield. OH^{5'} was subsequently masked with an orthogonal protection. TBDMSCl was chosen as silylating agent with excess imidazole in dry DMF to give **99**, purified by flash column chromatography (**Scheme 4.11**).

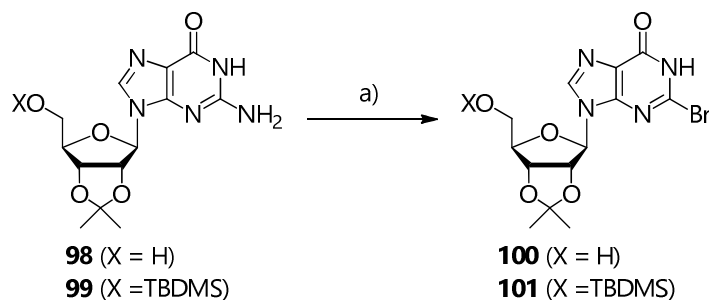


Reagents and conditions (yield): a) 2,2-DMP, *p*-TsOH·H₂O, acetone (96%); b) TBDMSCl, imidazole, DMF (95%).

Scheme 4.11. Protection of OH^{2'}, OH^{3'} and OH^{5'} of **55**

The bromination step was attempted directly on intermediate **98** to simplify the sequence. According to the previously optimized procedure, **98** was reacted with *t*-BuONO and TMSBr in CH₂Br₂ at -10°C. Reagents were carefully added dropwise under inert atmosphere and the mixture was allowed to warm to 5-10°C for 7 h, avoiding any exposure to light sources to prevent the decomposition of both intermediates, as well as of the newly formed C-Br bond. The progress of the reaction, likely to proceed *via* a radical Sandmeyer-type mechanism (see **6.1.4**)¹⁵⁸, was monitored by TLC in order to stop it prior to product decomposition. The subsequent work-up had to be performed quickly by solubilization of the crude in AcOEt and neutralization of HBr with a saturated aqueous NaHCO₃ solution. The crude product was quite unstable and had to be purified by double flash column chromatography as soon as possible, since TLC analysis showed the formation of a few by-products which could not be easily separated from the brominated derivative. It was not surprising that the yield was not very high. The same protocol was therefore applied to **99**, which was supposed to benefit from the TBDMS protection to reduce side reactions. This procedure resulted in a

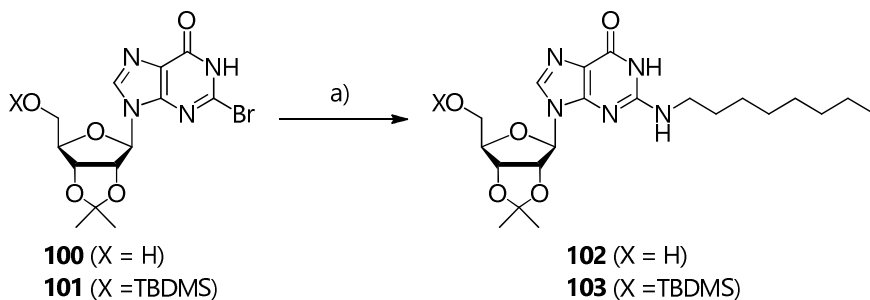
higher number of unexpected TLC spots, although only one flash column chromatography was necessary and the final yield was notably higher (70 vs. 21%) (**Scheme 4.12**).



Reagents and conditions (yield): a) TMSBr, *t*-BuONO, CH₂Br₂, -10°C → 5-10°C (21% for **100** and 70% for **101**).

Scheme 4.12. Bromination of **98** and **99**

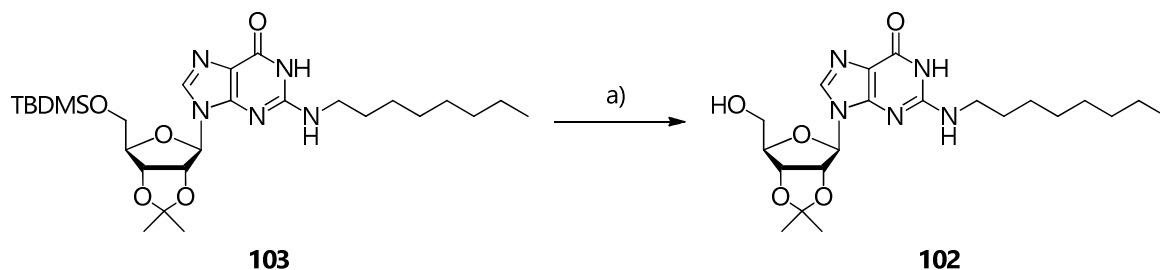
Both **100** and **101** were subjected to amination by bromide displacement with *n*-OctNH₂ in 2-methoxyethanol at 80°C, under previously optimized conditions (**Scheme 4.13**). As already noticed with similar products, the reaction required a long time to be completed (3 and 8 days to form **103** and **102**, respectively) and had to be protected from light exposure. After a mildly acidic work-up with 1 M HCl, flash column chromatography afforded **102** and **103**, the former in lower yield (39 vs. 69% yield).



Reagents and conditions (yield): a) *n*-OctNH₂, 2-methoxyethanol, 85°C (39% for **102** and 69% for **103**).

Scheme 4.13. Amination of **100** and **101**

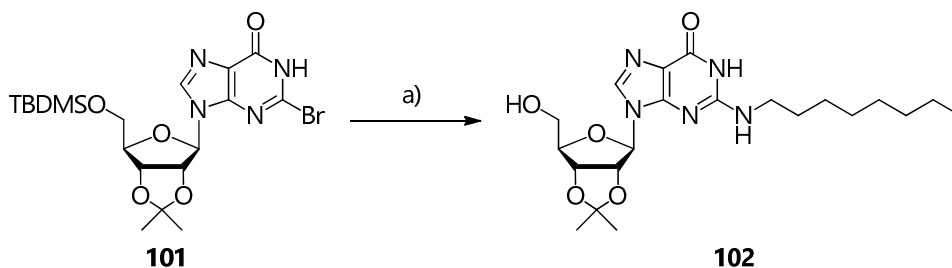
103 was then treated with TBAF·3H₂O in THF at RT to remove the 5'-*O*-silyl ether and obtain **102** after flash column chromatography, with free OH^{5'} ready for phosphorylation (**Scheme 4.14**).



Reagents and conditions (yield): a) TBAF·3H₂O, THF (60%).

Scheme 4.14. Desilylation of **103**

In addition, since a partial removal of the TBDMS group occurred in the course of the work-up of the amination reaction, the latter procedure was modified by filtering the crude product on a short silica pad and by increasing HCl concentration from 1 to 2 M (**Scheme 4.15**). Such modifications provided **102** in place of **103**, in overall higher yield with respect to the two sequential steps (55 vs.41%).

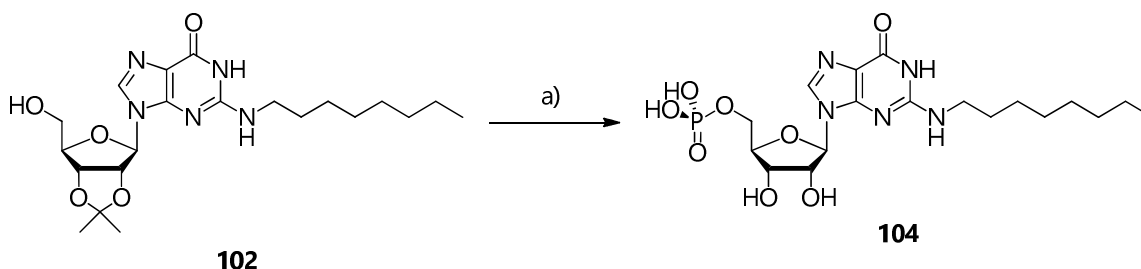


Reagents and conditions (yield): a) i) *n*-OctNH₂, 2-methoxyethanol, 85°C; ii) 2 M HCl (work-up) (55%).

Scheme 4.15. Sequential amination-desilylation of **102**

Based on the obtained results, the strategy of bromination and amination on the 5'-*O*-protected nucleoside appears to be more convenient.

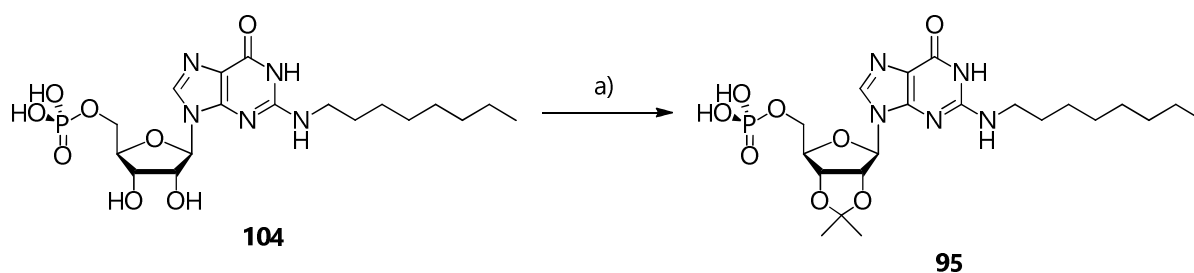
The same procedure carried out for the previous phosphorylation was applied to **102** with very few modifications (**Scheme 4.16**). The concomitant removal of the 2',3'-*O*-isopropylidene group could not be avoided, although undesired. Freeze-drying and purification by semi-preparative HPLC afforded **104**.



Reagents and conditions (yield): a) i) TEA, 50°C; ii) POCl₃, H₂O, 0°C; iii) 6 M NaOH (to pH 2); iv) 70°C (73%).

Scheme 4.16. Phosphorylation of **102**

The 2',3'-*O*-isopropylidene moiety was finally reintroduced with 2,2-dimethoxypropane (2,2-DMP) and stoichiometric *p*-TsOH·H₂O. This time, a dry 8:1 acetone-DMF mixture was necessary to overcome the scarce solubility of the phosphate ester and the reaction temperature was raised to reflux (**Scheme 4.17**). The final product **95** was isolated once again by semi-preparative HPLC.



Reagents and conditions (yield): a) 2,2-DMP, *p*-TsOH·H₂O, acetone/DMF, reflux (81%).

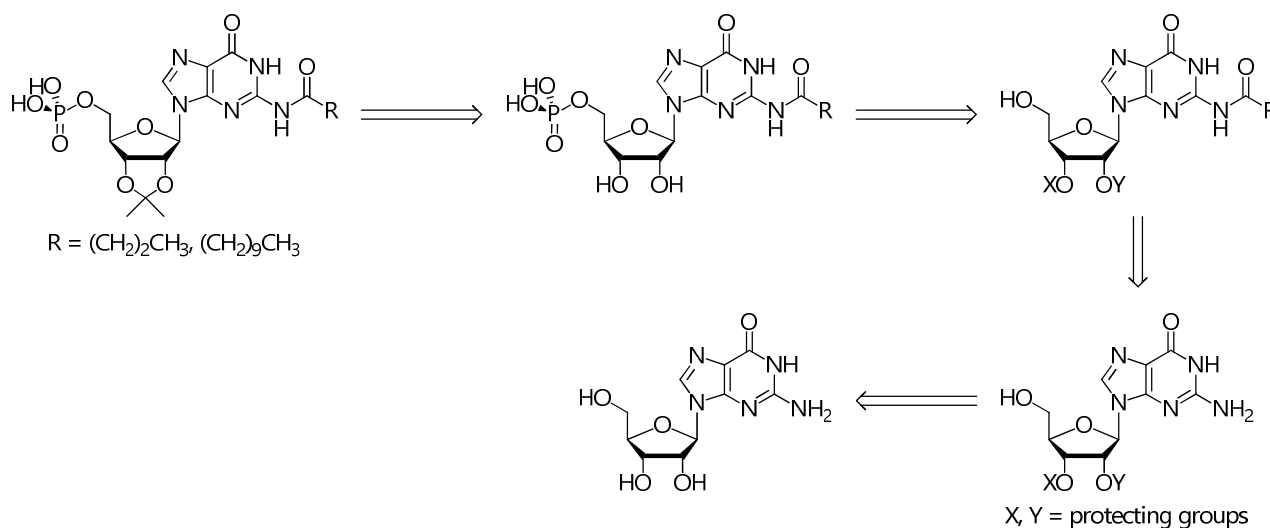
Scheme 4.17. Reintroduction of the 2',3'-*O*-isopropylidene moiety on **104**

Further studies are being carried out to run the last two reactions in one step, that it to perform nucleoside phosphorylation under conditions that preserve acid-labile moieties. The use of POCl₃ in trimethylphosphate (TMP) at 0°C over a limited time¹⁴⁷ and procedures requiring anhydrous H₃PO₄, tributylamine and catalytic *n*-butylimidazole in a DMF-CH₃CH₂NO₂ mixture¹⁴⁸, if necessary under microwave radiations¹⁴⁹, have already been tested and have produced very encouraging results.

However, none of these controlled conditions has yet allowed to obtain **95** directly from **102**.

4.2.3.4. Synthesis of *N*²-acyl-2',3'-*O*-isopropylidene-guanylic acids (**96-97**)

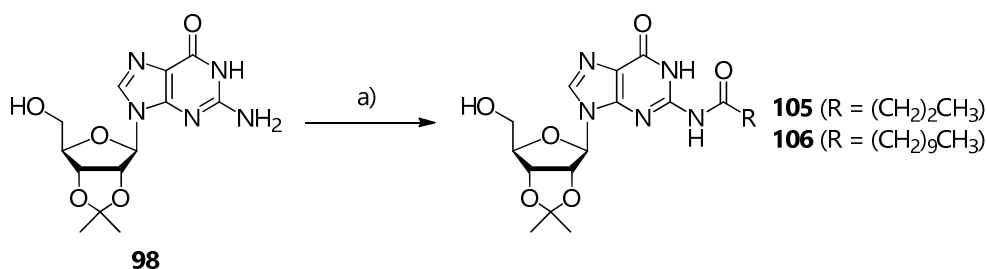
The already exploited synthetic route to obtain *N*²-acyl-2',3'-*O*-isopropylidene-guanylic acids (see **4.2.2**) was chosen again because of its simplicity and good yields, with no need for specific improvements. The retrosynthetic strategy for the corresponding guanylic acids includes the formation of a new amide bond as the key step and allows to operate on 2',3'-*O*-diprotected guanosine, thus eliminating the introduction and removal of protecting groups at position 5' (**Scheme 4.18**).



Scheme 4.18. Retrosynthetic analysis of *N*²-acylguanylic acids

The results of molecular modeling (see **4.2.1**) oriented the choice of the R residue. The butyryl residue matched the requirements for one of the less favorable poses. On the other hand, the undecanoyl moiety was added as the most promising candidate. The first molecule was selected as a negative control for GPR17 binding assays, while the second one as the potential best ligand.

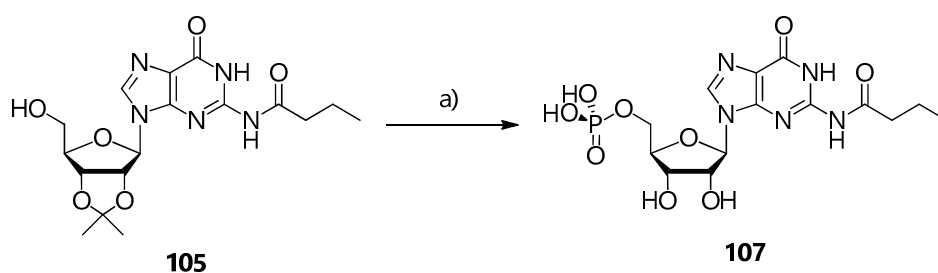
Since the 2',3'-*O*-isopropylidene ring is compatible with the conditions requested for acylation, this reaction was performed on the corresponding protected guanosine (**98**) as starting material (**Scheme 4.19**). The already reported *N*-acylation strategy was used again, starting with the transient protection of N²H, O⁶ and OH^{5'} with excess TMSCl (almost 7:1) and pyridine in dry CH₂Cl₂. Since reactions performed with large amounts of catalyst are usually complete after a relatively short time and TLC monitoring is hampered by acid-labile protecting groups, a 3 h time was always selected before adding either an acyl chloride or an anhydride. Due to the low stability of trimethylsilyl groups and the acidity of silica gel, CH₂Cl₂ had to be saturated with NH₃ in TLC control to deactivate the plate during elution. Although the moderately stable TMS moieties should be removed by a mild acidic workup, ¹H NMR analysis of the crude showed a mixture of still protected, partially silylated and unprotected intermediates. Treatment with 1 M HCl was thus necessary in all cases prior to flash column chromatography.



Reagents and conditions (yield): a) i) TMSCl, Py, CH₂Cl₂; ii) RCOX (X = OCO(CH₂)₂CH₃ for **105** and Cl for **106**); iii) 1 M HCl, THF (62-63%).

Scheme 4.19. *N*²-Acylation of **98**

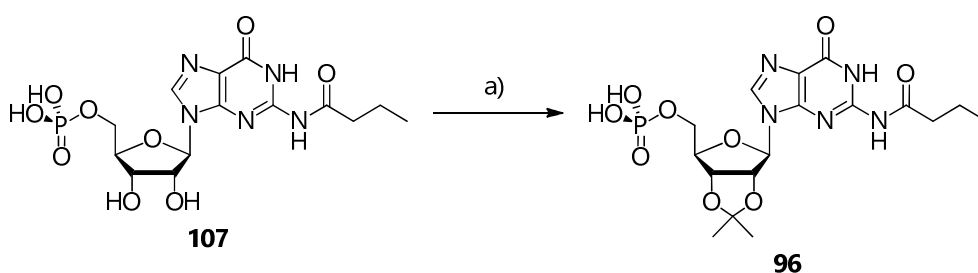
The usual protocol was followed to provide guanylic acid **107** after semi-preparative HPLC, with the concomitant removal of the 2',3'-*O*-isopropylidene moiety (**Scheme 4.20**).



Reagents and conditions (yield): a) i) TEP, 50°C; ii) POCl₃, H₂O, 0°C; iii) H₂O, 6 M NaOH (to pH 2); iv) 70°C (75%).

Scheme 4.20. Phosphorylation of **105**

Treatment with 2,2-dimethoxypropane (2,2-DMP) and *p*-TsOH·H₂O in a 4:1 acetone-DMF mixture once again allowed to reinsert the 2',3'-*O*-isopropylidene moiety on **107** (**Scheme 4.21**). After purifying the crude by semi-preparative HPLC, **96** was finally obtained in 30% yield.



Reagents and conditions (yield): a) 2,2-DMP, *p*-TsOH·H₂O, acetone/DMF, reflux (30%).

Scheme 4.21. Reintroduction of the 2',3'-*O*-isopropylidene moiety on **107**

To date, the synthetic sequence toward **97** has not been completed yet. *N*²-Undecanoyl intermediate **106** will be phosphorylated on OH^{5'} and subjected to 2',3'-*O*-isopropylidene reinsertion presumably by the same protocols exploited to convert **105** into **107** and then **96**.

The synthesized guanylic and inosinic acids (**94-97**) will be tested as potential ligands of GPR17 by Surface Plasmon Resonance (SPR).¹⁵⁰

5 | CONCLUSIONS

The first part of this PhD Thesis described the chemoenzymatic synthesis of 6-substituted purine ribonucleosides catalyzed by a purine nucleoside phosphorylase from *Aeromonas hydrophila* (*AhPNP*). Starting from the results reported in *Adv. Synth. Catal.* **2012**, 354, 96-104 and *J. Chromatogr. B* **2014**, 968, 79-86, the following goals were achieved:

- *AhPNP* was successfully exploited to catalyze the “one-pot, one-enzyme” regio- and stereoselective transfer of β -D-ribose from a proper sugar *donor* (7-methylguanosine iodide) to a library of 6-substituted purine *acceptors*, resulting in the “in batch” synthesis of twenty-four ribonucleosides. The conversions of the investigated transglycosylations allowed a preliminary assessment of the substrate specificity of *AhPNP* toward 6-modified purines. All results confirmed a broad tolerance and therefore highlighted the potential of *AhPNP* as biocatalyst, providing the necessary information to undertake the preparative synthesis of 6-modified purine nucleosides;
- *AhPNP* was immobilized in a stainless steel column resulting in a stable and active bioreactor (*AhPNP*-IMER, Immobilized Enzyme Reactor) that, upon on-line connection to a semi-preparative HPLC system, was used to run transglycosylation reactions in a flow mode. In such a set-up, biotransformation, on-line monitoring and product purification occurred in a single integrated platform, thus assisting the straightforward preparation of five nucleoside analogues at a mg scale in moderate to high yield (52-89%).

These results were described in *Curr. Org. Chem.* **2015**, 19, 2220-2225 and *Adv. Synth. Catal.* **2015**, 357, 2520-2528, respectively.

As a step forward, *AhPNP* was applied to the chemoenzymatic synthesis of sugar-modified purine nucleosides. In this frame, preliminary studies were performed as follows:

- the synthesis of arabinosyladenine was performed to explore the feasibility of a “one-pot, one-enzyme” chemoenzymatic approach toward arabinonucleosides. However, the necessary β -D-arabinose *donor* (7-methylarabinosylguanine iodide) was not phosphorylated by the catalyst and the application of the process already exploited for the synthesis of 6-substituted purine ribonucleosides starting from 7-methylguanosine iodide was not feasible in this case;
- the alternative “one-pot, two-enzyme” strategy was applied by coupling *AhPNP*-IMER with an analogous bioreactor based on a uridine phosphorylase from *Clostridium perfringens* (*CpUP*), covalently immobilized in a monolith column. The on-line apparatus of integrated synthesis and reaction monitoring obtained by connecting *CpUP*-IMER and *AhPNP*-IMER in series was tested in the synthesis of adenosine, 2'-deoxyadenosine and arabinosyladenine from uridine, 2'-deoxyuridine and arabinosyluracil as sugar *donors*, respectively. The corresponding nucleobases were transformed into the products in almost 90% conversion over 1 h for the ribosyl and 2'-deoxyribosyl derivatives. On the contrary, a 20% conversion was registered for arabinosyladenine after 5 h. Scale-up to a semi-

preparative synthesis is being developed (G. Cattaneo, M. Rabuffetti, G. Speranza, T. Kupfer, B. Peters, G. Massolini, D. Ubiali, E. Calleri *Submitted 2017*).

In the second part of this PhD Thesis, the PNP from *Mycobacterium tuberculosis* (*MtPNP*) was selected as a target to develop potential inhibitors:

- a new LC-ESI-MS/MS method was set up to evaluate the inhibition activity of 8-substituted purine ribonucleosides toward *MtPNP* and the selectivity against the microbial enzyme with respect to the corresponding human one (*HsPNP*). The enzymatic assay, based on the phosphorolysis of inosine, proved to be very convenient in terms of time (15' for plate processing and 2' for LC-MS analysis), as well as target amount, and was validated according to FDA guidelines. A series of seven 8-substituted purine ribonucleosides were screened, together with Acyclovir and Formycin A as positive and negative control, respectively. The library did not exert any significant effect up to 1 mM, with 8-bromoguanosine and 8-methylaminoguanosine being the only exceptions at 500 mM as weak inhibitors.

A complete description of the analytical protocol was published in *Anal. Chim. Acta* **2016**, *943*, 89-97.

The third and last part of this PhD Thesis was dedicated to the chemical synthesis of 8- and *N*²-substituted inosinic and guanylic acids as potential ligands of the human GPR17 receptor. Starting from studies aided by molecular modeling on a homology model of the protein target, the following goal was achieved:

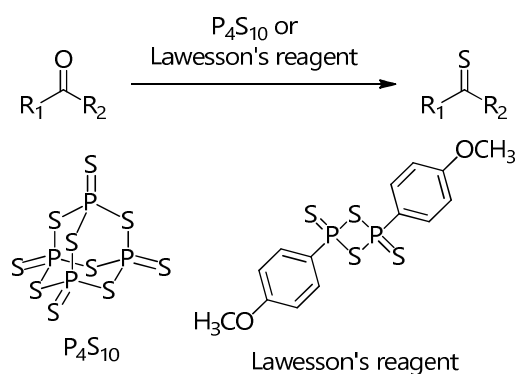
- a small library of 8- and *N*²-substituted derivatives of inosinic and guanylic acids were synthesized either by direct phosphorylation of 8-methylaminoinosine, previously prepared in the context of inhibition assays regarding *MtPNP*, or by proper alkylation/acylation of guanosine, followed by the introduction of a phosphate group in position 5'. Owing to the scarce nucleophilicity of the exocyclic NH₂ group in the synthesis of the *N*²-octyl derivative, the 2-position of the purine ring was activated as a bromo derivative, whose displacement with the proper amine afforded the desired functionalization. On the contrary, *N*²-acylations were carried out through a procedure involving the temporary protection of guanosine by silylation, nitrogen functionalization with a proper acyl chloride or anhydride and deprotection. An additional 2',3'-*O*-isopropylidene group was inserted after the phosphorylation step in all *N*²-functionalized nucleotides. Binding assays on GPR17 will be carried out.

6 | APPENDIX

6.1. Mechanisms of selected reactions

6.1.1. Carbonyl thiation with P_4S_{10} and Lawesson's reagent

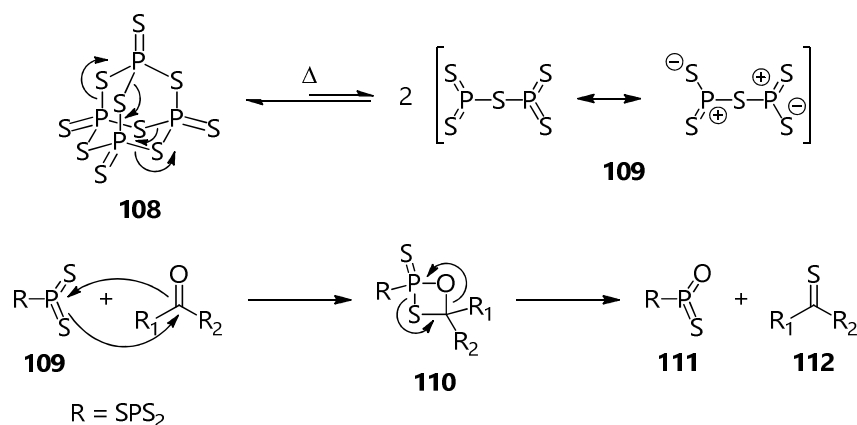
Tetraphosphorus decasulfide (P_4S_{10}) and Lawesson's reagent (2,4-bis(*p*-methoxyphenyl)-1,3-dithiadiphosphetane-2,4-disulfide) are useful reagents for the direct conversion of compounds containing carbonyl moieties (ketones, aldehydes, lactones, esters, amides and carboxylic acids) to the corresponding thiocarbonyl derivatives in generally good yields, as well as of alcohols to thiols (**Scheme 6.1**).



Scheme 6.1. Carbonyl thiation with P_4S_{10} and Lawesson's reagent

Thiation using P_4S_{10} is conducted in refluxing solvents such as benzene, toluene, 1,4-dioxane, xylene, THF, pyridine, CH_3CN and CS_2 and only seldom in CH_2Cl_2 or Et_2O at lower temperatures (usually $0^\circ C$). A base is often added (*e.g.* $NaHCO_3$, Na_2CO_3 , Na_2SO_3 , TEA, Al_2O_3 , ...).

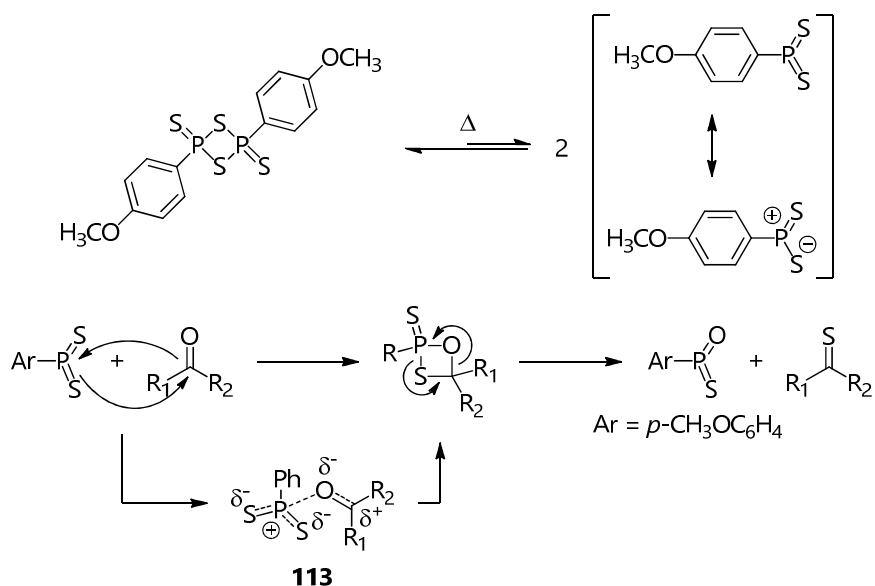
The generally accepted Wittig-type mechanism for thiation of carbonyl compounds by P_4S_{10} (**108**) (**Scheme 6.2**) consists of an initial thermal decomposition to the active dithiophosphine ylide P_2S_5 (**109**), which cycloadds to the carbonyl substrate and evolves to a thioxaphosphetane (**110**). The final step, which is rate-determining, is a cycloreversion to the thiocarbonyl product (**112**) and the oxathiophosphine ylide (**111**) of the initial reagent. Apart from the high stability of a new $P=O$ bond, the driving force of the whole process is the capacity of **111** to form trimers, instead of performing a second thiation hampered by a higher energy barrier.¹⁵¹



Scheme 6.2. Wittig-type mechanism of carbonyl thionation with P_4S_{10}

Hydroxyl groups are the most reactive moieties, followed by amides, ketones, aldehydes and esters. Lawesson's reagent was extensively studied by the Lawesson research group as a very convenient alternative to P_4S_{10} introduced in the 1950s.¹⁵² As its reactivity is not very high, an excess is often required in dry hydrocarbon solvents (benzene, toluene, xylene, ...) under heating, to obtain products in clean, fast and efficient reactions in terms of yield. Yields and manipulation are higher and easier, respectively, than P_2S_5 , with no significant by-product formation.

The thionation mechanism is almost identical to the previous one (**Scheme 6.3**).



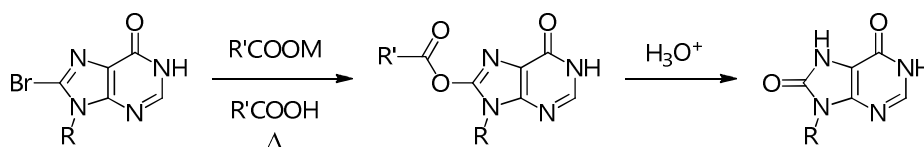
Scheme 6.3. Wittig-type mechanism of carbonyl thionation with Lawesson's reagent

Since the formation of the four-membered intermediate is concerted, no zwitterions are involved, but strong electrostatic interactions able to stabilize the carbonyl-ylide encounter pair (**113**) are essential to promote the second step, as computationally demonstrated by Legnani *et al.*¹⁵³

6.1.2. 8-Oxygenation of 8-bromopurine nucleosides

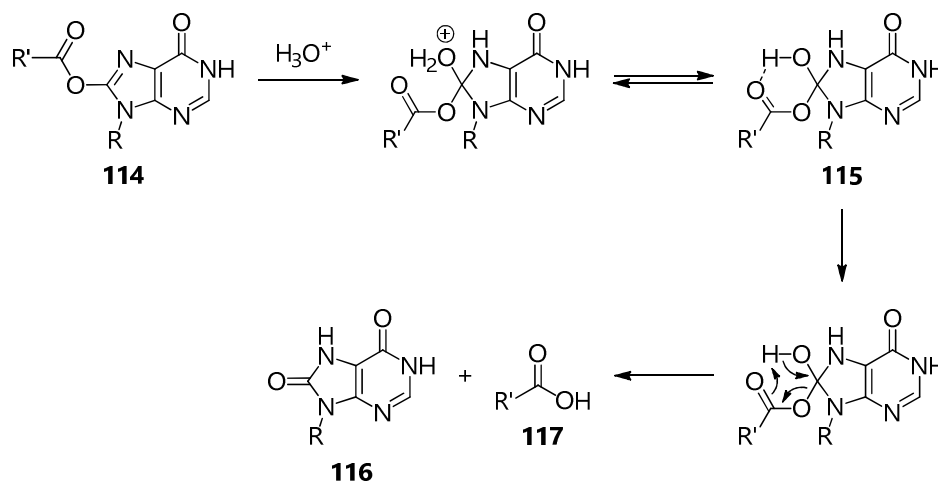
Due to their electrophilic nature, 8-bromopurine nucleosides are prone to reactions with a large number of nucleophiles ranging from mild (amines) to quite strong (alkoxydes, sulfides, ...).

In the case of carboxylate ions sources (**Scheme 6.4**), a 2-imidazolyl-type ester can be obtained at high temperatures in the presence of the analogous acid. The intermediate ester is significantly sensitive to acid- and base-catalyzed hydrolysis, not requiring harsh conditions. Like imine decomposition, this reaction is usually carried out *in situ* during the final work-up by a mildly acidic or basic wash. It is therefore possible to perform 8-oxygenation of 8-bromohypoxanthine nucleosides in a single step.



Scheme 6.4. 8-Oxygenation of 8-bromopurine nucleosides with a carboxylate salt

The first step is a bromide displacement by the carboxylate ion, whose already low nucleophilicity is made even scarcer by the presence of the acid. Quite high temperatures are thus necessary (often > 100°C). The resulting 2-imidazolyl-type ester undergoes a mild hydrolysis in acidic conditions by the same mechanism which leads to the analogous reaction of enol esters (**Scheme 6.5**).¹⁵⁴

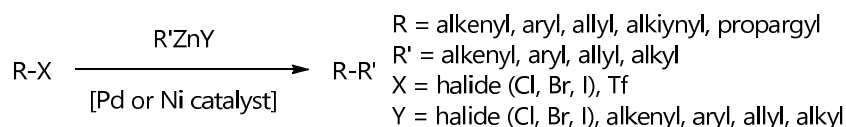


Scheme 6.5. Mechanism of the acid-catalyzed hydrolysis of 2-imidazolyl esters of purine derivatives

After an initial regioselective hydration of **114** aided by the ability of N⁷ to be protonated, the intermediate *O*-acylhemiactal **115** undergoes a cyclic six-membered transposition leading to the release of product **117** and the carboxylic acid corresponding to the initial ester (**116**). The formation of an intramolecular hydrogen bond between OH and the carbonyl moiety is likely to stabilize the transition state and promote the electron flow.

6.1.3. Negishi cross-coupling

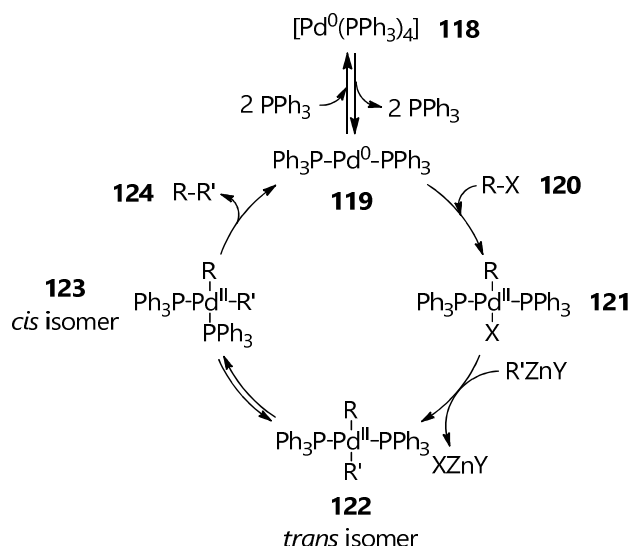
As a reaction involving an organozinc compound, an organic halide or triflate and either Ni or Pd as catalyst, the Negishi coupling is able to generate new C_{sp}³-C_{sp}³ or C_{sp}³-C_{sp}² bonds. Depending on a choice which seems to be totally empirical or based on the ease of access, organozinc reagents such as RZnY can be used (Y = halide or organic moiety) (**Scheme 6.6**).¹⁵⁵



Scheme 6.6. Negishi cross-coupling catalyzed by a Pd or Ni catalyst

Due to these very mild conditions, substrates and reagents bearing sensitive moieties (halides, esters, alcohols, amines, carboxylic acids, ...) can be involved in this kind of reaction with almost no need for protective groups.

All cross-couplings (Suzuki, Miyaura, Negishi, Stille, Sonogashira, ...) evolve through the same three steps (**Scheme 6.7**): an oxidative addition of the substrate containing a leaving group to the metal catalyst, the inter- or intramolecular transfer of an organic group toward the counterpart (organometals in general) by transmetalation and a final reductive elimination to form the new C-C bond. Pd, Ni and Cu are by far preferred over other metals, while the nature of the transfer agent depends on the reaction itself. For the Negishi cross-coupling reaction, a catalyst such as $[Pd(PPh_3)_4]$ is usually chosen.

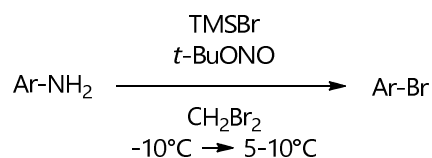


Scheme 6.7. Catalytic cycle of the Negishi cross-coupling

Although this general mechanism is widely accepted, each step may present specific features different from other cross-couplings, depending on reaction conditions. Before the oxidative addition, a preactivation step must occur in order to either reduce Pd^{II} (usually provided as salt) to Pd^0 or dissociate at least two ligands from the precatalyst (**118**), already in the lowest oxidation state, to form a $[Pd^0(PPh_3)_x]$ complex (usually $x = 2$). The active catalyst **119** then undergoes an oxidative addition with **120** to form a square planar triflate or halide Pd^{II} complex (**121**). The step may occur by a concerted mechanism or, more probably, a S_N1 -like stepwise one. The subsequent transmetalation strongly depends on the organozinc species, which can either be a diorgano or a monoorganohalide compound. Prior to the C-C bond formation, the diorganozinc intermediate **122** (*trans* isomer) must isomerize to the corresponding *cis* complex **123**.¹⁵⁶ Experimental data suggest that such an interconversion may not occur directly, but rather *via* retrotransmetalation.¹⁵⁷ The last reductive elimination affords product $R-R'$ (**124**) through a cyclic three-member transition state and regenerates the Pd^0 active catalyst.

6.1.4. Bromination by Sandmeyer-type reaction

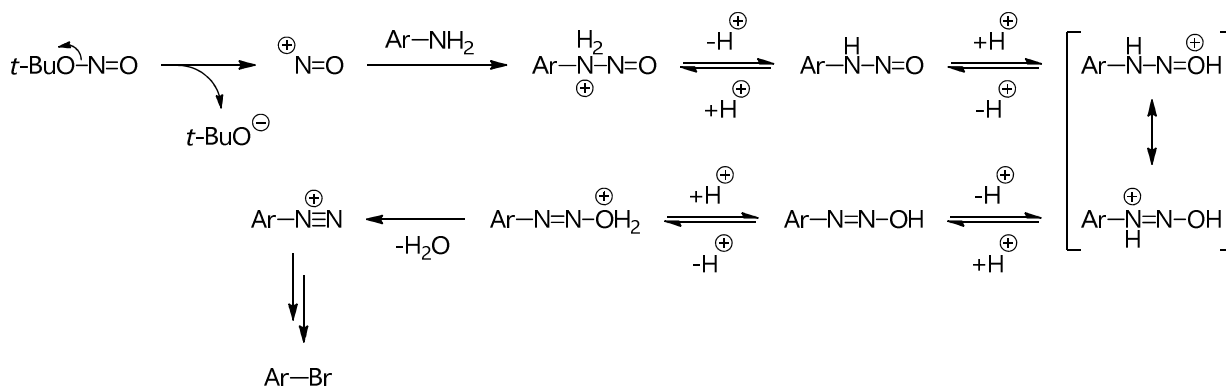
The exocyclic N^2H_2 moiety of arylamines can be converted into a bromine group by treatment with TMSBr and *t*-BuONO in CH_2Br_2 , between -10 and $5-10^\circ C$, following the Sandmeyer-type¹⁵⁸ procedure reported by Francom and Robins¹⁴⁵ (**Scheme 6.8**).



Scheme 6.8. Sandmeyer-type bromination of primary arylamines

A classic Sandmeyer reaction requires two steps, the first of which involves the formation of a diazonium salt by reaction of the amine with a source of HNO_2 to be formed *in situ* (usually $NaNO_2$ coupled with HCl , $AcOH$ or HBF_4). Excess KBr must be added as brominating agent, together with a $Cu^I Br-Cu^{II} Br_2$ catalytic mixture. CH_3CN is frequently the solvent of choice. In this Thesis, *t*-BuONO was selected as a good nitrosyl cation source to form the key aryldiazonium salt, TMSBr as bromine source and CH_2Br_2 as a compatible solvent which may also participate in the mechanism as halogen donor. It is worth pointing out that this choice allows a one-pot process and prevents the use of any Cu catalyst.

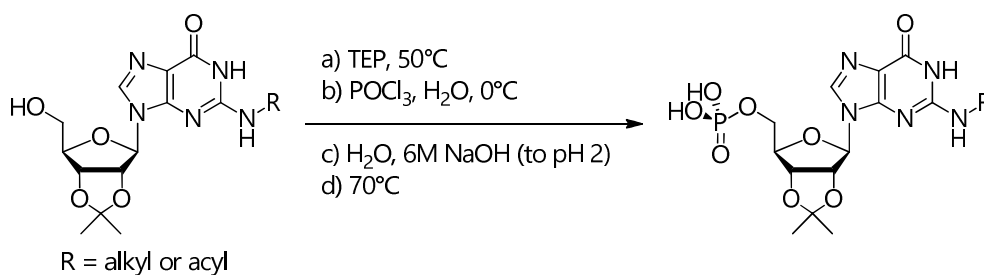
The reaction mechanism is reported in **Scheme 6.9**.



Scheme 6.9. Mechanism of a Sandmeyer-type bromination on a primary arylamine

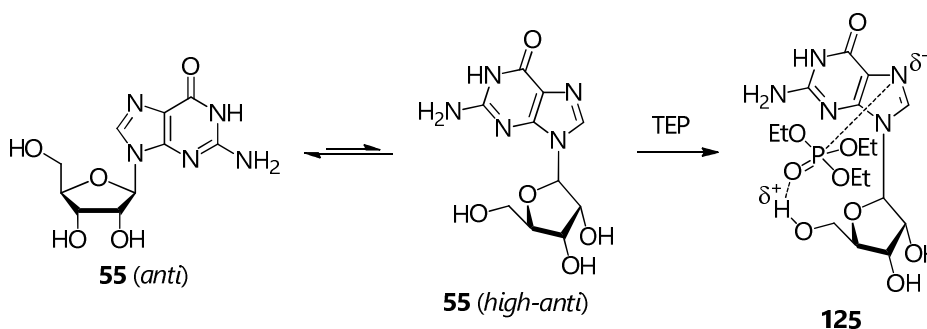
6.1.5. Phosphorylation of N^2 -alkyl- and N^2 -acylguanosines with $POCl_3$ /TEP

A phosphate group can be inserted on the primary hydroxyl group of N^2 -alkyl- and N^2 -acylguanosines using the protocol described by Ikemoto *et al.*¹⁴⁶ This procedure allows the direct phosphorylation of 5'-unprotected ribonucleosides to their respective phosphates, through $POCl_3$ as phosphorylating agent in the presence of a trialkylphosphate as solvent. Trimethyl- and triethylphosphate (TMP and TEP, respectively) may be selected. Furthermore, additions of H_2O accelerate the reaction. The general protocol, compatible with variably substituted substrates, proceeds through four steps (**Scheme 6.10**).



Scheme 6.10. Phosphorylation of N^2 -alkyl- and N^2 -acylguanosines with POCl_3/TEP

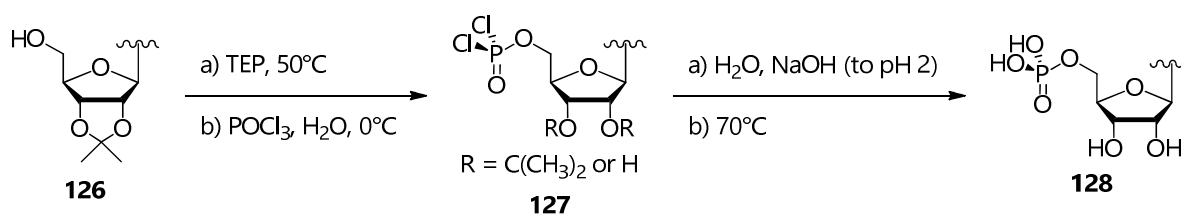
Before adding any phosphorylating agent, a binary nucleoside-TEP complex (**125**) must be formed at 50°C to properly promote the subsequent steps. The case of guanosine (**55**) is represented in **Scheme 6.11**.



Scheme 6.11. Formation of the **55**-TEP complex

125 was extensively studied and showed not only higher selectivity but also more excellent reactivity toward POCl_3 than **55** itself. This behavior is caused by an internal activation exerted by the phosphate unit bridging $\text{OH}^{5'}$ to N^7 . From various analytical data (IR spectra, XRD analysis, ^{13}C -NMR and dipolar diphasic determination), **125** was argued to be formed by the interaction of TEP with the *high-anti* conformer of **55**, disfavored in the equilibrium with its *anti* form. A hydrogen bond involves the first complexation site ($\text{OH}^{5'}$) and the $\text{P}=\text{O}$ oxygen in TEP, whereas a charge-transfer interaction likely relocates electron density from N^7 to the P atom. A significant partial charge is thus generated on the hydroxyl moiety and increases its nucleophilicity.

The conditions studied to optimize each step can be applied to 2'-3'-*O*-isopropylideneribonucleosides **126** (**Scheme 6.12**).



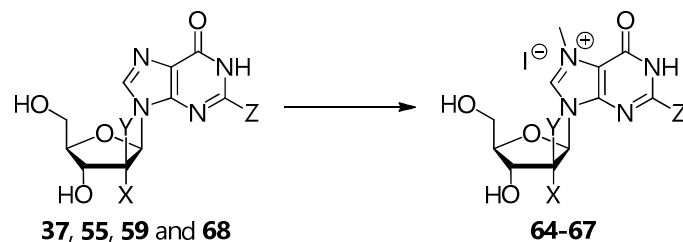
Scheme 6.12. Mechanism of the phosphorylation of 2',3'-*O*-isopropylideneribonucleosides

First of all, due to the incomplete formation of the **126**-TEP complex at $< 30^\circ\text{C}$, preheating at 40 - 50°C is necessary at the beginning of the reaction. As determined from the analysis of various trialkylphosphates, the overall rate diminishes with larger substituent sizes, probably because steric hindrance hampers the complex formation. The next step is the sequential addition of POCl_3 and H_2O . A reduction of the chloride amount from 3 to 1.5 equivalents underlines improved reactivity and selectivity of the complex if compared

to the free nucleoside. In addition, the presence of a little less than $\frac{1}{4}$ of H_2O for each POCl_3 equivalent markedly promotes the reaction, according to a curve characterized by an *optimum* point. The nucleophilic attack by $\text{OH}^{5'}$ on POCl_3 forms a dichlorophosphate intermediate (**127**) releasing one HCl equivalent. Product **128** results from the addition of concentrated NaOH until pH 2 and subsequent heating at 70°C , which hydrolyzes the intermediate to the final phosphate ester. It is worth noting that low pH and H_2O synergistically promote the removal of the acid-labile 2',3'-*O*-isopropylidene *in situ*.

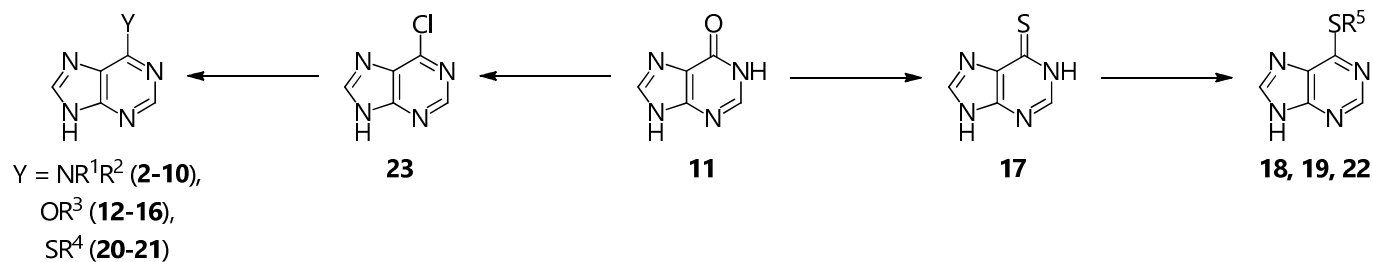
6.2. General synthetic schemes

6.2.1. General scheme of the synthesis of 7-methylpurine and 7-methylguanine nucleoside iodides (64-67)

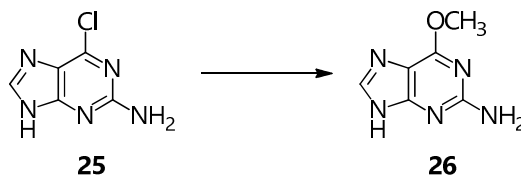


37 and **64**: X = OH, Y = H, Z = H; **55** and **65**: X = OH, Y = H, Z = NH₂;
68 and **66**: X = Y = H, Z = NH₂; **59** and **67**: X = H, Y = OH, Z = NH₂

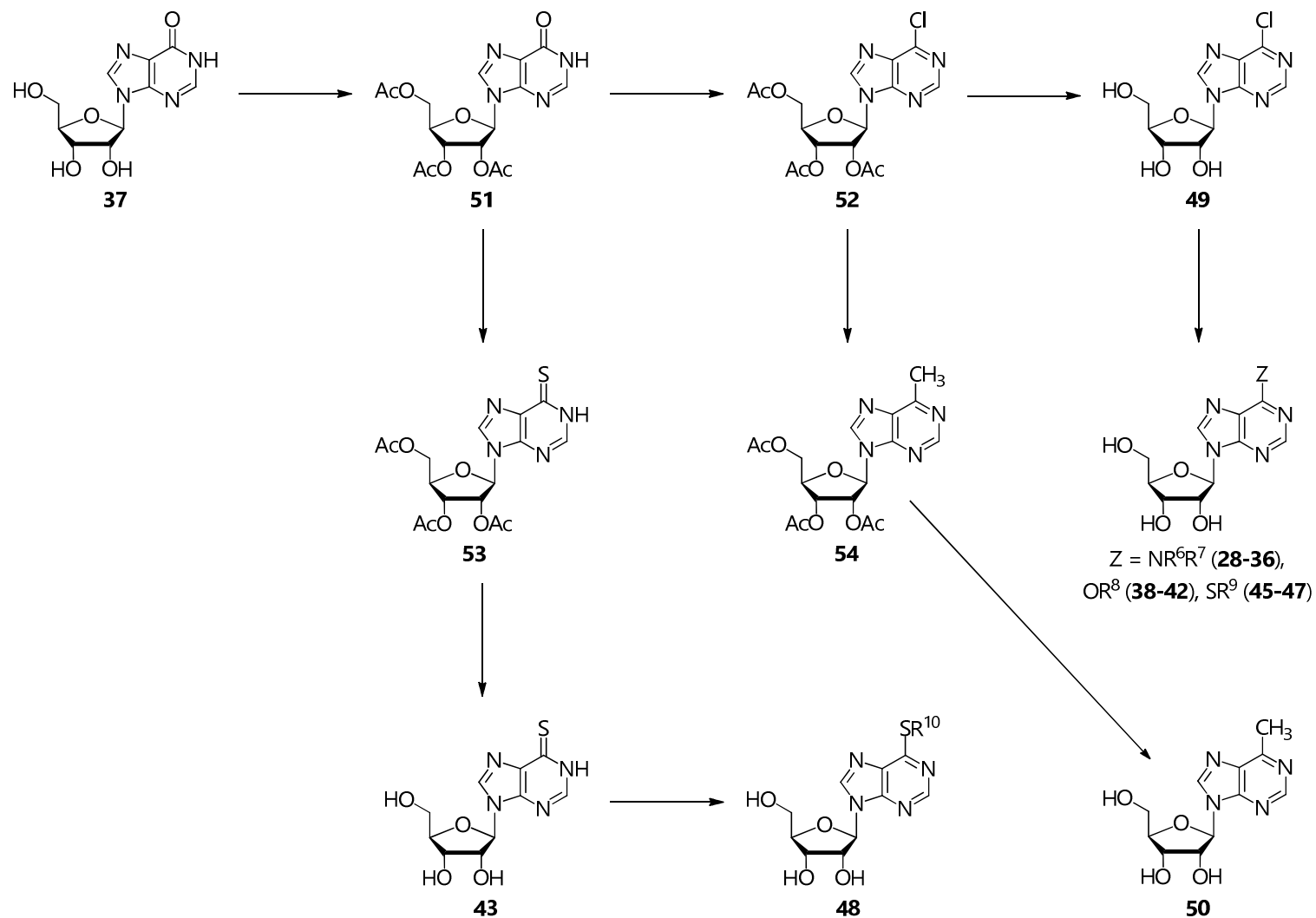
6.2.2. General scheme of the synthesis of 6-substituted purines and adenines (2-10, 12-22, 26)



2: R¹ = H, R² = CH₃; **3**: R¹ = H, R² = CH₂CH₃; **4**: R¹ = H, R² = CH(CH₃)₂; **5**: R¹ = H, R² = CH₂CH₂CH₂CH₃; **6**: R¹ = H, R² = cyclohexyl;
7: R¹ = H, R² = CH₂CH₂Ph; **8**: R¹ = H, R² = CH₂CH₂OH; **9**: R¹ = R² = CH₃; **10**: R¹ = R² = CH₂CH₂OH; **12**: R³ = CH₃; **13**: R³ = CH₂CH₃;
14: R³ = CH(CH₃)₂; **15**: R³ = CH₂CH₂CH₂CH₃; **16**: R³ = CH₂CH₂Ph; **18**: R⁵ = CH₃; **19**: R⁵ = CH₂CH₃; **20**: R⁴ = CH(CH₃)₂;
21: R⁴ = CH₂CH₂CH₂CH₃; **22**: R⁵ = CH₂CH₂Ph.

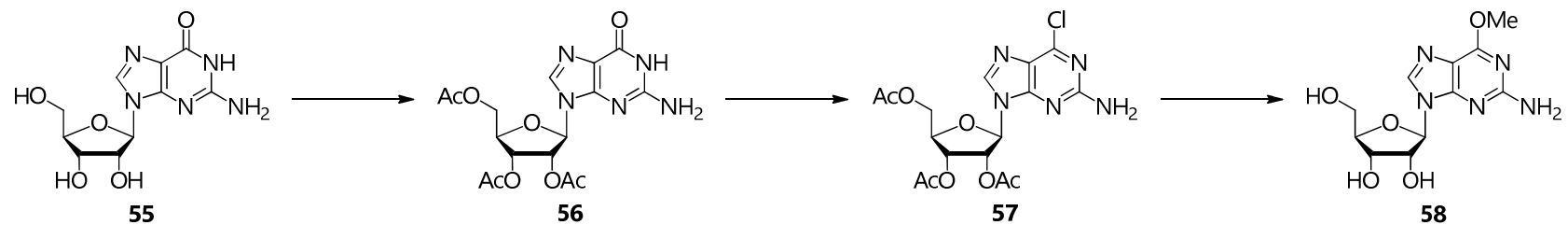


6.2.3. General scheme of the synthesis of 6-substituted inosines and adenosines (28-36, 38-50)

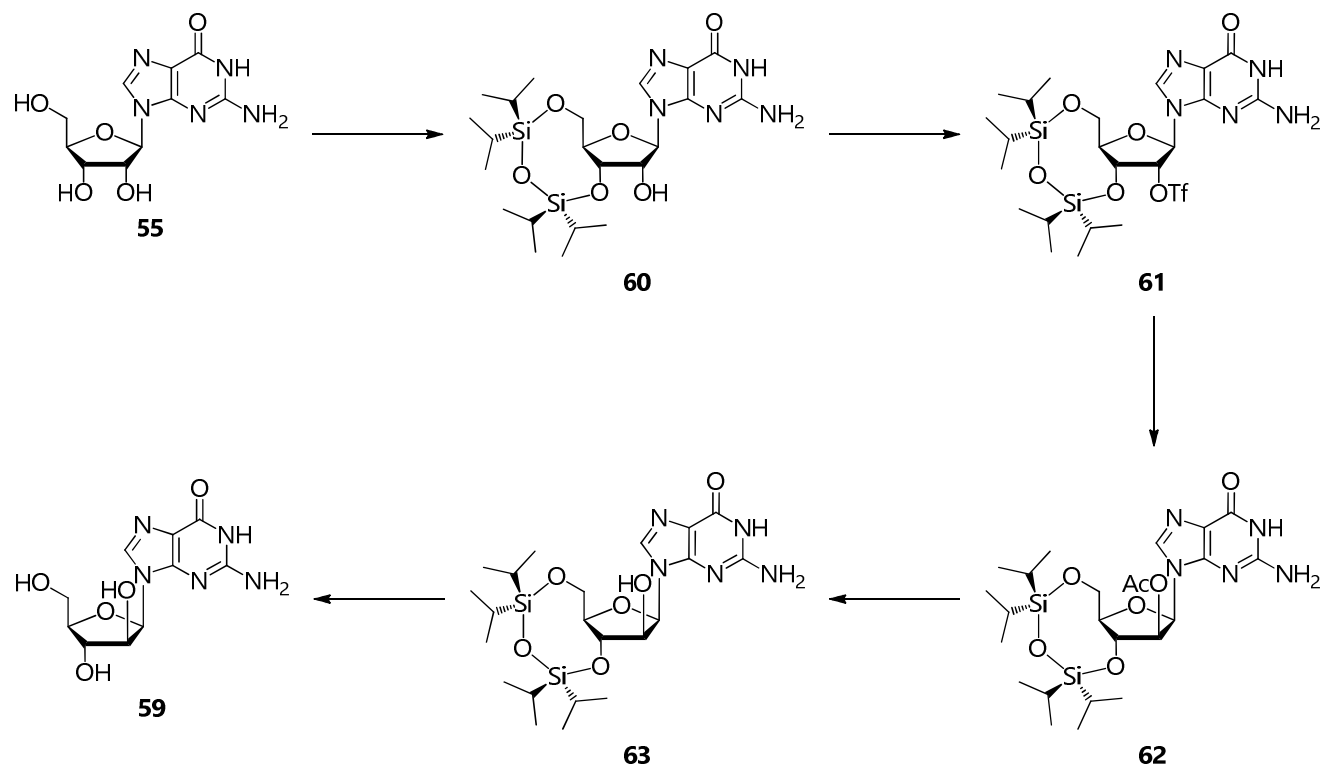


28: $\text{R}^6 = \text{H}, \text{R}^7 = \text{CH}_3$; **29:** $\text{R}^6 = \text{H}, \text{R}^7 = \text{CH}_2\text{CH}_3$; **30:** $\text{R}^6 = \text{H}, \text{R}^7 = \text{CH}(\text{CH}_3)_2$; **31:** $\text{R}^6 = \text{H}, \text{R}^7 = \text{CH}_2\text{CH}_2\text{CH}_2\text{CH}_3$; **32:** $\text{R}^6 = \text{H}, \text{R}^7 = \text{cyclohexyl}$;
33: $\text{R}^6 = \text{H}, \text{R}^7 = \text{CH}_2\text{CH}_2\text{Ph}$; **34:** $\text{R}^6 = \text{H}, \text{R}^7 = \text{CH}_2\text{CH}_2\text{OH}$; **35:** $\text{R}^6 = \text{R}^7 = \text{CH}_3$; **36:** $\text{R}^6 = \text{R}^7 = \text{CH}_2\text{CH}_2\text{OH}$; **38:** $\text{R}^8 = \text{CH}_3$; **39:** $\text{R}^8 = \text{CH}_2\text{CH}_3$;
40: $\text{R}^8 = \text{CH}(\text{CH}_3)_2$; **41:** $\text{R}^8 = \text{CH}_2\text{CH}_2\text{CH}_2\text{CH}_3$; **42:** $\text{R}^8 = \text{CH}_2\text{CH}_2\text{Ph}$; **45:** $\text{R}^9 = \text{CH}_2\text{CH}_3$; **46:** $\text{R}^9 = \text{CH}(\text{CH}_3)_2$; **47:** $\text{R}^9 = \text{CH}_2\text{CH}_2\text{CH}_2\text{CH}_3$; **48:** $\text{R}^{10} = \text{CH}_2\text{CH}_2\text{Ph}$.

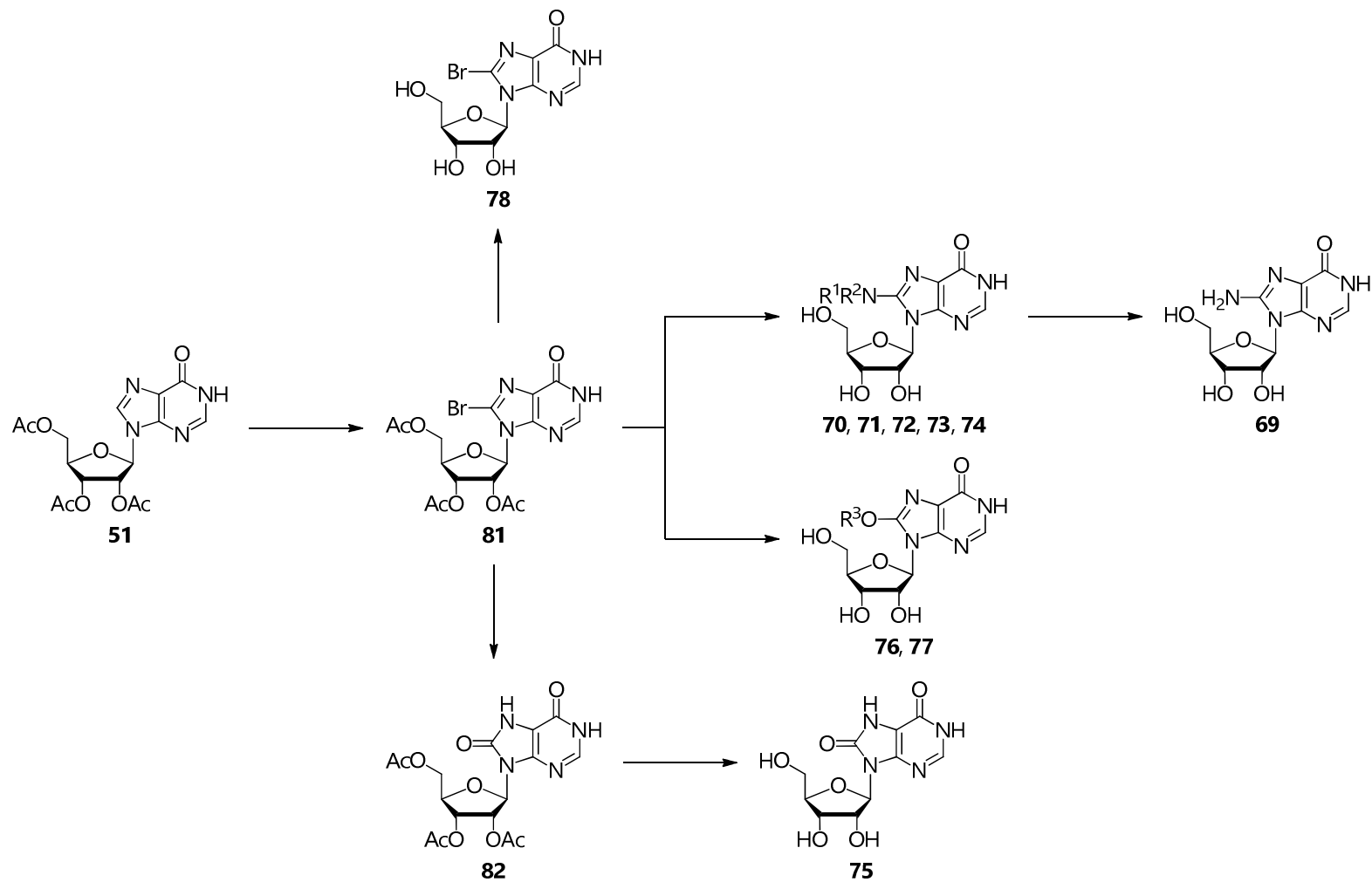
6.2.4. General scheme of the synthesis of 6-*O*-methylguanosine (58)



6.2.5. General scheme of the synthesis of arabinosylguanine (59)

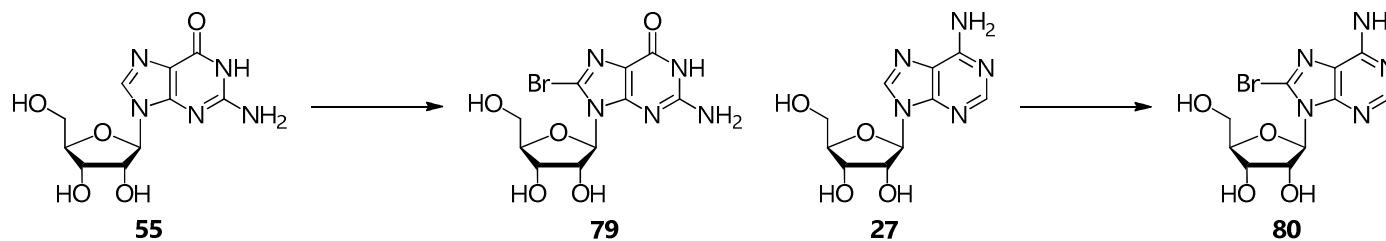


6.2.6. General scheme of the synthesis of 8-substituted inosines (69-78)

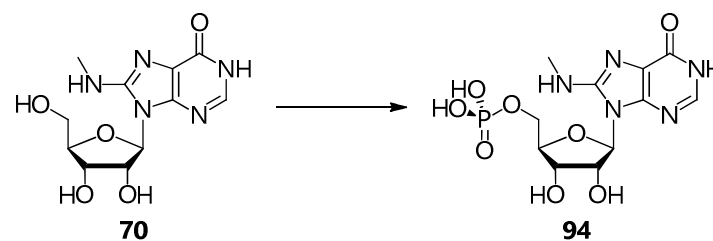


70: $R^2 = H, R^3 = CH_3$; **71:** $R^2 = H, R^3 = CH_2CH_3$; **72:** $R^2 = H, R^3 = CH(CH_3)_2$; **73:** $R^2 = H, R^3 = CH_2Ph$; **74:** $R^2 = R^3 = CH_3$; **76:** $R^1 = CH_3$; **77:** $R^1 = CH_2CH_3$;

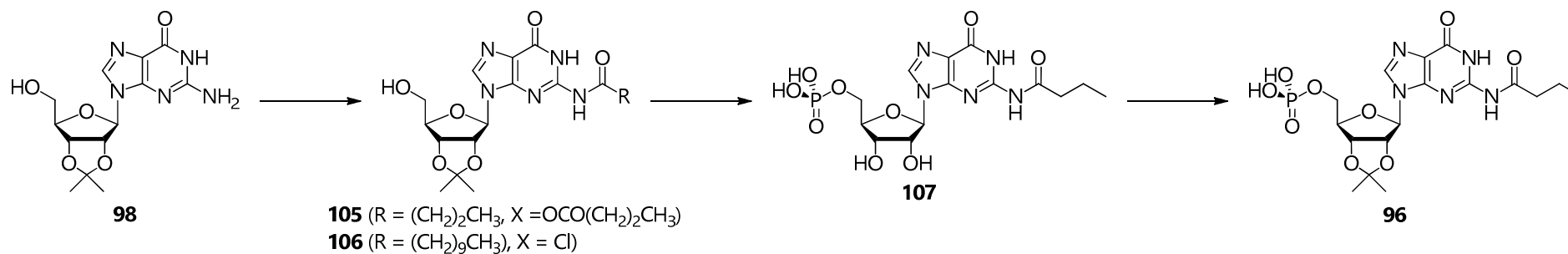
6.2.7. General scheme of the synthesis of 8-bromoguanosine and 8-bromoadenosine (79, 80)



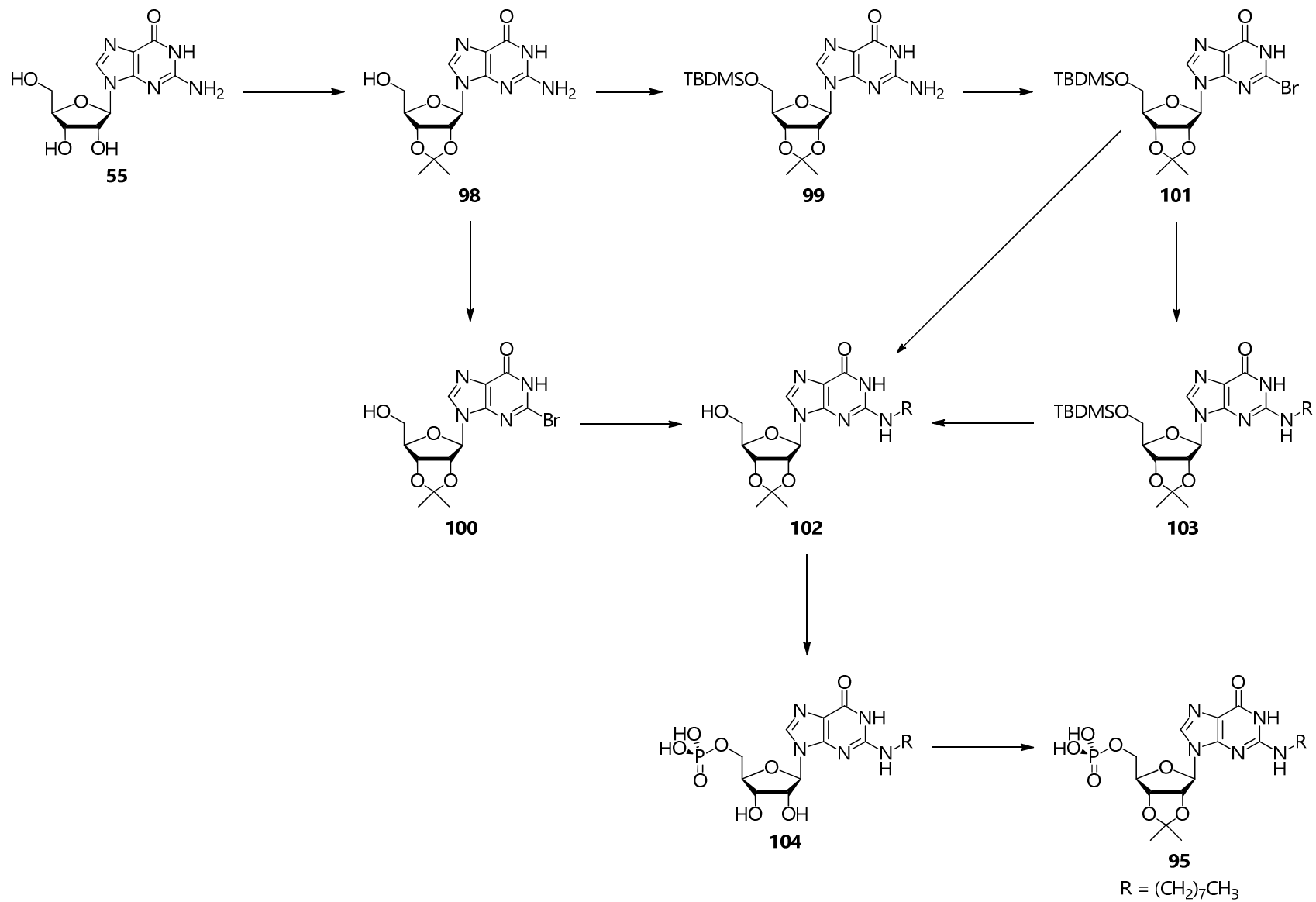
6.2.8. General scheme of the synthesis of 8-methylaminoinosinic acid (94)



6.2.9. General scheme of the synthesis of *N*²-butyryl-2',3'-*O*-isopropylidene-guanylic acid (96)



6.2.10. General scheme of the synthesis of N^2 -*n*-octyl-2',3'-*O*-isopropylidene-guanidylic acid (95)

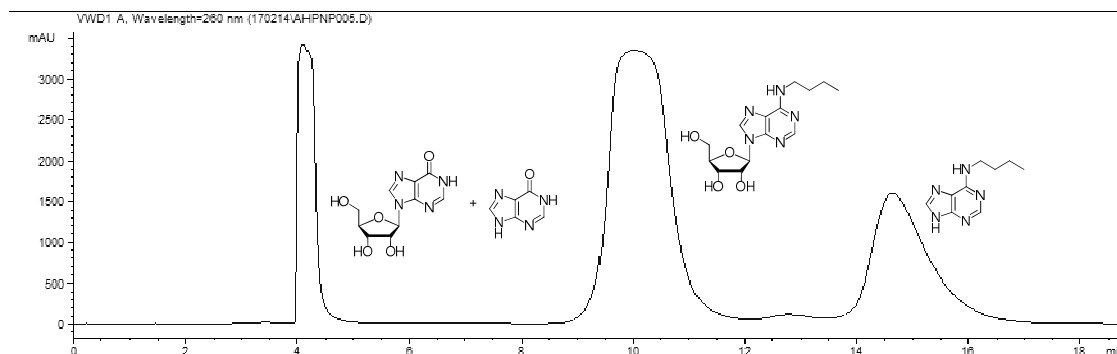


6.3. Semi-preparative chromatograms, $^1\text{H-NMR}$, $^{13}\text{C-NMR}$ and UV-Vis spectra of 6-substituted ribonucleosides synthesized by *Ah*PNP-IMER

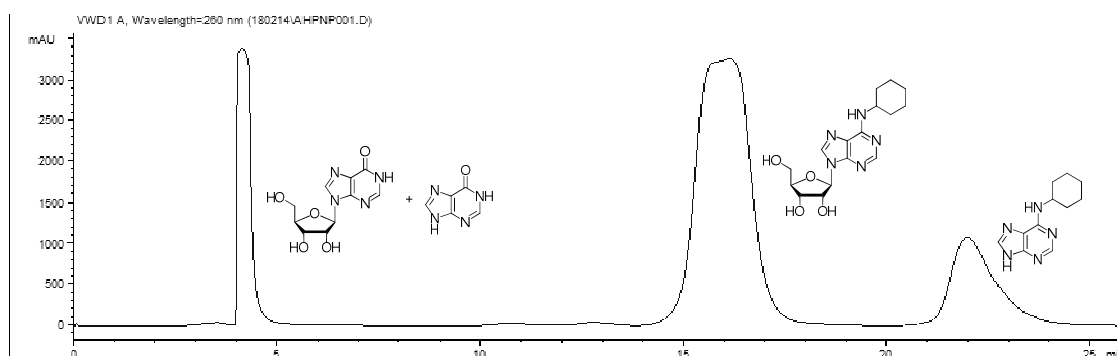
The following chromatograms and $^1\text{H-NMR}$, $^{13}\text{C-NMR}$ and UV-Vis spectra are adapted with permission from *Adv. Synth. Catal.* **2015**, 357, 2520-2528.¹¹⁰

6.3.1. Semi-preparative chromatograms

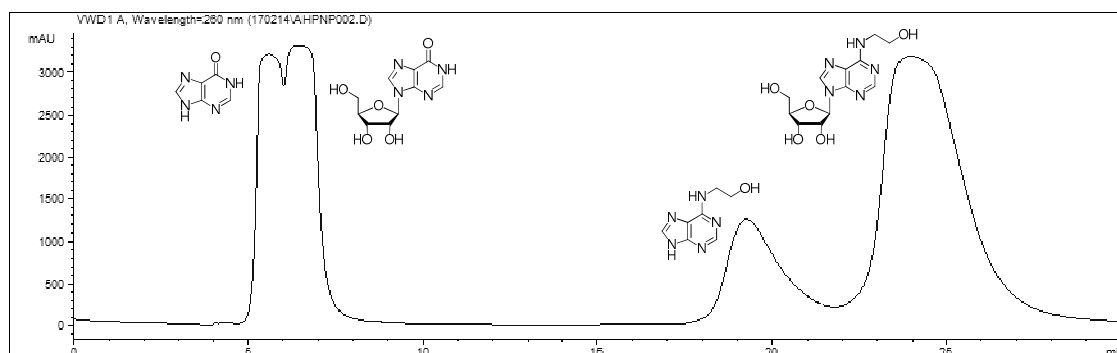
6.3.1.1. N^6 -Butyladenosine (31)



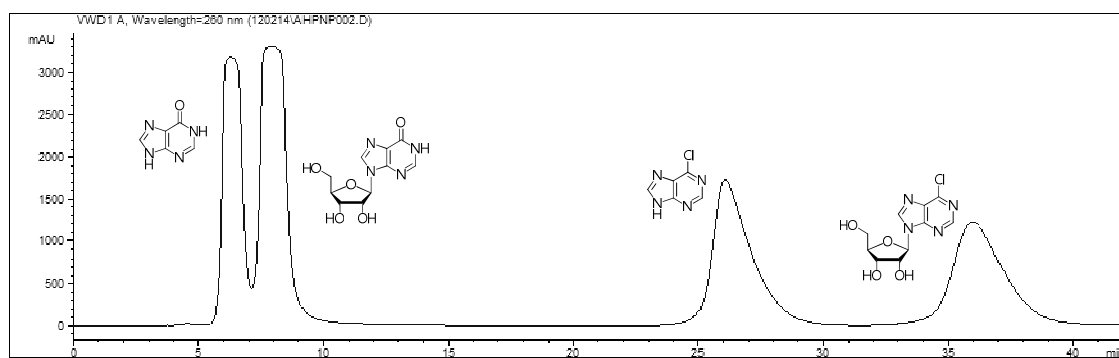
6.3.1.2. N^6 -Cyclohexyladenosine (32)



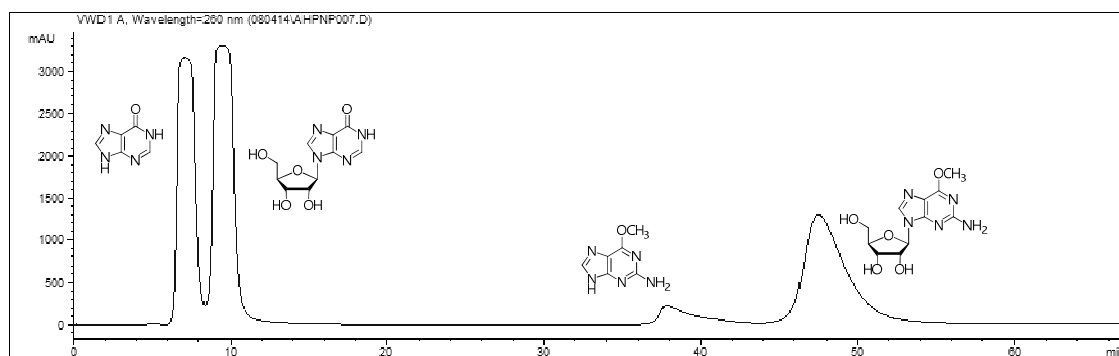
6.3.1.3. N^6 -Hydroxyethyladenosine (34)

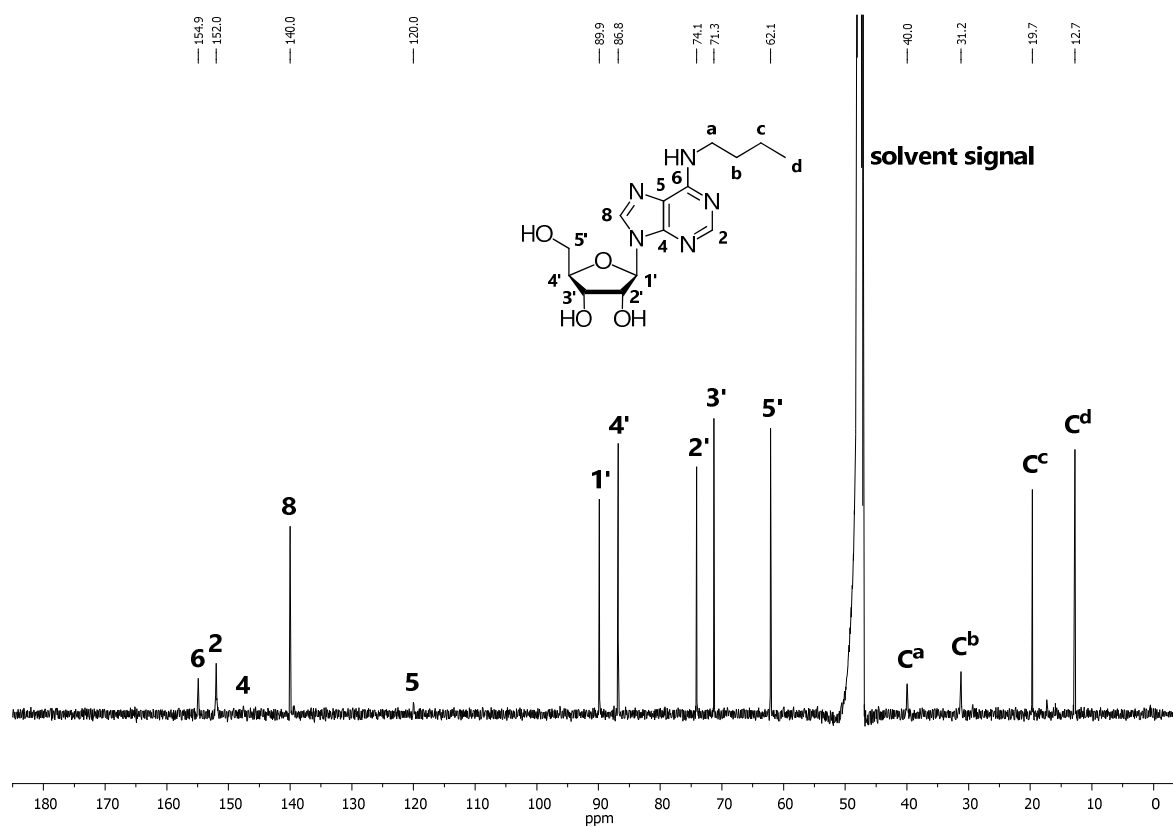
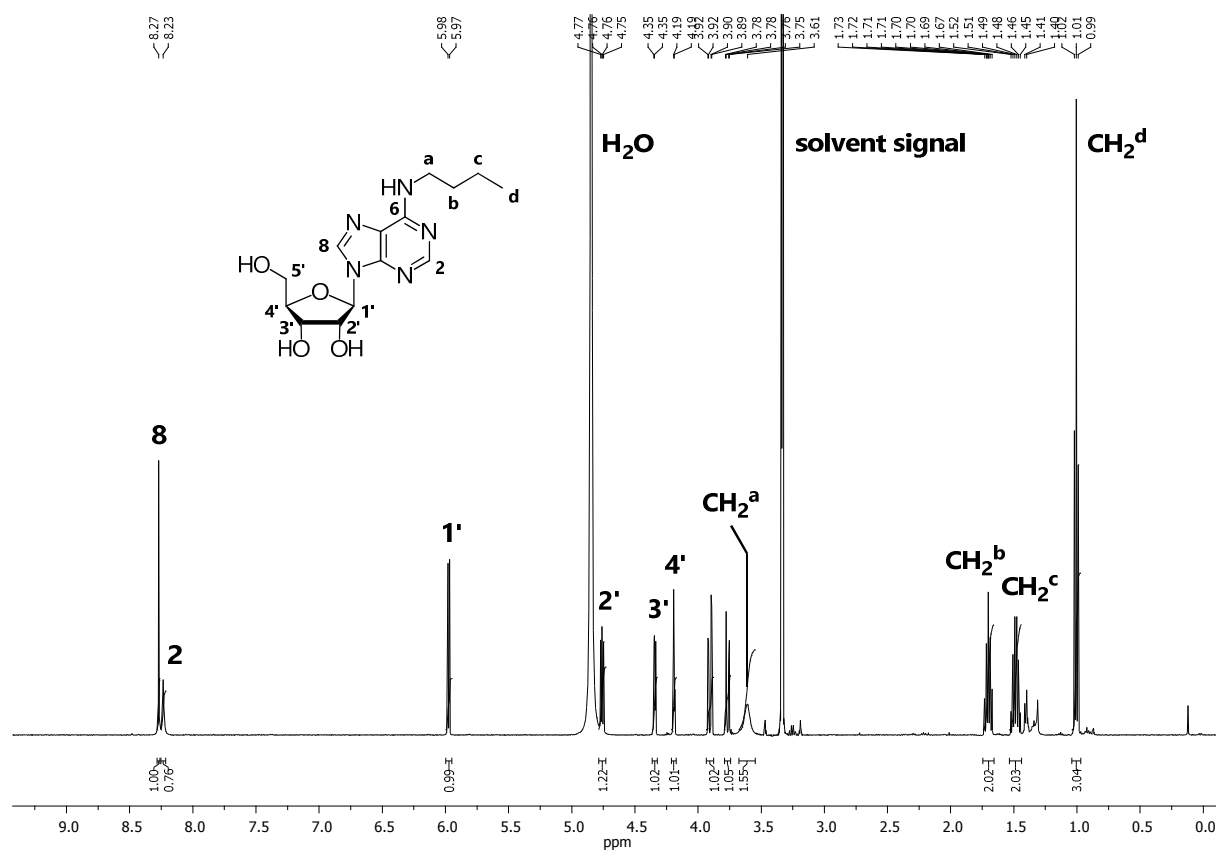


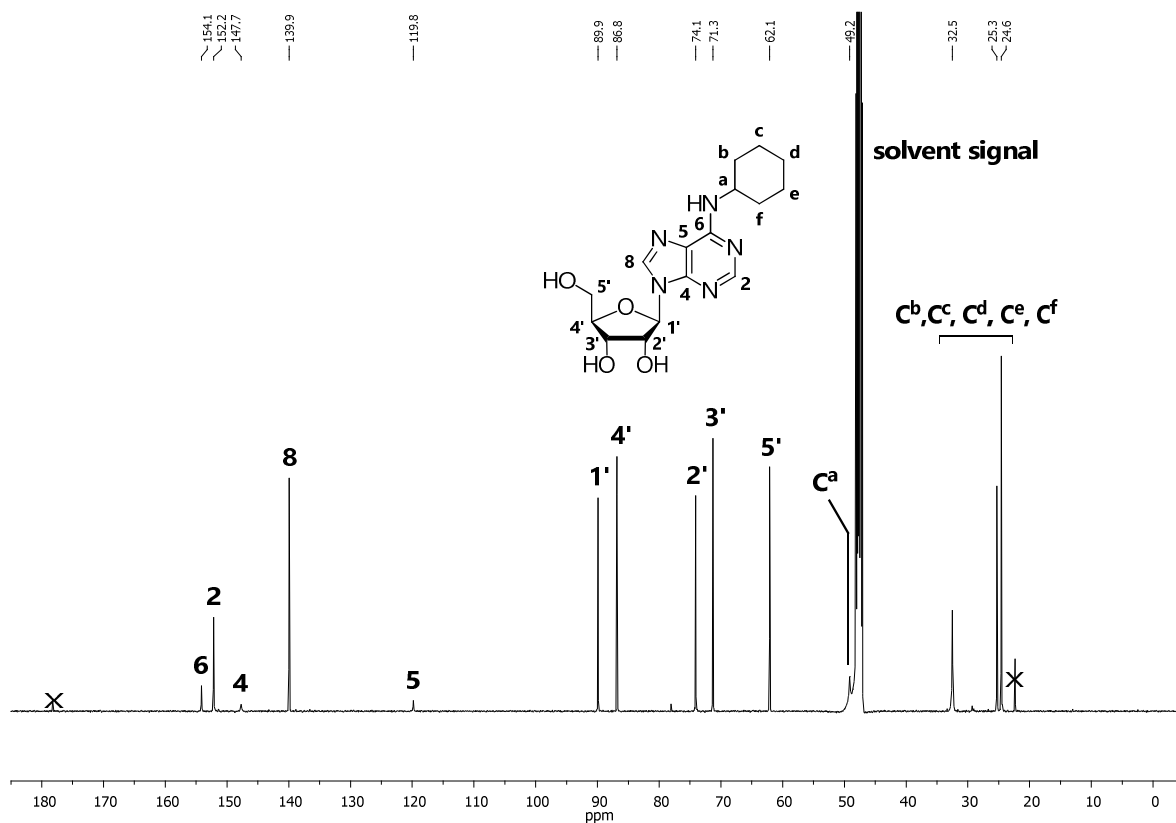
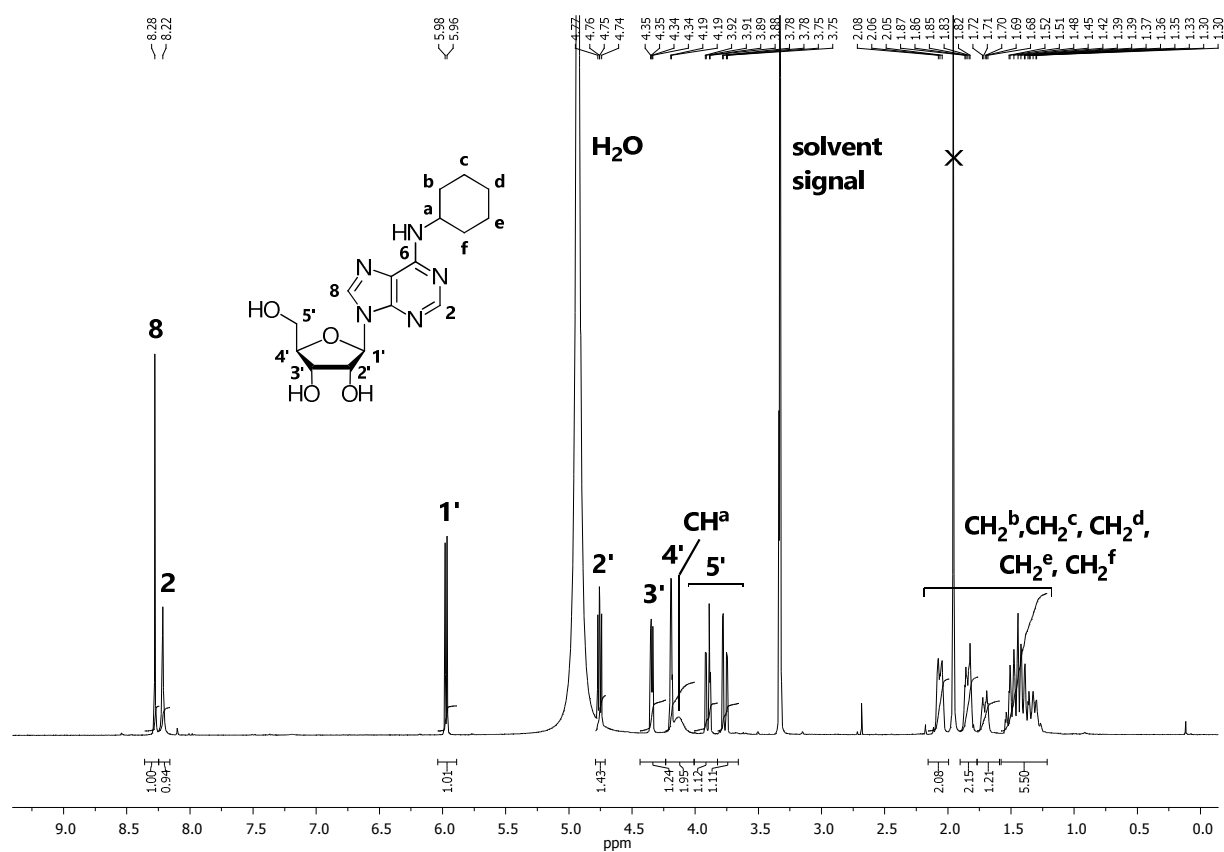
6.3.1.4. 6-Chloroinosine (49)

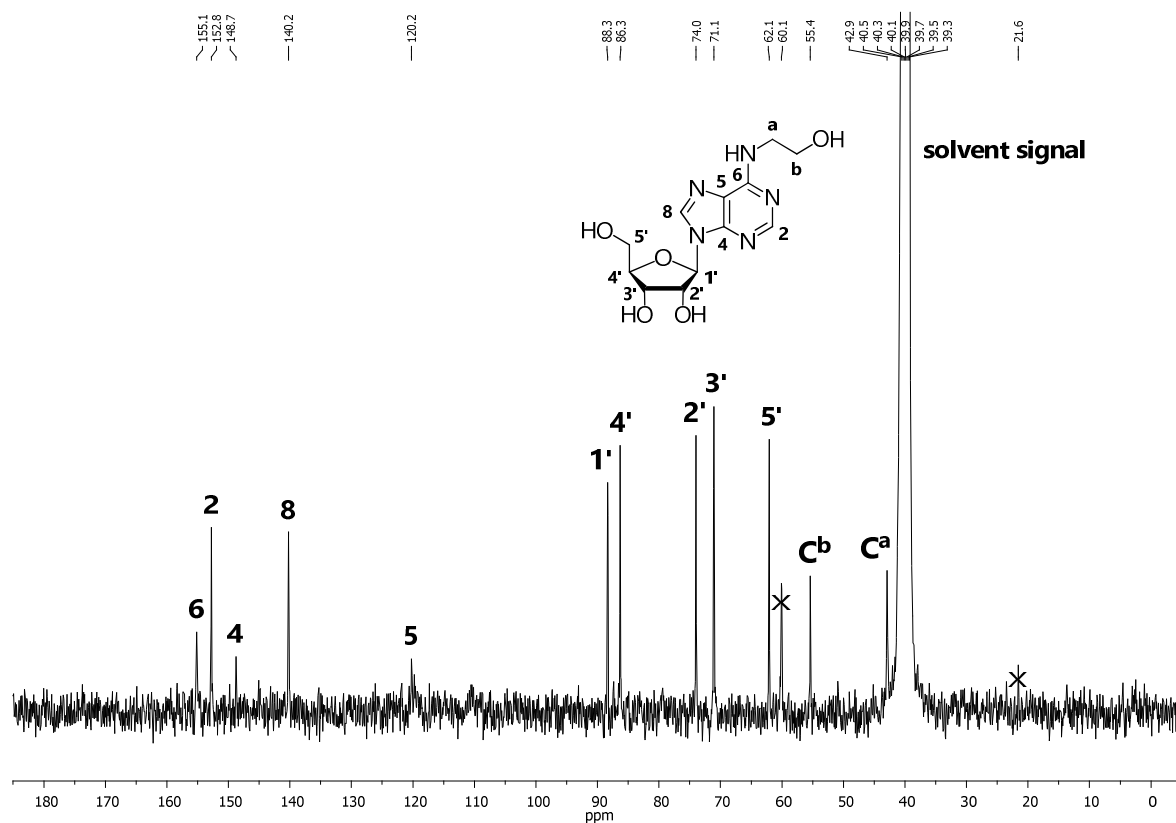
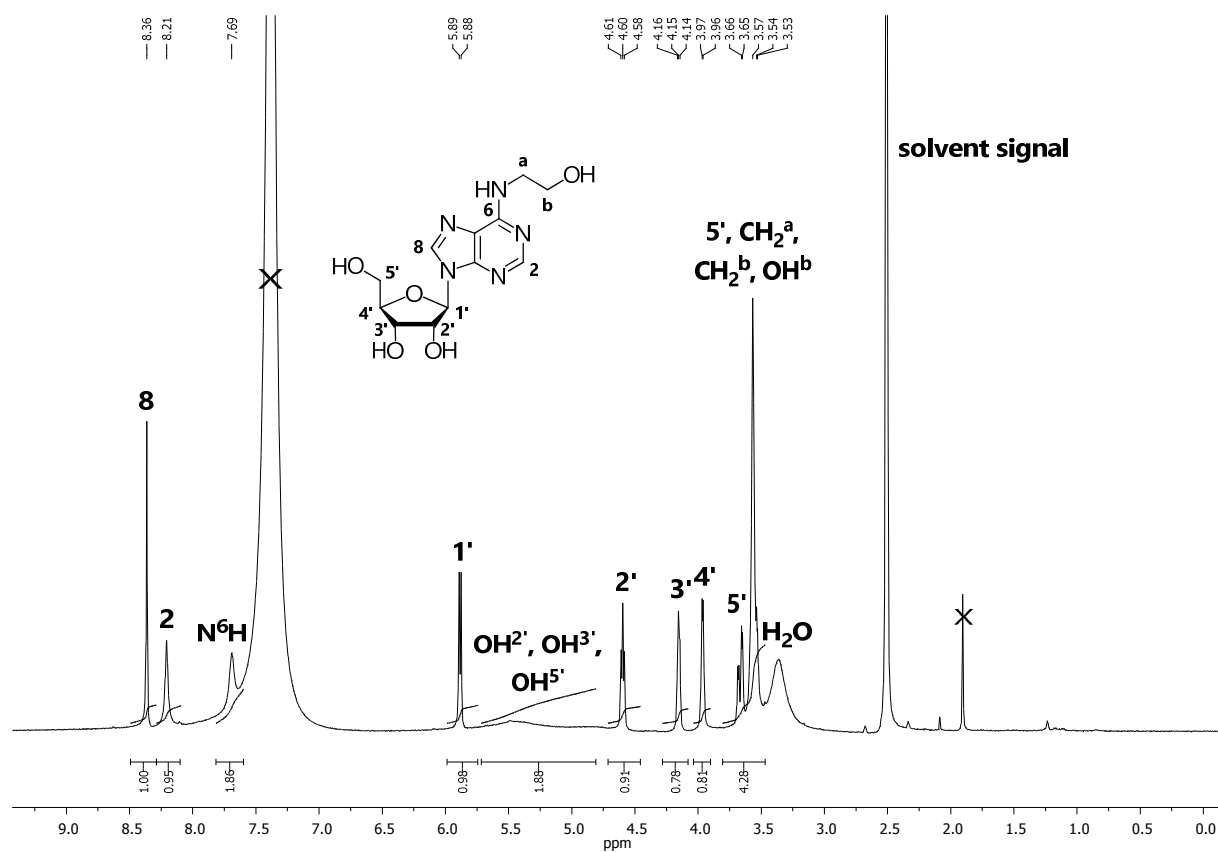


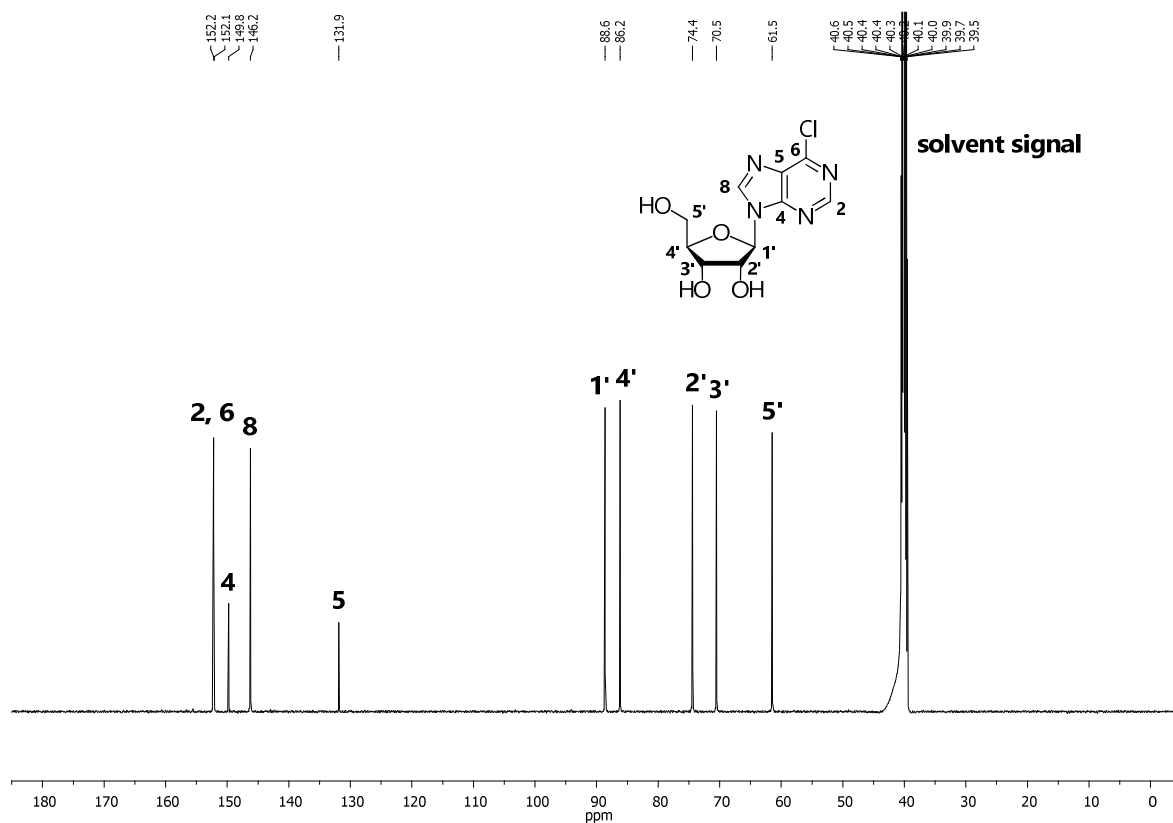
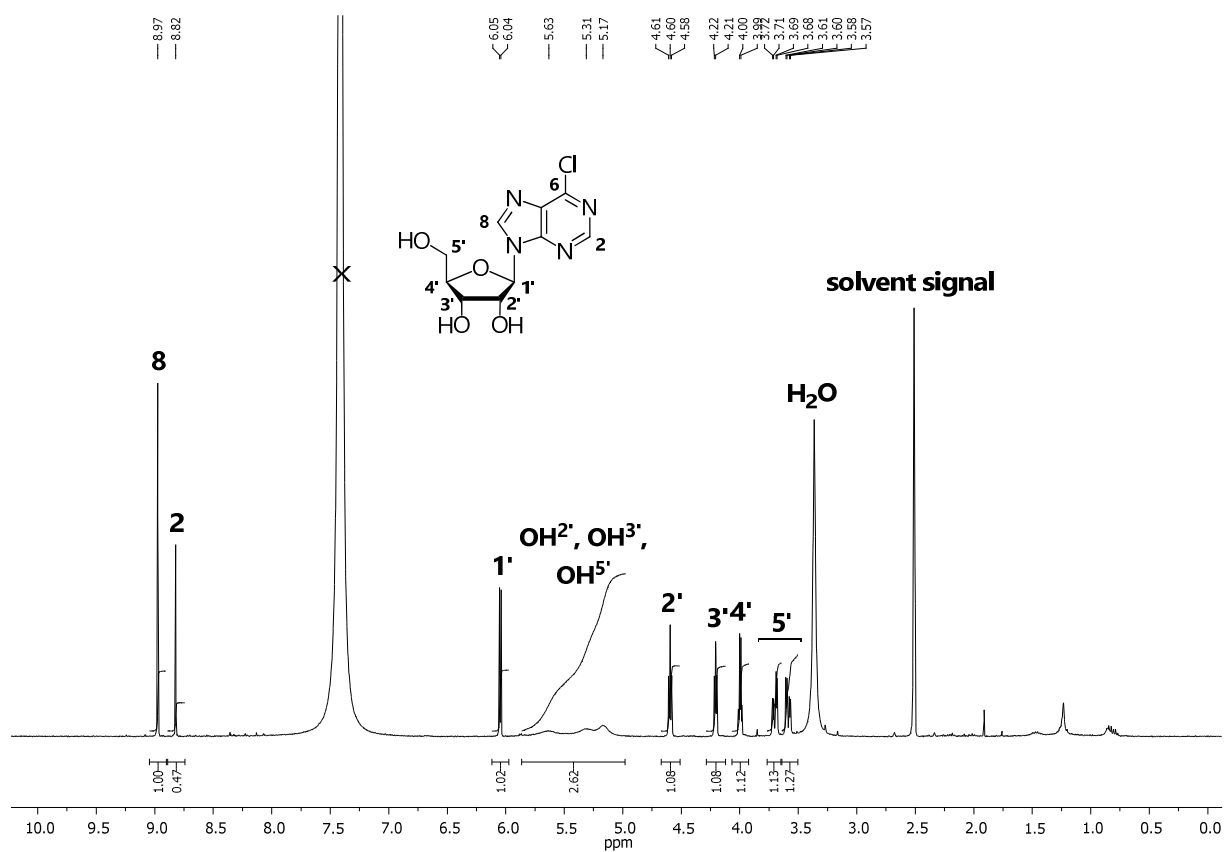
6.3.1.5. 6-O-Methylguanosine (58)

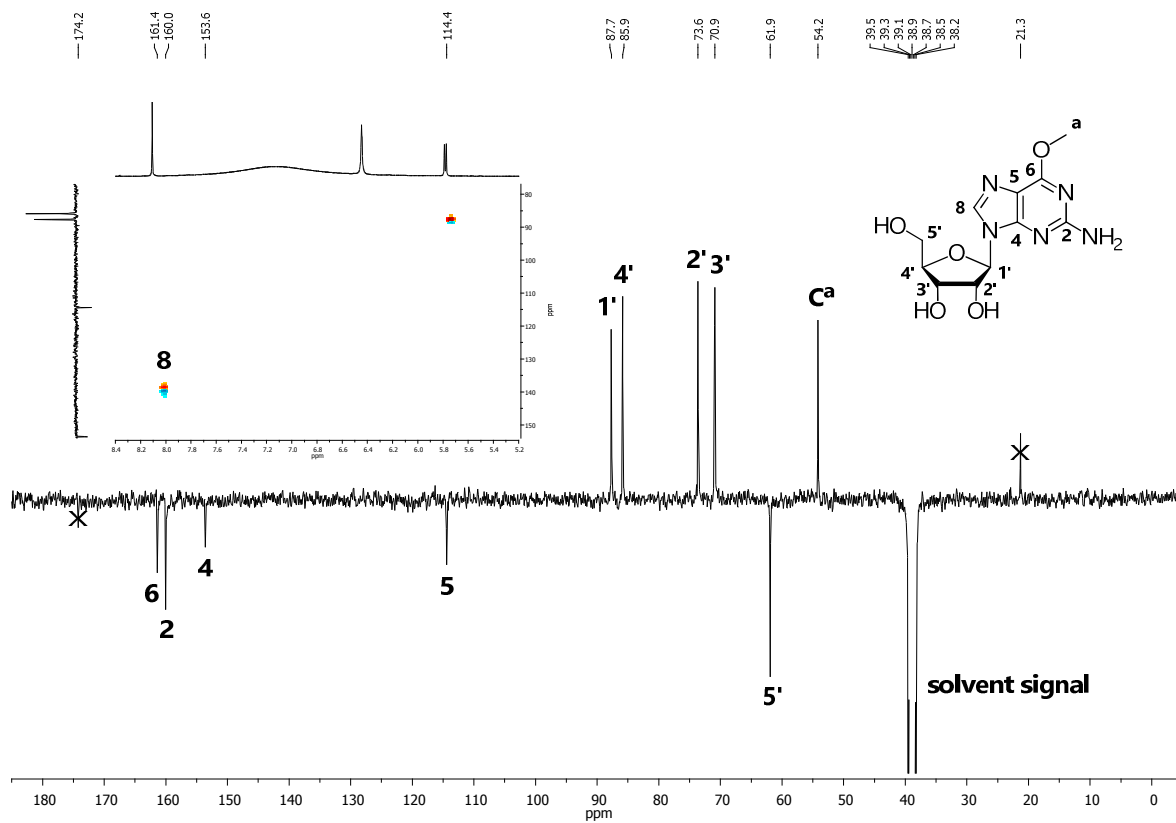
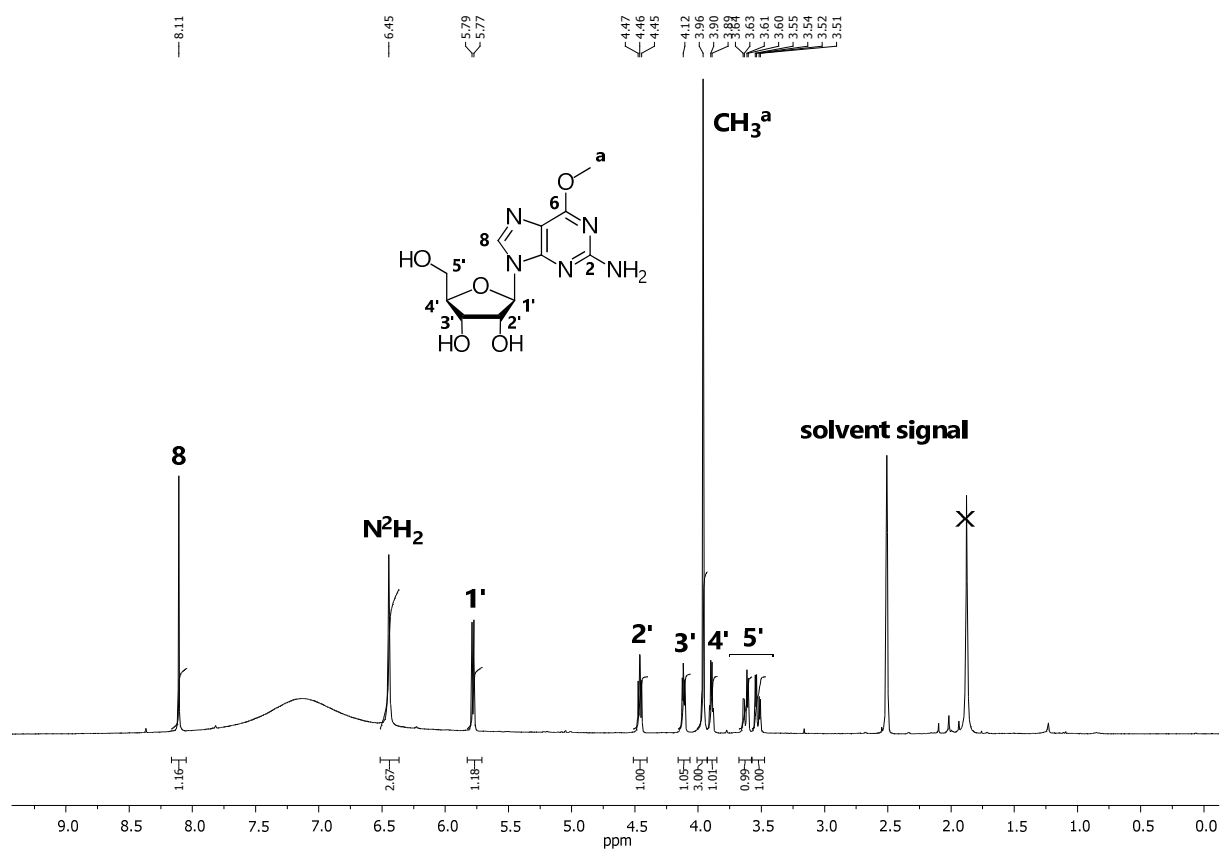


6.3.2. $^1\text{H-NMR}$ and $^{13}\text{C-NMR}$ spectra9.3.2.1. N^6 -Butyladenosine (31) (CD_3OD)

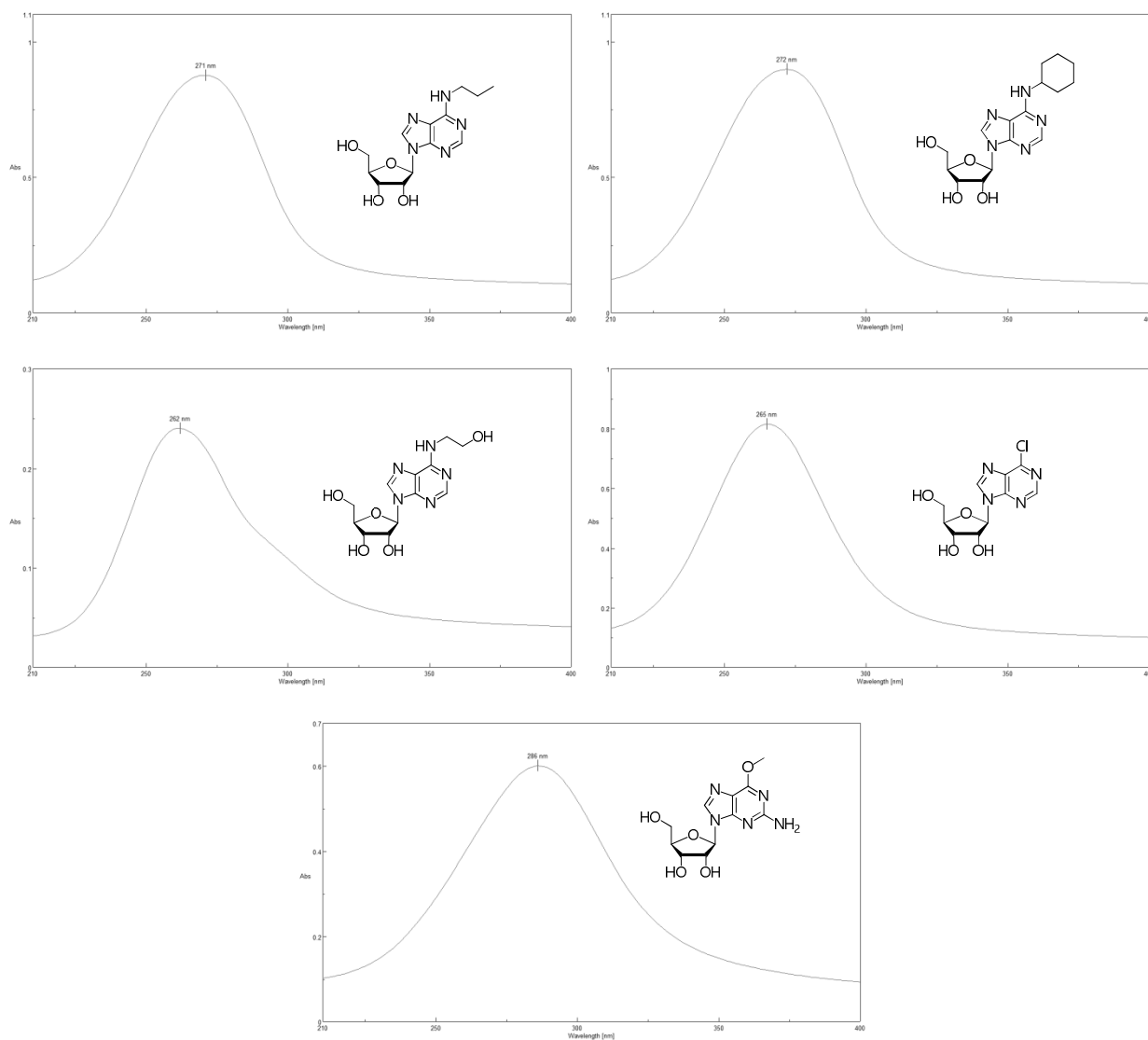
6.3.2.2. *N*⁶-Cyclohexyladenosine (32) (CD₃OD)

6.3.2.3. *N*⁶-Hydroxyethyladenosine (34) (DMSO-*d*₆)

6.3.2.4. 6-Chloroinosine (49) (DMSO- d_6)

6.3.2.5. 6-O-Methylguanosine (58) (DMSO- d_6)

6.3.3. Uv-Vis spectra



7 | EXPERIMENTAL SECTION

7.1. Materials and methods

Solvents and reagents

All solvents and reagents were purchased from Sigma-Aldrich, VWR International, Fluorochem, Fluka, Herk-Schuchardt, Merck, Carlo Erba reagents and Baker Analyzed reagents, and were used without further purification. CH_2Cl_2 , acetone and CH_3CN (dried over CaCl_2), MeOH, EtOH and *i*-PrOH (dried over CaO), *n*-BuOH (dried over K_2CO_3), THF (dried over LiAlH_4) and *N,N*-DMA (dried over CaH) were distilled before use. All other solvents were of HPLC grade.

Recombinant PNP from Aeromonas hydrophila, PNP from Mycobacterium tuberculosis, human PNP, and UP from Clostridium perfringens

Recombinant purine nucleoside phosphorylase from *Aeromonas hydrophila* and uridine phosphorylase from *Clostridium perfringens* prepared by Gnosis S.p.A. (Desio, MB, Italy).^{10c} Recombinant human purine nucleoside phosphorylase and the one from *Mycobacterium tuberculosis* were overexpressed and purified as previously described.^{75b, 159}

Specific activities toward inosine were $39 \text{ IU}\cdot\text{mg}^{-1}$ for *Ah*PNP (stock solution $21.5 \text{ mg}\cdot\text{mL}^{-1}$), $0.57 \text{ IU}\cdot\text{mg}^{-1}$ for *Hs*PNP (stock solution $0.4 \text{ mg}\cdot\text{mL}^{-1}$) and $0.10 \text{ IU}\cdot\text{mg}^{-1}$ for *Mt*PNP (stock solution $1.5 \text{ mg}\cdot\text{mL}^{-1}$). Specific activity of *Cp*UP toward 2'-deoxyuridine was $68 \text{ IU}\cdot\text{mg}^{-1}$ for *Ah*PNP (stock solution $7.0 \text{ mg}\cdot\text{mL}^{-1}$). pH measurements were performed with a 718 Stat Titrino pHmeter from Metrohm (Herisau, Switzerland).^{10c}

Analytical and flash column chromatography

Analytical TLC was performed on silica gel F₂₅₄ precoated aluminum sheets (0.2 mm layer, Merck); components were detected under an UV lamp (λ 254 nm) and by spraying with a $\text{CeSO}_4/(\text{NH}_4)_6\text{Mo}_7\text{O}_{24}\cdot 4\text{H}_2\text{O}$ solution or a 5% w/v ninhydrin solution in EtOH, followed by heating at 150°.

Silica gel 60, 40–63 μm (Merck, Darmstadt, Germany), was used for flash column chromatography. Amberlite® resin XAD-4 was purchased from Sigma-Aldrich.

NMR spectroscopy

^1H , ^{13}C and ^{31}P NMR spectra were recorded at 400.13, 100.61 and 161.98 Hz, respectively, on a Bruker AVANCE 400 spectrometer equipped with a TOPSPIN software package (Bruker, Karlsruhe, Germany) at 300 K, unless stated otherwise. ^1H and ^{13}C chemical shifts (δ) are given in parts per million and were referenced to the solvent signals (δ_{H} 7.26 - δ_{C} 77.16, δ_{H} 3.31 - δ_{C} 49.00, δ_{H} 2.50 - δ_{C} 39.52 and δ_{H} 4.79 ppm from

tetramethylsilane (TMS) for CDCl_3 , CD_3OD , $\text{DMSO}-d_6$ and D_2O respectively). ^{31}P chemical shifts are referred to 85% H_3PO_4 as external standard (δ_p 0.00 ppm).

^1H signals were assigned with the aid of ^1H - ^1H correlation spectroscopy (^1H - ^1H COSY). ^{13}C NMR signal multiplicities were based on APT (attached proton test) spectra. ^{13}C NMR signals were assigned with the aid of ^1H - ^{13}C correlation experiments (heteronuclear multiple quantum correlation spectroscopy, HMQC, and heteronuclear multiple bond correlation spectroscopy, HMBC).

Mass spectrometry

Electrospray ionization mass spectra (ESI-MS or ESI-Q-ToF-MS) were recorded on a *Thermo Finnigan LCQ Advantage* spectrometer (Hemel Hempstead, Hertfordshire, U.K.) and *Micromass Q-ToF* micro mass spectrometer (Waters, Milford, Massachusetts, U.S.A.), respectively.

UV-Vis spectroscopy

UV-Vis measurements were performed on a *Jasco V-360* spectrophotometer.

Analytical and semi-preparative HPLC for chemical synthesis

Analytical and semi-preparative HPLC were performed using an *Amersham pharmacia biotech (P900)* chromatographer equipped with a UV-Vis detector. Conditions were as follows: column, Jupiter® 10u Proteo 90A (10 μm , 250 x 4.6 mm (analytical HPLC) and 250 x 10.0 mm (semi-preparative HPLC), Phenomenex); flow rate, 0.5 $\text{mL}\cdot\text{min}^{-1}$ (analytical HPLC) and 5 $\text{mL}\cdot\text{min}^{-1}$ (semi-preparative HPLC); λ , 226 and 250 nm. Elution methods are reported in each paragraph describing the preparation of the corresponding product. HPLC t_R is always referred to analytical conditions (flow rate: 0.5 $\text{mL}\cdot\text{min}^{-1}$).

Analytical HPLC for enzyme-catalyzed batch synthesis

HPLC analysis to monitor the progress of transglycosylation reactions and to check the purity of compounds was performed using a *Merck Hitachi L-7000 La-Chrom* liquid chromatographer equipped with a UV-Vis detector, an autosampler (injection volume: 20 μL) and a column oven (temperature: 40 $^\circ\text{C}$). Conditions were as follows: column, Kromasil C_{18} (5 μm particles, 250 x 4.6 mm, Supelco); flow rate, 1 $\text{mL}\cdot\text{min}^{-1}$; λ , 260 nm; eluent, 10 mM K_2HPO_4 buffer pH 4.5 or 3.2 (A) and MeOH (B). Elution methods are reported in each paragraph describing the preparation of the corresponding product.

Immobilized Enzyme Reactor apparatus

Enzyme immobilization and flow biotransformations were performed by two HPLC modular systems (system 1 and 2) interfaced by a 6-way switching valve (V) and used in two different settings (analytical and semi-preparative set-up).

System 1 consisted of an *Agilent HP-1100* pump (Palo Alto, CA, USA), directly connected to the bioreactor(s) (*AhpNP-IMER* or/and *CpUP-IMER*) and to a 6-way switching valve (V) containing a loop (5 and 2 μL or 1.4 mL for analytical or semi-preparative purposes, respectively). In the semi-preparative setting, a 3-way junction (Y) was inserted between the reactor(s) and V.

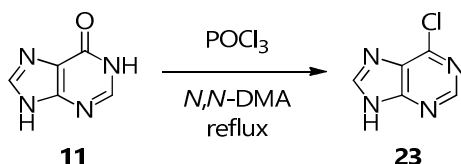
System 2 consisted of an *Agilent HP-1100* pump (Palo Alto, CA, USA) connected through V to a chromatographic column (Gemini® RP-18, 5 μm , 250 x 4.6 mm Phenomenex equipped with an RP-18 precolumn (analytical HPLC) or Lichrocart Lichrosphere® RP-18, 10 μm , 300 x 10 mm, Phenomenex (for semi-preparative HPLC)) and a UV-Vis detector (λ 260 nm). The systems were controlled by an *HPLC ChemStation* (Revision A.04.01).

7.2. Synthesis of structurally modified nucleobases and nucleosides

7.2.1. Synthesis of 6-substituted purines and guanines (2-10, 12-24)

7.2.1.1. 6-Chloropurine (23)

$C_5H_3ClN_4$; MW 154.56



11 (1.00 g, 7.35 mmol) was suspended in freshly dry *N,N*-DMA (2.50 mL) under inert atmosphere. The mixture was cooled to 0°C, POCl₃ (25.00 mL, 268.21 mmol) was added dropwise in 1 h and the resulting yellow suspension was allowed to warm to RT and then refluxed for 4 h.

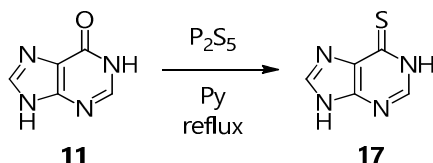
The solvent was evaporated under reduced pressure and the resulting brown oil was diluted with H₂O (30 mL). The solution was cooled to 0°C and pH was adjusted to 9 with 33% aqueous NH₄OH. After removing the solvent under reduced pressure, the pale yellow crude was recrystallized from H₂O twice and freeze-dried to get **23** as a pale yellow powder (1.01 g, 6.53 mmol).

Yield: **89%**

R_f: 0.47 (CH₂Cl₂-MeOH, 9:1)

¹H NMR (DMSO-*d*₆, 400 MHz): δ (ppm) 13.94 (br s, 1H, N⁹H), 8.75 (s, 1H, H²), 8.70 (s, 1H, H⁸).

MS (ESI⁺): *m/z* calcd for [C₅H₃ClN₄]⁺: 154.00; found: 155.1 [M+H]⁺, 177.0 [M+Na]⁺.

7.2.1.2. 6-Thiopurine (**17**)C₅H₄N₄S; MW 152.18

P₂S₅ (9.80 g, 44.09 mmol) was added to a suspension of **11** (1.00 g, 7.35 mmol) in pyridine (30 mL) under inert atmosphere and the resulting orange mixture was refluxed overnight.

The solvent was evaporated under reduced pressure and the obtained oil was diluted with H₂O (100 mL). The mixture was heated at 90°C, KOH was added until complete dissolution of the oil and the resulting solution was treated with activated charcoal. The suspension was filtered on celite and AcOH was added to the hot solution to precipitate a yellow powder, which was washed with few cold H₂O and dried under reduced pressure. The filtrate solution was concentrated to half its volume, freeze-dried and diluted with H₂O (100 mL). The resulting precipitate was filtered, washed with few cold H₂O and recrystallized from absolute EtOH.

The two solids were reunited to get **17** as a pale yellow powder (894 mg, 5.87 mmol).

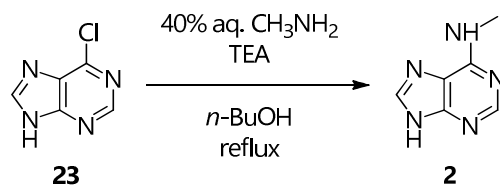
Yield: **80%**

R_f: 0.77 (EtOH-H₂O, 7:3)

¹H NMR (DMSO-*d*₆, 400 MHz): δ (ppm) 13.31 (br s, 1H, N⁹H), 8.37 (s, 1H, H⁸), 8.19 (s, 1H, H²).

¹³C NMR (DMSO-*d*₆, 100 MHz): δ (ppm) 171.4 (C⁶), 151.1 (C⁴), 145.2 (C⁸), 145.0 (C²), 129.0 (C⁵).

MS (ESI⁺): *m/z* calcd for [C₅H₄N₄S]⁺: 152.02; found: 153.4 [M+H]⁺, 175.4 [M+Na]⁺, 327.2 [2M+Na]⁺.

7.2.1.3. N⁶-Methyladenine (2)C₆H₇N₅; MW 149.15

40% aqueous CH₃NH₂ (0.10 mL, 1.16 mmol) was added to a suspension of **23** (154 mg, 1.00 mmol) and TEA (0.15 mL, 1.08 mmol) in *n*-BuOH (2.5 mL) under inert atmosphere. The resulting yellow suspension was refluxed for 2 h, during which time it became a light brown solution.

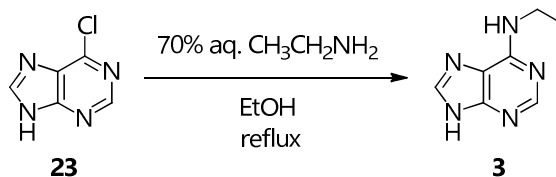
It was then cooled to RT to precipitate **2** as a pale yellow crystalline solid, which was filtered, washed with few cold H₂O and dried under reduced pressure (96 mg, 0.64 mmol).

Yield: **64%**

R_f: 0.59 (CH₂Cl₂ saturated with NH₃-MeOH, 6:1)

¹H NMR (DMSO-*d*₆, 400 MHz): δ (ppm) 12.83 (br s, 1H, N⁹H), 8.20 (s, 1H, H²), 8.08 (s, 1H, H⁸), 7.56 (br s, 1H, N⁶H), 2.96 (br s, 3H, NHCH₃).

MS (ESI⁺): *m/z* calcd for [C₆H₇N₅]⁺: 149.07; found: 149.6 [M]⁺, 150.3 [M+H]⁺, 172.2 [M+Na]⁺, 321.1 [2M+Na]⁺.

7.2.1.4. *N*⁶-Ethyladenine (**3**)C₇H₉N₅; MW 163.18

70% aqueous CH₃CH₂NH₂ (1.30 mL, 16.35 mmol) was added to a suspension of **23** (134 mg, 0.87 mmol) in EtOH (1.7 mL) under inert atmosphere. The resulting pale brown mixture was refluxed for 24 h, during which time it turned to a dark brown solution.

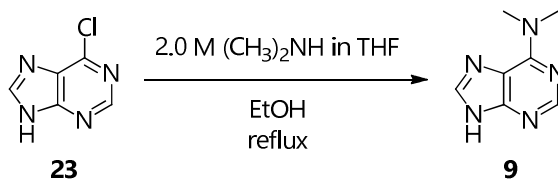
The solvent was removed under reduced pressure and the resulting brown crude was purified by flash column chromatography (CH₂Cl₂-MeOH, 9.3:0.7) to get **3** as a white powder (111 mg, 0.68 mmol).

Yield: **78%**

*R*_f: 0.68 (CH₂Cl₂ saturated with NH₃-MeOH, 6:1)

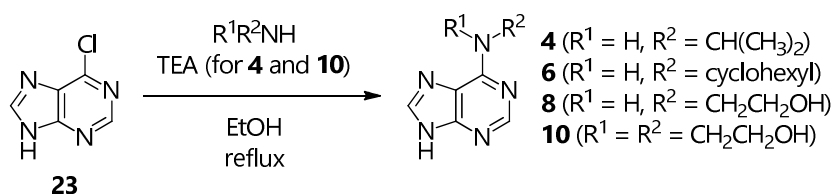
¹H NMR (DMSO-*d*₆, 400 MHz): δ (ppm) 12.81 (br s, 1H, N⁹H), 8.17 (s, 1H, H²), 8.08 (s, 1H, H⁸), 7.57 (br s, 1H, N⁶H), 3.52 (br s, 1H, NHCH₂) 1.18 (t, *J* = 7.1 Hz, 3H, CH₃).

MS (ESI⁺): *m/z* calcd for [C₇H₉N₅]⁺: 163.09; found: 164.2 [M+H]⁺, 186.1 [M+Na]⁺, 349.2 [2M+Na]⁺.

7.2.1.5. *N*⁶,*N*⁶-Dimethyladenine (**9**)C₇H₉N₅; MW 163.18

A 2.0M Me₂NH solution in THF (5.00 mL, 10.00 mmol) was added to a suspension of **23** (155 mg, 1.00 mmol) in EtOH (6.0 mL). The resulting yellow mixture was refluxed for 17 h, becoming a brown solution. The solvent was removed under reduced pressure and the brown crude was suspended in CH₂Cl₂ to separate the product from the exceeding amount of Me₂NH, then Et₂O was added to cause the precipitation of a pale yellow solid, which was filtered and purified by flash column chromatography (CH₂Cl₂-MeOH, 9.6:0.4) to get **9** as a very pale yellow powder (66 mg, 0.40 mmol).

Yield: **40%***R*_f: 0.41 (CH₂Cl₂-MeOH, 9:1)¹H NMR (CD₃OD, 400 MHz): δ (ppm) 8.20 (s, 1H, H²), 8.01 (s, 1H, H⁸), 3.53 (br s, 6H, N(CH₃)₂).HRMS (ESI-Q-ToF): *m/z* calcd for [C₇H₉N₅]⁺: 163.09; found: 164.1285 [M+H]⁺, 186.1132 [M+Na]⁺.

7.2.1.6. General procedure for the synthesis of N^6 -alkyl- and N^6,N^6 -dialkyladenines **4**, **6**, **8** and **10**

The appropriate amine (10.00 mmol) was added to a suspension of **23** (100 mg, 0.65 mmol) in EtOH (2.0 mL) under inert atmosphere. In the case of **4** and **10**, TEA (0.11 mL, 0.79 mmol) was also added. The resulting mixture was refluxed and monitored by TLC (CH_2Cl_2 -MeOH, 9:1) until consumption of the starting reagent (between 15 and 36 h).

10: The formed precipitate was filtered and dried under high vacuum.

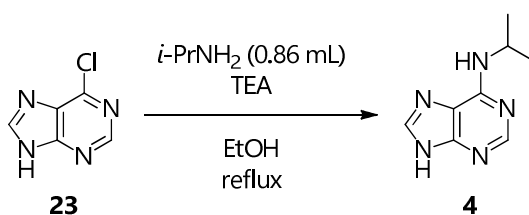
4: After removing the solvent under reduced pressure, the product was purified by flash column chromatography (CH_2Cl_2 saturated with NH_3 -MeOH, 9.4:0.6).

6 and **8**: The solvent was removed under reduced pressure. H_2O (3.0 mL) was added and the solution was neutralized with 2 M HCl, then the solvent was removed under reduced pressure and the crude was purified by semi-preparative HPLC.

Time (min)	Column volumes	% A (H_2O)	% B (MeOH)
0 - 2	0.5	97	0
2 - 18	4	97 \rightarrow 0	0 \rightarrow 100
18 - 30	3	0	100

7.2.1.6.1. N^6 -*i*-Propyladenine (**4**)

$\text{C}_8\text{H}_{11}\text{N}_5$; MW 177.21



Brown powder (93 mg, 0.52 mmol).

Yield: **81%**

R_f : 0.73 (CH_2Cl_2 saturated with NH_3 -MeOH, 6:1)

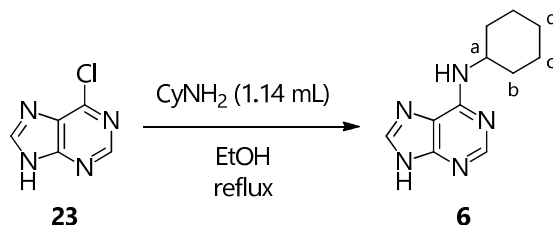
$^1\text{H NMR}$ ($\text{DMSO}-d_6$, 400 MHz): δ (ppm) 12.86 (br s, 1H, N^9H), 8.16 (br s, 1H, H^2), 8.07 (s, 1H, H^8), 7.34 (br d, $J = 7.1$ Hz, 1H, N^6H), 4.45 (br, 1H, NHCH), 1.22 (d, $J = 6.5$ Hz, 6H, $\text{CH}(\text{CH}_3)_2$).

$^1\text{H NMR}$ (CD_3OD , 400 MHz): δ (ppm) 8.24 (br s, 1H, H^2), 8.07 (s, 1H, H^8), 4.47 (br s, 1H, NHCH), 1.34 (d, $J = 6.5$ Hz, 6H, $\text{CH}(\text{CH}_3)_2$).

MS (ESI⁺): m/z calcd for $[C_8H_{11}N_5]^+$: 177.10; found: 178.3 $[M+H]^+$, 200.3 $[M+Na]^+$, 377.3 $[2M+Na]^+$.

7.2.1.6.2. *N*⁶-Cyclohexyladenine (6)

$C_{11}H_{15}N_5$; MW 217.27



Pale yellow powder (110 mg, 0.51 mmol).

Yield: **78%**

R_f : 0.67 (CH_2Cl_2 saturated with NH_3 -MeOH, 6:1)

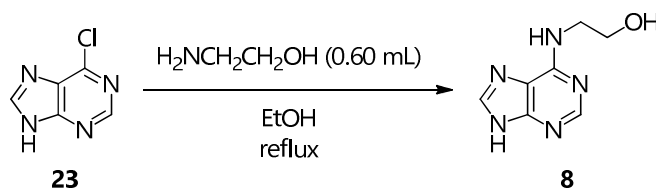
HPLC t_R : 36.0' (100% B)

¹H NMR (DMSO-*d*₆, 400 MHz): δ (ppm) 12.83 (br s, 1H, N⁹H), 8.16 (s, 1H, H²), 8.07 (s, 1H, H⁸), 7.33 (br s, 1H, N⁶H), 4.05 (br s, 1H, H^a), 1.90 (v br d, $J = 5.0$ Hz, 2H, H^b), 1.75 (br dd, $J = 8.9, 3.2$ Hz, 2H, H^c), 1.62 (br d, $J = 12.7$ Hz, 1H, H^d), 1.45-1.08 (m, 5H, H^b, H^c).

MS (ESI⁺): m/z calcd for $[C_{11}H_{15}N_5]^+$: 217.13; found: 218.3 $[M+H]^+$, 869.3 $[4M+H]^+$.

7.2.1.6.3. *N*⁶-Hydroxyethyladenine (8)

$C_7H_9N_5O$; MW 179.18



White powder (100 mg, 0.56 mmol).

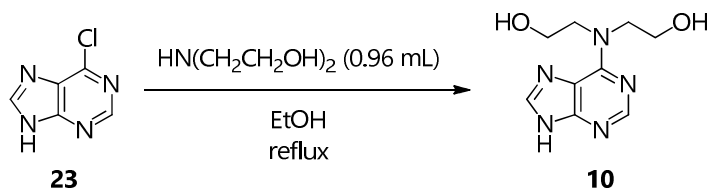
Yield: **86%**

R_f : 0.22 (CH_2Cl_2 saturated with NH_3 -MeOH, 6:1)

HPLC t_R : 24.1' (63.3% B)

¹H NMR (DMSO-*d*₆, 400 MHz): δ (ppm) 12.78 (v br s, 1H, N⁹H), 8.18 (s, 1H, H²), 8.10 (s, 1H, H⁸), 7.43 (br s, 1H, N⁶H), 4.81 (br s, 1H, OH), 3.67-3.49 (m, 4H, CH_2CH_2).

MS (ESI⁺): m/z calcd for $[C_7H_9N_5O]^+$: 179.08; found: 180.2 $[M+H]^+$, 716.3 $[4M]^+$.

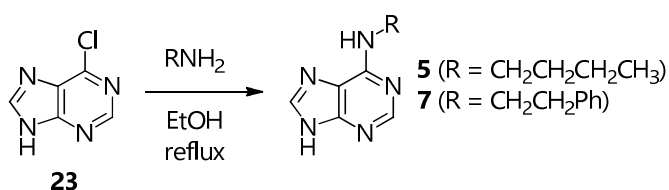
7.2.1.6.4. *N*⁶,*N*⁶-Bis-Hydroxyethyladenine (10)C₉H₁₃N₅O₂; MW 223.23

Very pale yellow powder (90 mg, 0.40 mmol).

Yield: **62%**

¹H NMR (DMSO-*d*₆, 400 MHz): δ (ppm) 8.17 (s, 1H, H²), 8.09 (s, 1H, H⁸), 4.76 (v br s, 2H, OH), 4.49-3.77 (m, 4H, CH₂CH₂OH), 3.68 (br t, *J* = 6.0 Hz, 4H, CH₂CH₂OH).

MS (ESI⁺): *m/z* calcd for [C₉H₁₃N₅O₂]⁺: 223.11; found: 224.3 [M+H]⁺, 246.2 [M+Na]⁺, 469.2 [2M+Na]⁺.

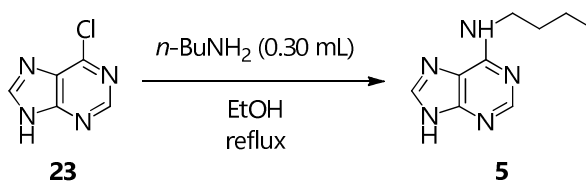
7.2.1.7. General procedure for the synthesis of *N*⁶-alkyladenines **5** and **7**

The appropriate amine (3.00 mmol) was added to a suspension of **23** (155 mg, 1.00 mmol) in EtOH (5.9 mL) under inert atmosphere. The resulting mixture was refluxed and monitored by TLC (CH₂Cl₂-MeOH, 9:1) until consumption of the starting reagent (5 h).

The solvent was removed under reduced pressure, then the crude was suspended in H₂O, filtered, washed with few cold H₂O and dried under reduced pressure.

7.2.1.7.1. *N*⁶-*n*-Butyladenine (**5**)

C₉H₁₃N₅; MW 191.23



White powder (153 mg, 0.80 mmol).

Yield: **80%**

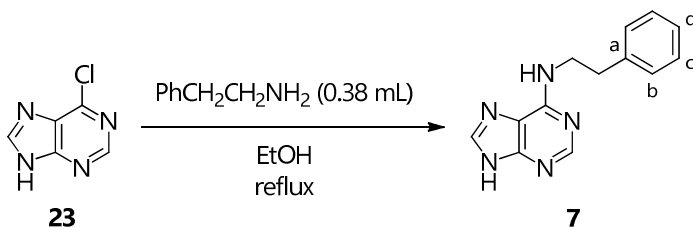
*R*_f: 0.63 (CH₂Cl₂ saturated with NH₃-MeOH, 6:1)

¹H NMR (CD₃OD, 400 MHz): δ (ppm) 8.24 (s, 1H, H²), 8.08 (s, 1H, H⁸), 3.69-3.55 (br s, 2H, NHCH₂), 1.71 (dt, *J* = 14.8, 7.5 Hz, 2H, CH₂CH₂CH₃), 1.50 (dq, *J* = 14.6, 7.3 Hz, 2H, CH₂CH₃), 1.01 (t, *J* = 7.4 Hz, 3H, CH₃).

MS (ESI⁺): *m/z* calcd for [C₉H₁₃N₅]⁺: 191.12; found: 192.2 [M+H]⁺, 214.2 [M+Na]⁺, 405.1 [2M+Na]⁺.

7.2.1.7.2. *N*⁶-(2-Phenyl)ethyladenine (**7**)

C₁₃H₁₃N₅; MW 239.28



Very pale yellow powder (211 mg, 0.88 mmol).

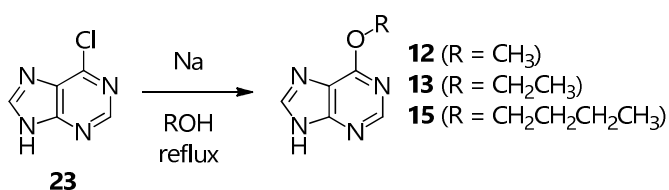
Yield: **88%**

*R*_f: 0.66 (CH₂Cl₂ saturated with NH₃-MeOH, 6:1)

¹H NMR (DMSO-*d*₆, 400 MHz): δ (ppm) 12.69 (br, 1H, N⁹H), 8.21 (br s, 1H, H²), 8.09 (s, 1H, H⁸), 7.63 (br s, 1H, N⁶H), 7.34-7.15 (m, 5H, C₆H₅), 3.73 (br s, 2H, NHCH₂), 2.93 (t, *J* = 7.5 Hz, 2H, CH₂C₆H₅).

¹³C NMR (DMSO-*d*₆, 400 MHz): δ (ppm) 154.5 (C⁶), 152.9 (C²), 150.9 (C⁴), 140.1 (C^a), 139.4 (C⁸), 129.1, 128.8, 126.5 (C^b, C^c, C^d), 118.4 (C⁵), 41.8 (NHCH₂), 35.6 (CH₂C₆H₅).

MS (ESI⁺): *m/z* calcd for [C₁₃H₁₃N₅]⁺: 239.12; found: 240.3 [M+H]⁺, 262.3 [M+Na]⁺, 501.2 [2M+Na]⁺.

7.2.1.8. General procedure for the synthesis of 6-alkoxypurines **12**, **13** and **15**

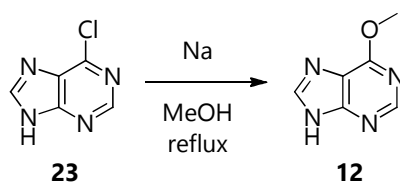
Na (60 mg, 2.61 mmol) was dissolved in the appropriate dry alcohol (2.00 mL) under inert atmosphere. **2** (100 mg, 0.65 mmol) was added and the resulting suspension was refluxed and monitored by TLC (CH₂Cl₂-MeOH, 9:1) until consumption of the starting reagent (15 h).

The solvent was removed under reduced pressure and the product was purified by semi-preparative HPLC.

Time (min)	Column volumes	% A (H ₂ O)	% B (MeOH)
0 - 2	0.5	97	3
2 - 18	4	97 → 0	3 → 100
18 - 30	3	0	100

7.2.1.8.1. 6-Methoxypurine (**12**)

C₆H₆N₄O; MW 150.14



White powder (72 mg, 0.48 mmol).

Yield: **73%**

R_f: 0.38 (CH₂Cl₂-MeOH, 9:1)

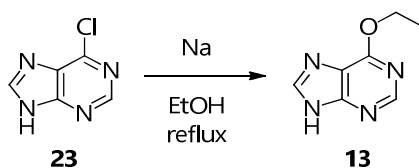
HPLC *t_R*: 25.2' (72.6% B)

¹H NMR (DMSO-*d*₆, 400 MHz): 13.42 (br s, 1H, N⁹H), 8.50 (s, 1H, H²), 8.37 (s, 1H, H⁸), 4.09 (s, 3H, OCH₃).

MS (ESI⁺): *m/z* calcd for [C₆H₆N₄O]⁺: 150.05; found: 151.0 [M+H]⁺, 172.9 [M+Na]⁺.

7.2.1.8.2. 6-Ethoxypurine (**13**)

C₇H₈N₄O; MW 164.16



Ochre powder (90 mg, 0.55 mmol).

Yield: **84%**

R_f : 0.42 (CH₂Cl₂-MeOH, 9:1)

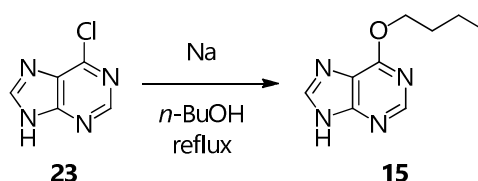
HPLC t_R : 28.0' (79.2% B)

¹H NMR (DMSO-*d*₆, 400 MHz): 8.32 (s, 1H, H²), 8.12 (s, 1H, H⁸), 4.54 (q, *J* = 7.1 Hz, 2H, OCH₂), 1.40 (t, *J* = 7.1 Hz, 3H, CH₃).

MS (ESI⁺): *m/z* calcd for [C₇H₈N₄O]⁺: 164.07; found: 165.0 [M+H]⁺, 187.0 [M+Na]⁺, 350.9 [2M+Na]⁺.

7.2.1.8.3. 6-*n*-Butoxypurine (15)

C₉H₁₂N₄O; MW 192.22



Pale yellow powder (62 mg, 0.32 mmol).

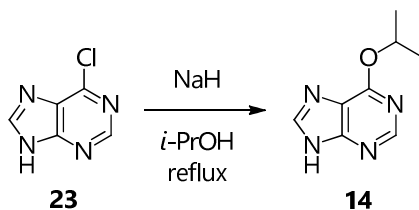
Yield: **50%**

R_f : 0.44 (CH₂Cl₂-MeOH, 9:1)

HPLC t_R : 43.1' (92.5% B)

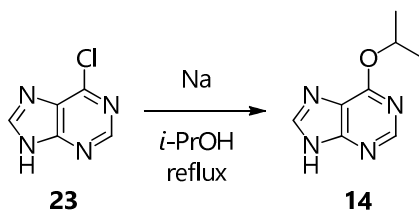
¹H NMR (DMSO-*d*₆, 400 MHz): 8.26 (s, 1H, H²), 8.02 (s, 1H, H⁸), 4.48 (t, *J* = 6.7 Hz, 2H, OCH₂), 1.77 (quin, *J* = 7.1 Hz, 2H, CH₂CH₂CH₃), 1.46 (sext, *J* = 7.4 Hz, 2H, CH₂CH₃), 0.95 (t, *J* = 7.4 Hz, 3H, CH₃).

MS (ESI⁺): *m/z* calcd for [C₉H₁₂N₄O]⁺: 192.10; found: 215.0 [M+Na]⁺, 385.1 [2M+H]⁺, 406.9 [2M+Na]⁺, 769.1 [4M+H]⁺.

7.2.1.9. 6-*i*-Propoxypurine (**14**)C₈H₁₀N₄O; MW 178.19

A 60% NaH dispersion in mineral oil (180 mg, 4.50 mmol) was added to dry *i*-PrOH (7.5 mL) portionwise in 3 h under inert atmosphere, forming a yellow suspension. **23** (133 mg, 0.86 mmol) was added and the resulting mixture was refluxed for 15 h.

The solvent was removed under reduced pressure and the light brown crude was purified by flash column chromatography (CH₂Cl₂ saturated with NH₃-MeOH, 9.4:0.6) to obtain **14** as a pale yellow powder (149 mg, 0.84 mmol).

Yield: **97%**

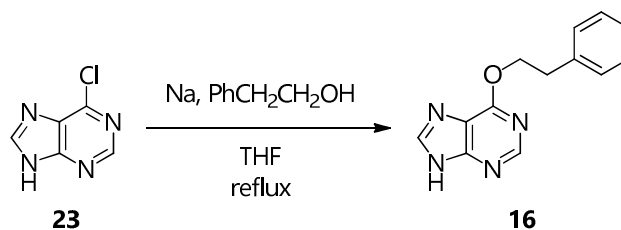
Na (109 mg, 4.74 mmol) was dissolved in dry *i*-PrOH (7.3 mL) under inert atmosphere and **23** (132 mg, 0.85 mmol) was added to the white suspension. The resulting mixture was refluxed for 13 h.

The solvent was removed under reduced pressure, the crude was dissolved in H₂O (3.0 mL) and extracted with Et₂O (7x3 mL). The reunited organic phases were dried over Na₂SO₄ and evaporated under reduced pressure to obtain **14** as a pale yellow powder (24 mg, 0.13 mmol).

Yield: **16%****R_f**: 0.49 (CH₂Cl₂-MeOH, 9:1)

¹H NMR (CD₃OD, 400 MHz): δ (ppm) 8.50 (s, 1H, H²), 8.29 (s, 1H, H⁸), 5.69 (hept, *J* = 6.2 Hz, 1H, OCH), 1.48 (d, *J* = 6.2 Hz, 6H, CH(CH₃)₂).

MS (ESI⁺): *m/z* calcd for [C₈H₁₀N₄O]⁺: 178.09; found: 179.0 [M+H]⁺, 201.2 [M+Na]⁺, 379.2 [2M+Na]⁺.

7.2.1.10. 6-(2-Phenyl)ethoxypurine (16) $C_{13}H_{12}N_4O$; MW 240.26

Na (101 mg, 4.39 mmol) was added portionwise to a solution of PhCH₂CH₂OH (0.50 mL, 4.17 mmol) in dry THF (3.0 mL) under inert atmosphere, forming an orange suspension which was stirred at RT for 15 h. **23** (154 mg, 1.00 mmol) was added and the suspension was refluxed for 16 h.

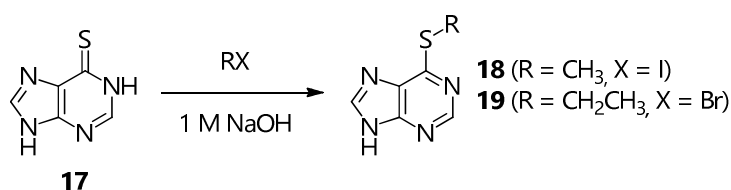
The solvent was removed under reduced pressure and the resulting brown crude was purified by flash column chromatography (CH₂Cl₂-MeOH, 9.4:0.6) to get **16** as a white powder (180 mg, 0.75 mmol).

Yield: **75%**

R_f: 0.53 (CH₂Cl₂-MeOH, 9:1)

¹H NMR (CD₃OD, 400 MHz): δ (ppm) 8.50 (s, 1H, H²), 8.30 (s, 1H, H⁸), 7.37-7.18 (m, 5H, C₆H₅), 4.84 (t, *J* = 7.0 Hz, 2H, OCH₂), 3.21 (t, *J* = 7.0 Hz, 2H, CH₂C₆H₅).

MS (ESI⁺): *m/z* calcd for [C₁₃H₁₂N₄O]⁺: 240.10; found: 241.4 [M+H]⁺, 263.4 [M+Na]⁺, 503.3 [2M+Na]⁺.

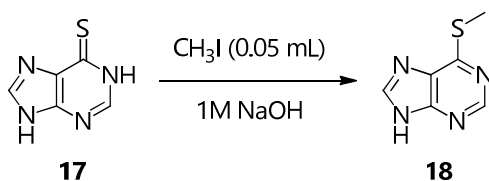
7.2.1.11. General procedure for the synthesis of 6-alkylthiopyrimidines **18** and **19**

A suspension of **17** (100 mg, 0.66 mmol) in 1 M aqueous NaOH (1.7 mL) was stirred at RT for 30', until almost complete dissolution of the starting reagent, and the appropriate alkyl halide (0.80 mmol for **18** and 1.20 mmol for **19**) was added dropwise. The mixture was stirred at RT and monitored by TLC (CH₂Cl₂-MeOH, 9:1) until consumption of the starting reagent (between 2 and 15 h).

The solution was either acidified to pH 5 with AcOH (for **18**) or neutralized with 2 M HCl (for **19**) to precipitate the product, which was filtered, washed with few precipitation solvent and dried under high vacuum.

7.2.1.11.1. 6-Methylthiopyrimidine (**18**)

C₆H₆N₄S; MW 166.20



Pale brown powder (65 mg, 0.39 mmol).

Yield: **59%**

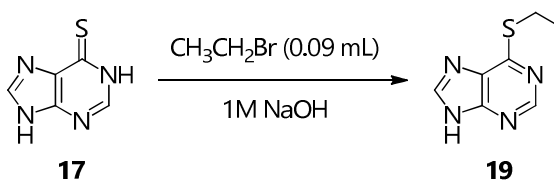
R_f: 0.50 (CH₂Cl₂-MeOH, 9:1)

¹H NMR (DMSO-*d*₆, 400 MHz): δ (ppm) 8.66 (s, 1H, H²), 8.37 (s, 1H, H⁸), 2.66 (s, 3H, SCH₃).

MS (ESI⁺): *m/z* calcd for [C₆H₆N₄S]⁺: 166.03; found: 167.4 [M+H]⁺, 189.2 [M+Na]⁺, 355.2 [2M+Na]⁺.

7.2.1.11.2. 6-Ethylthiopyrimidine (**19**)

C₇H₈N₄S; MW 180.23



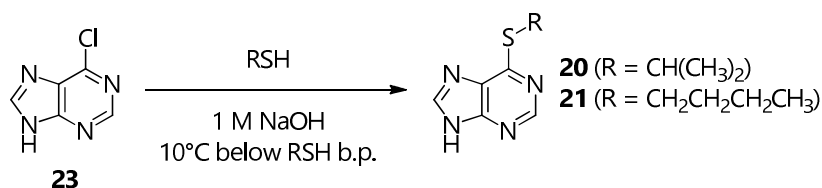
White powder (87 mg, 0.48 mmol).

Yield: **73%**

R_f: 0.53 (CH₂Cl₂-MeOH, 9:1)

¹H NMR (DMSO-*d*₆, 400 MHz): δ (ppm) 8.49 (s, 1H, H²), 8.11 (s, 1H, H⁸), 3.29 (q, $J = 7.3$ Hz, 2H, SCH₂), 1.33 (t, $J = 7.3$ Hz, 3H, CH₃).

MS (ESI⁺): m/z calcd for [C₇H₈N₄S]⁺: 180.05; found: 181.3 [M+H]⁺, 203.2 [M+Na]⁺, 383.5 [2M+Na]⁺.

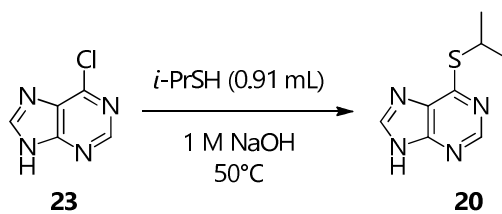
7.2.1.12. General procedure for the synthesis of 6-alkylthiopurines **20** and **21**

The appropriate thiol (9.80 mmol for **20** and 2.80 mmol for **21**) was dissolved in 1 M aqueous NaOH (1.7 mL) and the resulting solution was stirred at RT for 30'. **23** (100 mg, 0.65 mmol) was added, then the suspension was stirred at 10°C below the boiling point of the thiol and monitored by TLC (CH₂Cl₂-MeOH, 9:1) until consumption of the starting reagent (between 15 and 48 h).

The solution was neutralized with 2 M HCl to precipitate the product, which was filtered, washed with few cold H₂O and dried under high vacuum

7.2.1.12.1. 6-*i*-Propylthiopurine (**20**)

C₈H₁₀N₄S; MW 194.26



White powder (107 mg, 0.55 mmol).

Yield: **85%**

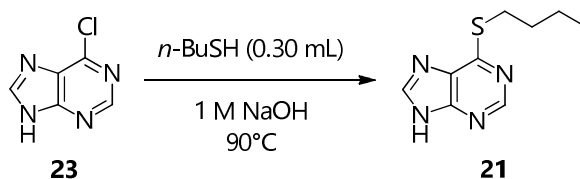
R_f: 0.56 (CH₂Cl₂-MeOH, 9:1)

¹H NMR (DMSO-*d*₆, 400 MHz): δ (ppm) 13.47 (br, 1H, N⁹H), 8.69 (s, 1H, H²), 8.42 (s, 1H, H⁸), 4.31 (sept, *J* = 6.8 Hz, 1H, SCH), 1.44 (d, *J* = 6.8 Hz, 6H, CH(CH₃)₂).

MS (ESI⁺): *m/z* calcd for [C₈H₁₀N₄S]⁺: 194.06; found: 195.1 [M+H]⁺, 217.1 [M+Na]⁺, 410.9 [2M+Na]⁺.

7.2.1.12.2. 6-*n*-Butylthiopurine (**21**)

C₉H₁₂N₄S; MW 208.28



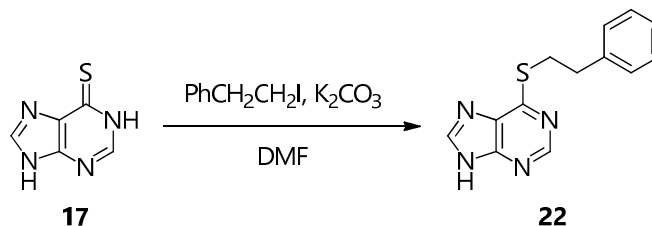
Yellow solid (67 mg, 0.32 mmol).

Yield: **50%**

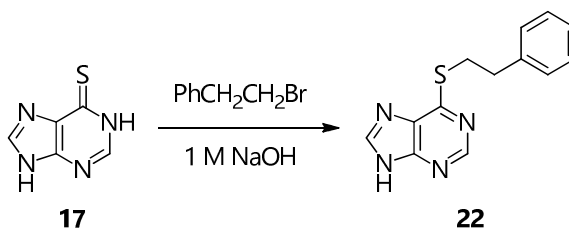
R_f: 0.54 (CH₂Cl₂-MeOH, 9:1)

¹H NMR (DMSO-*d*₆, 400 MHz): δ (ppm) 8.56 (s, 1H, H²), 8.22 (s, 1H, H⁸), 3.33 (t, $J = 7.3$ Hz, 2H, SCH₂), 1.68 (quin, $J = 7.4$ Hz, 2H, CH₂CH₂CH₃), 1.44 (sext, $J = 7.4$ Hz, 2H, CH₂CH₃), 0.92 (t, $J = 7.4$ Hz, 3H, CH₃).

MS (ESI⁺): m/z calcd for [C₉H₁₂N₄S]⁺: 208.08; found: 209.0 [M+H]⁺, 231.1 [M+Na]⁺.

7.2.1.13. 6-(2-Phenyl)ethylthiopurine (**22**)C₁₃H₁₂N₄S; MW 256.33

17 (152 mg, 1.00 mmol) and K₂CO₃ (155 mg, 1.12 mmol) were suspended in dry DMF (1.0 mL) and the resulting mixture was stirred at RT for 30'. PhCH₂CH₂I (0.20 mL, 1.38 mmol) was then added dropwise. After stirring at RT for 1 h 30', H₂O (3.0 mL) was added and the solution was neutralized with 2 M HCl at 0°C to precipitate **22** as a very pale yellow powder, which was filtered, washed with few cold H₂O and dried under high vacuum (169 mg, 0.66 mmol).

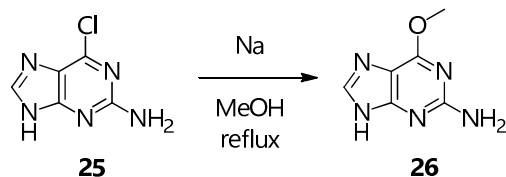
Yield: **66%**

PhCH₂CH₂Br (0.19 mL, 1.39 mmol) was added to a suspension of **17** (100 mg, 0.66 mmol) in 1 M aqueous NaOH (1.7 mL) under inert atmosphere. The resulting mixture was stirred at RT overnight. The solution was neutralized with 1 M HCl to precipitate a solid, which was filtered, washed with few cold H₂O and with very few cold MeOH and dried under vacuum to get **22** as a white powder (20 mg, 0.08 mmol).

Yield: **12%***R_f*: 0.57 (CH₂Cl₂-MeOH, 9:1)

¹H NMR (DMSO-*d*₆, 400 MHz): δ (ppm) 8.72 (s, 1H, H²), 8.43 (s, 1H, H⁸), 7.36-7.19 (m, 5H, C₆H₅), 3.62 (t, *J* = 7.6 Hz, 2H, SCH₂), 3.04 (t, *J* = 7.5 Hz, 2H, CH₂C₆H₅).

MS (ESI⁺): *m/z* calcd for [C₁₃H₁₂N₄S]⁺: 256.08; found: 279.2 [M+Na]⁺.

7.2.1.14. 2-Amino-6-methoxypurine (**26**)C₆H₇N₅O; MW 165.15

Na (69 mg, 3.00 mmol) was dissolved in dry MeOH (1.83 mL) under inert atmosphere and **25** (102 mg, 0.60 mmol) was added to the mixture, forming a yellow suspension which was refluxed for 24 h.

The resulting mixture was evaporated under reduced pressure and purified by flash column chromatography (CH₂Cl₂-MeOH, 9.7:0.3) to get **26** as a white powder (93 mg, 0.56 mmol).

Yield: **94%**

Na (69 mg, 3.00 mmol) was dissolved in dry MeOH (1.83 mL) under inert atmosphere and 6-chloroguanine (102 mg, 0.60 mmol) was added to the mixture, forming a yellow suspension which was refluxed for 24 h.

The resulting mixture was diluted with MeOH (0.5 mL), NH₄Cl (161 mg, 3.01 mmol) was added and the suspension was stirred at RT for 30'. The solvent was evaporated under reduced pressure, H₂O was added (3.0 mL) and the resulting suspension was neutralized with 2 M NaOH to precipitate **Z** as a white powder, which was filtered, washed with few cold H₂O and dried under reduced pressure (69 mg, 0.42 mmol).

Yield: **70%**

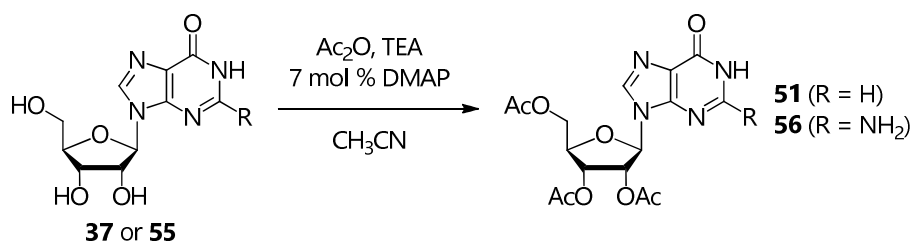
R_f: 0.38 (CH₂Cl₂-MeOH, 9:1)

¹H NMR (DMSO-*d*₆, 400 MHz): δ (ppm) 13.19 (v br s, 1H, N⁹H), 8.06 (s, 1H, H⁸), 6.61 (br s, 2H, N²H₂), 3.99 (s, 3H, OCH₃).

¹³C NMR (DMSO-*d*₆, 100 MHz): δ (ppm) 160.4 (C⁶), 159.7 (C²), 155.3 (C⁴), 139.5 (C⁸), 111.7 (C⁵), 53.9 (OCH₃).

MS (ESI⁺): *m/z* calcd for [C₆H₇N₅O]⁺: 165.07; found: 166.2 [M+H]⁺, 188.2 [M+Na]⁺, 331.1 [2M+H]⁺, 353.2 [2M+Na]⁺.

7.2.2. Synthesis of 6-substituted inosines and guanosines (28-36, 38-48, 58)

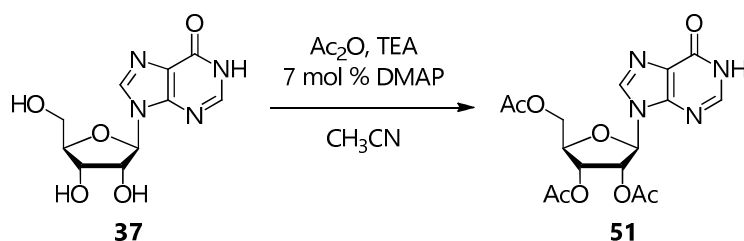
7.2.2.1. General procedure for the synthesis of 2',3',5'-tri-*O*-acetylinosine (51) and guanosine (56)

Ac₂O (13.20 mL, 139.64 mmol) and TEA (20.41 mL, 146.43 mmol) were added dropwise to a suspension of **37** (10.73 g, 40.00 mmol for **51**) or **55** (11.33 g, 40.00 mmol for **56**) and DMAP (347 mg, 2.84 mmol) in CH₃CN (380 mL) under inert atmosphere. The mixture was stirred at RT for 2 h, during which time it became a transparent solution.

The solvent was removed under reduced pressure and the resulting white crude was treated with *i*-PrOH (100 mL) to precipitate the product, which was filtered, washed with few cold *i*-PrOH and dried under reduced pressure.

7.2.2.1.1. 2',3',5'-Tri-*O*-acetylinosine (51)

C₁₆H₁₈N₄O₈; MW 394.34



White powder (15.06 g, 38.19 mmol).

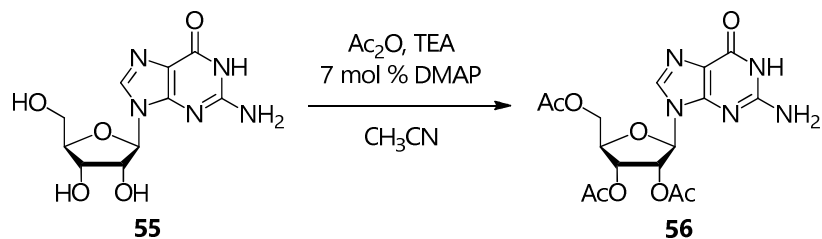
Yield: **95%**

*R*_f: 0.71 (CH₂Cl₂-MeOH, 12:1) or 0.63 (CH₂Cl₂-MeOH, 9:1)

¹H NMR (CDCl₃, 400 MHz): δ (ppm) 12.91 (br s, 1H, N¹H), 8.21 (s, 1H, H²), 8.02 (s, 1H, H⁸), 6.18 (d, *J* = 5.3 Hz, 1H, H¹), 5.89 (t, *J* = 5.4 Hz, 1H, H²), 5.62 (t, *J* = 5.0 Hz, 1H, H³), 4.50-4.47 (m, 1H, H⁴), 4.46 (dd, *J* = 8.3, 3.4 Hz, 1H, H^{5a}), 4.40 (dd, *J* = 12.6, 4.9 Hz, 1H, H^{5b}), 2.17 (s, 3H, CH₃CO), 2.16 (s, 3H, CH₃CO), 2.12 (s, 3H, CH₃CO).

¹³C NMR (CDCl₃, 100 MHz): δ (ppm) 171.2, 170.6, 170.4 (CH₃CO), 157.6 (C⁶), 149.1 (C⁴), 147.5 (C²), 138.7 (C⁸), 125.9 (C⁵), 86.7 (C¹), 80.6 (C⁴), 73.3 (C²), 71.1 (C³), 63.9 (C⁵), 21.6, 21.5, 21.3 (CH₃CO).

MS (ESI⁺): *m/z* calcd for [C₁₆H₁₈N₄O₈]⁺: 394.11; found: 417.1 [M+Na]⁺, 811.2 [2M+Na]⁺, 1204.9 [3M+Na]⁺.

7.2.2.1.2. 2',3',5'-Tri-*O*-acetylguanosine (56)C₁₆H₁₉N₅O₈; MW 409.35

White powder (15.39 g, 37.60 mmol).

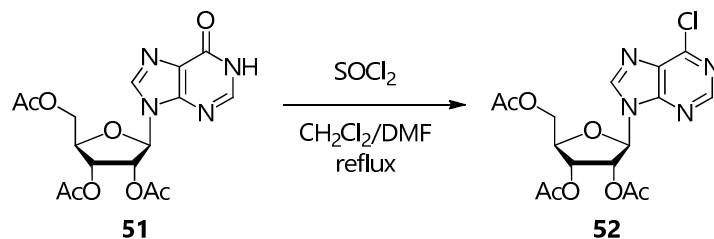
Yield: 94%

R_f: 0.45 (CH₂Cl₂-MeOH, 9:1)

¹H NMR (DMSO-*d*₆, 400 MHz): δ (ppm) 10.78 (br s, 1H, N¹H), 7.93 (s, 1H, H⁸), 6.56 (br s, 2H, N²H₂), 5.99 (d, *J* = 6.2 Hz, 1H, H^{1'}), 5.79 (t, *J* = 6.0 Hz, 1H, H^{2'}), 5.50 (dd, *J* = 5.9, 4.1 Hz, 1H, H^{3'}), 4.38 (dd, *J* = 11.3, 3.7 Hz, 1H, H^{5'a}), 4.32 (dd, *J* = 8.8, 4.6 Hz, 1H, H^{4'}), 4.26 (dd, *J* = 11.2, 5.6 Hz, 1H, H^{5'b}), 2.12 (s, 3H, CH₃CO), 2.05 (s, 3H, CH₃CO), 2.04 (s, 3H, CH₃CO).

¹³C NMR (DMSO-*d*₆, 100 MHz): δ (ppm) 170.4, 169.8, 169.6 (CH₃CO), 156.6 (C⁶), 153.8 (C²), 151.1 (C⁴), 135.6 (C⁸), 116.9 (C⁵), 84.5 (C^{1'}), 79.5 (C^{4'}), 72.1 (C^{2'}), 70.3 (C^{3'}), 63.0 (C^{5'}), 20.4, 20.3, 20.1 (CH₃CO).

MS (ESI⁺): *m/z* calcd for [C₁₆H₁₉N₅O₈]⁺: 409.12; found: 410.1 [M+H]⁺, 432.2 [M+Na]⁺, 841.1 [2M+Na]⁺, 1249.8 [3M+Na]⁺, 1659.5 [4M+Na]⁺.

7.2.2.2. 6-Chloro-2',3',5'-tri-*O*-acetylinosine (**52**)C₁₆H₁₇ClN₄O₇; MW 412.78

Under inert atmosphere, a solution of SOCl₂ (1.40 mL, 19.19 mmol) and dry DMF (0.8 mL) in dry CH₂Cl₂ (35 mL) was added dropwise to one of **51** (1.40 g, 3.55 mmol) in dry CH₂Cl₂ (92 mL) at 0°C. The resulting colourless mixture was refluxed for 16 h.

The resulting light yellow solution was washed with saturated aqueous NaHCO₃ (3x40 mL) until no more CO₂ evolution was observed, brine (2x50 mL) and H₂O (2x50 mL) and dried over Na₂SO₄. After removing the solvent under reduced pressure, the oil crude was filtered on silica (CH₂Cl₂-MeOH, 6:1) to get **52** as a very dense yellow oil (1.44 g, 3.49 mmol).

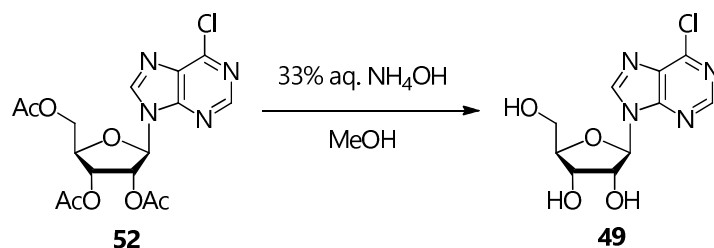
Yield: **98%**

R_f: 0.71 (CH₂Cl₂-MeOH, 12:1)

¹H NMR (CDCl₃, 400 MHz): δ (ppm) 8.80 (s, 1H, H²⁸), 8.31 (s, 1H, H⁸), 6.26 (d, *J* = 5.2 Hz, 1H, H^{1'}), 5.97 (t, *J* = 5.3 Hz, 1H, H^{2'}), 5.67 (t, *J* = 5.0 Hz, 1H, H^{3'}), 4.51 (dd, *J* = 7.3, 3.9 Hz, 1H, H^{5'a}), 4.46 (d, *J* = 3.2 Hz, 1H, H^{4'}), 4.41 (dd, *J* = 12.1, 4.2 Hz, 1H, H^{5'b}), 2.18 (s, 3H, CH₃CO), 2.15 (s, 3H, CH₃CO), 2.11 (s, 3H, CH₃CO).

¹³C NMR (DMSO-*d*₆, 100 MHz): δ (ppm) 170.1, 169.5, 169.3 (CH₃CO), 152.1 (C², C⁶), 151.2 (C⁴), 134.9 (C⁸), 132.2 (C⁵), 86.8 (C^{1'}), 80.4 (C^{4'}), 73.0 (C^{2'}), 70.3 (C^{3'}), 62.8 (C^{5'}), 20.6, 20.4, 20.3 (CH₃CO).

MS (ESI⁺): *m/z* calcd for [C₁₆H₁₇ClN₄O₇]⁺: 412.08; found: 413.5 [M+H]⁺, 435.2 [M+Na]⁺, 825.1 [2M+H]⁺, 846.8 [2M+Na]⁺.

7.2.2.3. 6-Chloroinosine (**49**)C₁₀H₁₁ClN₄O₄; MW 286.67

33% aqueous NH₄OH (16.6 mL, 140.66 mmol) was added to a solution of **52** (2.00 g, 4.85 mmol) in MeOH (60 mL). The resulting yellow mixture was stirred at RT, monitored by TLC (CH₂Cl₂-MeOH, 9:1) until consumption of the starting reagent and complete formation of the product (1 h 30') and quenched by neutralization with 6 M HCl at 0°C.

After filtering the insoluble crystalline residue, the solvent was removed under reduced pressure and the resulting white crude was purified by flash column chromatography (CH₂Cl₂-MeOH, 9.3:0.7) to obtain **49** as a very pale yellow powder (960 mg, 3.35 mmol).

Yield: 69%

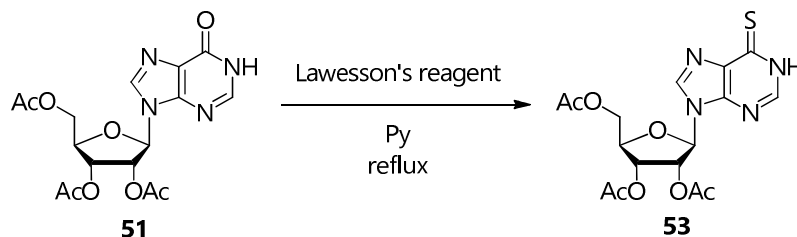
R_f: 0.35 (CH₂Cl₂-MeOH, 9:1)

¹H NMR (DMSO-*d*₆, 400 MHz): δ (ppm) 8.96 (s, 1H, H⁸), 8.83 (s, 1H, H²), 6.05 (d, *J* = 5.2 Hz, 1H, H^{1'}), 5.58 (d, *J* = 5.8 Hz, 1H, OH^{2'}), 5.26 (d, *J* = 5.2 Hz, 1H, OH^{3'}), 5.10 (t, *J* = 5.4 Hz, 1H, OH^{5'}), 4.60 (dd, *J* = 10.5, 5.3 Hz, 1H, H^{2'}), 4.20 (dd, *J* = 9.2, 4.7 Hz, 1H, H^{3'}), 4.00 (q, *J* = 3.9 Hz, 1H, H^{4'}), 3.72 (dt, *J* = 12.0, 4.6 Hz, 1H, H^{5'a}), 3.59 (ddd, *J* = 11.9, 5.4, 4.1 Hz, 1H, H^{5'b}).

¹³C NMR (DMSO-*d*₆, 100 MHz): δ (ppm) 152.2 (C²), 152.1 (C⁶), 149.8 (C⁴), 146.2 (C⁸), 131.9 (C⁵), 88.7 (C^{1'}), 86.2 (C^{4'}), 74.4 (C^{2'}), 70.5 (C^{3'}), 61.5 (C^{5'}).

MS (ESI⁺): *m/z* calcd for [C₁₀H₁₁ClN₄O₄]⁺: 286.05; found: 287.1 [M+H]⁺, 309.2 [M+Na]⁺.

UV-Vis (CH₃OH): λ_{max} = 265 nm.

7.2.2.4. 6-Thio-2',3',5'-tri-*O*-acetylthiosine (**53**)C₁₆H₁₈N₄O₇S; MW 410.40

51 (1.97 g, 5.00 mmol) was dissolved in pyridine (10.0 mL) under inert atmosphere and Lawesson's reagent (4.04 g, 9.99 mmol) was added. The solution was refluxed for 7 h.

The solvent was concentrated under reduced pressure to half its volume, then the resulting solution was washed with saturated aqueous NaHCO₃ (2x5 mL) and extracted with CH₂Cl₂ (3x15 mL). The reunited organic phases were washed with 1 M HCl (2x5 mL), dried over Na₂SO₄ and evaporated under reduced pressure. Further volatiles were removed with a mechanic pump to obtain **53** as a brown-yellow solid (1.58 g, 3.85 mmol).

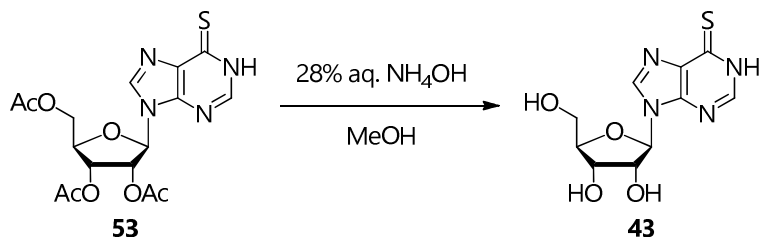
Yield: **77%**

R_f: 0.39 (CH₂Cl₂-MeOH, 9:1)

¹H NMR (DMSO-*d*₆, 400 MHz): δ (ppm) 13.90 (s, 1H, N⁶H), 8.51 (s, 1H, H⁸), 8.25 (d, *J* = 3.4 Hz, 1H, H²), 6.22 (d, *J* = 5.5 Hz, 1H, H¹), 5.91 (t, *J* = 5.7 Hz, 1H, H^{2'}), 5.55 (dd, *J* = 5.8, 4.9 Hz, 1H, H^{3'}), 4.44-4.36 (m, 2H, H^{4'}, H^{5'a}), 4.27 (dd, *J* = 12.8, 6.5 Hz, 1H, H^{5'b}), 2.12 (s, 3H, CH₃CO), 2.05 (s, 3H, CH₃CO), 2.04 (s, 3H, CH₃CO).

¹³C NMR (DMSO-*d*₆, 100 MHz): δ (ppm) 176.8 (C⁶), 170.5, 169.9, 169.7 (CH₃CO), 146.0 (C²), 144.1 (C⁴), 142.2 (C⁸), 136.2 (C⁵), 86.2 (C^{1'}), 80.2 (C^{4'}), 72.8 (C^{2'}), 70.4 (C^{3'}), 63.2 (C^{5'}), 21.0, 20.8, 20.6 (CH₃CO).

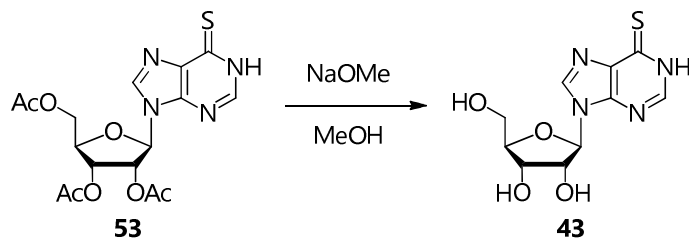
MS (ESI⁺): *m/z* calcd for [C₁₆H₁₈N₄O₇S]⁺: 410.09; found: 433.3 [M+Na]⁺, 843.3 [2M+Na]⁺.

7.2.2.5. 6-Thioinosine (**43**)C₁₀H₁₂N₄O₄S; MW 284.29

28% aqueous NH₄OH (1.26 mL, 9.06 mmol) was added to a solution of **53** (143 mg, 0.35 mmol) in MeOH (7.0 mL). The resulting mixture was stirred at RT for 15 h.

After neutralization with 2 M AcOH, the solvent was removed under reduced pressure and **43** was recrystallized from Et₂O as a yellow powder (74 mg, 0.26 mmol).

Yield: **74%**



Under inert atmosphere, **53** (1.25 g, 3.05 mmol) was dissolved in MeOH (60 mL) and a 25% NaOMe solution in MeOH (3.10 mL, 13.56 mmol) was added. The resulting solution was stirred at RT for 2 h.

After quenching by adding NH₄Cl (193 mg, 3.61 mmol), the light yellow precipitate was filtered and repeatedly washed with acetone. The solvent from the filtered solution was removed under reduced pressure to obtain product **43** as a light brown solid (503 mg, 1.77 mmol).

Yield: **58%**

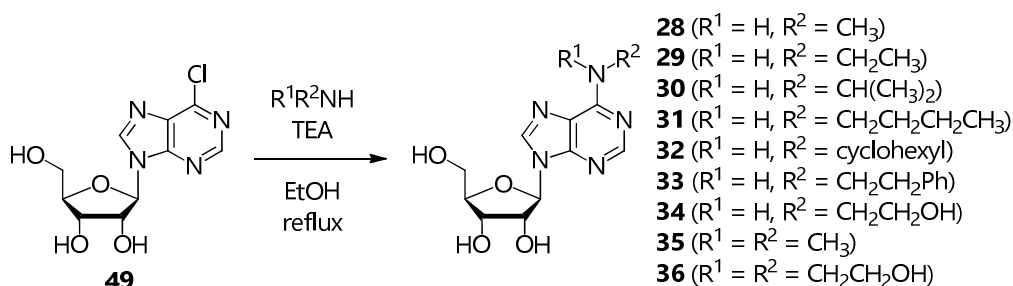
R_f: 0.84 (EtOH-H₂O, 7:3)

¹H NMR (DMSO-*d*₆, 400 MHz): δ (ppm) 13.80 (s, 1H, N¹H), 8.55 (s, 1H, H⁸), 8.23 (s, 1H, H²), 5.90 (d, *J* = 5.5 Hz, 1H, H^{1'}), 5.53 (d, *J* = 5.8 Hz, 1H, OH^{2'}), 5.22 (d, *J* = 4.5 Hz, 1H, OH^{3'}), 5.07 (d, *J* = 4.4 Hz, 1H, OH^{5'}), 4.48 (ps q, *J* = 5.2 Hz, 1H, H^{2'}), 4.15 (d, *J* = 4.0 Hz, 1H, H^{3'}), 3.96 (ps q, *J* = 3.8 Hz, 1H, H^{4'}), 3.67 (dt, *J* = 11.8, 4.6 Hz, 1H, H^{5'}), 3.57 (ddd, *J* = 11.8, 5.1, 4.4 Hz, 1H, H^{5'}).

¹³C NMR (DMSO-*d*₆, 100 MHz): δ (ppm) 176.5 (C⁶), 145.7 (C²), 144.4 (C⁴), 141.7 (C⁸), 135.9 (C⁵), 88.0 (C^{1'}), 86.1 (C^{4'}), 74.7 (C^{2'}), 70.6 (C^{3'}), 61.6 (C^{5'}).

MS (ESI⁺): *m/z* calcd for [C₁₀H₁₂N₄O₄S]⁺: 284.06; found: 307.0170 [M+Na]⁺.

7.2.2.6. General procedure for the synthesis of *N*⁶-alkyl- and *N*⁶,*N*⁶-dialkyladenosines (**28**, **29**, **30**, **31**, **32**, **33**, **34**, **35**, **36**)



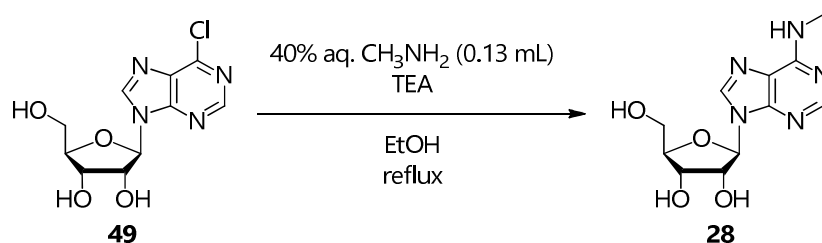
The appropriate amine or amine solution (1.50 mmol for **28**, **29**, **31**, **32**, **33**, **34** and **36**, 10.00 mmol for **30** and 5.00 mmol for **35**) and TEA (0.14 mL, 1.00 mmol) were added to a suspension of **49** (143 mg, 0.50 mmol) in EtOH (3.5 mL) under inert atmosphere. The resulting mixture was refluxed and monitored by TLC (CH_2Cl_2 -MeOH, 9:1) until consumption of the starting reagent (between 2 and 55 h).

28, **30**, **32** and **35**: The solvent was removed under reduced pressure and the resulting crude was purified by flash column chromatography (CH_2Cl_2 -MeOH, 8.9:1.1 for **28**, 9.1:0.9 for **30**, 9.3:0.7 for **32** and **35**).

29, **31**, **33**, **34** and **36**: The mixture was stored at 4°C overnight, then the resulting precipitate was filtered, washed with very few cold EtOH and dried under reduced pressure.

7.2.2.6.1. *N*⁶-Methyladenosine (**28**)

$C_{11}H_{15}N_5O_4$; MW 281.27



White powder (116 mg, 0.41 mmol).

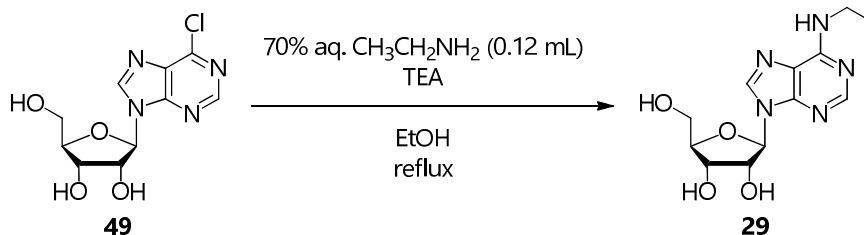
Yield: **82%**

R_f : 0.22 (CH_2Cl_2 -MeOH, 9:1)

¹H NMR (DMSO-*d*₆, 400 MHz): δ (ppm) 8.34 (s, 1H, H⁸), 8.23 (br s, 1H, H²), 7.81 (br s, 1H, N⁶H), 5.88 (d, $J = 6.2$ Hz, 1H, H^{1'}), 5.45-5.39 (m, 2H, OH^{2'}, OH^{5'}), 5.17 (d, $J = 4.6$ Hz, 1H, OH^{3'}), 4.61 (dd, $J = 11.3, 6.1$ Hz, 1H, H^{2'}), 4.14 (dd, $J = 7.8, 4.7$ Hz, 1H, H^{3'}), 3.96 (br q, $J = 3.3$ Hz, 1H, H^{4'}), 3.68 (dt, $J = 12.0, 4.1$ Hz, 1H, H^{5'a}), 3.55 (ddd, $J = 11.8, 7.6, 3.9$ Hz, 1H, H^{5'b}), 2.96 (br s, 1H, NHCH₃).

¹³C NMR (DMSO-*d*₆, 100 MHz): δ (ppm) 155.2 (C⁶), 152.5 (C²), 148.1 (C⁴), 139.7 (C⁸), 119.9 (C⁵), 88.0 (C^{1'}), 86.0 (C^{4'}), 73.6 (C^{2'}), 70.7 (C^{3'}), 61.7 (C^{5'}), 27.1 (CH₃).

MS (ESI⁺): m/z calcd for $[C_{11}H_{15}N_5O_4]^+$: 281.11; found: 282.0 [M+H]⁺, 303.9 [M+Na]⁺, 584.8 [2M+Na]⁺.

7.2.2.6.2. *N*⁶-Ethyladenosine (29)C₁₂H₁₇N₅O₄; MW 295.29

White powder (124 mg, 0.42 mmol).

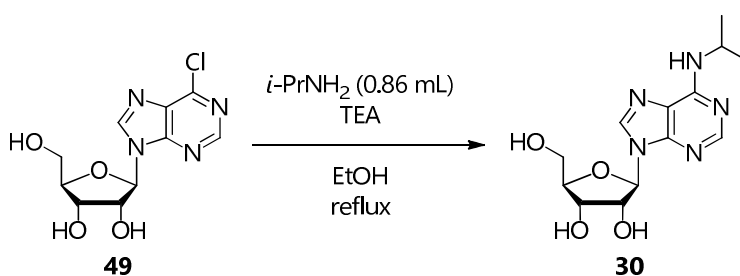
Yield: 84%

*R*_f: 0.27 (CH₂Cl₂-MeOH, 9:1)

¹H NMR (DMSO-*d*₆, 400 MHz): δ (ppm) 8.34 (s, 1H, H⁸), 8.20 (br s, 1H, H²), 7.86 (br s, 1H, N⁶H), 5.88 (d, *J* = 6.2 Hz, 1H, H^{1'}), 5.46-5.39 (m, 2H, OH^{2'}, OH^{5'}), 5.17 (d, *J* = 4.6 Hz, 1H, OH^{3'}), 4.61 (dd, *J* = 11.3, 6.0 Hz, 1H, H^{2'}), 4.14 (dd, *J* = 7.7, 4.6 Hz, 1H, H^{3'}), 3.96 (br q, *J* = 3.1 Hz, 1H, H^{3'}), 3.67 (dt, *J* = 12.0, 4.0 Hz, 1H, H^{5'a}), 3.60-3.44 (m, 2H, H^{5'b}, NHCH₂), 1.17 (t, *J* = 7.1 Hz, 3H, CH₃).

¹³C NMR (DMSO-*d*₆, 100 MHz): δ (ppm) 155.0 (C⁶), 152.8 (C²), 148.7 (C⁴), 140.1 (C⁸), 120.2 (C⁵), 88.4 (C^{1'}), 86.4 (C^{4'}), 73.9 (C^{2'}), 71.1 (C^{3'}), 62.1 (C^{5'}), 35.0 (NHCH₂), 15.3 (CH₃).

MS (ESI)⁺: *m/z* calcd for [C₁₂H₁₇N₅O₄]⁺: 295.13; found: 296.1 [M+H]⁺, 318.0 [M+Na]⁺, 591.4 [2M+H]⁺, 612.8 [2M+Na]⁺.

7.2.2.6.3. *N*⁶-*i*-Propyladenosine (30)C₁₃H₁₉N₅O₄; MW 309.32

White powder (146 mg, 0.47 mmol).

Yield: 94%

*R*_f: 0.32 (CH₂Cl₂-MeOH, 9:1)

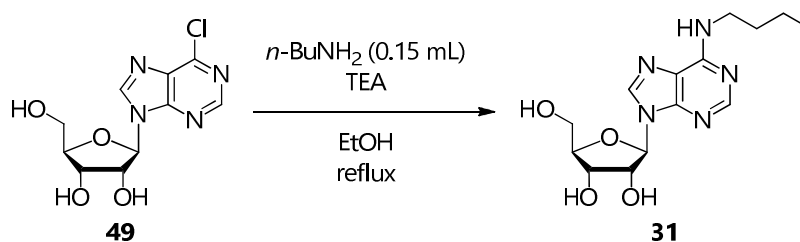
¹H NMR (DMSO-*d*₆, 400 MHz): δ (ppm) 8.34 (s, 1H, H⁸), 8.20 (br s, 1H, H²), 7.61 (br d, *J* = 7.9 Hz, 1H, N⁶H), 5.89 (d, *J* = 6.2 Hz, 1H, H^{1'}), 5.46-5.38 (m, 2H, OH^{2'}, OH^{5'}), 5.17 (br d, *J* = 4.1 Hz, 1H, OH^{4'}), 4.62 (dd, *J* = 10.6, 5.4 Hz, 1H, H^{2'}), 4.47 (br s, 1H, NHCH), 4.16 (br dd, *J* = 6.9, 3.7 Hz, 1H, H^{3'}), 3.98 (q, *J* = 3.3 Hz, 1H, H^{4'}), 3.69 (dt, *J* = 11.9, 3.7 Hz, 1H, H^{5'a}), 3.61-3.52 (m, 1H, H^{5'b}), 1.23 (d, *J* = 6.5 Hz, 6H, CH(CH₃)₂).

^{13}C NMR (DMSO- d_6 , 100 MHz): δ (ppm) 154.5 (C^6), 152.8 (C^2), 148.9 (C^4), 140.0 (C^8), 120.1 (C^5), 88.5 ($\text{C}^{1'}$), 86.4 ($\text{C}^{4'}$), 74.0 ($\text{C}^{2'}$), 71.1 ($\text{C}^{3'}$), 62.2 ($\text{C}^{5'}$), 41.8 (NHCH), 22.8 ($\text{CH}(\text{CH}_3)_2$).

MS (ESI $^+$): m/z calcd for $[\text{C}_{13}\text{H}_{19}\text{N}_5\text{O}_4]^+$: 309.14; found: 310.2 $[\text{M}+\text{H}]^+$, 332.2 $[\text{M}+\text{Na}]^+$, 641.0 $[\text{2M}+\text{Na}]^+$.

7.2.2.6.4. *N*⁶-*n*-Butyladenosine (31)

$\text{C}_{14}\text{H}_{21}\text{N}_5\text{O}_4$; MW 323.35



White powder (115 mg, 0.36 mmol).

Yield: **71%**

R_f : 0.33 (CH_2Cl_2 -MeOH, 9:1)

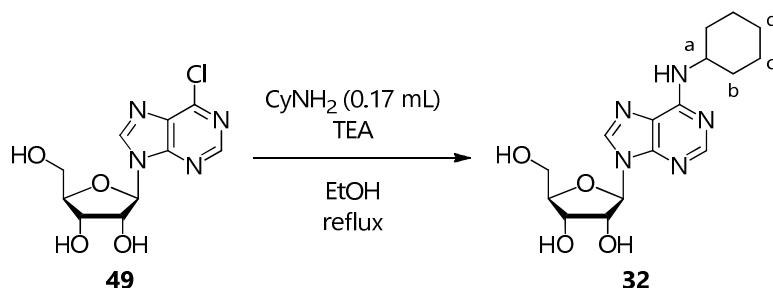
^1H NMR (CD_3OD , 400 MHz): δ (ppm) 8.26 (s, 1H, H^8), 8.23 (br s, 1H, H^2), 5.97 (d, $J = 6.4$ Hz, 1H, $\text{H}^{1'}$), 4.76 (dd, $J = 6.1, 5.5$ Hz, 1H, $\text{H}^{2'}$), 4.34 (dd, $J = 5.0, 2.4$ Hz, 1H, $\text{H}^{3'}$), 4.19 (br q, $J = 2.4$ Hz, 1H, $\text{H}^{4'}$), 3.91 (dd, $J = 12.6, 2.3$ Hz, 1H, $\text{H}^{5'a}$), 3.76 (dd, $J = 12.6, 2.5$ Hz, 1H, $\text{H}^{5'b}$), 3.62 (br s, 1H, NHCH_2), 1.70 (quint, $J = 7.3$ Hz, 2H, $\text{CH}_2\text{CH}_2\text{CH}_3$), 1.48 (sext, $J = 7.4$ Hz, 2H, CH_2CH_3), 1.00 (t, $J = 7.4$ Hz, 3H, CH_3).

^1H NMR (DMSO- d_6 , 400 MHz): δ (ppm) 8.34 (s, 1H, H^8), 8.21 (br s, 1H, H^2), 7.90 (br s, 1H, N^6H), 5.88 (d, $J = 6.1$ Hz, 1H, $\text{H}^{1'}$), 5.49-5.41 (m, 2H, $\text{OH}^{2'}$, $\text{OH}^{5'}$), 5.20 (d, $J = 4.4$ Hz, 1H, $\text{OH}^{3'}$), 4.62 (dd, $J = 11.1, 5.6$ Hz, 1H, $\text{H}^{2'}$), 4.15 (br dd, $J = 7.2, 4.2$ Hz, 1H, $\text{H}^{3'}$), 3.97 (br d, $J = 2.7$ Hz, 1H, $\text{H}^{4'}$), 3.73-3.63 (dt, $J = 11.8, 3.6$ Hz, 1H, $\text{H}^{5'a}$), 3.55 (ddd, $J = 11.6, 7.6, 3.7$ Hz, 1H, $\text{H}^{5'b}$), 3.52-3.40 (m, 1H, NHCH_2), 1.58 (ps quint, $J = 7.3$ Hz, 2H, $\text{CH}_2\text{CH}_2\text{CH}_3$), 1.33 (dq, $J = 14.3, 7.1$ Hz, 2H, CH_2CH_3), 0.90 (t, $J = 7.3$ Hz, 3H, CH_3).

^{13}C NMR (DMSO- d_6 , 100 MHz): δ (ppm) 155.8 (C^6), 153.5 (C^2), 149.3 (C^4), 140.7 (C^8), 120.9 (C^5), 89.1 ($\text{C}^{1'}$), 87.0 ($\text{C}^{4'}$), 74.6 ($\text{C}^{2'}$), 71.8 ($\text{C}^{3'}$), 62.8 ($\text{C}^{5'}$), 39.7 (NHCH_2), 32.3 ($\text{CH}_2\text{CH}_2\text{CH}_3$), 20.7 (CH_2CH_3), 14.9 (CH_3).

MS (ESI $^+$): m/z calcd for $[\text{C}_{14}\text{H}_{21}\text{N}_5\text{O}_4]^+$: 323.16; found: 324.5 $[\text{M}+\text{H}]^+$, 668.9 $[\text{2M}+\text{Na}]^+$.

UV-Vis (CH_3OH): $\lambda_{\text{max}} = 271$ nm.

7.2.2.6.5. *N*⁶-Cyclohexyladenosine (**32**)C₁₆H₂₃N₅O₄; MW 349.38

White powder (139 mg, 0.40 mmol).

Yield: 79%

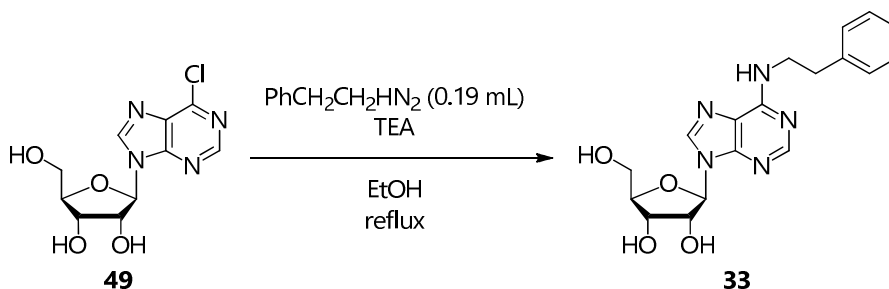
*R*_f: 0.47 (CH₂Cl₂-MeOH, 9:1)

¹H NMR (CD₃OD, 400 MHz): δ (ppm) 8.27 (s, 1H, H⁸), 8.22 (s, 1H, H²), 5.97 (d, *J* = 6.4 Hz, 1H, H^{1'}), 4.76 (dd, *J* = 6.3, 5.3 Hz, 1H, H^{2'}), 4.34 (dd, *J* = 5.1, 2.5 Hz, 1H, H^{3'}), 4.19 (q, *J* = 2.5 Hz, 1H, H^{4'}), 4.14 (v br s, 1H, H^a), 3.91 (dd, *J* = 12.6, 2.4 Hz, 1H, H^{5'a}), 3.76 (dd, *J* = 12.6, 2.6 Hz, 1H, H^{5'b}), 2.12-2.02 (m, 2H, H^b), 1.89-1.80 (m, 2H, H^c), 1.75-1.66 (m, 1H, H^d), 1.56-1.25 (m, 5H, H^b, H^c).

¹³C NMR (CD₃OD, 100 MHz): δ (ppm) 154.1 (C⁶), 152.2 (C²), 147.7 (C⁴), 139.9 (C⁸), 119.8 (C⁵), 89.9 (C^{1'}), 86.8 (C^{4'}), 74.1 (C^{2'}), 71.3 (C^{3'}), 62.1 (C^{5'}), 49.3 (C^a), 32.5 (C^b), 25.3 (C^d), 24.6 (C^c).

MS (ESI⁺): *m/z* calcd for [C₁₆H₂₃N₅O₄]⁺: 349.18; found: 350.3 [M+H]⁺, 372.3 [M+Na]⁺.

UV-Vis (CH₃OH): λ_{max} = 272 nm.

7.2.2.6.6. *N*⁶-(2-Phenyl)ethyladenosine (**33**)C₁₈H₂₁N₅O₄; MW 371.39

White powder (121 mg, 0.33 mmol).

Yield: 65%

*R*_f: 0.53 (CH₂Cl₂-MeOH, 10:1)

¹H NMR (DMSO-*d*₆, 400 MHz): δ (ppm) 8.36 (br s, 1H, H⁸), 8.25 (br s, 1H, H²), 7.95 (br s, 1H, N⁶H), 7.34-7.17 (m, 5H, C₆H₅), 5.89 (d, *J* = 6.1 Hz, 1H, H^{1'}), 5.45 (d, *J* = 6.1 Hz, 1H, OH^{2'}), 5.41 (dd, *J* = 7.1, 4.6 Hz, 1H, OH^{5'}),

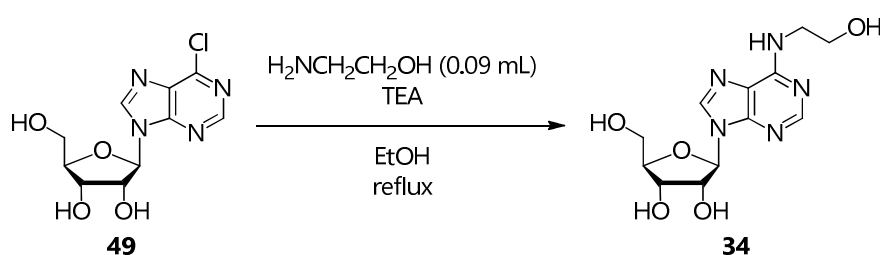
5.19 (d, $J = 4.5$ Hz, 1H, OH^{3'}), 4.62 (dd, $J = 11.1, 5.8$ Hz, 1H, H^{2'}), 4.15 (dd, $J = 7.6, 4.5$ Hz, 1H, H^{3'}), 3.97 (br dd, $J = 6.4, 3.3$ Hz, 1H, H^{4'}), 3.80-3.64 (m, 3H, NHCH₂, H^{5'a}), 3.61-3.51 (ddd, $J = 11.8, 7.5, 3.9$ Hz, 1H, H^{5'b}), 2.93 (t, $J = 7.5$ Hz, 2H, CH₂C₆H₅).

¹³C NMR (DMSO-*d*₆, 100 MHz): δ (ppm) 155.0 (C⁶), 152.9 (C²), 148.8 (C⁴), 140.2 (C⁸), 140.0 (C^a), 129.1, 128.8 (C^b, C^c), 126.5 (C^d), 120.3 (C⁵), 88.4 (C^{1'}), 86.4 (C^{4'}), 74.0 (C^{2'}), 71.1 (C^{3'}), 62.1 (C^{5'}), 41.8 (NHCH₂), 35.5 (CH₂C₆H₅).

MS (ESI⁺): m/z calcd for [C₁₈H₂₁N₅O₄]⁺: 371.16; found: 372.3 [M+H]⁺, 394.3 [M+Na]⁺, 765.3 [2M+Na]⁺.

7.2.2.6.7. N⁶-Hydroxyethyladenosine (34)

C₁₂H₁₇N₅O₅; MW 311.29



White powder (129 mg, 0.41 mmol).

Yield: **83%**

R_f : 0.18 (CH₂Cl₂-MeOH, 7:1)

¹H NMR (DMSO-*d*₆, 400 MHz): δ (ppm) 8.36 (s, 1H, H⁸), 8.22 (s, 1H, H²), 7.69 (br s, 1H, N⁶H), 5.89 (d, $J = 6.1$ Hz, 1H, H^{1'}), 5.50-5.35 (m, 2H, OH^{2'}, OH^{5'}), 5.19 (br s, 1H, OH^{3'}), 4.76 (br s, 1H, CH₂CH₂OH), 4.61 (br dd, $J = 8.6, 5.2$ Hz, 1H, H^{2'}), 4.15 (br s, 1H, H^{3'}), 3.97 (q, $J = 3.3$ Hz, 1H, H^{4'}), 3.68 (br dt, $J = 12.0, 3.2$ Hz, 1H, H^{5'a}), 3.63-3.51 (m, 5H, H^{5'b}, NHCH₂CH₂OH).

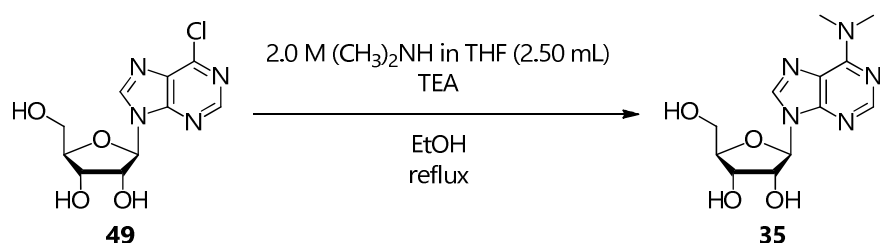
¹³C NMR (DMSO-*d*₆, 100 MHz): δ (ppm) 155.3 (C⁶), 152.8 (C²), 148.9 (C⁴), 140.2 (C⁸), 120.3 (C⁵), 88.4 (C^{1'}), 86.4 (C^{4'}), 74.0 (C^{2'}), 71.1 (C^{3'}), 62.1 (C^{5'}), 60.2 (CH₂OH), 43.0 (NHCH₂).

MS (ESI⁺): m/z calcd for [C₁₂H₁₇N₅O₅]⁺: 311.12; found: 312.3 [M+H]⁺, 334.3 [M+Na]⁺, 645.2 [2M+Na]⁺.

UV-Vis (CH₃OH): $\lambda_{\text{max}} = 262$ nm.

7.2.2.6.8. N⁶,N⁶-Dimethyladenosine (35)

C₁₂H₁₇N₅O₄; MW 295.29



White powder (102 mg, 0.35 mmol).

Yield: 69%

R_f : 0.51 (CH₂Cl₂-MeOH, 9:1)

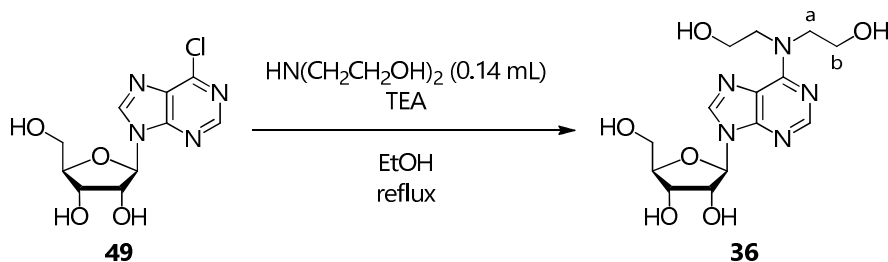
¹H NMR (CD₃OD, 400 MHz): δ (ppm) 8.22 (s, 1H, H⁸), 8.20 (s, 1H, H²), 5.97 (d, J = 6.4 Hz, 1H, H¹), 4.76 (dd, J = 6.0, 5.4 Hz, 1H, H²), 4.34 (dd, J = 5.0, 2.4 Hz, 1H, H³), 4.19 (br dd, J = 4.5, 2.5 Hz, 1H, H⁴), 3.90 (dd, J = 12.5, 2.2 Hz, 1H, H^{5a}), 3.76 (dd, J = 12.5, 2.2 Hz, 1H, H^{5b}), 3.53 (br s, 6H, N(CH₃)₂).

¹³C NMR (CD₃OD, 100 MHz): δ (ppm) 154.9 (C⁶), 151.3 (C²), 149.3 (C⁴), 138.8 (C⁸), 120.6 (C⁵), 89.8 (C¹), 86.7 (C^{4'}), 73.9 (C^{2'}), 71.3 (C^{3'}), 62.1 (C^{5'}), 37.6 (N(CH₃)₂).

MS (ESI⁺): m/z calcd for [C₁₂H₁₇N₅O₄]⁺: 295.13; found: 296.2 [M+H]⁺, 318.3 [M+Na]⁺, 613.4 [2M+Na]⁺.

7.2.2.6.9. N⁶,N⁶-Bis-Hydroxyethyladenosine (36)

C₁₄H₂₁N₅O₆; MW 355.35



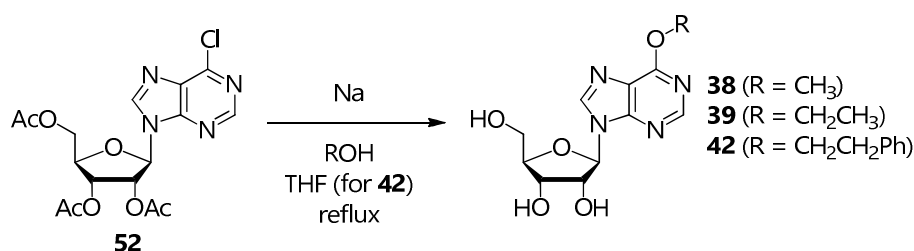
White powder (165 mg, 0.46 mmol).

Yield: 93%

¹H NMR (DMSO-*d*₆, 400 MHz): δ (ppm) 8.38 (s, 1H, H⁸), 8.21 (s, 1H, H²), 5.91 (d, J = 6.0 Hz, 1H, H¹), 5.44 (d, J = 6.2 Hz, 1H, OH^{2'}), 5.36 (dd, J = 6.8, 4.7 Hz, 1H, OH^{5'}), 5.17 (d, J = 4.7 Hz, 1H, OH^{3'}), 4.79 (br t, J = 5.2 Hz, 2H, N(CH₂CH₂OH)₂), 4.59 (dd, J = 11.2, 5.9 Hz, 1H, H²), 4.37-4.19 (br s, 2H, H^a), 4.15 (dd, J = 8.1, 4.7 Hz, 1H, H³), 3.97 (br q, J = 3.3 Hz, 1H, H⁴), 3.92-3.76 (br, 2H, H^a), 3.74-3.62 (m, 5H, H^b, H^{5b}), 3.56 (ddd, J = 11.7, 7.3, 3.9 Hz, 1H, H^{5b}).

¹³C NMR (DMSO-*d*₆, 100 MHz): δ (ppm) 154.3 (C⁶), 152.1 (C²), 150.4 (C⁴), 139.4 (C⁸), 120.0 (C⁵), 88.3 (C¹), 86.2 (C^{4'}), 73.9 (C^{2'}), 71.0 (C^{3'}), 62.0 (C^{5'}), 60.6, 58.9 (C^b), 52.8, 52.6 (C^a).

MS (ESI⁺): m/z calcd for [C₁₄H₂₁N₅O₆]⁺: 355.15; found: 356.2 [M+H]⁺, 378.3 [M+Na]⁺, 733.2 [2M+Na]⁺.

7.2.2.7. General procedure for the synthesis of 6-alkoxyinosines **38**, **39** and **42**

Na (69 mg, 3.00 mmol) was dissolved in the appropriate dry alcohol (3.00 mL) (for **38** and **39**) or in a solution of it (3.00 mmol) in dry THF (4.0 mL) (for **42**) under inert atmosphere. A solution of **52** (206 mg, 0.50 mmol) in the same dry alcohol (3.00 mL) or in dry THF (2.0 mL) was added, respectively, and the resulting mixture was refluxed and monitored by TLC (CH₂Cl₂-MeOH, 9:1) until consumption of the starting reagent and complete formation of the product (between 1 and 6 h).

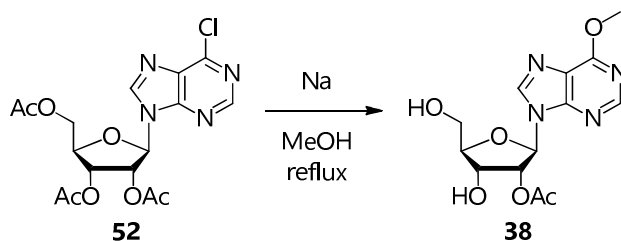
NH₄Cl (160 mg, 3.00 mmol) was added, the suspension was stirred at RT for 15', filtered to eliminate the residue solid and the solvent was removed under reduced pressure.

38 and **42**: The product was purified by flash column chromatography (CH₂Cl₂-MeOH, 9.1:0.9 for **38** and 9.4:0.6 for **42**).

39: The crude residue was suspended in acetone and filtered. The operation was repeated twice after evaporation of the filtrate.

7.2.2.7.1. 6-Methoxyinosine (**38**)

C₁₁H₁₄N₄O₅; MW 282.25



Light brown powder (128 mg, 0.45 mmol).

Yield: **91%**

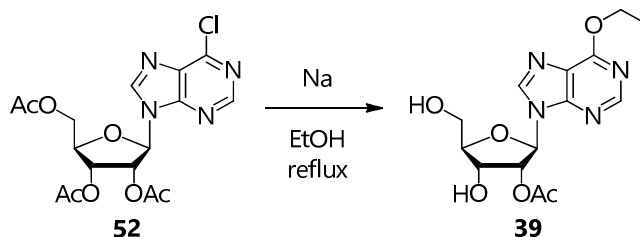
R_f: 0.33 (CH₂Cl₂-MeOH, 9:1)

¹H NMR (CD₃OD, 400 MHz): δ (ppm) 8.56 (s, 1H, H⁸), 8.54 (s, 1H, H²), 6.10 (d, *J* = 5.9 Hz, 1H, H^{1'}), 4.76 (t, *J* = 5.5 Hz, 1H, H^{2'}), 4.38 (dd, *J* = 5.1, 3.2 Hz, 1H, H^{3'}), 4.22-4.18 (m, 4H, H^{4'}, OCH₃), 3.91 (dd, *J* = 12.4, 2.8 Hz, 1H, H^{5'a}), 3.79 (dd, *J* = 12.4, 3.1 Hz, 1H, H^{5'b}).

¹H NMR (CD₃OD, 100 MHz): δ (ppm) 161.0 (C⁶), 151.8 (C²), 151.1 (C⁴), 142.5 (C⁸), 121.4 (C⁵), 89.6 (C^{1'}), 86.5 (C^{4'}), 74.3 (C^{2'}), 70.9 (C^{3'}), 61.8 (C^{5'}), 53.5 (OCH₃).

MS (ESI⁺): *m/z* calcd for [C₁₁H₁₄N₄O₅]⁺: 282.10; found: 305.3 [M+Na]⁺, 587.2 [2M+Na]⁺.

7.2.2.7.2. 6-Ethoxyinosine (39)

C₁₂H₁₆N₄O₅; MW 296.28

Ochre powder (148 mg, 0.50 mmol).

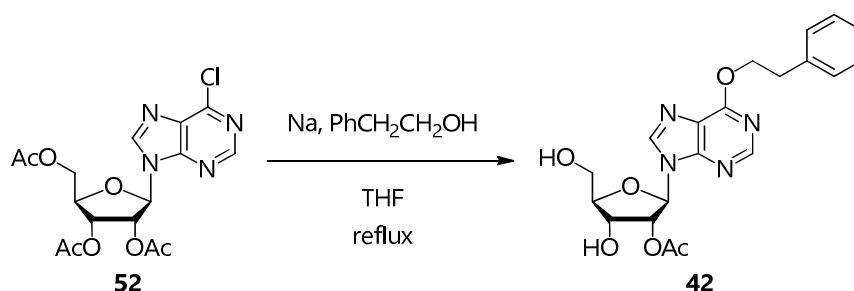
Yield: **quantitative***R_f*: 0.38 (CH₂Cl₂-MeOH, 9:1)

¹H NMR (CD₃OD, 400 MHz): δ (ppm) 8.53 (s, 1H, H⁸), 8.51 (s, 1H, H²), 6.09 (d, *J* = 6.0 Hz, 1H, H^{1'}), 4.76 (t, *J* = 5.5 Hz, 1H, H^{2'}), 4.69 (q, *J* = 7.1 Hz, 2H, OCH₂), 4.37 (dd, *J* = 5.2, 3.1 Hz, 1H, H^{3'}), 4.19 (q, *J* = 3.0 Hz, 1H, H^{4'}), 3.91 (dd, *J* = 12.4, 2.8 Hz, 1H, H^{5'a}), 3.79 (dd, *J* = 12.4, 3.0 Hz, 1H, H^{5'b}), 1.51 (t, *J* = 7.1 Hz, 3H, CH₂CH₃).

¹H NMR (CD₃OD, 100 MHz): δ (ppm) 160.8 (C⁶), 151.8 (C²), 151.2 (C⁴), 142.4 (C⁸), 121.5 (C⁵), 89.7 (C^{1'}), 86.5 (C^{4'}), 74.3 (C^{2'}), 71.0 (C^{3'}), 63.1 (OCH₂), 61.8 (C^{5'}), 13.3 (CH₃).

MS (ESI⁺): *m/z* calcd for [C₁₂H₁₆N₄O₅]⁺: 296.11; found: 319.2 [M+Na]⁺, 615.1 [2M+Na]⁺.

7.2.2.7.3. 6-(2-Phenyl)ethoxyinosine (42)

C₁₈H₂₀N₄O₅; MW 372.38

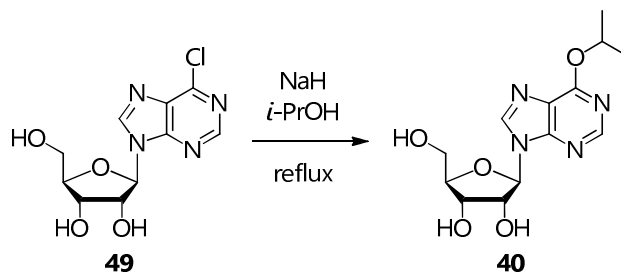
White solid (54 mg, 0.15 mmol).

Yield: **29%***R_f*: 0.48 (CH₂Cl₂-MeOH, 9:1)

¹H NMR (DMSO-*d*₆, 400 MHz): δ (ppm) 8.63 (s, 1H, H⁸), 8.55 (s, 1H, H²), 7.38-7.17 (m, 5H, C₆H₅), 6.02 (d, *J* = 5.7 Hz, 1H, H^{1'}), 5.52 (br d, *J* = 5.7 Hz, 1H, OH^{2'}), 5.24 (br d, *J* = 4.4 Hz, 1H, OH^{3'}), 5.16 (t, *J* = 5.4 Hz, 1H, OH^{5'}), 4.78 (t, *J* = 6.9 Hz, 1H, OCH₂), 4.61 (dd, *J* = 10.3, 5.1 Hz, 1H, H^{2'}), 4.20 (br d, *J* = 3.7 Hz, 1H, H^{3'}), 4.00 (br dd, *J* = 3.5, 3.6 Hz, 1H, H^{4'}), 3.71 (dt, *J* = 11.4, 4.1 Hz, 1H, H^{5'a}), 3.59 (br ddd, *J* = 11.9, 5.4, 4.2 Hz, 1H, H^{5'b}), 3.15 (t, *J* = 6.9 Hz, 2H, CH₂C₆H₅).

¹³C NMR (DMSO-*d*₆, 100 MHz): δ (ppm) 160.5 (C⁶), 152.4 (C⁴), 152.1 (C²), 142.9 (C⁸), 138.5, 129.4, 128.8, 126.8 (C₆H₅), 121.6 (C⁵), 88.3 (C^{1'}), 86.2 (C^{4'}), 74.3 (C^{2'}), 70.8 (C^{3'}), 67.5 (OCH₂), 61.8 (C^{5'}), 35.0 (CH₂C₆H₅).

MS (ESI⁺): *m/z* calcd for [C₁₈H₂₀N₄O₅]⁺: 372.14; found: 373.0 [M+H]⁺, 395.2 [M+Na]⁺, 767.1 [2M+Na]⁺.

7.2.2.8. 6-*i*-Propoxyinosine (**40**)C₁₃H₁₈N₄O₅; MW 310.31

A 60% NaH dispersion in mineral oil (100 mg, 2.50 mmol) was added to dry *i*-PrOH (10.0 mL) portionwise in 2 h at 50°C, under inert atmosphere. **49** (143 mg, 0.50 mmol) was added and the resulting suspension was refluxed for 4 h.

After treatment with NH₄Cl (134 mg, 2.51 mmol), the mixture was stirred at RT for 15' and the solvent was removed under reduced pressure. The crude was purified by flash column chromatography (CH₂Cl₂-MeOH, 9.2:0.8) to obtain **40** as a pale yellow powder (50 mg, 0.16 mmol).

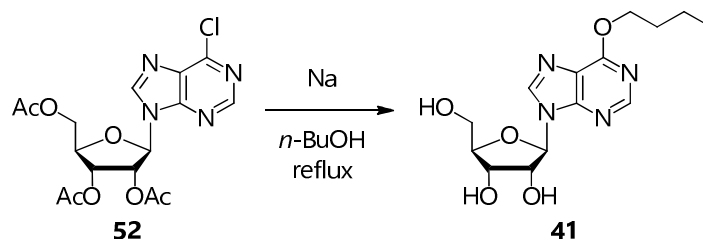
Yield: **32%**

R_f: 0.36 (CH₂Cl₂-MeOH, 9:1)

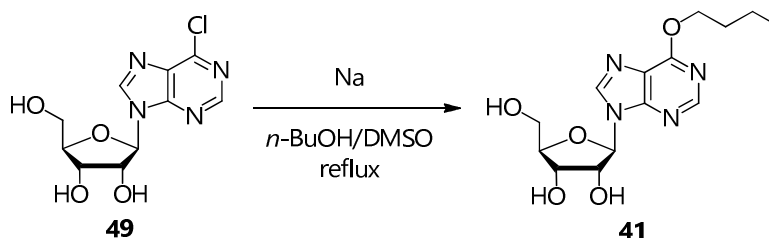
¹H NMR (CD₃OD, 400 MHz): δ (ppm) 8.52 (s, 1H, H⁸), 8.50 (s, 1H, H²), 6.08 (d, *J* = 6.0 Hz, 1H, H^{1'}), 5.70 (sept, *J* = 6.2 Hz, 1H, OCH), 4.75 (t, *J* = 5.5 Hz, 1H, H^{2'}), 4.37 (dd, *J* = 5.0, 3.2 Hz, 1H, H^{3'}), 4.19 (q, *J* = 2.9 Hz, 1H, H^{4'}), 3.91 (dd, *J* = 12.4, 2.7 Hz, 1H, H^{5'a}), 3.79 (dd, *J* = 12.4, 3.0 Hz, 1H, H^{5'b}), 1.48 (d, *J* = 6.2 Hz, 6H, CH(CH₃)₂).

¹³C NMR (CD₃OD, 100 MHz): δ (ppm) 160.4 (C⁶), 151.8 (C²), 151.2 (C⁴), 142.3 (C⁸), 121.7 (C⁵), 89.7 (C^{1'}), 86.5 (C^{4'}), 74.3 (C^{2'}), 71.0 (C^{3'}), 70.5 (OCH₂), 61.8 (C^{5'}), 20.8 (CH(CH₃)₂).

MS (ESI⁺): *m/z* calcd for [C₁₃H₁₈N₄O₅]⁺: 310.13; found: 311.0 [M+H]⁺, 333.2 [M+Na]⁺, 643.1 [2M+Na]⁺.

7.2.2.9. 6-*n*-Butoxyinosine (**41**)C₁₄H₂₀N₄O₅; MW 324.33

Na (79 mg, 3.44 mmol) was dissolved in dry *n*-BuOH (3.00 mL) under inert atmosphere and a solution of **52** (235 mg, 0.57 mmol) in dry *n*-BuOH (3.00 mL) was added. The resulting mixture was refluxed for 6 h. NH₄Cl (193 mg, 3.61 mmol) was added, the suspension was stirred at RT for 15', filtered to eliminate the residue solid and the solvent was removed under reduced pressure. The crude residue was suspended in acetone and filtered. The operation was repeated twice to obtain **41** as an ochre solid (159 mg, 0.49 mmol) after removing the solvent of the filtrate solution under reduced pressure.

Yield: **86%**

Under inert atmosphere, Na (23 mg, 1.00 mmol) was dissolved in dry *n*-BuOH (1.0 mL) and the resulting solution was added to a one of **49** (143 mg, 0.50 mmol) in dry DMSO (1.2 mL). The transparent solution immediately became a white suspension, which was stirred at RT for 3 h, during which time it became less opaque.

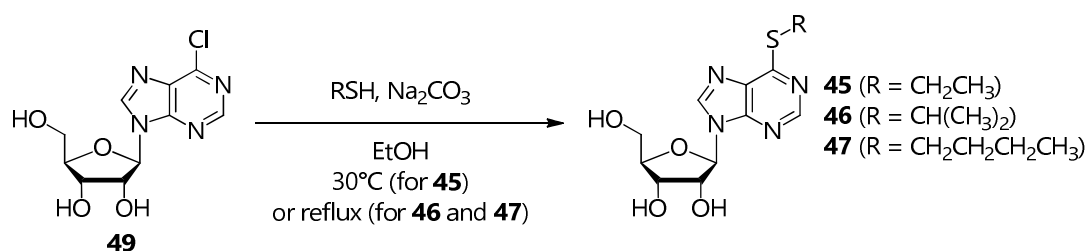
NH₄Cl (40 mg, 0.75 mmol) was added and **41** was obtained by flash column chromatography (CH₂Cl₂-MeOH, 9.4:0.6) as a solution in DMSO. It was then diluted in water and lyophilized to get a pale grey solid (96 mg, 0.30 mmol).

Yield: **59%***R*_f: 0.41 (CH₂Cl₂-MeOH, 9:1)

¹H NMR (DMSO-*d*₆, 400 MHz): δ (ppm) 8.62 (s, 1H, H⁸), 8.53 (s, 1H, H²), 6.00 (d, *J* = 5.7 Hz, 1H, H^{1'}), 5.49 (d, *J* = 6.0 Hz, 1H, OH^{2'}), 5.22 (d, *J* = 4.9 Hz, 1H, OH^{3'}), 5.14 (t, *J* = 5.6 Hz, 1H, OH^{5'}), 4.64-4.53 (m, 3H, H^{2'}, OCH₂), 4.18 (dd, *J* = 8.6, 4.6 Hz, 1H, H^{3'}), 3.98 (q, *J* = 3.7 Hz, 1H, H^{4'}), 3.70 (dt, *J* = 11.8, 4.5 Hz, 1H, H^{5'a}), 3.58 (ddd, *J* = 12.0, 6.1, 4.2, 1H, H^{5'b}), 1.80 (quin, *J* = 7.1 Hz, 2H, CH₂CH₂CH₃), 1.46 (sext, *J* = 7.4 Hz, 2H, CH₂CH₃), 0.95 (t, *J* = 7.4 Hz, 3H, CH₃).

¹³C NMR (DMSO-*d*₆, 100 MHz): δ (ppm) 160.7 (C⁶), 152.3 (C⁴), 152.1 (C²), 142.8 (C⁸), 121.6 (C⁵), 88.3 (C^{1'}), 86.2 (C^{4'}), 74.2 (C^{2'}), 70.8 (C^{3'}), 66.8 (OCH₂), 61.8 (C^{5'}), 30.9 (CH₂CH₂CH₃), 19.1 (CH₂CH₃), 14.1 (CH₃).

MS (ESI⁺): *m/z* calcd for [C₁₄H₂₀N₄O₅]⁺: 324.14; found: 325.2 [M+H]⁺, 347.3 [M+Na]⁺, 647.7 [2M]⁺, 671.2 [2M+Na]⁺, 972.5 [3M]⁺, 973.6 [3M+H]⁺.

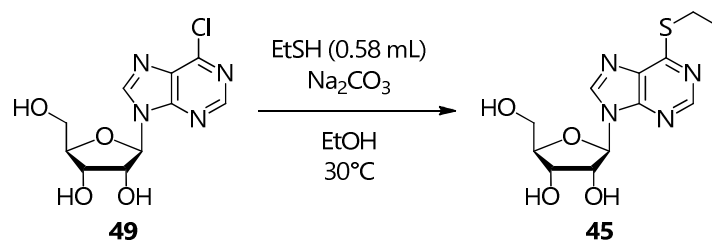
7.2.2.10. General procedure for the synthesis of 6-alkylthioinosines **45**, **46** and **47**

The appropriate thiol (7.80 mmol for **45** and 2.50 mmol for **46** and **47**) was added to a suspension of Na₂CO₃ (318 mg, 3.00 mmol) in EtOH (5.0 mL) and the resulting mixture was stirred at RT for 30'. **49** (143 mg, 0.50 mmol) was added and the suspension was stirred at 30 °C for 48 h (for **45**) or refluxed for 15 h (for **46** and **47**).

After removing the solvent under reduced pressure, the product was purified by flash chromatography (AcOEt-*n*-hexane, 1:1 for **45** and CH₂Cl₂-MeOH, 9.3:0.7 for **46** and 9.5:0.5 for **47**).

7.2.2.10.1. 6-Ethylthioinosine (**45**)

C₁₂H₁₆N₄O₄S; MW 312.34



White powder (104 mg, 0.33 mmol).

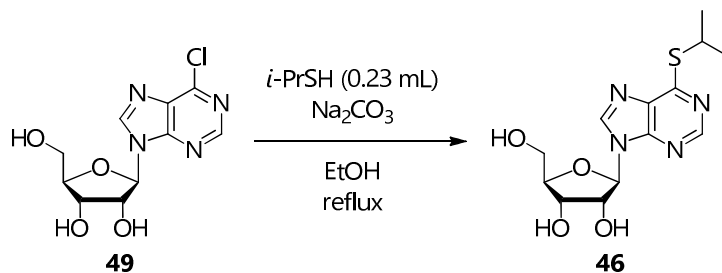
Yield: **67%**

R_f: 0.45 (CH₂Cl₂-MeOH, 9:1)

¹H NMR (DMSO-*d*₆, 400 MHz): δ (ppm) 8.74 (s, 1H, H²), 8.71 (s, 1H, H⁸), 6.00 (d, *J* = 5.6 Hz, 1H, H^{1'}), 5.53 (d, *J* = 5.9 Hz, 1H, OH^{2'}), 5.24 (d, *J* = 5.0 Hz, 1H, OH^{3'}), 5.12 (t, *J* = 5.6 Hz, 1H, OH^{5'}), 4.61 (dd, *J* = 10.9, 5.5 Hz, 1H, H^{2'}), 4.18 (dd, *J* = 8.7, 4.7 Hz, 1H, H^{3'}), 3.98 (q, *J* = 3.8 Hz, 1H, H^{4'}), 3.69 (dt, *J* = 11.9, 4.6 Hz, 1H, H^{5'a}), 3.57 (ddd, *J* = 11.9, 6.0, 4.1 Hz, 1H, H^{5'b}), 3.36 (q, *J* = 7.3 Hz, 2H, SCH₂), 1.37 (t, *J* = 7.3 Hz, 3H, CH₃).

¹H NMR (DMSO-*d*₆, 100 MHz): δ (ppm) 160.4 (C⁶), 152.0 (C²), 148.6 (C⁴), 143.9 (C⁸), 131.7 (C⁵), 88.2 (C^{1'}), 86.2 (C^{4'}), 74.2 (C^{2'}), 70.7 (C^{3'}), 61.7 (C^{5'}), 22.9 (SCH₂), 15.4 (CH₃).

HRMS (ESI-Q-ToF⁺): *m/z* calcd for [C₁₂H₁₆N₄O₄S]⁺: 312.0892; found: 335.1109 [M+Na]⁺.

7.2.2.10.2. 6-*i*-Propylthioinosine (46)C₁₃H₁₈N₄O₄S; MW 326.37

White powder (96 mg, 0.29 mmol).

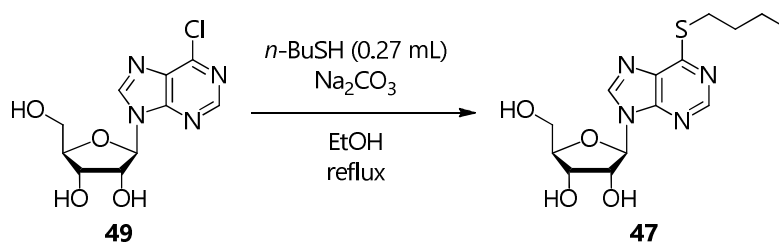
Yield: 59%

R_f: 0.48 (CH₂Cl₂-MeOH, 9:1)

¹H NMR (CD₃OD, 400 MHz): δ (ppm) 8.69 (s, 1H, H²), 8.59 (s, 1H, H⁸), 6.09 (d, *J* = 5.8 Hz, 1H, H^{1'}), 4.75 (t, *J* = 5.4 Hz, 1H, H^{2'}), 4.46-4.35 (m, 2H, H^{3'}, SCH), 4.18 (dd, *J* = 5.9, 2.9 Hz, 1H, H^{4'}), 3.91 (dd, *J* = 12.4, 2.7 Hz, 1H, H^{5'a}), 3.79 (dd, *J* = 12.4, 3.0 Hz, 1H, H^{5'b}), 1.51 (d, *J* = 6.8 Hz, 6H, CH(CH₃)₂).

¹H NMR (CD₃OD, 100 MHz): δ (ppm) 161.8 (C⁶), 151.3 (C²), 147.7 (C⁴), 143.0 (C⁸), 131.2 (C⁵), 89.5 (C^{1'}), 86.4 (C^{4'}), 74.3 (C^{2'}), 70.9 (C^{3'}), 61.7 (C^{5'}), 34.1 (SCH), 22.1 (CH(CH₃)₂).

MS (ESI⁺): *m/z* calcd for [C₁₃H₁₈N₄O₄S]⁺: 326.10; found: 349.2 [M+Na]⁺, 675.2 [2M+Na]⁺

7.2.2.10.3. 6-*n*-Butylthioinosine (47)C₁₄H₂₀N₄O₄S; MW 340.40

Pale ochre powder (150 mg, 0.44 mmol).

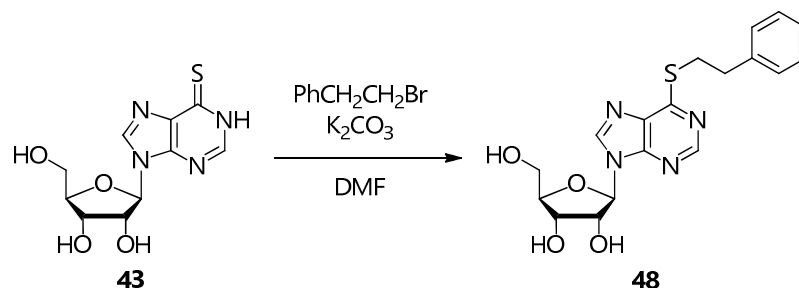
Yield: 88%

R_f: 0.47 (CH₂Cl₂-MeOH, 9:1)

¹H NMR (DMSO-*d*₆, 400 MHz): δ (ppm) 8.74 (s, 1H, H²), 8.70 (s, 1H, H⁸), 5.99 (d, *J* = 5.6 Hz, 1H, H^{1'}), 5.53 (d, *J* = 5.9 Hz, 1H, OH^{2'}), 5.24 (d, *J* = 5.0 Hz, 1H, OH^{3'}), 5.12 (t, *J* = 5.5 Hz, 1H, OH^{5'}), 4.60 (dd, *J* = 10.9, 5.6 Hz, 1H, H^{2'}), 4.18 (dd, *J* = 8.7, 4.8 Hz, 1H, H^{3'}), 3.98 (q, *J* = 3.8 Hz, 1H, H^{4'}), 3.69 (dt, *J* = 11.9, 4.6 Hz, 1H, H^{5'a}), 3.57 (ddd, *J* = 12.0, 6.0, 4.1 Hz, 1H, H^{5'b}), 3.37 (t, *J* = 7.3 Hz, 2H, SCH₂), 1.70 (quin, *J* = 7.4 Hz, 2H, CH₂CH₂CH₃), 1.45 (sext, *J* = 7.4 Hz, 2H, CH₂CH₃), 0.92 (t, *J* = 7.4 Hz, 3H, CH₃).

¹H NMR (DMSO-*d*₆, 100 MHz): δ (ppm) 160.5 (C⁶), 152.0 (C²), 148.6 (C⁴), 143.9 (C⁸), 131.7 (C⁵), 88.2 (C^{1'}), 86.2 (C^{4'}), 74.2 (C^{2'}), 70.7 (C^{3'}), 61.7 (C^{5'}), 31.7 (CH₂CH₂CH₃), 28.0 (SCH₂), 21.9 (CH₂CH₃), 14.0 (CH₃).

HRMS (ESI-Q-ToF⁺): m/z calcd for [C₁₄H₂₀N₄O₄S]⁺: 340.1205; found: 363.1116 [M+Na]⁺.

7.2.2.11. 6-(2-Phenyl)ethylthioinosine (**48**)C₁₈H₂₀N₄O₄S; MW 388.44

43 (143 mg, 0.50 mmol) and K₂CO₃ (83 mg, 0.60 mmol) were suspended in dry DMF (1.0 mL) and the resulting mixture was stirred at RT for 30', then PhCH₂CH₂Br (0.14 mL, 1.00 mmol) was added. The mixture was stirred at RT for 1 h.

The solution was diluted with a CH₂Cl₂-MeOH, 8:2 mixture and filtered on silica, then the solvent was removed under reduced pressure. The resulting crude was suspended in MeOH to precipitate **48** as a brown powder, which was filtered, washed with few cold precipitation solvent and dried under vacuum (92 mg, 0.24 mmol).

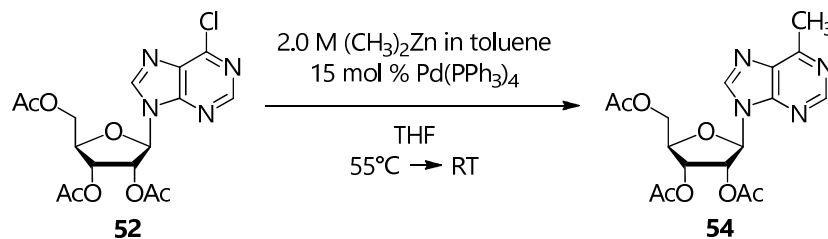
Yield: **47%**

*R*_f: 0.51 (CH₂Cl₂-MeOH, 9:1)

¹H NMR (DMSO-*d*₆, 400 MHz): δ (ppm) 8.78 (s, 1H, H²), 8.71 (s, 1H, H⁸), 7.39-7.18 (m, 5H, C₆H₅), 6.01 (d, *J* = 5.5 Hz, 1H, H^{1'}), 5.53 (d, *J* = 5.9 Hz, 1H, OH^{2'}), 5.24 (d, *J* = 4.9 Hz, 1H, OH^{3'}), 5.12 (t, *J* = 5.4 Hz, 1H, OH^{5'}), 4.61 (dd, *J* = 10.7, 5.4 Hz, 1H, H^{2'}), 4.19 (dd, *J* = 8.3, 4.3 Hz, 1H, H^{3'}), 3.98 (br dd, *J* = 7.3, 3.7 Hz, 1H, H^{4'}), 3.70 (dt, *J* = 12.0, 4.3 Hz, 1H, H^{5'a}), 3.66-3.54 (m, 3H, H^{5'b}, SCH₂), 3.04 (t, *J* = 7.5 Hz, 2H, CH₂C₆H₅).

¹³C NMR (DMSO-*d*₆, 100 MHz): δ (ppm) 160.2 (C⁶), 152.1 (C²), 148.7 (C⁴), 143.7 (C⁸), 140.5, 129.1, 128.9, 126.9 (C₆H₅), 131.7 (C⁵), 88.2 (C^{1'}), 86.2 (C^{4'}), 74.2 (C^{2'}), 70.7 (C^{3'}), 61.7 (C^{5'}), 35.6 (CH₂C₆H₅), 29.7 (SCH₂).

HRMS (ESI-Q-ToF⁺): *m/z* calcd for [C₁₈H₂₀N₄O₄S]⁺: 388.1205; found: 411.1547 [M+Na]⁺.

7.2.2.12. 6-Methyl-2',3',5'-tri-*O*-acetylinosine (**54**)C₁₇H₂₀N₄O₇; MW 392.36

Under inert atmosphere, a 2.0 M solution of Me₂Zn in toluene (1.6 mL, 3.2 mmol) was diluted in dry THF (5.0 mL) and a solution of **52** (233 mg, 0.56 mmol) in dry THF (2.0 mL) was added to it dropwise at 0°C. The formation of a light yellow solid was immediately observed. Pd(PPh₃)₄ (104 mg, 0.09 mmol) was added and the resulting brown suspension was stirred at 55°C for 10 h, then at RT for 5 days.

After adding NH₄Cl (626 mg, 11.70 mmol) and filtering the brown precipitate, the solvent was removed under reduced pressure to get a brown crude, which was purified by flash column chromatography (AcOEt-*n*-hexane, 7.5:2.5) to obtain **54** as a yellow oil (179 mg, 0.46 mmol).

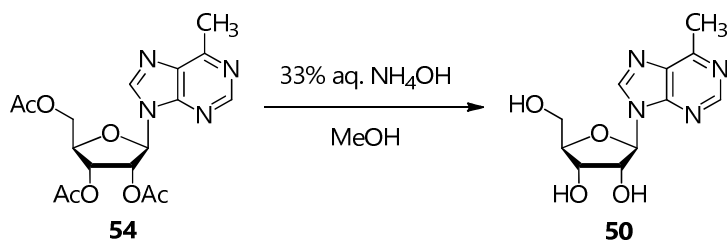
Yield: **81%**

*R*_f: 0.33 (AcOEt-*n*-hexane, 7.5:2.5)

¹H NMR (CDCl₃, 400 MHz): δ (ppm) 8.84 (s, 1H, H⁸), 8.61 (s, 1H, H²), 6.35 (d, *J* = 5.0 Hz, 1H, H^{1'}), 6.12 (ps t, *J* = 5.4 Hz, 1H, H^{2'}), 5.77 (ps t, *J* = 5.3 Hz, 1H, H^{3'}), 4.52-4.49 (m, 1H, H^{5'a}), 4.47 (q, *J* = 4.0 Hz, 1H, H^{4'}), 4.40 (dd, 1H, *J* = 12.9, 5.6 Hz, H^{5'b}), 2.85 (s, 3H, CH₃), 2.17 (s, 3H, CH₃CO), 2.08 (s, 3H, CH₃CO), 2.07 (s, 3H, CH₃CO).

MS (ESI⁺): *m/z* calcd for [C₁₇H₂₀N₄O₇]⁺: 392.13; found: 393.3 [M+H]⁺, 415.3 [M+Na]⁺, 807.2 [2M+Na]⁺.

7.2.2.13. 6-Methylinosine (50)

C₁₁H₁₄N₄O₄; MW 266.25

54 (166 mg, 0.42 mmol) was dissolved in MeOH (6.0 mL) under inert atmosphere and 33% aqueous NH₄OH (0.6 mL, 5.03 mmol) was added. The yellow solution was stirred at RT for 2 h 30'.

After removing the solvent under reduced pressure, the resulting crude was purified by flash column chromatography (CH₂Cl₂-MeOH, 9:1) to obtain **50** as a white solid (74 mg, 0.28 mmol).

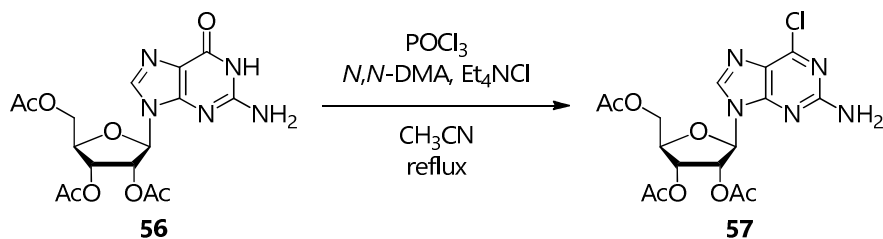
Yield: **66%**

R_f: 0.46 (CH₂Cl₂-MeOH, 9:1)

¹H NMR (DMSO-*d*₆, 400 MHz): δ (ppm) 8.80 (s, 1H, H²), 8.76 (s, 1H, H⁸), 6.02 (d, *J* = 5.7 Hz, 1H, H^{1'}), 5.52 (d, *J* = 6.0 Hz, 1H, OH^{2'}), 5.23 (d, *J* = 5.0 Hz, 1H, OH^{3'}), 5.12 (t, *J* = 5.6 Hz, 1H, OH^{5'}), 4.63 (dd, *J* = 11.0, 5.7 Hz, 1H, H²), 4.19 (dd, *J* = 8.6, 4.8 Hz, 1H, H^{3'}), 3.98 (q, *J* = 3.8 Hz, 1H, H^{4'}), 3.70 (dt, *J* = 11.9, 4.6 Hz, 1H, H^{5'a}), 3.58 (ddd, *J* = 11.9, 6.0, 4.1 Hz, 1H, H^{5'b}), 2.74 (s, 3H, CH₃).

¹³C NMR (DMSO-*d*₆, 100 MHz): δ (ppm) 158.8 (C⁶), 152.1 (C²), 150.5 (C⁴), 144.5 (C⁸), 133.4 (C⁵), 88.1 (C^{1'}), 86.1 (C^{4'}), 74.1 (C^{2'}), 70.8 (C^{3'}), 61.8 (C^{5'}), 19.6 (CH₃).

MS (ESI⁺): *m/z* calcd for [C₁₁H₁₄N₄O₄]⁺: 266.10; found: 267.3 [M+H]⁺, 289.2 [M+Na]⁺.

7.2.2.14. 6-Chloro-2',3',5'-tri-*O*-acetylguanosine (**57**)C₁₆H₁₈ClN₅O₇; MW 427.80

Under inert atmosphere, **56** (10.23 g, 24.99 mmol), *N,N*-DMA (3.16 mL, 24.93 mmol) and Et₄NCl (8.29 g, 50.03 mmol), pre-dried *in vacuo* over P₂O₅ at 80°C for 1 day, were dissolved in dry CH₃CN (50 mL). After stirring the mixture for 2', POCl₃ (13.7 mL, 146.98 mmol) was added dropwise and the resulting solution was refluxed and monitored by TLC (CH₂Cl₂-MeOH, 9.5:0.5) until complete disappearance of the reagent (35').

The solvent was removed under reduced pressure and the resulting yellow foam was dissolved in CHCl₃ (150 mL) and stirred vigorously with crushed ice for 15'. The layers were separated and the aqueous phase was extracted with CHCl₃ (4x50 mL). The combined organic phases were washed with cold H₂O (3x60 mL), 5% aqueous NaHCO₃ until neutralization (3x50 mL) and brine (2x50 mL), dried over Na₂SO₄, filtered and concentrated to half its starting volume. *i*-PrOH (60 mL) was added and the solution was slowly concentrated under reduced pressure to 40 mL, then stored at 4 °C overnight. The formed precipitate was filtered, washed with cold *i*-PrOH and recrystallized from *i*-PrOH to obtain **57** (8.10 g, 18.93 mmol) as white crystals.

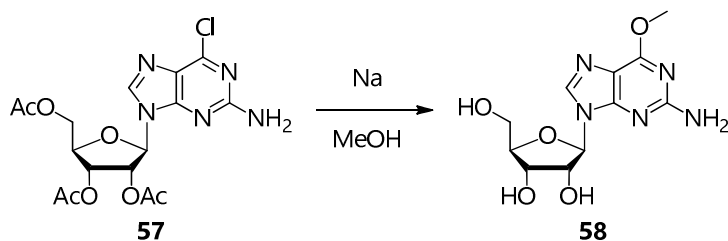
Yield: **76%**

*R*_f: 0.45 (CH₂Cl₂-MeOH, 9.5:0.5)

¹H NMR (CDCl₃, 400 MHz): δ (ppm) 7.89 (s, 1H, H⁸), 6.02 (d, *J* = 4.9 Hz, 1H, H¹), 5.97 (t, *J* = 5.1 Hz, 1H, H²), 5.76 (t, *J* = 4.97 Hz, 1H, H³), 5.25 (br s, 2H, N²H₂), 4.50-4.43 (m, 2H, H⁴, H^{5'a}), 4.42-4.36 (m, 1H, H^{5'b}), 2.16 (s, 3H, CH₃CO), 2.12 (s, 3H, CH₃CO), 2.10 (s, 3H, CH₃CO).

¹³C NMR (DMSO-*d*₆, 100 MHz): δ (ppm) 170.4, 169.5, 169.3 (CH₃CO), 159.1 (C²), 153.1 (C⁴), 152.0 (C⁶), 140.7 (C⁸), 125.9 (C⁵), 86.7 (C¹), 80.1 (C⁴), 72.8 (C²), 70.5 (C³), 62.9 (C⁵), 20.7, 20.5, 20.4 (CH₃CO).

MS (ESI⁺): *m/z* calcd for [C₁₆H₁₈ClN₅O₇]⁺: 427.09; found: 428.2 [M+H]⁺, 450.4 [M+Na]⁺.

7.2.2.15. 6-O-Methylguanosine (**58**)C₁₁H₁₅N₅O₅; MW 297.27

Na (35 mg, 1.52 mmol) was dissolved in MeOH (1.50 mL) under inert atmosphere and **57** (128 mg, 0.30 mmol) was added. The resulting transparent solution was stirred at RT for 23 h.

The solvent was removed under reduced pressure and the crude was purified by flash column chromatography (CH₂Cl₂-MeOH, 9.1:0.9) to obtain **58** as a white powder (51 mg, 0.17 mmol).

Yield: **57%**

R_f: 0.32 (CH₂Cl₂-MeOH, 9:1)

¹H NMR (CD₃OD, 400 MHz): δ (ppm) 8.04 (s, 1H, H⁸), 5.87 (d, *J* = 6.4 Hz, 1H, H^{1'}), 4.74 (dd, *J* = 6.2, 5.3 Hz, 1H, H^{2'}), 4.33 (dd, *J* = 5.2, 2.6 Hz, 1H, H^{3'}), 4.16 (q, *J* = 2.5 Hz, 1H, H^{4'}), 4.08 (s, 3H, OCH₃), 3.90 (dd, *J* = 12.4, 2.5 Hz, 1H, H^{5'a}), 3.76 (dd, *J* = 12.4, 2.7 Hz, 1H, H^{5'b}).

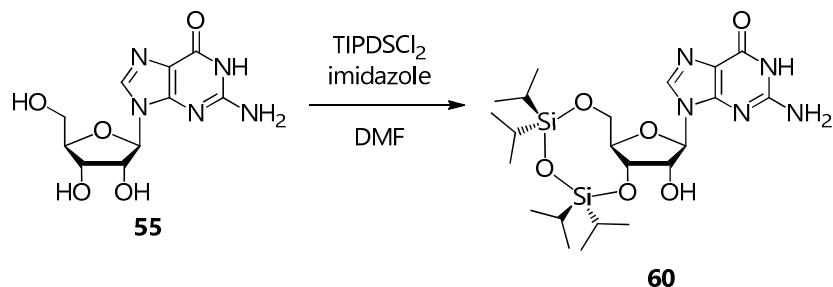
¹³C NMR (CD₃OD, 100 MHz): δ (ppm) 161.4 (C⁶), 160.0 (C²), 153.6 (C⁴), 139.2 (C⁸), 114.4 (C⁵), 87.7 (C^{1'}), 85.9 (C^{4'}), 73.6 (C^{2'}), 70.9 (C^{3'}), 61.9 (C^{5'}), 54.2 (CH₃).

HRMS (ESI-Q-ToF⁺): *m/z* calcd for [C₁₁H₁₅N₅O₅]⁺: 297.107; found: 320.177 [M+Na]⁺, 617.370 [2M+Na]⁺.

UV-Vis (CH₃OH): λ_{max} = 286 nm.

7.2.3. Synthesis of arabinosylguanine (**59**)7.2.3.1. 3',5'-*O*-Tetra-*i*-propyldisiloxanylguanosine (**60**)

$C_{22}H_{39}N_5O_6Si_2$; MW 525.75



TIPDSCl₂ (1.28 mL, 4.00 mmol) was added dropwise to a stirred suspension of **55** (1.13 g, 3.99 mmol) and imidazole (654 mg, 9.61 mmol) in dry DMF (11.8 mL) under inert atmosphere. The resulting mixture was stirred for 2 h 30' at RT, becoming a colourless solution.

Cold H₂O (15 mL) was added to the solution to precipitate **60** as a white powder, which was filtered, washed several times with cold H₂O and dried under reduced pressure (2.06 g, 3.92 mmol).

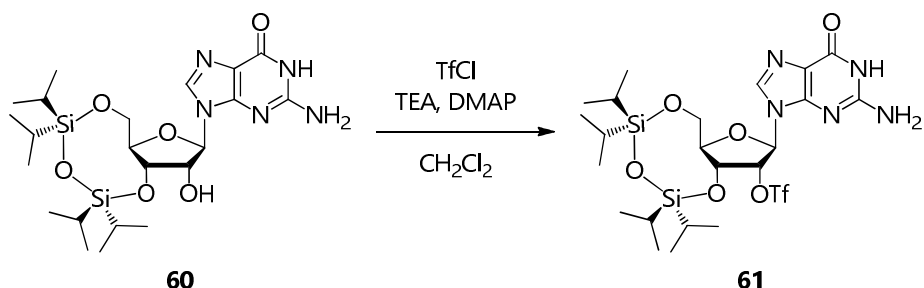
Yield: **98%**

*R*_f: 0.34 (CH₂Cl₂-MeOH, 9:1)

¹H NMR (DMSO-*d*₆, 400 MHz): δ (ppm) 10.64 (br s, 1H, N¹H), 7.76 (s, 1H, H⁸), 6.50 (br s, 2H, N²H₂), 5.68 (br d, *J* = 1.7 Hz, 1H, H^{1'}), 5.62 (d, *J* = 5.1 Hz, 1H, OH^{2'}), 4.35 (dd, *J* = 8.0, 5.1 Hz, 1H, H^{3'}), 4.26 (td, *J* = 5.1, 1.7 Hz, 1H, H^{2'}), 4.09 (dd, *J* = 12.8, 3.2 Hz, 1H, H^{5'a}), 3.99 (dt, *J* = 8.0, 2.9 Hz, 1H, H^{4'}), 3.93 (dd, *J* = 12.7, 2.7 Hz, 1H, H^{5'b}), 1.10-0.92 (m, 28H, CH(CH₃)₂).

¹³C NMR (DMSO-*d*₆, 100 MHz): δ (ppm) 157.1 (C⁶), 154.3 (C⁴), 151.0 (C²), 134.6 (C⁸), 117.2 (C⁵), 88.3 (C^{1'}), 81.5 (C^{4'}), 74.3 (C^{2'}), 70.1 (C^{3'}), 61.2 (C^{5'}), 17.8, 17.7, 17.6, 17.42, 17.35, 17.32, 17.27 (CH(CH₃)₂), 13.2, 12.9, 12.8, 12.5 (CH(CH₃)₂).

MS (ESI⁺): *m/z* calcd for [C₂₂H₃₉N₅O₆Si₂]⁺: 525.24; found: 526.7 [M+H]⁺, 548.8 [M+Na]⁺, 1051.7 [2M+H]⁺, 1073.8 [2M+Na]⁺.

7.2.3.2. 2'-*O*-Trifluoromethanesulfonyl-3',5'-*O*-tetra-*i*-propyldisiloxanylguanosine (**61**)C₂₃H₃₈F₃N₅O₈SSi₂; MW 657.81

60 (314 mg, 0.60 mmol), TEA (96 μ L, 0.69 mmol) and DMAP (85 mg, 0.70 mmol) were suspended in dry CH₂Cl₂ (3.9 mL) under inert atmosphere. The mixture was stirred at RT for 10' to form an opalescent colourless solution, which was cooled to 0°C, and TfCl (94 μ L, 0.88 mmol) was added dropwise. The resulting yellow transparent solution was allowed to warm to RT and stirred for 3 h at RT.

The mixture was diluted with H₂O (3.0 mL), then the organic phase was separated from the aqueous one and washed with 1 M HCl (2x5 mL). Both aqueous phases were extracted with CH₂Cl₂ (2x10 mL). The reunited organic phases were evaporated under reduced pressure and the resulting yellow crude was purified by flash column chromatography (CH₂Cl₂-MeOH, 9.5:0.5) to get **61** as a white solid (273 mg, 0.42 mmol).

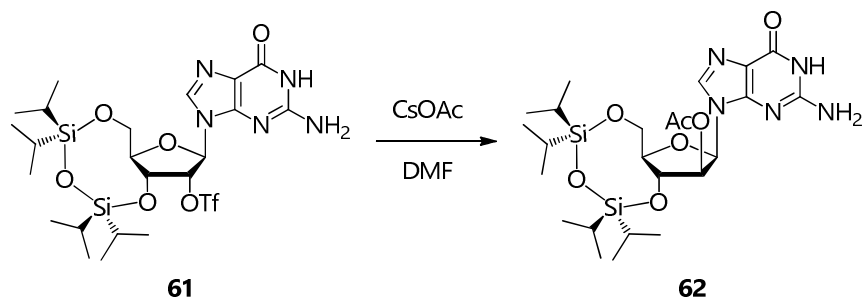
Yield: **69%**

R_f: 0.55 (CH₂Cl₂-MeOH, 9:1)

¹H NMR (DMSO-*d*₆, 400 MHz): δ (ppm) 10.75 (br s, 1H, N¹H), 7.81 (s, 1H, H⁸), 6.34 (br s, 2H, N²H₂), 6.13 (d, J = 1.2 Hz, 1H, H^{1'}), 5.94 (d, J = 5.0 Hz, 1H, H^{2'}), 4.77 (dd, J = 8.9, 5.1 Hz, 1H, H^{3'}), 4.10 (dd, J = 9.3, 4.0 Hz, 1H, H^{5'a}), 4.04-3.95 (m, 2H, H^{4'}, H^{5'b}), 1.26-0.92 (m, 28H, CH(CH₃)₂).

¹³C NMR (DMSO-*d*₆, 100 MHz): δ (ppm) 157.0 (C⁶), 154.4 (C²), 151.0 (C⁴), 135.5 (C⁸), 117.0 (q, J = 319.8 Hz, CF₃), 116.9 (C⁵), 89.2 (C^{2'}), 84.8 (C^{1'}), 81.2 (C^{4'}), 68.9 (C^{3'}), 60.5 (C^{5'}), 17.7, 17.6, 17.5, 17.4, 17.3, 17.18, 17.16 (CH(CH₃)₂), 13.1, 12.8, 12.7, 12.6 (CH(CH₃)₂).

MS (ESI⁺): m/z calcd for [C₂₃H₃₈F₃N₅O₈SSi₂]⁺: 657.19; found: 658.6 [M+H]⁺, 680.6 [2M+Na]⁺, 1315.2 [2M+H]⁺, 1337.3 [2M+Na]⁺.

7.2.3.3. 2'-*O*-Acetyl-3',5'-*O*-tetra-*i*-propyldisiloxanylarabinosylguanine (**62**)C₂₄H₄₁N₅O₇Si₂; MW 567.78

61 (323 mg, 0.49 mmol) was dissolved in dry DMF (4.5 mL) under inert atmosphere, then CsOAc (941 mg, 4.90 mmol) was added and the resulting pale yellow suspension was stirred at RT for 24 h, during which time it became dark orange.

After filtering the colourless precipitate, the brown solution was diluted with AcOEt (30 mL) and washed with H₂O (3x10 mL) until a colourless aqueous phase was obtained. The organic phase was dried over Na₂SO₄ and concentrated under reduced pressure. The pale orange crude was purified by flash column chromatography (CH₂Cl₂-MeOH, 9.4:0.6) to obtain **62** as a very pale yellow solid (154 mg, 0.27 mmol).

Yield: **55%**

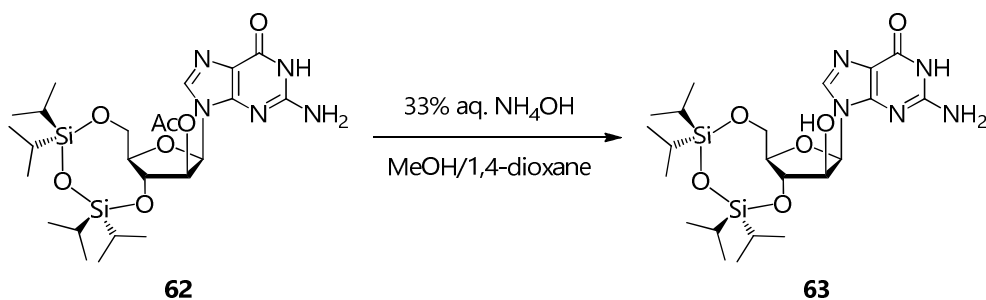
R_f: 0.53 (CH₂Cl₂-MeOH, 9:1)

¹H NMR (DMSO-*d*₆, 400 MHz): δ (ppm) 10.65 (br s, 1H, N¹H), 7.66 (s, 1H, H⁸), 6.50 (br s, 2H, N²H₂), 6.17 (d, *J* = 6.7 Hz, 1H, H^{1'}), 5.55 (br dd, *J* = 7.8, 7.0 Hz, 1H, H^{2'}), 4.57 (t, *J* = 8.3 Hz, 1H, H^{3'}), 4.09 (dd, *J* = 13.3, 4.0 Hz, 1H, H^{5'a}), 3.99-3.92 (m, 2H, H^{4'}, H^{5'b}), 1.75 (s, 3H, COCH₃), 1.16-0.91 (m, 28H, CH(CH₃)₂).

¹H NMR (CD₃OD, 400 MHz): δ (ppm) 7.87 (s, 1H, H⁸), 6.28 (d, *J* = 6.3 Hz, 1H, H^{1'}), 5.62 (dd, *J* = 8.0, 6.4 Hz, 1H, H^{2'}), 4.67 (t, *J* = 8.4 Hz, 1H, H^{3'}), 4.18 (dd, *J* = 13.2, 2.8 Hz, 1H, H^{5'a}), 4.13 (dd, *J* = 13.2, 2.9 Hz, 1H, H^{5'b}), 3.99 (dt, *J* = 8.6, 2.8 Hz, 1H, H^{4'}), 1.82 (s, 3H, COCH₃), 1.22-0.97 (m, 28H, CH(CH₃)₂).

¹³C NMR (CD₃OD, 100 MHz): δ (ppm) 169.7 (COCH₃), 157.9 (C⁶), 154.1 (C²), 151.5 (C⁴), 136.0 (C⁸), 115.9 (C⁵), 80.5 (C^{1'}), 80.2 (C^{4'}), 76.1 (C^{2'}), 71.4 (C^{3'}), 60.5 (C^{5'}), 18.8 (COCH₃), 16.50, 16.48, 16.4, 16.02, 15.97, 15.9 (CH(CH₃)₂), 13.3, 12.83, 12.81, 12.3 (CH(CH₃)₂).

MS (ESI+): *m/z* calcd for [C₂₄H₄₁N₅O₇Si₂]⁺: 567.25; found: 568.4 [M+H]⁺, 590.7 [M+Na]⁺, 1133.6 [2M-H]⁺, 1157.5 [2M+Na]⁺.

7.2.3.4. 3',5'-*O*-Tetra-*i*-propyldisiloxanylarabinosylguanine (**63**)C₂₂H₃₉N₅O₆Si₂; MW 525.75

33% aqueous NH₄OH (1.04 mL, 8.81 mmol) was added dropwise to a solution of **62** (149 mg, 0.26 mmol) in a 5:2 MeOH/1,4-dioxane mixture (2.40 mL). A white precipitate was immediately formed. The resulting suspension was stirred at RT for 24 h, during which time it became a yellow solution.

The solvent was removed under reduced pressure and **63** was isolated from the resulting dark yellow crude by flash column chromatography (CH₂Cl₂-MeOH, 9:1) as a pale yellow solid (109 mg, 0.21 mmol).

Yield: **80%**

R_f: 0.32 (CH₂Cl₂-MeOH, 9:1)

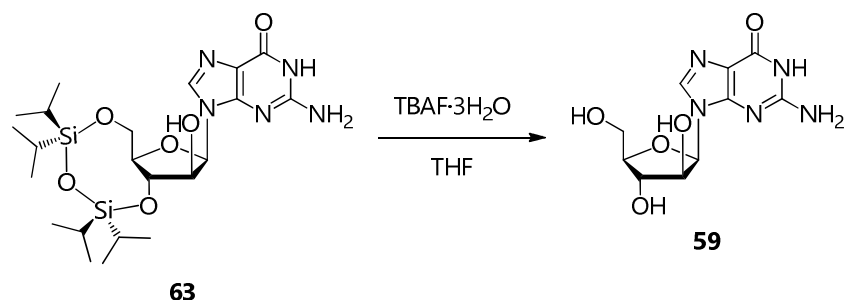
¹H NMR (DMSO-*d*₆, 400 MHz): δ (ppm) 10.59 (br s, 1H, N¹H), 7.61 (s, 1H, H⁸), 6.46 (br s, 2H, N²H₂), 5.96 (d, *J* = 6.5 Hz, 1H, H^{1'}), 5.79 (d, *J* = 5.9 Hz, 1H, OH^{2'}), 4.43 (dd, *J* = 13.3, 6.7 Hz, 1H, H^{2'}), 4.31 (t, *J* = 7.8 Hz, 1H, H^{3'}), 3.98 (dd, *J* = 12.8, 3.7 Hz, 1H, H^{5'a}), 3.92 (dd, *J* = 12.8, 2.5 Hz, 1H, H^{5'b}), 3.78-3.72 (m, 1H, H^{4'}), 1.21-1.05 (m, 28H, CH(CH₃)₂).

¹H NMR (CD₃OD, 400 MHz): δ (ppm) 7.85 (br s, 1H, H⁸), 6.13 (d, *J* = 5.6 Hz, 1H, H^{1'}), 4.47 (t, *J* = 6.2 Hz, 1H, H^{2'}), 4.43 (t, *J* = 6.9 Hz, 1H, H^{3'}), 4.10 (dd, *J* = 12.7, 3.3 Hz, 1H, H^{5'a}), 4.04 (dd, *J* = 12.7, 4.2 Hz, 1H, H^{5'b}), 3.85 (dt, *J* = 7.3, 3.8 Hz, 1H, H^{4'}), 1.21-0.87 (m, 28H, CH(CH₃)₂).

¹³C NMR (CD₃OD, 100 MHz): δ (ppm) 158.0 (C⁶), 154.0 (C²), 151.7 (C⁴), 137.4 (C⁸), 115.7 (C⁵), 82.5 (C^{1'}), 81.0 (C^{4'}), 75.7 (C^{2'}, C^{3'}), 61.6 (C^{5'}), 16.54, 16.50, 16.4, 16.13, 16.08, 16.0 (CH(CH₃)₂), 13.4, 13.0, 12.9, 12.4 (CH(CH₃)₂).

MS (ESI+): *m/z* calcd for [C₂₂H₃₉N₅O₆Si₂]⁺: 525.24; found: 526.5 [M+H]⁺, 548.6 [M+Na]⁺, 1051.3 [2M+H]⁺, 1073.5 [2M+Na]⁺.

7.2.3.5. Arabinosylguanine (59)

C₁₀H₁₃N₅O₅; MW 283.24

TBAF·3H₂O (48 mg, 152 μmol) was added to a solution of **63** (38 mg, 72 μmol) in THF (0.53 mL). The resulting yellow opaque solution was stirred at RT for 30' to precipitate a light grey glass.

The solvent was removed under reduced pressure and the brown crude was purified by semi-preparative HPLC to get **59** as a white powder (13.6 mg, 48 μmol).

Yield: **67%**

Time (min)	Column volumes	% A (H ₂ O)	% B (MeOH)
0 - 2	0.5	97	3
2 - 18	4	97 → 0	3 → 100
18 - 20	1	0	100

HPLC t_R: 19.8' (39.4% B)

R_f: 0.83 (EtOH-H₂O, 7:3)

¹H NMR (DMSO-*d*₆, 400 MHz): δ (ppm) 10.59 (br s, 1H, N¹H), 7.76 (s, 1H, H⁸), 6.50 (br s, 2H, N²H₂), 6.02 (d, *J* = 4.6 Hz, 1H, H^{1'}), 5.62 (br d, *J* = 5.1 Hz, 1H, OH^{2'}), 5.50 (d, *J* = 4.0 Hz, 1H, OH^{3'}), 5.06 (br t, *J* = 4.5 Hz, 1H, OH^{5'}), 4.07 (dd, *J* = 7.9, 4.0 Hz, 1H, H^{3'}), 4.03 (dd, *J* = 9.3, 4.7 Hz, 1H, H^{2'}), 3.74 (dd, *J* = 8.9, 4.4 Hz, 1H, H^{4'}), 3.65 (dd, *J* = 11.7, 4.3 Hz, 1H, H^{5'a}), 3.59 (dd, *J* = 11.7, 5.3 Hz, 1H, H^{5'b}).

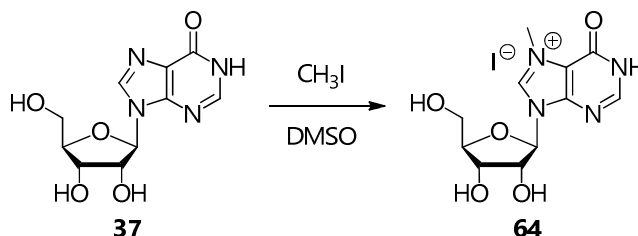
¹³C NMR (DMSO-*d*₆, 100 MHz): δ (ppm) 157.3 (C⁶), 154.1 (C²), 151.5 (C⁴), 137.3 (C⁸), 116.3 (C⁵), 84.7 (C^{4'}), 83.8 (C^{1'}), 75.9 (C^{2'}), 75.8 (C^{3'}), 61.4 (C^{5'}).

MS (ESI⁺): *m/z* calcd for [C₁₀H₁₃N₅O₅]⁺: 283.09; found: 284.17 [M+H]⁺, 306.17 [M+Na]⁺, 589.17 [2M+Na]⁺, 1155.0 [4M+Na]⁺.

7.2.4. Synthesis of 7-methylpurine and 7-methylguanine nucleoside iodides (64-67)

7.2.4.1. 7-Methylinosine iodide (64)

$C_{11}H_{15}IN_4O_5$; MW 410.17



CH_3I (1.80 mL, 28.91 mmol) was added dropwise to a solution of **37** (805 mg, 3.00 mmol) in dry DMSO (8.7 mL) under inert atmosphere. The resulting colourless solution was protected from light exposure and stirred at RT for 24 h, during which time the solution slowly turned to dark red and then brown. The disappearance of the substrate was monitored by TLC (EtOH- H_2O , 7:3; R_f = 0.80).

The solution was cooled to 0°C and diluted with $CHCl_3$ (75 mL) to precipitate a dark orange syrup. The supernatant was discarded and the syrup was ground in acetone to precipitate **64** as a white powder, which was filtered, washed with few cold acetone, dried under reduced pressure and stored at -20°C (825 mg, 2.01 mmol).

Yield: **67%**

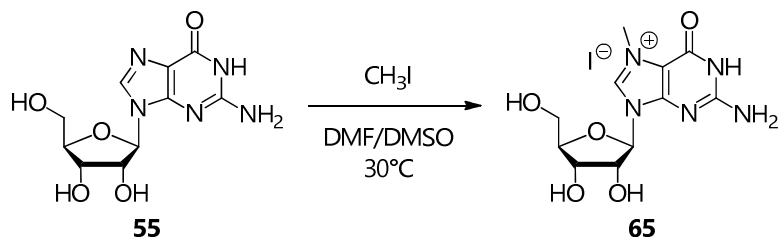
R_f : 0.23 (EtOH- H_2O , 4:1)

1H NMR (DMSO- d_6 , 400 MHz): δ (ppm) 13.50 (br s, 1H, N^1H), 9.68 (s, 1H, H^8), 8.46 (s, 1H, H^2), 6.03 (d, J = 3.1 Hz, 1H, $H^{1'}$), 5.80 (br d, J = 4.9 Hz, 1H, $OH^{2'}$), 5.34 (br d, J = 5.4 Hz, 1H, $OH^{3'}$), 5.16 (br t, J = 4.8 Hz, 1H, $OH^{5'}$), 4.43 (dd, J = 7.7, 4.5 Hz, 1H, $H^{2'}$), 4.17 (dd, J = 10.1, 5.2 Hz, 1H, $H^{3'}$), 4.13 (s, 3H, CH_3), 4.06 (dt, J = 6.2, 3.3 Hz, 1H, $H^{4'}$), 3.78 (dd, J = 12.3, 3.1 Hz, 1H, $H^{5'a}$), 3.65 (dd, J = 12.3, 3.6 Hz, 1H, $H^{5'b}$).

^{13}C NMR (DMSO- d_6 , 100 MHz): δ (ppm) 153.5 (C^6), 150.6 (C^2), 146.3 (C^4), 139.4 (C^8), 116.1 (C^5), 90.7 ($C^{1'}$), 86.3 ($C^{4'}$), 75.0 ($C^{2'}$), 69.4 ($C^{3'}$), 60.6 ($C^{5'}$), 36.6 (CH_3).

MS (ESI $^+$): m/z calcd for $[C_{11}H_{15}N_4O_5]^+$: 283.10; found: 283.0 $[M]^+$, 305.1 $[M+Na]^+$, 565.3 $[2M-H]^+$.

MS (ESI $^-$): m/z calcd for $[I]^-$: 126.91; found: 127.2 $[I]^-$.

7.2.4.2. 7-Methylguanosine iodide (**65**)C₁₁H₁₆IN₅O₅; MW 425.18

CH₃I (0.13 mL, 2.09 mmol) was added dropwise to a suspension of **55** (200 mg, 0.71 mmol) at 30°C in a dry 3:1 DMF/DMSO mixture (2.0 mL) under inert atmosphere. The resulting colourless solution was protected from light exposure and stirred at 30°C for 4 h, during which time the solution slowly turned to brown. The disappearance of the substrate was monitored by TLC (EtOH-H₂O, 7:3; R_f = 0.79).

The solution was diluted with H₂O (50 mL) and freeze-dried twice to get a very dense brown oil. Acetone (20 mL) was added, the resulting mixture was cooled to 0°C and sonicated to get **65** as a white powder, which was filtered, washed with few cold acetone, dried under reduced pressure and stored at -20°C (263 mg, 0.62 mmol).

Yield: **87%**

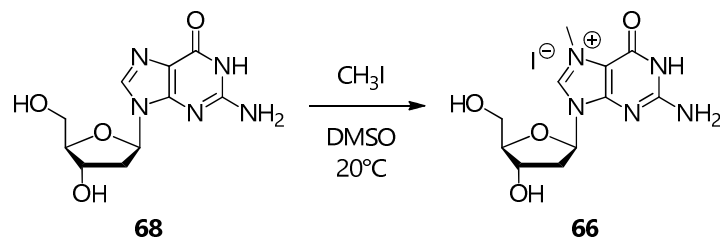
R_f: 0.18 (EtOH-H₂O, 4:1)

¹H NMR (DMSO-*d*₆, 400 MHz): δ (ppm) 11.74 (br s, 1H, N¹H), 9.35 (s, 1H, H⁸), 7.22 (br s, 2H, N²H₂), 5.84 (d, *J* = 3.9 Hz, 1H, H^{1'}), 5.64 (br d, *J* = 5.1 Hz, 1H, OH^{2'}), 5.33 (d, *J* = 5.4 Hz, 1H, OH^{3'}), 5.12 (t, *J* = 5.1 Hz, 1H, OH^{5'}), 4.37 (dd, *J* = 8.5, 4.3 Hz, 1H, H^{2'}), 4.16 (dd, *J* = 10.0, 5.1 Hz, 1H, H^{3'}), 4.05-3.97 (m, 4H, H^{4'}, CH₃), 3.72 (dt, *J* = 11.8, 3.9 Hz, 1H, H^{5'a}), 3.61 (dt, *J* = 9.0, 4.3 Hz, 1H, H^{5'b}).

¹³C NMR (DMSO-*d*₆, 100 MHz): δ (ppm) 156.1 (C²), 153.8 (C⁶), 149.7 (C⁴), 136.8 (C⁸), 108.1 (C⁵), 89.2 (C^{1'}), 86.2 (C^{4'}), 74.7 (C^{2'}), 69.8 (C^{3'}), 60.9 (C^{5'}), 36.3 (CH₃).

MS (ESI⁺): *m/z* calcd for [C₁₁H₁₆N₅O₅]⁺: 298.11; found: 297.5 [M-H]⁺, 298.1 [M]⁺, 595.2 [2M-H]⁺, 894.3 [3M-2H]⁺.

MS (ESI⁻): *m/z* calcd for [I]⁻: 126.91; found: 127.2 [I]⁻.

7.2.4.3. 7-Methyl-2'-deoxyguanosine iodide (**66**)C₁₁H₁₆IN₅O₄; MW 409.18

CH₃I (0.26 mL, 4.18 mmol) was added to a solution of **68** (160 mg, 0.60 mmol) in dry DMSO (1.20 mL) under inert atmosphere. The resulting colourless mixture was protected from light exposure and stirred at 20°C for 3 h 30', during which time it turned brown-red. More CH₃I (37 μL, 0.59 mmol) was added and the mixture was stirred at 20°C for 1 h. Throughout the reaction, the disappearance of the substrate was monitored by TLC (EtOH-H₂O, 4:1; R_f = 0.80).

Cold CHCl₃ (15 mL) was added to precipitate a pale yellow powder and the suspension was decanted at 0°C for 2 h. The precipitate was filtered, washed with few cold CHCl₃ and dried under reduced pressure to obtain **66** as a pale yellow powder, which was stored at -20°C (197 mg, 0.48 mmol).

Yield: **80%**

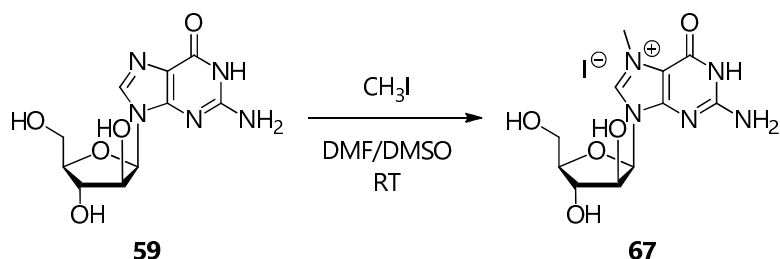
R_f: 0.21 (EtOH-H₂O, 4:1)

¹H NMR (DMSO-d₆, 400 MHz): δ (ppm) 11.67 (s, 1H, N¹H), 9.28 (s, 1H, H⁸), 7.18 (br s, 2H, N²H₂), 6.20 (t, J = 6.0 Hz, 1H, H^{1'}), 5.40 (br s, 1H, OH^{3'}), 4.98 (br s, 1H, OH^{5'}), 4.37 (dd, J = 9.1, 4.6 Hz, 1H, H^{3'}), 4.00 (s, 3H, CH₃), 3.93 (q, J = 3.9 Hz, 1H, H^{4'}), 3.62 (dd, J = 12.1, 4.2 Hz, 1H, H^{5'a}), 3.57 (dd, J = 12.1, 4.2 Hz, 1H, H^{5'b}), 2.55-2.47 (m, 1H, H^{2'a}), 2.40 (ddd, J = 13.4, 6.2, 4.8 Hz, 1H, H^{2'b}).

¹³C NMR (DMSO-d₆, 100 MHz): δ (ppm) 156.0 (C²), 153.9 (C⁶), 149.3 (C⁴), 136.7 (C⁸), 108.1 (C⁵), 89.1 (C^{4'}), 85.8 (C^{1'}), 70.2 (C^{3'}), 61.3 (C^{5'}), 40.5 (C^{2'}), 36.1 (CH₃).

MS (ESI⁺): m/z calcd for [C₁₁H₁₆N₅O₄]⁺: 282.12; found: 280.8 [M-H]⁺, 282.1 [M]⁺, 304.1 [M-H+Na]⁺, 305.3 [M+Na]⁺, 563.0 [2M-H]⁺, 563.7 [2M]⁺, 585.5 [2M-2H+Na]⁺.

MS (ESI⁻): m/z calcd for [I]⁻: 126.91; found: 127.2 [M]⁻.

7.2.4.4. 7-Methylarabinofuranosylguanine iodide (**67**)C₁₁H₁₆IN₅O₅; MW 425.18

CH₃I (0.14 mL, 2.25 mmol) was added to a solution of **59** (100 mg, 0.35 mmol) in a dry 3:1 DMF/DMSO mixture (0.96 mL) under inert atmosphere. The resulting colourless mixture was protected from light exposure and stirred at RT for 6 h, during which time it turned yellow. The disappearance of the substrate was monitored by TLC (EtOH-H₂O, 7:3; *R_f* = 0.83).

The solution was diluted with H₂O (50 mL) and freeze-dried until complete removal of DMSO. The resulting pale yellow crude was suspended in dry acetone (2.5 mL), filtered, washed with few cold dry acetone and dried under reduced pressure to obtain **67** as an off-white powder, which was stored at -20°C (133 mg, 0.31 mmol).

Yield: **89%**

R_f: 0.53 (EtOH-H₂O, 7:3)

¹H NMR (DMSO-*d*₆, 400 MHz): δ (ppm) 11.68 (br s, 1H, N¹H), 9.22 (s, 1H, H⁸), 7.21 (br s, 2H, N²H₂), 6.17 (d, *J* = 4.3 Hz, 1H, H^{1'}), 5.82 (d, *J* = 5.3 Hz, 1H, OH^{2'}), 5.64 (d, *J* = 4.3 Hz, 1H, OH^{3'}), 5.04 (t, *J* = 5.4 Hz, 1H, OH^{5'}), 4.17 (dd, *J* = 8.6, 4.4 Hz, 1H, H^{2'}), 4.11 (dd, *J* = 7.5, 3.7 Hz, 1H, H^{3'}), 4.06 (s, 3H, CH₃), 3.90 (dd, *J* = 8.9, 5.1 Hz, 1H, H^{4'}), 3.70 (dd, *J* = 11.5, 5.0 Hz, 1H, H^{5'a}), 3.64 (dd, *J* = 11.6, 5.4 Hz, 1H, H^{5'b}).

¹³C NMR (DMSO-*d*₆, 100 MHz): δ (ppm) 156.2 (C²), 153.8 (C⁶), 149.6 (C⁴), 137.8 (C⁸), 107.6 (C⁵), 86.5 (C^{4'}), 86.0 (C^{1'}), 75.5 (C^{2'}), 75.4 (C^{3'}), 61.3 (C^{5'}), 36.1 (CH₃).

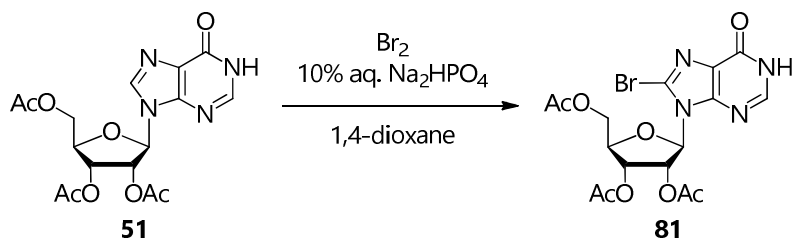
MS (ESI⁺): *m/z* calcd for [C₁₁H₁₆N₅O₅]⁺: 298.11; found: 297.1 [M-H]⁺, 298.0 [M]⁺, 319.9 [M-H+Na]⁺, 594.9 [2M-H]⁺, 617.0 [2M-2H+Na]⁺, 1192.1 [4M]⁺.

MS (ESI⁻): *m/z* calcd for [I]⁻: 126.91; found: 127.1 [M]⁻.

7.2.5. Synthesis of 8-substituted inosines, guanosines and adenosines (69-80)

7.2.5.1. 8-Bromo-2',3',5'-tri-*O*-acetylribose (81)

$C_{16}H_{17}BrN_4O_8$; MW 473.23



51 (3.40 g, 8.62 mmol) was suspended in 1,4-dioxane (130 mL) under inert atmosphere and decanted solutions of Br_2 (1.60 mL) in 10% aqueous Na_2HPO_4 (70 mL) were added at 0, 24, 48, 72, 96 and 120 h, during which time the mixture was protected from light exposure and stirred at RT. At 8 days, the resulting red solution was decolorized with NaHSO_3 and extracted with CH_2Cl_2 (3x120 mL). The reunited organic phases were dried over Na_2SO_4 and evaporated under reduced pressure, and the resulting crude was purified by flash column chromatography (CH_2Cl_2 -MeOH, 9.5:0.5) to obtain **81** as a white powder (3.39 g, 7.16 mmol).

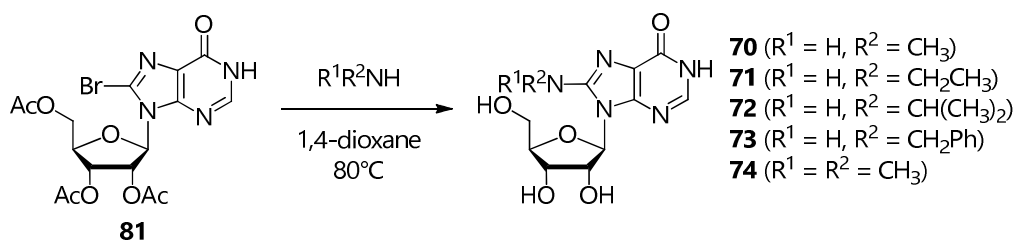
Yield: **83%**

R_f : 0.59 (CH_2Cl_2 -MeOH, 9:1) or 0.93 (CH_2Cl_2 -MeOH, 4:1)

$^1\text{H NMR}$ (CDCl_3 , 400 MHz): δ (ppm) 12.76 (br s, 1H, N^1H), 8.17 (s, 1H, H^2), 6.24 (dd, $J = 6.0, 4.8$ Hz, 1H, H^2), 6.12 (d, $J = 4.7$ Hz, 1H, H^1), 5.79 (t, $J = 5.9$ Hz, 1H, H^3), 4.51 (dd, $J = 11.7, 3.6$ Hz, 1H, H^{5a}), 4.40 (td, $J = 5.8, 3.7$ Hz, 1H, H^4), 4.33 (dd, $J = 11.7, 6.1$ Hz, 1H, H^{5b}), 2.17 (s, 3H, CH_3CO), 2.12 (s, 3H, CH_3CO), 2.08 (s, 3H, CH_3CO).

$^{13}\text{C NMR}$ (CDCl_3 , 100 MHz): δ (ppm) 170.5, 169.5, 169.4 (CH_3CO), 157.5 (C^6), 149.8 (C^4), 145.3 (C^2), 126.6 (C^8), 125.8 (C^5), 88.8 (C^1), 80.2 (C^4), 72.1 (C^2), 70.3 (C^3), 63.0 (C^5), 20.7, 20.5, 20.4 (CH_3CO).

MS (ESI) $^+$: m/z calcd for $[\text{C}_{16}\text{H}_{17}^{79}\text{BrN}_4\text{O}_8]^+$: 472.02; found: 237.1 [^{79}Br]M-(2',3',5'-tri-*O*-acetylribose)+ Na^+ , 239.0 [^{81}Br]M-(2',3',5'-tri-*O*-acetylribose)+ Na^+ , 494.9 [^{79}Br]M+ Na^+ , 496.9 [^{81}Br]M+ Na^+ , 966.7 [2^{79}Br]M+ Na^+ , 968.8 [^{79}Br]M+ ^{81}Br]M+ Na^+ , 970.8 [2^{81}Br]M+ Na^+ .

7.2.5.2. General procedure for the synthesis of 8-alkylaminoinosines (**70**, **71**, **72**, **73** and **74**)

The appropriate amine or amine solution (13.98 mmol for **70**, 14.21 mmol for **71**, 37.48 mmol for **72**, 5.58 mmol for **73** and 11.95 mmol for **74**) was added to a solution of **81** (189 mg, 0.40 mmol) in dry 1,4-dioxane (0.90 mL) under inert atmosphere. The resulting mixture was stirred at 80°C and monitored by TLC (CH_2Cl_2 -MeOH, 4:1 for **70**, **71** and **72** and 9:1 for **73**) or analytical HPLC (for **74**) until complete consumption of the starting material and formation of the product (between 1 and 15 days).

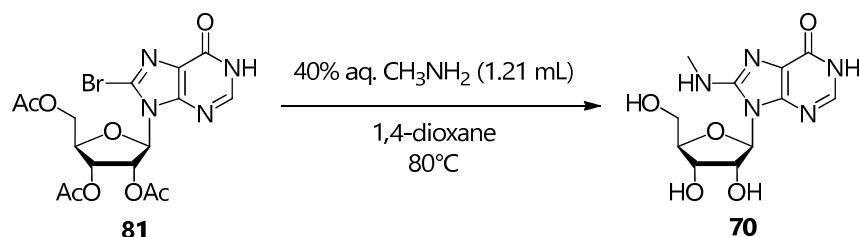
70, **71**, **72** and **74**: The solvent was removed under reduced pressure and the crude was purified by semi-preparative HPLC.

73: The mixture was concentrated under reduced pressure to get a dark orange oil residue. *n*-Hexane (25 mL) was added, the two-phase mixture was stirred at RT for 10' and the upper layer was removed. Et_2O (25 mL) was added to precipitate a very dense brown syrup, which was sonicated to form an ochre powder, then the yellow supernatant was discarded. The procedure was repeated four times, until the organic phase became colourless and no more amine was detected by TLC (CH_2Cl_2 /MeOH, 9:1). The residue was evaporated under reduced pressure and the light orange crude was purified by semi-preparative HPLC.

Time (min)	Column volumes	% A (H_2O)	% B (MeOH)
0 - 2	0.5	97	3
2 - 30	7	97 → 0	3 → 100
30 - 32	0.5	0	100

7.2.5.2.1. 8-Methylaminoinosine (**70**)

$C_{11}H_{15}N_5O_5$; MW 297.27



White powder (96 mg, 0.32 mmol).

Yield: **81%**

R_f : 0.18 (CH_2Cl_2 -MeOH, 4:1)

HPLC t_R : 17.8' (48.1% B)

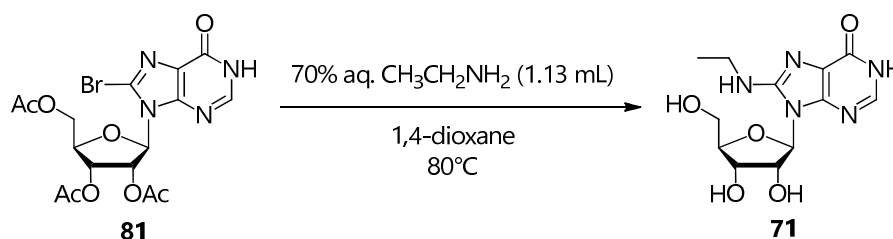
^1H NMR (DMSO- d_6 , 400 MHz): δ (ppm) 12.08 (br s, 1H, N^1H), 7.82 (s, 1H, H^2), 6.81 (q, $J = 4.5$ Hz, 1H, N^8H), 5.86 (d, $J = 7.3$ Hz, 1H, H^1), 5.68 (t, $J = 4.6$ Hz, 1H, $\text{OH}^{5'}$), 5.29 (d, $J = 6.5$ Hz, 1H, $\text{OH}^{2'}$), 5.13 (d, $J = 4.3$ Hz, 1H, $\text{OH}^{3'}$), 4.57 (dd, $J = 12.6, 6.7$ Hz, 1H, $\text{H}^{2'}$), 4.13-4.08 (m, 1H, $\text{H}^{3'}$), 3.96 (q, $J = 2.3$ Hz, 1H, $\text{H}^{4'}$), 3.68-3.62 (m, 2H, $\text{H}^{5'a}, \text{H}^{5'b}$), 2.84 (d, $J = 4.6$ Hz, 3H, NHCH_3).

^{13}C NMR (DMSO- d_6 , 100 MHz): δ (ppm) 156.3 (C^6), 152.2 (C^8), 148.5 (C^4), 143.1 (C^2), 122.6 (C^5), 87.4 (C^1), 86.4 ($\text{C}^{4'}$), 71.7 ($\text{C}^{3'}$), 71.3 ($\text{C}^{2'}$), 62.2 ($\text{C}^{5'}$), 29.8 (NHCH_3).

MS (ESI $^+$): m/z calcd for $[\text{C}_{11}\text{H}_{15}\text{N}_5\text{O}_5]^+$: 297.11; found: 166.1 $[\text{M-ribose}+\text{H}]^+$, 188.1 $[\text{M-ribose}+\text{Na}]^+$, 298.1 $[\text{M}+\text{H}]^+$, 320.1 $[\text{M}+\text{Na}]^+$, 617.1 $[\text{2M}+\text{Na}]^+$.

7.2.5.2.2. 8-Ethylaminoinosine (71)

$\text{C}_{12}\text{H}_{17}\text{N}_5\text{O}_5$; MW 311.29



White powder (98 mg, 0.31 mmol).

Yield: **78%**

R_f : 0.28 (CH_2Cl_2 -MeOH, 4:1)

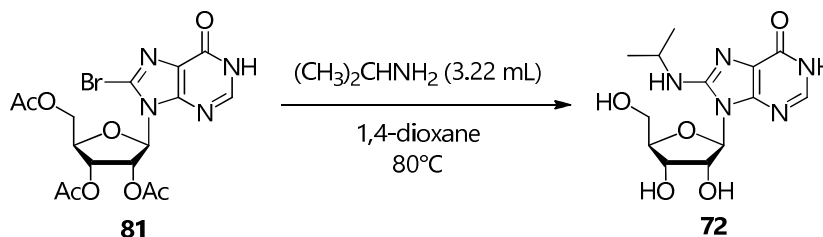
HPLC t_R : 19.3' (53.0% B)

^1H NMR (CD $_3$ OD, 300 MHz): δ (ppm) 7.84 (s, 1H, H^2), 6.06 (d, $J = 7.2$ Hz, 1H, H^1), 4.68 (dd, $J = 7.6, 5.8$ Hz, 1H, H^2), 4.27 (dd, $J = 5.8, 1.8$ Hz, 1H, $\text{H}^{3'}$), 4.10 (br d, $J = 1.8$ Hz, 1H, $\text{H}^{4'}$), 3.87-3.76 (m, 2H, $\text{H}^{5'a}, \text{H}^{5'b}$), 3.42 (ddd, $J = 14.4, 7.0, 3.7$ Hz, 2H, NHCH_2), 1.24 (t, $J = 7.3$ Hz, 3H, CH_3).

^1H NMR (DMSO- d_6 , 400 MHz): δ (ppm) 12.06 (br s, 1H, N^1H), 7.81 (s, 1H, H^2), 6.79 (t, $J = 5.3$ Hz, 1H, N^8H), 5.88 (d, $J = 7.4$ Hz, 1H, H^1), 5.64 (br t, $J = 4.2$ Hz, 1H, $\text{OH}^{5'}$), 5.27 (d, $J = 6.3$ Hz, 1H, $\text{OH}^{2'}$), 5.12 (br d, $J = 3.2$ Hz, 1H, $\text{OH}^{3'}$), 4.57 (q, $J = 6.2$ Hz, 1H, $\text{H}^{2'}$), 4.15-4.09 (m, 1H, $\text{H}^{3'}$), 3.96 (br q, $J = 2.2$ Hz, 1H, $\text{H}^{4'}$), 3.69-3.62 (m, 2H, $\text{H}^{5'a}, \text{H}^{5'b}$), 3.40-3.24 (m, 2H, NHCH_2), 1.17 (t, $J = 7.2$ Hz, 3H, CH_3).

^{13}C NMR (DMSO- d_6 , 100 MHz): δ (ppm) 155.9 (C^6), 151.1 (C^8), 148.0 (C^4), 142.6 (C^2), 122.2 (C^5), 87.1 (C^1), 86.0 ($\text{C}^{4'}$), 71.2 ($\text{C}^{3'}$), 71.0 ($\text{C}^{2'}$), 61.8 ($\text{C}^{5'}$), 37.5 (NHCH_2), 15.1 (CH_3).

MS (ESI $^+$): m/z calcd for $[\text{C}_{12}\text{H}_{17}\text{N}_5\text{O}_5]^+$: 311.12; found: 180.4 $[\text{M-ribose}+\text{H}]^+$, 202.2 $[\text{M-ribose}+\text{Na}]^+$, 334.2 $[\text{M}+\text{Na}]^+$, 645.1 $[\text{2M}+\text{Na}]^+$.

7.2.5.2.3. 8-*i*-Propylaminoinosine (72)C₁₃H₁₉N₅O₅; MW 325.32

White powder (23 mg, 0.07 mmol).

Yield: 18%

R_f: 0.32 (CH₂Cl₂-MeOH, 4:1)HPLC *t_R*: 19.1' (52.2% B)

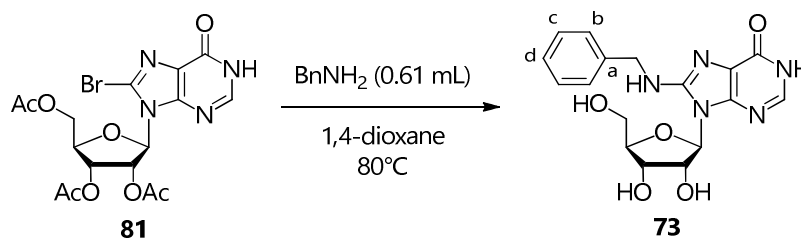
¹H NMR (CD₃OD, 300 MHz): δ (ppm) 7.83 (s, 1H, H²), 6.06 (d, *J* = 7.7 Hz, 1H, H^{1'}), 4.67 (dd, *J* = 7.2, 5.7 Hz, 1H, H^{2'}), 4.26 (dd, *J* = 5.8, 1.8 Hz, 1H, H^{3'}), 4.18-4.06 (m, 2H, NHCH, H^{4'}), 3.87-3.76 (m, 2H, H^{5'a}, H^{5'b}), 1.24 (d, *J* = 6.7 Hz, 6H, CH(CH₃)₂).

¹H NMR (DMSO-*d*₆, 400 MHz): δ (ppm) 12.01 (br s, 1H, N¹H), 7.81 (s, 1H, H²), 6.59 (d, *J* = 7.6 Hz, 1H, N⁸H), 5.89 (d, *J* = 7.4 Hz, 1H, H^{1'}), 5.63 (br s, 1H, OH^{5'}), 5.48-4.96 (m, 2H, OH^{2'}, OH^{3'}), 4.54 (dd, *J* = 7.1, 5.8 Hz, 1H, H^{2'}), 4.12 (dd, *J* = 5.5, 2.0 Hz, 1H, H^{3'}), 4.07-3.97 (m, 1H, NHCH), 3.95 (br q, *J* = 2.1 Hz, 1H, H^{4'}), 3.71-3.61 (m, 2H, H^{5'a}, H^{5'b}), 1.20 (d, *J* = 3.5 Hz, 3H, CH(CH₃)₂), 1.18 (d, *J* = 3.4 Hz, 3H, CH(CH₃)₂).

¹³C NMR (DMSO-*d*₆, 100 MHz): δ (ppm) 155.9 (C⁶), 150.5 (C⁸), 147.9 (C⁴), 142.5 (C²), 122.2 (C⁵), 87.0 (C^{1'}), 86.0 (C^{4'}), 71.2 (C^{3'}), 70.9 (C^{2'}), 61.8 (C^{5'}), 44.4 (NHCH), 23.1, 22.8 (CH(CH₃)₂).

MS (ESI⁺): *m/z* calcd for [C₁₃H₁₉N₅O₅]⁺: 325.14; found: 326.0 [M+H]⁺, 348.2 [M+Na]⁺, 673.1 [2M+Na]⁺.

7.2.5.2.5. 8-Benzylaminoinosine (73)

C₁₇H₁₉N₅O₅; MW 373.36

White powder (123 mg, 0.33 mmol).

Yield: 83%

R_f: 0.13 (CH₂Cl₂-MeOH, 9:1)HPLC *t_R*: 21.6' (60.8% B)

¹H NMR (CD₃OD, 400 MHz): δ (ppm) 7.86 (s, 1H, H²), 7.43-7.19 (m, 5H, C₆H₅), 6.12 (d, J = 7.5 Hz, 1H, H^{1'}), 4.74 (dd, J = 7.5, 5.6 Hz, 1H, H^{2'}), 4.68 (d, J = 15.3 Hz, 1H, NHCH^a), 4.59 (d, J = 15.3 Hz, 1H, NHCH^b), 4.29 (dd, J = 5.6, 2.0 Hz, 1H, H^{3'}), 4.14 (br q, J = 2.0 Hz, 1H, H^{4'}), 3.82 (dd, J = 11.8, 2.3 Hz, 1H, H^{5'a}), 3.78 (dd, J = 11.8, 1.9 Hz, 1H, H^{5'b}).

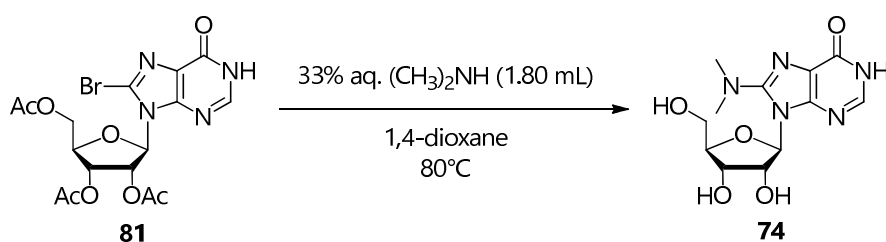
¹H NMR (DMSO-*d*₆, 400 MHz): δ (ppm) 12.05 (br s, 1H, N¹H), 7.82 (s, 1H, H²), 7.50 (br t, J = 5.8 Hz, 1H, N⁸H), 7.39-7.20 (m, 5H, C₆H₅), 5.93 (d, J = 7.4 Hz, 1H, H^{1'}), 5.69 (br s, 1H, OH^{5'}), 5.47-5.05 (m, 2H, OH^{2'}, OH^{3'}), 4.64 (br t, J = 6.1 Hz, 1H, H^{2'}), 4.59-4.46 (m, 2H, NHCH₂), 4.14 (br d, J = 4.3 Hz, 1H, H^{3'}), 4.00 (br s, 1H, H^{4'}), 3.66 (br s, 2H, H^{5'a}, H^{5'b}).

¹³C NMR (DMSO-*d*₆, 100 MHz): δ (ppm) 155.9 (C⁶), 151.0 (C⁸), 148.1 (C⁴), 142.7 (C²), 140.5 (C^a), 128.6, 127.5, 127.1 (C^b, C^c, C^d), 122.1 (C⁵), 87.1 (C^{1'}), 86.2 (C^{4'}), 71.4 (C^{3'}), 71.2 (C^{2'}), 61.9 (C^{5'}), 45.7 (NHCH₂).

MS (ESI⁺): m/z calcd for [C₁₇H₁₉N₅O₅]⁺: 373.14; found: 396.3 [M+Na]⁺, 769.3 [2M+Na]⁺.

7.2.5.2.4. 8-*N,N*-Dimethylaminoinosine (74)

C₁₂H₁₇N₅O₅; MW 311.29



White powder (109 mg, 0.35 mmol).

Yield: **87%**

R_f: 0.54 (CH₂Cl₂-MeOH, 4:1)

HPLC t_R: 18.4' (50.0% B)

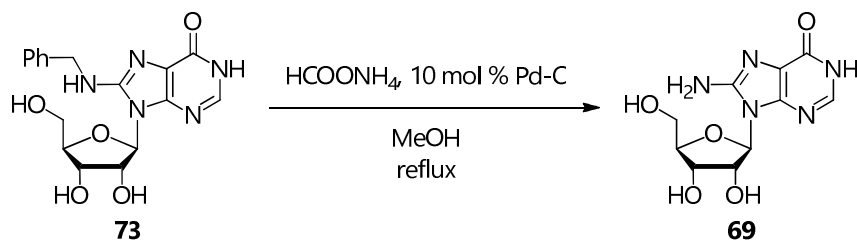
¹H NMR (CD₃OD, 400 MHz): δ (ppm) 7.97 (s, 1H, H²), 5.91 (d, J = 6.9 Hz, 1H, H^{1'}), 5.11 (br dd, J = 6.6, 5.7 Hz, 1H, H^{2'}), 4.38 (dd, J = 5.4, 2.6 Hz, 1H, H^{3'}), 4.11 (dd, J = 6.2, 3.2 Hz, 1H, H^{4'}), 3.86 (dd, J = 12.3, 3.1 Hz, 1H, H^{5'a}), 3.75 (dd, J = 12.3, 3.8 Hz, 1H, H^{5'b}), 2.99 (s, 6H, N(CH₃)₂).

¹H NMR (DMSO-*d*₆, 400 MHz): δ (ppm) 11.90 (v br s, 1H, N¹H), 7.97 (s, 1H, H²), 5.68 (d, J = 6.7 Hz, 1H, H^{1'}), 5.61-5.07 (m, 2H, OH), 5.06-4.84 (br s, 1H, OH), 5.01 (t, J = 6.0 Hz, 1H, H^{2'}), 4.16 (dd, J = 5.3, 3.0 Hz, 1H, H^{3'}), 3.90 (dd, J = 7.7, 4.7 Hz, 1H, H^{4'}), 3.66 (dd, J = 11.9, 4.6 Hz, 1H, H^{5'a}), 3.52 (dd, J = 11.9, 5.0 Hz, 1H, H^{5'b}), 2.84 (s, 6H, N(CH₃)₂).

¹³C NMR (DMSO-*d*₆, 100 MHz): δ (ppm) 156.2 (C⁶), 156.1 (C⁸), 148.2 (C⁴), 144.5 (C²), 122.7 (C⁵), 88.8 (C^{1'}), 86.2 (C^{4'}), 71.4 (C^{2'}), 71.1 (C^{3'}), 62.5 (C^{5'}), 43.3 (N(CH₃)₂).

MS (ESI⁺): m/z calcd for [C₁₂H₁₇N₅O₅]⁺: 311.12; found: 180.1 [M-ribose+H]⁺, 201.9 [M-ribose+Na]⁺, 267.0 [M-N(CH₃)₂-H]⁺, 297.1 [M-CH₃]⁺, 334.0 [M+Na]⁺, 645.0 [2M+Na]⁺.

7.2.5.3. 8-Aminoinosine (69)

C₁₀H₁₃N₅O₅; MW 283.24

73 (60 mg, 0.16 mmol) and 10% Pd-C (90 mg, 84.6 μmol) were suspended in MeOH (2.50 mL) under inert atmosphere. Portions of HCOONH₄ were added at 0 h and 24 h (202 mg, 3.20 mmol), 96 h (404 mg, 6.41 mmol) and 120 h (101 mg, 1.60 mmol) and the resulting mixture was refluxed and monitored by TLC (CH₂Cl₂-MeOH, 4:1).

At 6 days, the suspension was filtered on celite and evaporated under reduced pressure to get **69** as a very pale yellow powder (43 mg, 0.15 mmol).

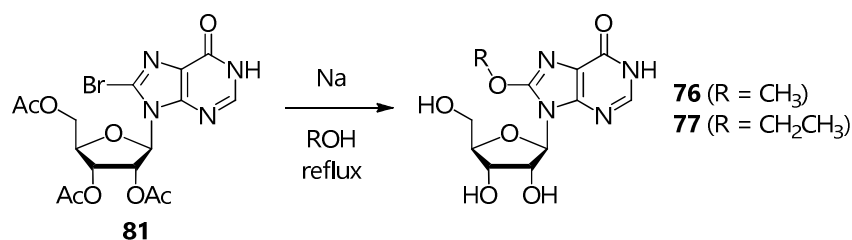
Yield: **96%**

R_f: 0.10 (CH₂Cl₂-MeOH, 8:2)

¹H NMR (DMSO-*d*₆, 400 MHz): δ (ppm) 12.04 (br s, 1H, N¹H), 7.79 (s, 1H, H²), 6.50 (br s, 2H, N⁸H₂), 5.85 (d, *J* = 7.3 Hz, 1H, H^{1'}), 5.56 (br s, 1H, OH^{5'}), 5.30 (br s, 1H, OH^{2'}), 5.16 (br s, 1H, OH^{3'}), 4.59 (t, *J* = 6.4 Hz, 1H, H^{2'}), 4.12 (dd, *J* = 5.4, 2.0 Hz, 1H, H^{3'}), 3.94 (br q, *J* = 2.3 Hz, 1H, H^{4'}), 3.63 (br s, 2H, H^{5'a}, H^{5'b}).

¹³C NMR (DMSO-*d*₆, 100 MHz): δ (ppm) 155.4 (C⁶), 151.1 (C⁸), 147.5 (C⁴), 143.0 (C²), 120.9 (C⁵), 87.2 (C^{1'}), 86.2 (C^{4'}), 71.2 (C^{3'}), 71.0 (C^{2'}), 61.8 (C^{5'}).

MS (ESI⁺): *m/z* calcd for [C₁₀H₁₃N₅O₅]⁺: 283.09; found: 284.0 [M+H]⁺, 306.1 [M+Na]⁺, 567.0 [2M+H]⁺, 589.0 [2M+Na]⁺.

7.2.5.4. General procedure for the synthesis of 8-alkoxyinosines (**76**, **77**)

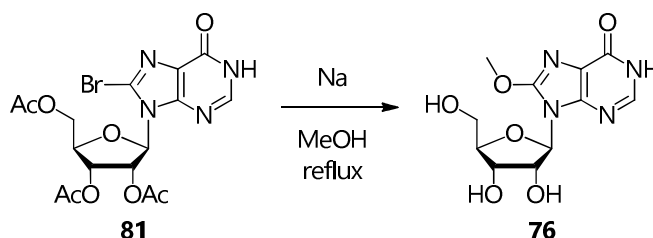
81 (189 mg, 0.40 mmol) was added to a solution of the appropriate alkoxide, freshly prepared by dissolving Na (46 mg, 2.00 mmol) in the corresponding dry alcohol (3.00 mL) under inert atmosphere. The resulting mixture was refluxed and monitored by TLC (CH₂Cl₂-MeOH, 4:1) until complete consumption of the starting material and formation of the product (between 2 and 3 h).

76 and **77**: The solvent was removed under reduced pressure and the crude was purified by semi-preparative HPLC.

Time (min)	Column volumes	% A (H ₂ O)	% B (MeOH)
0 - 2	0.5	97	3
2 - 30	7	97 → 0	3 → 100
30 - 32	0.5	0	100

7.2.5.4.1. 8-Methoxyinosine (**76**)

C₁₁H₁₄N₄O₆; MW 298.25



White powder (104 mg, 0.35 mmol).

Yield: **87%**

R_f: 0.47 (CH₂Cl₂-MeOH, 4:1)

HPLC *t_R*: 17.5' (47.2% B)

¹H NMR (CD₃OD, 300 MHz): δ (ppm) 7.94 (s, 1H, H²), 5.88 (d, *J* = 6.8 Hz, 1H, H^{1'}), 4.97-4.82 (m, 1H, H^{2'}), 4.30 (dd, *J* = 5.1, 2.6 Hz, 1H, H^{3'}), 4.15 (s, 3H, OCH₃), 4.07 (q, *J* = 2.9 Hz, 1H, H^{4'}), 3.82 (dd, *J* = 12.6, 2.9 Hz, 1H, H^{5'a}), 3.68 (dd, *J* = 12.6, 3.8 Hz, 1H, H^{5'b}).

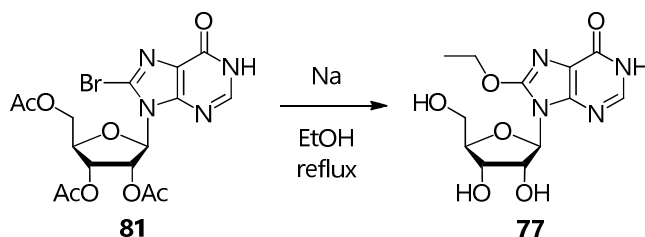
¹H NMR (DMSO-*d*₆, 400 MHz): δ (ppm) 7.88 (s, 1H, H²), 5.68 (d, *J* = 6.7 Hz, 1H, H^{1'}), 4.84 (dd, *J* = 6.5, 5.4 Hz, 1H, H^{2'}), 4.11 (dd, *J* = 5.1, 2.5 Hz, 1H, H^{3'}), 4.04 (s, 3H, OCH₃), 3.90 (dd, *J* = 6.3, 3.6 Hz, 1H, H^{4'}), 3.61 (dd, *J* = 12.1, 3.8 Hz, 1H, H^{5'a}), 3.48 (dd, *J* = 12.1, 4.2 Hz, 1H, H^{5'b}).

¹³C NMR (DMSO-*d*₆, 100 MHz): δ (ppm) 161.0 (C⁶), 153.3 (C⁸), 148.3 (C²), 148.0 (C⁴), 120.2 (C⁵), 87.3 (C^{1'}), 86.5 (C^{4'}), 71.8 (C^{2'}), 71.4 (C^{3'}), 62.8 (C^{5'}), 57.2 (OCH₃).

MS (ESI⁺): *m/z* calcd for [C₁₁H₁₄N₄O₆]⁺: 298.09; found: 165.0 [M-ribosyl-H]⁺, 189.1 [M-ribosyl+Na]⁺, 321.1 [M+Na]⁺, 619.1 [2M+Na]⁺.

7.2.5.4.2. 8-Ethoxyinosine (77)

C₁₂H₁₆N₄O₆; MW 312.28



White powder (93 mg, 0.30 mmol).

Yield: **74%**

R_f: 0.57 (CH₂Cl₂-MeOH, 4:1)

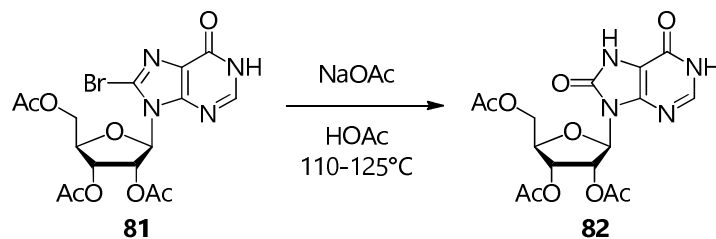
HPLC t_R: 19.8' (54.7% B)

¹H NMR (CD₃OD, 300 MHz): δ (ppm) 7.94 (s, 1H, H²), 5.91 (d, *J* = 6.6 Hz, 1H, H^{1'}), 4.93-4.81 (m, 1H, H^{2'}), 4.56 (q, *J* = 7.1 Hz, 2H, OCH₂), 4.32 (dd, *J* = 5.6, 2.8 Hz, 1H, H^{3'}), 4.07 (q, *J* = 3.2 Hz, 1H, H^{4'}), 3.82 (dd, *J* = 12.3, 3.2 Hz, 1H, H^{5'a}), 3.69 (dd, *J* = 12.6, 3.8 Hz, 1H, H^{5'b}), 1.47 (t, *J* = 7.3 Hz, 3H, CH₃).

¹H NMR (DMSO-*d*₆, 400 MHz): δ (ppm) 7.93 (s, 1H, H²), 5.71 (d, *J* = 6.4 Hz, 1H, H^{1'}), 4.83 (t, *J* = 5.8 Hz, 1H, H^{2'}), 4.47 (q, *J* = 7.3 Hz, 2H, OCH₂), 4.12 (dd, *J* = 5.1, 3.2 Hz, 1H, H^{3'}), 3.88 (dd, *J* = 7.6, 4.4 Hz, 1H, H^{4'}), 3.61 (dd, *J* = 11.9, 4.4 Hz, 1H, H^{5'a}), 3.48 (dd, *J* = 11.9, 4.8 Hz, 1H, H^{5'b}), 1.39 (t, *J* = 7.1 Hz, 3H, CH₃).

¹³C NMR (DMSO-*d*₆, 100 MHz): δ (ppm) 158.7 (C⁶), 153.1 (C⁸), 147.7 (C⁴), 146.7 (C²), 120.4 (C⁵), 87.2 (C^{1'}), 86.2 (C^{4'}), 71.7 (C^{2'}), 71.2 (C^{3'}), 66.4 (OCH₂), 62.6 (C^{5'}), 14.8 (CH₃).

MS (ESI⁺): *m/z* calcd for [C₁₂H₁₆N₄O₆]⁺: 312.11; found: 203.1 [M-ribosyl+Na]⁺, 335.1 [M+Na]⁺, 647.1 [2M+Na]⁺, 935.3 [3M-H]⁺.

7.2.5.5. 2',3',5'-Tri-*O*-acetyl-8-pxoinosine (**82**)C₁₆H₁₈N₄O₉; MW 410.34

81 (189 mg, 0.40 mmol) and well-dried NaOAc (98 mg, 1.19 mmol) were dissolved in AcOH (2.40 mL) under inert atmosphere and the resulting solution was stirred at 110-125°C for 3 h.

The mixture was partitioned between CH₂Cl₂ (20 mL) and H₂O (10 mL) and the aqueous phase was extracted with CH₂Cl₂ (2x20 mL). The reunited organic phases were dried over Na₂SO₄ and evaporated under first reduced pressure and then high vacuum. The resulting crude was purified by flash column chromatography (CH₂Cl₂-MeOH, 9.4:0.6) to obtain **82** as a white solid (152 mg, 0.37 mmol).

Yield: **93%**

R_f: 0.49 (CH₂Cl₂-MeOH, 9:1)

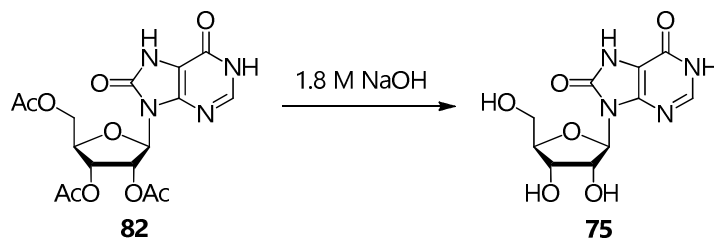
¹H NMR (DMSO-*d*₆, 300 MHz): δ (ppm) 11.60 (br m, 2H, N¹H, N⁷H), 8.02 (s, 1H, H²), 6.00 (t, *J* = 4.8 Hz, 1H, H^{2'}), 5.84 (d, *J* = 4.5 Hz, 1H, H^{1'}), 5.55 (t, *J* = 6.0 Hz, 1H, H^{3'}), 4.37 (dd, *J* = 12.0, 3.6 Hz, 1H H^{5'a}), 4.24 (dd, *J* = 9.3, 5.4 Hz, 1H, H^{4'}), 4.11 (dd, *J* = 12.0, 5.7 Hz, 1H, H^{5'b}), 2.08 (s, 3H, CH₃CO), 2.06 (s, 3H, CH₃CO), 2.00 (s, 3H, CH₃CO).

¹H NMR (CDCl₃, 400 MHz): δ (ppm) 12.48 (v br s, 1H, N¹H), 11.22 (br s, 1H, N⁷H), 8.04 (s, 1H, H²), 6.21 (br s, 1H, H^{2'}), 6.12 (br d, *J* = 2.4 Hz, 1H, H^{1'}), 5.75 (br t, *J* = 5.0 Hz, 1H, H^{3'}), 4.51 (br d, *J* = 9.1 Hz, 1H H^{5'a}), 4.41-4.29 (m, 2H, H^{4'}, H^{5'b}), 2.17 (s, 3H, CH₃CO), 2.15 (s, 3H, CH₃CO), 2.11 (s, 3H, CH₃CO).

¹³C NMR (DMSO-*d*₆, 100 MHz): δ (ppm) 170.7, 169.8, 169.7 (CH₃CO), 152.7 (C⁸), 152.4 (C⁶), 145.3 (C⁴), 144.4 (C²), 109.2 (C⁵), 84.3 (C^{1'}), 79.5 (C^{4'}), 71.8 (C^{2'}), 70.8 (C^{3'}), 63.4 (C^{5'}), 20.9, 20.8, 20.6 (CH₃CO).

MS (ESI⁺): *m/z* calcd for [C₁₆H₁₈N₄O₉]⁺: 410.11; found: 433.3 [M+Na]⁺, 842.9 [2M+Na]⁺.

7.2.5.6. 8-Oxoinosine (75)

C₁₀H₁₂N₄O₆; MW 284.23

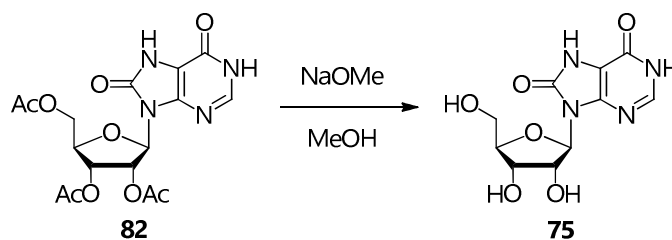
82 (75 mg, 0.18 mmol) was dissolved in 1.8 M NaOH (0.40 mL, 0.72 mmol) and the resulting colourless solution was stirred at RT for 15'.

The mixture was neutralized with KH₂PO₄, the solvent was removed under reduced pressure and the crude was purified by semi-preparative HPLC. The resulting white solid was suspended in dry MeOH, filtered, washed with few cold MeOH and dried under reduced pressure to get **75** as a white powder (33 mg, 0.12 mmol).

Yield: **65%**

Time (min)	Column volumes	% A (H ₂ O)	% B (MeOH)
0 - 2	0.5	100	0
2 - 30	7	100 → 0	0 → 100
30 - 32	0.5	0	100

HPLC *t_R*: 8.4' (16.8% B)



A 25% NaOMe solution in MeOH (0.12 mL, 0.52 mmol) was added to a suspension of **82** (50 mg, 0.12 mmol) in dry MeOH (0.38 mL) and the resulting mixture was stirred at RT for 2 h 30'.

The resulting precipitate was filtered, washed with few cold MeOH and dried under reduced pressure to obtain **75** as a white powder (17 mg, 0.06 mmol).

Yield: **50%**

R_f: 0.12 (CH₂Cl₂-MeOH, 9:1)

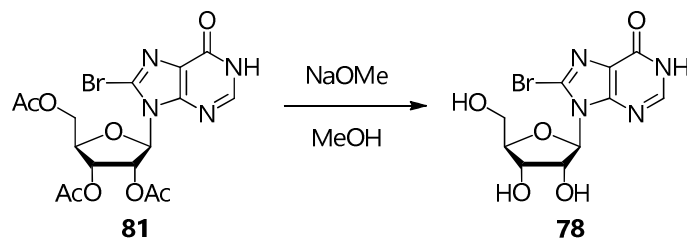
¹H NMR (DMSO-*d*₆, 400 MHz): δ (ppm) 11.47 (v br s, 2H, N¹H, N⁸H), 7.71 (s, 1H, H²), 6.17 (br s, 1H, OH⁵), 5.65 (d, *J* = 7.1 Hz, 1H, H¹), 5.29-4.88 (m, 2H, OH^{2'}, OH^{3'}), 4.83 (dd, *J* = 6.8, 5.3 Hz, 1H, H^{2'}), 4.09 (dd, *J* = 5.0, 1.6 Hz, 1H, H^{3'}), 3.88 (br dd, *J* = 4.5, 2.5 Hz, 1H, H^{4'}), 3.60 (dd, *J* = 12.2, 2.6 Hz, 1H, H^{5'a}), 3.46 (br d, *J* = 11.9 Hz, 1H, H^{5'b}).

^{13}C NMR (DMSO- d_6 , 100 MHz): δ (ppm) 159.6 (C^6), 152.6 (C^8), 150.4 (C^2), 145.0 (C^4), 108.6 (C^5), 86.2 ($\text{C}^{4'}$), 86.1 ($\text{C}^{1'}$), 71.9 ($\text{C}^{2'}$), 71.2 ($\text{C}^{3'}$), 63.2 (C^5).

MS (ESI $^+$): m/z calcd for $[\text{C}_{10}\text{H}_{12}\text{N}_4\text{O}_6]^+$: 284.08; found: 284.9 $[\text{M}+\text{H}]^+$, 307.1 $[\text{M}+\text{Na}]^+$.

MS (ESI $^+$): m/z calcd for $[\text{C}_{10}\text{H}_{12}\text{N}_4\text{O}_6]^-$: 284.08; found: 283.1 $[\text{M}-\text{H}]^+$, 566.8 $[2\text{M}-\text{H}]^-$.

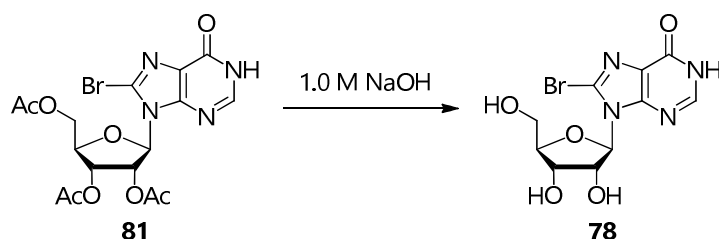
7.2.5.7. 8-Bromoinosine (78)

C₁₀H₁₁BrN₄O₅; MW 347.12

25% NaOMe in MeOH (0.38 mL, 1.66 mmol) was added to a suspension of **81** (189 mg, 0.40 mmol) in dry MeOH (1.0 mL) and the resulting solution was stirred at RT for 55'.

The solvent was removed under reduced pressure, the crude was suspended in H₂O (2.0 mL) and the mixture was neutralized with 6 M HCl to precipitate **78** as a white powder, which was filtered, washed with few cold H₂O and dried under reduced pressure (125 mg, 0.36 mmol).

Yield: **90%**



81 (62 mg, 0.13 mmol) was dissolved in 1.0 M NaOH (1.30 mL, 1.30 mmol) and the resulting opalescent solution was stirred at RT for 1 h.

The mixture was diluted with H₂O (0.5 mL) and neutralized with NaH₂PO₄ to precipitate **78** as a white powder, which was filtered, washed with few cold H₂O and dried under reduced pressure (29 mg, 0.08 mmol).

Yield: **64%**

R_f: 0.26 (CH₂Cl₂-MeOH, 8.1:1.5)

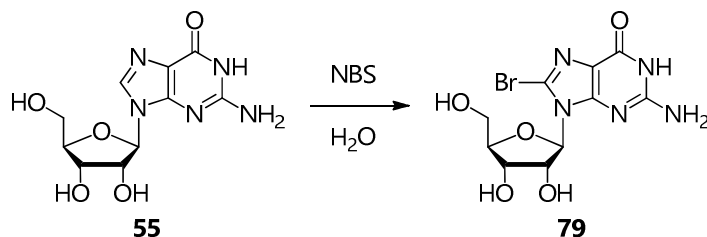
¹H NMR (DMSO-*d*₆, 400 MHz): δ (ppm) 12.63 (br s, 1H, N¹H), 8.11 (s, 1H, H²), 5.83 (d, *J* = 6.3 Hz, 1H, H^{1'}), 5.50 (br d, *J* = 4.0 Hz, 1H, OH^{2'}), 5.24 (br s, 1H, OH^{3'}), 5.03 (br t, *J* = 5.1 Hz, 1H, H^{2'}), 4.94 (br t, *J* = 5.6 Hz, 1H, OH^{5'}), 4.20 (br s, 1H, H^{3'}), 3.93 (dd, *J* = 8.2, 4.9 Hz, 1H, H^{4'}), 3.66 (dt, *J* = 10.9, 4.2 Hz, 1H, H^{5'a}), 3.52 (dt, *J* = 11.8, 5.7 Hz, 1H, H^{5'b}).

¹³C NMR (DMSO-*d*₆, 100 MHz): δ (ppm) 155.7 (C⁶), 149.6 (C⁴), 146.7 (C²), 126.4 (C⁸), 125.8 (C⁵), 91.0 (C^{1'}), 86.7 (C^{4'}), 71.7 (C^{2'}), 70.9 (C^{3'}), 62.3 (C^{5'}).

MS (ESI⁺): *m/z* calcd for [C₁₀H₁₁⁷⁹BrN₄O₅]⁺: 345.99; found: 369.0 [(⁷⁹Br)M+Na]⁺, 371.0 [(⁸¹Br)M+Na]⁺, 714.9 [2(⁷⁹Br)M+Na]⁺, 716.9 [(⁷⁹Br)M+(⁸¹Br)M+Na]⁺, 718.9 [2(⁸¹Br)M+Na]⁺.

7.2.5.8. 8-Bromoguanosine (**79**)

$C_{10}H_{12}BrN_5O_5$; MW 362.14



NBS (890 mg, 5.00 mmol) was added to a suspension of **55** (1.42 mg, 5.01 mmol) in distilled H_2O (9.0 mL) at $0^\circ C$. The resulting white mixture was stirred at $0^\circ C$ for 1 h, allowed to warm at RT and stirred for 5 h, during which time it turned light orange.

The suspension was filtered and washed once with few cold distilled H_2O . The resulting pale pink crude was recrystallized from H_2O to obtain **79** as white crystals (1.61 g, 4.45 mmol).

Yield: **89%**

R_f : 0.80 (EtOH- H_2O , 4:1)

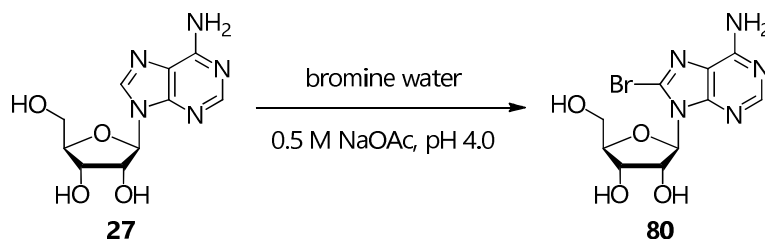
1H NMR (DMSO- d_6 , 400 MHz): δ (ppm) 10.83 (br s, 1H, N^1H), 6.50 (br s, 2H, N^2H_2), 5.68 (d, $J = 6.3$ Hz, 1H, H^1), 5.45 (d, $J = 6.2$ Hz, 1H, OH^2), 5.10 (d, $J = 5.1$ Hz, 1H, OH^3), 5.00 (dd, $J = 11.9, 6.1$ Hz, 1H, H^2), 4.93 (t, $J = 6.0$ Hz, 1H, OH^5), 4.12 (dd, $J = 8.6, 5.1$ Hz, 1H, H^3), 3.84 (dd, $J = 8.6, 5.2$ Hz, 1H, H^4), 3.64 (dt, $J = 10.6, 5.2$ Hz, 1H, H^{5a}), 3.50 (dt, $J = 12.0, 6.0$ Hz, 1H, H^{5b}).

^{13}C NMR (DMSO- d_6 , 100 MHz): δ (ppm) 156.0 (C^2), 154.0 (C^6), 152.6 (C^4), 121.5 (C^8), 118.0 (C^5), 90.2 (C^1), 86.4 (C^4), 71.0 (C^3), 70.8 (C^2), 62.5 (C^5).

MS (ESI $^+$): m/z calcd for $[C_{10}H_{12}^{79}BrN_5O_5]^+$: 361.00; found: 230.2 [$(^{79}Br)M$ -ribosyl+H] $^+$, 232.3 [$(^{81}Br)M$ -ribosyl+H] $^+$, 384.0 [$(^{79}Br)M$ +Na] $^+$, 386.0 [$(^{81}Br)M$ +Na] $^+$, 744.8 [$2(^{79}Br)M$ +Na] $^+$, 746.9 [$(^{79}Br)M$ + $(^{81}Br)M$ +Na] $^+$, 748.9 [$2(^{81}Br)M$ +Na] $^+$.

7.2.5.9. 8-Bromoadenosine (**80**)

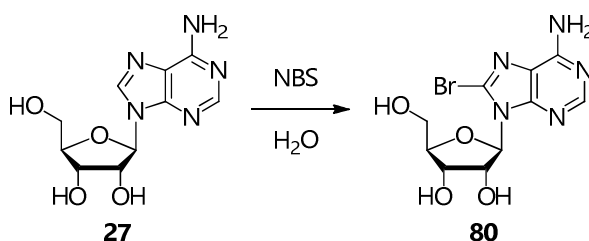
$C_{10}H_{12}BrN_5O_4$; MW 346.14



Aliquots of decanted saturated bromine water (9.90 and 5.00 mL) were added at 0 and 24 h, respectively, to a suspension of **27** (267 mg, 1.00 mmol) in 0.5 M NaOAc pH 4.0 (6.0 mL) under inert atmosphere. The resulting yellow solution was protected from light exposure and stirred at RT, during which time it became dark and a white precipitate was formed.

At 48 h the suspension was decolorized with NaHSO_3 and neutralized with 6 M NaOH. The precipitate was filtered, washed with few cold H_2O and dried under reduced pressure to obtain **80** as a white powder (287 mg, 0.83 mmol).

Yield: **83%**



Additions of NBS (534 mg, 3.00 mmol) were made at 0', 24 h and 7 2 h to a suspension of **27** (802 mg, 3.00 mmol) in distilled H_2O (15.0 mmol) under inert atmosphere. The resulting mixture was protected from light exposure and stirred at RT, during which time it became brown.

At 4 days, the suspension was filtered and washed with cold H_2O until a clear colourless solution was obtained. The pink solid was washed once with cold Et_2O , few cold *i*-PrOH and cold Et_2O and dried under reduced pressure. The crude was recrystallized from distilled H_2O to obtain **80** as brown needles (601 mg, 1.74 mmol)

Yield: **58%**

R_f : 0.32 (CH_2Cl_2 -MeOH, 9:1)

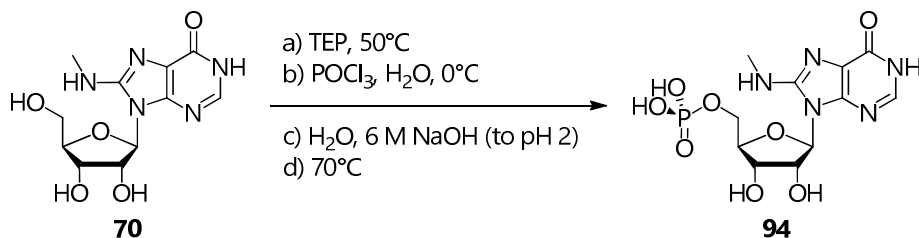
^1H NMR (DMSO- d_6 , 400 MHz): δ (ppm) 8.13 (s, 1H, H^2), 7.57 (br s, 2H, NH_2), 5.84 (d, $J = 6.7$ Hz, 1H, H^1), 5.50 (dd, $J = 8.6, 3.8$ Hz, 1H, OH^5), 5.46 (d, $J = 6.2$ Hz, 1H, OH^2), 5.23 (d, $J = 4.3$ Hz, 1H, OH^3), 5.10 (dd, $J = 11.8, 6.1$ Hz, 1H, H^2), 4.20 (br dd, $J = 5.5, 4.6$ Hz, 1H, H^3), 3.99 (br dd, $J = 5.8, 4.1$ Hz, 1H, H^4), 3.69 (dt, $J = 11.7, 3.5$ Hz, 1H, H^{5a}), 3.53 (ddd, $J = 11.9, 8.6, 3.7$ Hz, 1H, H^{5b}).

^{13}C NMR (DMSO- d_6 , 100 MHz): δ (ppm) 155.6 (C^6), 152.9 (C^2), 150.4 (C^4), 127.6 (C^8), 120.2 (C^5), 90.9 (C^1), 87.2 (C^4), 71.6 (C^2), 71.3 (C^3), 62.6 (C^5).

MS (ESI⁺): *m/z* calcd for [C₁₀H₁₂⁷⁹BrN₅O₄]⁺: 345.01; found: 212.3 [(⁷⁹Br)M-ribosyl-H]⁺, 214.1 [(⁸¹Br)M-ribosyl-H]⁺, 344.1 [(⁷⁹Br)M-H]⁺, 346.2 [(⁸¹Br)M-H]⁺, 689.2 [2(⁷⁹Br)M-H]⁺, 691.0 [(⁷⁹Br)M+(⁸¹Br)M)-H]⁺, 693.0 [2(⁸¹Br)M-H]⁺.

7.2.6. Synthesis of 8- and N^2 -substituted inosinic and guanylic acids (94-97)7.2.6.1. 8-Methylaminoinosinic acid (**94**)

$C_{11}H_{16}N_5O_8P$; MW 377.25



A suspension of **70** (25 mg, 84 μ mol) in TEP (278 μ L) was stirred at 50°C for 15'. POCl₃ (47 μ L, 504 μ mol) and H₂O (1.5 μ L, 83 μ mol) were added at 0°C and the resulting transparent colourless mixture was stirred at 0°C for 6 h. The disappearance of the substrate was monitored by TLC (EtOH-H₂O, 7:3; R_f = 0.88). After adding H₂O (556 μ L), pH was adjusted to 2 with 6 M NaOH and the resulting solution was stirred at 70°C for 1 h 30'. The mixture was neutralized with 6 M NaOH, diluted with H₂O (15 mL) and freeze-dried twice. The crude was purified by semi-preparative HPLC to get **94** as an off-white powder (24 mg, 64 μ mol).

Yield: **75%**

Time (min)	Column volumes	% A (H ₂ O/0.1% TFA)	% B ((H ₂ O/0.1% TFA)-CH ₃ CN, 4:1)
0 - 32	8	100 \rightarrow 70	0 \rightarrow 30

R_f : 0.67 (EtOH-H₂O, 7:3)

HPLC t_R : 14.9' (11.5% B)

¹H NMR (DMSO-*d*₆, 400 MHz): δ (ppm) 12.12 (br s, 1H, N¹H), 7.83 (s, 1H, H²), 6.27 (br s, 1H, N⁸H), 5.79 (d, J = 6.4 Hz, 1H, H^{1'}), 5.51-5.30 (m, 2H, OH^{2'}, OH^{3'}), 4.68 (br t, J = 5.8 Hz, 1H, H^{2'}), 4.20-4.13 (m, 1H, H^{3'}), 4.09-3.95 (m, 3H, H^{4'}, H^{5'a}, H^{5'b}), 2.88 (s, 3H, NHCH₃).

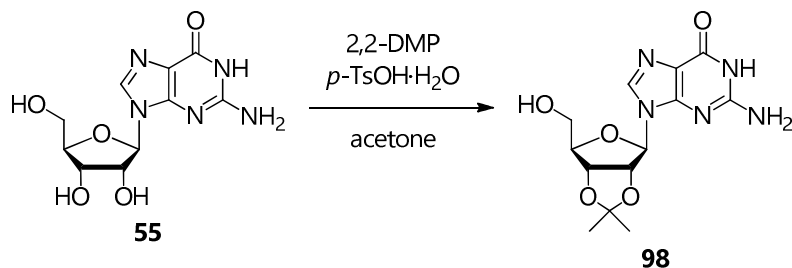
¹H NMR (D₂O, 400 MHz): δ (ppm) 8.15 (s, 1H, H²), 6.07 (d, J = 7.1 Hz, 1H, H^{1'}), 4.68 (br dd, J = 7.0, 5.9 Hz, 1H, H^{2'}), 4.40 (dd, J = 5.6, 2.5 Hz, 1H, H^{3'}), 4.33 (br t, J = 1.8 Hz, 1H, H^{4'}), 4.14 (br dd, J = 11.4, 7.0 Hz, 1H, H^{5'a}), 4.12-4.06 (m, 1H, H^{5'b}), 3.11 (s, 3H, NHCH₃).

¹³C NMR (D₂O, 100 MHz): δ (ppm) 153.2 (C⁶), 148.9 (C⁸), 147.1 (C²), 146.8 (C⁴), 111.4 (C⁵), 87.8 (C^{1'}), 85.0 (d, ³ J_{CP} = 8.2 Hz, C^{4'}), 71.3 (C^{2'}), 70.1 (C^{3'}), 64.6 (br d, ² J_{CP} = 3.0 Hz, C^{5'}), 29.7 (CH₃).

³¹P NMR (D₂O, 161 MHz): δ (ppm) 0.78.

MS (ESI⁺): m/z calcd for [C₁₁H₁₆N₅O₈P]⁺: 377.07; found: 377.2 [M]⁺, 399.0 [M-H+Na]⁺, 1507.3 [4M-H]⁺.

MS (ESI⁺): m/z calcd for [C₁₁H₁₆N₅O₈P]⁻: 377.07; found: 376.0 [M-H]⁻, 753.0 [2M-H]⁻, 775.1 [2M-2H+Na]⁻, 1529.9 [4M-H+Na]⁺.

7.2.6.2. 2',3'-*O*-Isopropylideneadenosine (**98**)C₁₃H₁₇N₅O₅; MW 323.30

2,2-DMP (34.30 mL, 278.94 mmol) and *p*-TsOH·H₂O (6.72 g, 35.33 mmol) were added to a suspension of **55** (10.00 g, 35.31 mmol) in acetone (250 mL) under inert atmosphere. The resulting mixture was stirred at RT for 24 h.

The solvent was removed under reduced pressure and the resulting foam was suspended in 5% aqueous NH₄OH (215 mL) to precipitate **98** as a white powder, which was filtered, washed with cold H₂O and dried under reduced pressure (10.93 g, 33.81 mmol).

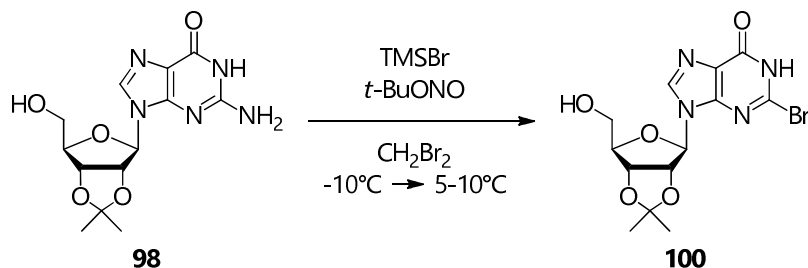
Yield: **96%**

*R*_f: 0.32 (CH₂Cl₂-MeOH, 9:1)

¹H NMR (DMSO-*d*₆, 400 MHz): δ (ppm) 10.55 (br s, 1H, N¹H), 7.92 (s, 1H, H²), 6.52 (br s, 2H, N²H₂), 5.93 (d, *J* = 2.8 Hz, 1H, H^{1'}), 5.19 (dd, *J* = 6.3, 2.8 Hz, 1H, H^{2'}), 5.11 (t, *J* = 5.4 Hz, 1H, OH^{5'}), 4.97 (dd, *J* = 6.3, 3.0 Hz, 1H, H^{3'}), 4.12 (td, *J* = 5.1, 3.2 Hz, 1H, H^{4'}), 3.56 (dd, *J* = 11.2, 4.8 Hz, 1H, H^{5'a}), 3.51 (dd, *J* = 11.6, 5.2 Hz, 1H, H^{5'b}), 1.51 (s, 3H, C(CH₃)₂), 1.31 (s, 3H, C(CH₃)₂).

¹³C NMR (DMSO-*d*₆, 400 MHz): δ (ppm) 157.2 (C⁶), 154.2 (C²), 151.2 (C⁴), 136.3 (C⁸), 117.2 (C⁵), 113.5 (C(CH₃)₂), 88.9 (C^{1'}), 87.1 (C^{4'}), 84.0 (C^{2'}), 81.6 (C^{3'}), 62.1 (C^{5'}), 27.5, 25.7 (C(CH₃)₂).

MS (ESI⁺): *m/z* calcd for [C₁₃H₁₇N₅O₅]⁺: 323.12; found: 345.9 [M+Na]⁺, 669.0 [2M+Na]⁺, 991.9 [3M-H+Na]⁺, 1315.3 [4M+Na]⁺.

7.2.6.3. 2-Bromo-2',3'-*O*-isopropylideneinosine (**100**)C₁₃H₁₅BrN₄O₅; MW 387.19

TMSBr (3.17 mL, 24.02 mmol) and *t*-BuONO (5.95 mL, 50.03 mmol) were added dropwise at -10°C to a suspension of **98** (646 mg, 2.00 mmol) in CH₂Br₂ (10.0 mL) under inert atmosphere. The resulting dark brown solution was protected from light exposure and allowed to warm to 5-10°C for 7 h under stirring.

The solution was added dropwise to a 1:1 AcOEt/saturated aqueous NaHCO₃ mixture (300 mL) and vigorously stirred at 0°C for 10'. After separating the layers, the aqueous one was extracted with AcOEt (1x50 mL), then the reunited organic phases were washed with H₂O (1x50 mL) and dried over Na₂SO₄. The solvent was removed under reduced pressure and the resulting yellow foam was purified by flash column chromatography twice (CH₂Cl₂-MeOH, 8.8:1.2 and 9.1:0.9) to obtain **100** as a light yellow powder (163 mg, 0.42 mmol).

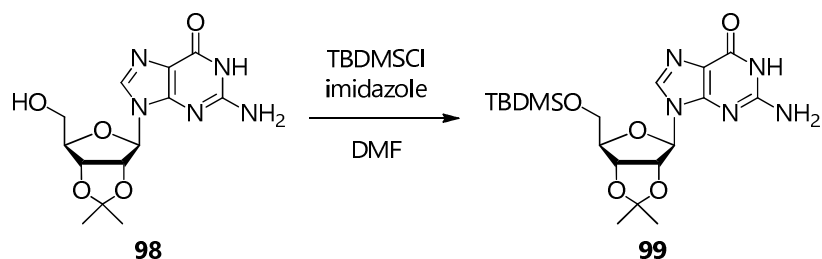
Yield: **21%**

*R*_f: 0.36 (CH₂Cl₂-MeOH, 9:1)

¹H NMR (DMSO-*d*₆, 400 MHz): δ (ppm) 13.37 (br s, 1H, N¹H), 8.30 (s, 1H, H⁸), 6.05 (d, *J* = 2.7 Hz, 1H, H^{1'}), 5.24 (dd, *J* = 6.2, 2.7 Hz, 1H, H^{2'}), 5.08 (br t, *J* = 4.8 Hz, 1H, OH^{5'}), 4.92 (dd, *J* = 6.2, 2.7 Hz, 1H, H^{3'}), 4.22 (td, *J* = 4.8, 2.8 Hz, 1H, H^{4'}), 3.57-3.51 (m, 2H, H^{5'a}, H^{5'b}), 1.54 (s, 3H, C(CH₃)₂), 1.33 (s, 3H, C(CH₃)₂).

¹³C NMR (DMSO-*d*₆, 100 MHz): δ (ppm) 157.6 (C⁶), 148.2 (C⁴), 139.2 (C⁸), 134.6 (C²), 123.9 (C⁵), 113.6 (C(CH₃)₂), 89.9 (C^{1'}), 87.4 (C^{4'}), 84.3 (C^{2'}), 81.7 (C^{3'}), 61.9 (C^{5'}), 27.5, 25.6 (C(CH₃)₂).

MS (ESI⁺): *m/z* calcd for [C₁₃H₁₅BrN₄O₅]⁺: 386.02; found: 409.2 [(⁷⁹Br)M+Na]⁺, 411.0 [(⁸¹Br)M+Na]⁺, 795.1 [2(⁷⁹Br)M+Na]⁺, 797.1 [(⁷⁹Br)M+(⁸¹Br)M+Na]⁺, 799.1 [2(⁸¹Br)M+Na]⁺.

7.2.6.4. 2',3'-*O*-Isopropylidene-5'-*O*-*t*-butyldimethylsilylguanosine (**99**)C₁₉H₃₁N₅O₅Si; MW 437.57

TBDMSCl (1.09 g, 7.23 mmol) and imidazole (950 mg, 13.95 mmol) were added to a suspension of **98** (2.00 g, 6.19 mmol) in dry DMF (15.0 mL) under inert atmosphere and the resulting mixture was stirred at RT for 4 h.

The suspension was diluted with H₂O (50 mL) and extracted with AcOEt (1x50 mL), then the reunited organic phases were washed with H₂O (1x50 mL) and brine (1x50 mL) and evaporated under reduced pressure. The resulting crude was purified by flash column chromatography (CH₂Cl₂-MeOH, 12.5:1.0) to obtain **99** as a white powder (2.57 g, 6.95 mmol).

Yield: **95%**

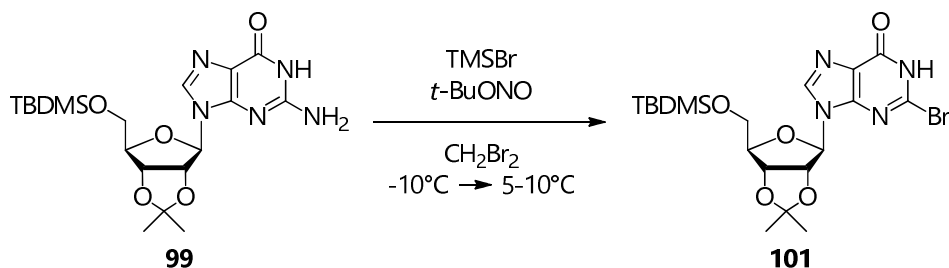
R_f: 0.54 (CH₂Cl₂-MeOH, 9:1)

¹H NMR (DMSO-*d*₆, 400 MHz): δ (ppm) 10.70 (br s, 1H, N¹H), 7.83 (s, 1H, H⁸), 6.53 (br s, 2H, N²H₂), 5.96 (br d, *J* = 1.8 Hz, 1H, H^{1'}), 5.22 (dd, *J* = 6.1, 1.7 Hz, 1H, H^{2'}), 4.97 (dd, *J* = 6.1, 3.1 Hz, 1H, H^{3'}), 4.12 (dd, *J* = 8.5, 5.2 Hz, 1H, H^{4'}), 3.76-3.66 (m, 2H, H^{5'a}, H^{5'b}), 1.51 (s, 3H, C(CH₃)₂), 1.32 (s, 3H, C(CH₃)₂), 0.82 (s, 9H, Si(C(CH₃)₃)), -0.04 (s, 3H, Si(CH₃)₂), -0.05 (s, 3H, Si(CH₃)₂).

¹H NMR (CDCl₃, 400 MHz): δ (ppm) 12.05 (br s, 1H, N¹H), 7.79 (s, 1H, H⁸), 6.29 (br s, 2H, N²H₂), 6.02 (br d, *J* = 2.3 Hz, 1H, H^{1'}), 5.19 (br dd, *J* = 6.0, 2.0 Hz, 1H, H^{2'}), 4.94 (dd, *J* = 6.2, 2.8 Hz, 1H, H^{3'}), 4.36 (dd, *J* = 7.0, 4.0 Hz, 1H, H^{4'}), 3.87 (dd, *J* = 11.2, 4.0 Hz, 1H, H^{5'a}), 3.80 (dd, *J* = 11.3, 4.0 Hz, 1H, H^{5'b}), 1.64 (s, 3H, C(CH₃)₂), 1.43 (s, 3H, C(CH₃)₂), 0.90 (s, 9H, Si(C(CH₃)₃)), 0.073 (s, 3H, Si(CH₃)₂), 0.068 (s, 3H, Si(CH₃)₂).

¹³C NMR (CDCl₃, 100 MHz): δ (ppm) 159.0 (C⁶), 153.6 (C²), 151.3 (C⁴), 136.4 (C⁸), 117.4 (C⁵), 114.1 (C(CH₃)₂), 90.3 (C^{1'}), 87.0 (C^{4'}), 84.7 (C^{2'}), 81.2 (C^{3'}), 63.5 (C^{5'}), 27.3, 25.5 (C(CH₃)₂), 25.9 (Si(C(CH₃)₃)), 18.4 (Si(C(CH₃)₃)), -5.4, -5.5 (Si(CH₃)₂).

MS (ESI⁺): *m/z* calcd for [C₁₉H₃₁N₅O₅Si]⁺: 437.21; found: 438.1 [M+H]⁺, 460.2 [M+Na]⁺, 897.2 [2M+Na]⁺, 1772.4 [4M+H+Na]⁺.

7.2.6.5. 2-Bromo-2',3'-*O*-isopropylidene-5'-*O*-*t*-butyldimethylsilylinosine (**101**)C₁₉H₂₉BrN₄O₅Si; MW 501.45

TMSBr (1.20 mL, 9.09 mmol) and *t*-BuONO (2.40 mL, 20.18 mmol) were added dropwise at -10°C to a solution of **99** (438 mg, 1.00 mmol) in CH_2Br_2 (7.0 mL) under inert atmosphere. The resulting dark brown solution was protected from light exposure and stirred at -10°C for 2 h, allowed to warm and stirred at $5-10^{\circ}\text{C}$ for 5 h.

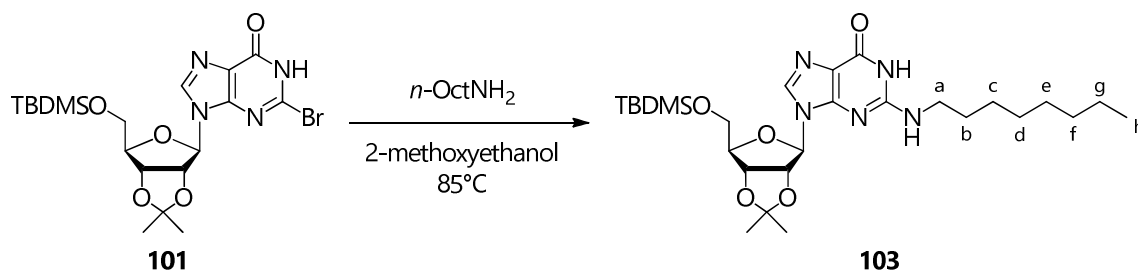
The solution was added dropwise to a 1:1 CH_2Cl_2 /saturated aqueous NaHCO_3 mixture (300 mL) and vigorously stirred at 0°C for 10'. After separating the layers, the aqueous one was extracted with cold CH_2Cl_2 (1x70 mL), then the reunited organic phases were washed with H_2O (2x70 mL) and brine (1x70 mL) and dried over Na_2SO_4 . The solvent was removed under reduced pressure and the resulting yellow foamy crude was purified by flash column chromatography (CH_2Cl_2 -MeOH, 9.5:0.5) to obtain **101** as a yellow crystalline solid (350 mg, 0.70 mmol).

Yield: **70%***R*_f: 0.56 (CH_2Cl_2 -MeOH, 9:1)

¹H NMR (CDCl₃, 400 MHz): δ (ppm) 12.85 (br s, 1H, N¹H), 8.10 (s, 1H, H⁸), 6.15 (d, $J = 2.8$ Hz, 1H, H¹), 5.06 (dd, $J = 6.1, 2.6$ Hz, 1H, H^{2'}), 4.95 (dd, $J = 6.1, 2.7$ Hz, 1H, H^{3'}), 4.41 (q, $J = 3.4$ Hz, 1H, H^{4'}), 3.92 (dd, $J = 11.4, 3.4$ Hz, 1H, H^{5'a}), 3.83 (dd, $J = 11.3, 3.7$ Hz, 1H, H^{5'b}), 1.66 (s, 3H, C(CH₃)₂), 1.42 (s, 3H, C(CH₃)₂), 0.91 (s, 9H, Si(C(CH₃)₃)), 0.094 (s, 3H, Si(CH₃)₂), 0.089 (s, 3H, Si(CH₃)₂).

¹³C NMR (CDCl₃, 100 MHz): δ (ppm) 158.9 (C⁶), 148.3 (C⁴), 138.8 (C⁸), 133.1 (C²), 123.8 (C⁵), 114.4 (C(CH₃)₂), 90.7 (C^{1'}), 87.1 (C^{4'}), 85.2 (C^{2'}), 81.1 (C^{3'}), 63.5 (C^{5'}), 27.3, 25.4 (C(CH₃)₂), 25.9 (Si(C(CH₃)₃)), 18.4 (Si(C(CH₃)₃)), -5.4, -5.5 (Si(CH₃)₂).

MS (ESI⁺): m/z calcd for [C₁₉H₂₉⁷⁹BrN₄O₅Si]⁺: 500.11; found: 523.0 [(⁷⁹Br)M+Na]⁺, 525.1 [(⁸¹Br)M+Na]⁺, 1023.0 [2(⁷⁹Br)M+Na]⁺, 1025.0 [(⁷⁹Br)M+(⁸¹Br)M+Na]⁺, 1027.0 [2(⁸¹Br)M+Na]⁺.

7.2.6.6. *N*²-*n*-Octyl-2',3'-*O*-isopropylidene-5'-*O*-*t*-butyldimethylsilylguanosine (**103**)C₂₇H₄₇N₅O₅Si; MW 549.78

n-OctNH₂ (0.18 mL, 1.09 mmol) was added to a solution of **101** (111 mg, 0.22 mmol) in 2-methoxyethanol (2.70 mL) under inert atmosphere. The resulting dark brown solution was protected from light exposure and stirred at 85°C for 3 days, during which time it became first yellow and then orange.

The mixture was diluted with AcOEt (5 mL), washed with 1 M HCl (4x5 mL), saturated aqueous Na₂S₂O₃ (1x5 mL) and brine (1x5 mL) and dried over Na₂SO₄. The solvent was removed under reduced pressure and the orange oil crude was purified by flash column chromatography (CH₂Cl₂-MeOH, 9.5:0.5) to obtain **103** as a dense yellow foam (84 mg, 0.15 mmol).

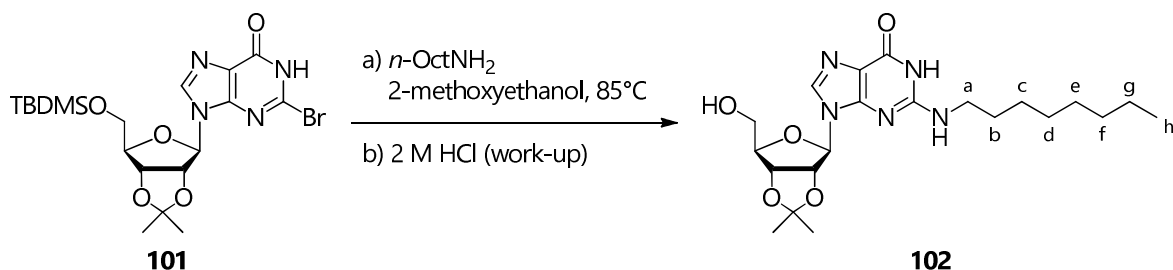
Yield: **69%**

*R*_f: 0.59 (CH₂Cl₂-MeOH, 9:1)

¹H NMR (CDCl₃, 400 MHz): δ (ppm) 11.81 (br s, 1H, N¹H), 7.71 (br s, 1H, H⁸), 6.93 (br s, 1H, N²H), 5.94 (br s, 1H, H^{1'}), 5.18 (br d, *J* = 4.3 Hz, 1H, H^{2'}), 4.84 (br dd, *J* = 5.2, 2.1 Hz, 1H, H^{3'}), 4.27 (br dd, *J* = 6.8, 4.2 Hz, 1H, H^{4'}), 3.78 (br dd, *J* = 11.1, 3.5 Hz, 1H, H^{5'a}), 3.70 (dd, *J* = 11.0, 4.6 Hz, 1H, H^{5'b}), 3.32 (br t, *J* = 5.4 Hz, 2H, CH₂^a), 1.64-1.50 (m, 5H, C(CH₃)₂, CH₂^b), 1.36-1.05 (m, 13H, C(CH₃)₂, CH₂^c, CH₂^d, CH₂^e, CH₂^f, CH₂^g), 0.86-0.71 (m, 12H, CH₃^h, Si(CH₃)₃), -0.04 (s, 3H, Si(CH₃)₂), -0.05 (s, 3H, Si(CH₃)₂).

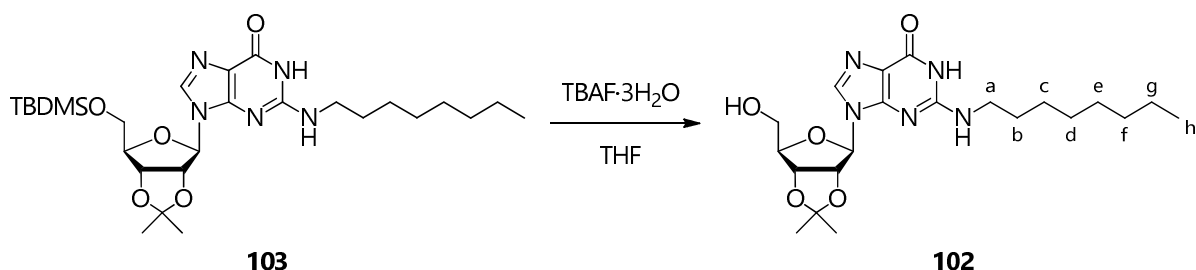
¹³C NMR (CDCl₃, 100 MHz): δ (ppm) 158.1 (C⁶), 153.1 (C²), 151.2 (C⁴), 132.9 (C⁸), 117.8 (C⁵), 113.9 (C(CH₃)₂), 90.5 (C^{1'}), 87.2 (C^{4'}), 84.6 (C^{2'}), 81.5 (C^{3'}), 63.6 (C^{5'}), 41.6 (C^a), 31.9 (C^b), 31.9, 29.4, 29.3 (C^c, C^d, C^e), 27.2, 25.4 (C(CH₃)₂), 27.1 (C^f), 25.9 (SiC(CH₃)₃), 22.6 (C^g), 18.3 (SiC(CH₃)₃), 14.1 (C^h), -5.4, -5.5 (Si(CH₃)₂).

MS (ESI⁺): *m/z* calcd for [C₂₇H₄₇N₅O₅Si]⁺: 549.33; found: 550.2 [M+H]⁺, 572.3 [M+Na]⁺, 1121.4 [2M+Na]⁺.

7.2.6.7. *N*²-*n*-Octyl-2',3'-*O*-isopropylidenguanosine (**102**)C₂₁H₃₃N₅O₅; MW 435.52

n-OctNH₂ (0.41 mL, 2.48 mmol) was added to a solution of **101** (253 mg, 0.50 mmol) in 2-methoxyethanol (6.10 mL) under inert atmosphere. The resulting dark brown solution was protected from light exposure and stirred at 85°C for 3 days. The mixture was concentrated under reduced pressure and filtered on silica (CH₂Cl₂-MeOH, 8.6:1.4), diluted with AcOEt (10 mL), washed with 2 M HCl (4x5 mL) and dried over Na₂SO₄. The organic phase was concentrated under reduced pressure and the brown oil crude was purified by flash column chromatography (CH₂Cl₂-MeOH, 9.2:0.8) to obtain **102** as a yellow foam (119 mg, 0.27 mmol).

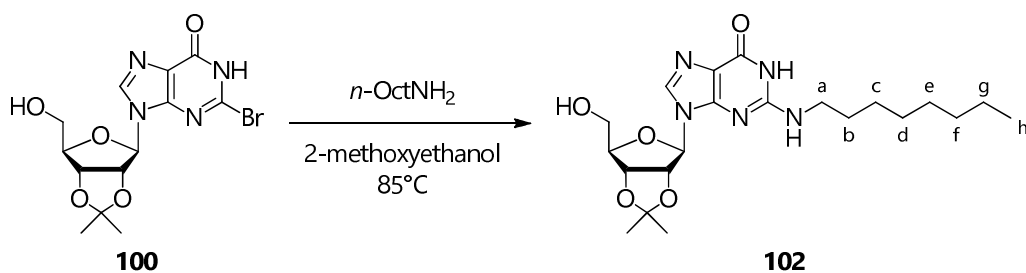
Yield: 55%



TBAF·3H₂O (51 mg, 0.16 mmol) was added to a solution of **103** (74 mg, 0.13 mmol) in THF (1.50 mL) under inert atmosphere. The resulting yellow solution was stirred at RT for 6 h, during which time it became pale orange and a precipitate was formed.

The mixture was diluted with CH₂Cl₂ (3 mL), washed with H₂O (2x2 mL) and dried over Na₂SO₄. The solvent was removed under reduced pressure and the yellow oil crude was purified by flash column chromatography (CH₂Cl₂-MeOH, 9.2:0.8) to obtain **102** as an off-white powder (34 mg, 0.08 mmol).

Yield: 60%



n-OctNH₂ (0.47 mL, 2.84 mmol) was added to a solution of **100** (138 mg, 0.36 mmol) in 2-methoxyethanol (4.40 mL) under inert atmosphere. The resulting orange solution was protected from light exposure and stirred at 85°C for 8 days.

The mixture was diluted with AcOEt (10 mL), washed with 2 M HCl (4x5 mL) and dried over Na₂SO₄. The solvent was removed under reduced pressure and the yellow oil crude was purified by flash column chromatography (CH₂Cl₂-MeOH, 9.3:0.7) to obtain **102** as a yellow foam (61 mg, 0.14 mmol).

Yield: **39%**

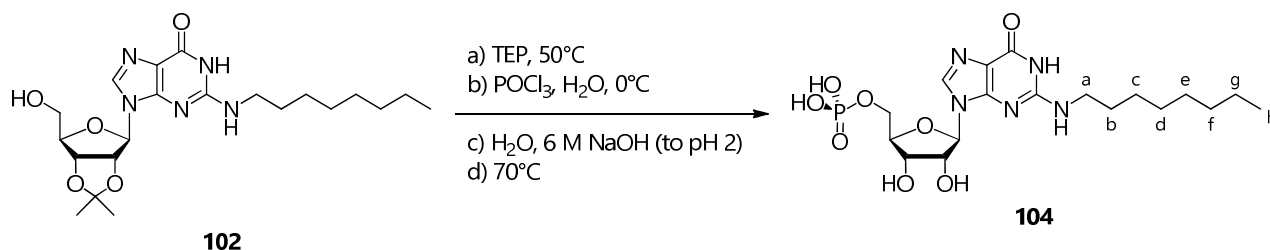
R_f: 0.35 (CH₂Cl₂-MeOH, 9:1)

¹H NMR (DMSO-*d*₆, 400 MHz): δ (ppm) 10.62 (br s, 1H N¹H), 7.88 (s, 1H, H⁸), 6.53 (t, *J* = 5.4 Hz, 1H, NHCH₂), 5.99 (d, *J* = 2.8 Hz, 1H, H¹), 5.31 (dd, *J* = 6.0, 2.8 Hz, 1H, H²), 4.98 (t, *J* = 5.6 Hz, 1H, OH⁵), 4.91 (dd, *J* = 6.2, 3.1 Hz, 1H, H³), 4.12 (dt, *J* = 5.3, 2.8 Hz, 1H, H⁴), 3.47-3.57 (m, 2H, H^{5a}, H^{5b}), 3.31-3.21 (m, 2H, CH₂^a), 1.64-1.50 (m, 2H, CH₂^b), 1.53 (s, 3H, C(CH₃)₂), 1.32 (s, 3H, C(CH₃)₂), 1.24-1.29 (m, 10H, CH₂^c, CH₂^d, CH₂^e, CH₂^f, CH₂^g), 0.85 (t, *J* = 6.8 Hz, 3H, CH₃^h).

¹³C NMR (DMSO-*d*₆, 100 MHz): δ (ppm) 157.6 (C⁶), 153.5 (C²), 151.1 (C⁴), 137.2 (C⁸), 117.8 (C⁵), 113.8 (C(CH₃)₂), 89.6 (C¹), 87.4 (C⁴), 84.2 (C²), 82.2 (C³), 62.5 (C⁵), 41.4 (C^a), 32.1 (C^b), 29.6, 29.51, 29.45 (C^c, C^d, C^e), 27.9, 26.0 (C(CH₃)₂), 27.2 (C^f), 22.9 (C^g), 14.7 (C^h).

MS (ESI⁺): *m/z* calcd for [C₂₁H₃₃N₅O₅]⁺: 435.25; found: 436.08 [M+H]⁺, 458.30 [M+Na]⁺, 871.21 [2M]⁺, 893.15 [2M+Na]⁺.

MS (ESI-Q-ToF⁺): *m/z* calcd for [C₂₁H₃₃N₅O₅]⁺: 435.25; found: 458.83 [M+Na]⁺, 894.18 [2M+H+Na]⁺.

7.2.6.8. *N*²-*n*-Octylguanylic acid (**104**)C₁₈H₃₀N₅O₈P; MW 475.43

A suspension of **102** (30 mg, 69 μ mol) in TEP (230 μ L) was stirred at 50°C for 15' under inert atmosphere. POCl₃ (39 μ L, 418 μ mol) and H₂O (1.4 μ L, 78 μ mol) were added at 0°C and the resulting mixture was stirred at 0°C for 6 h. The disappearance of the substrate was monitored by TLC (EtOH-H₂O, 7:3; *R*_f = 0.87). After adding H₂O (344 μ L), pH was adjusted to 2 with 6 M NaOH and the resulting colourless solution was stirred at 70-80°C for 2 h.

The mixture was neutralized with 6 M NaOH, diluted with H₂O (60 mL) and freeze-dried. The resulting crude was purified by semi-preparative HPLC to get **104** as a white powder (24 mg, 50 μ mol).

Yield: **73%**

Time (min)	Column volumes	% A (H ₂ O/0.1% TFA)	% B ((H ₂ O/0.1% TFA)-CH ₃ CN, 4:1)
0 - 2	0.5	100	0
2 - 50	12	60 \rightarrow 0	40 \rightarrow 100

*R*_f: 0.74 (EtOH-H₂O, 7:3)HPLC *t*_R: 17.3' (55.4% B)

¹H NMR (DMSO-*d*₆, 400 MHz): δ (ppm) 10.52 (br s, 1H, N¹H), 7.90 (s, 1H, H⁸), 6.50 (br s, 1H, NHCH₂), 5.73 (br d, *J* = 5.4 Hz, 1H, H^{1'}), 4.53 (br t, *J* = 4.4 Hz, 1H, H^{2'}), 4.15 (br s, 1H, H^{3'}), 4.07-3.86 (m, 3H, H^{4'}, H^{5'a}, H^{5'b}), 3.32-3.20 (m, 2H, CH₂^a), 1.58-1.46 (br t, *J* = 5.4 Hz, 2H, CH₂^b), 1.38-1.17 (m, 10H, CH₂^c, CH₂^d, CH₂^e, CH₂^f, CH₂^g), 0.85 (br t, *J* = 6.0 Hz, 3H, CH₃^h).

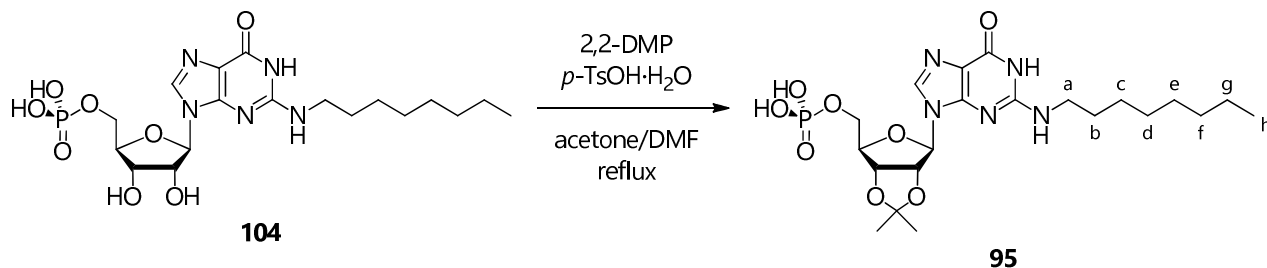
¹H NMR (D₂O, 400 MHz): δ (ppm) 8.00 (s, 1H, H⁸), 5.91 (d, *J* = 5.6 Hz, 1H, H^{1'}), 4.68 (t, *J* = 5.4 Hz, 1H, H^{2'}), 4.42 (t, *J* = 4.5 Hz, 1H, H^{3'}), 4.22 (br d, *J* = 2.5 Hz, 1H, H^{4'}), 4.02 (dd, *J* = 11.7, 4.4 Hz, 1H, H^{5'a}), 3.97 (dd, *J* = 12.0, 4.6 Hz, 1H, H^{5'b}), 3.28 (qt, *J* = 3.4, 6.9 Hz, 2H, CH₂^a), 1.55-1.45 (m, 2H, CH₂^b), 1.30-1.06 (m, 10H, CH₂^c, CH₂^d, CH₂^e, CH₂^f, CH₂^g), 0.72 (t, *J* = 6.6 Hz, 3H, CH₃^h).

¹³C NMR (D₂O, 100 MHz): δ (ppm) 158.0 (C⁶), 152.6 (C²), 151.7 (C⁴), 137.0 (C⁸), 114.6 (C⁵), 86.9 (C^{1'}), 83.5 (d, ³*J*_{CP} = 7.1 Hz, C^{4'}), 74.6 (C^{2'}), 70.2 (C^{3'}), 64.8 (br d, ²*J*_{CP} = 3.2 Hz, C^{5'}), 41.0 (C^a), 29.0 (C^b), 31.6, 29.1, 28.8 (C^c, C^d, C^e), 26.8 (C^f), 22.3 (C^g), 13.6 (C^h).

³¹P NMR (D₂O, 161 MHz): δ (ppm) 1.44.

MS (ESI⁻): *m/z* calcd for [C₁₈H₃₀N₅O₈P]⁻: 475.18; found: 474.32 [M-H]⁻, 496.34 [M-2H+Na]⁻, 949.10 [2M-H]⁻, 971.15 [2M-2H+Na]⁻.

MS (ESI-Q-ToF⁺): *m/z* calcd for [C₁₈H₃₀N₅O₈P]⁺: 475.18; found: 476.29 [M+H]⁺, 498.27 [M+Na]⁺.

7.2.6.9. *N*²-*n*-Octyl-2',3'-*O*-isopropylidene-guanylic acid (**95**)C₂₁H₃₄N₅O₈P; MW 515.50

2,2-DMP (2.14 mL, 17.40 mmol) and *p*-TsOH·H₂O (16 mg, 84.11 μmol) were added to a suspension of **104** (40 mg, 84.13 μmol) in a dry 8:1 acetone-DMF mixture (2.40 mL) under inert atmosphere and the resulting mixture was refluxed for 26 h.

The suspension was neutralized with saturated aqueous NaHCO₃ and freeze-dried. The crude was purified by semi-preparative HPLC to obtain **95** as a white solid (35 mg, 68 μmol).

Yield: **81%**

Time (min)	Column volumes	% A (H ₂ O)	% B (H ₂ O-CH ₃ CN, 4:1)
0 - 2	0.5	95	5
2 - 50	12	95 → 40	5 → 60

*R*_f: 0.35 (*n*-BuOH-AcOH-H₂O, 4:1:1)HPLC *t*_R: 42.8' (47.5% B)

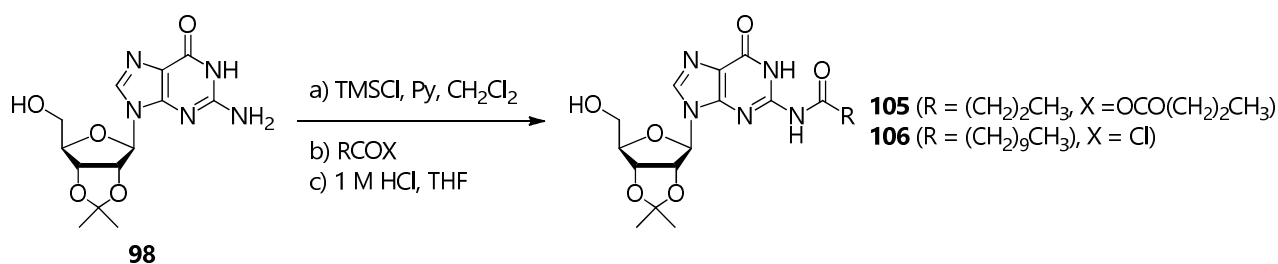
¹H NMR (D₂O, 400 MHz): δ (ppm) 8.01 (s, 1H, H⁸), 6.06 (br d, *J* = 2.0 Hz, 1H, H^{1'}), 5.30 (br dd, *J* = 5.0, 2.8 Hz, 1H, H^{2'}), 5.05 (br dd, *J* = 6.0, 1.9 Hz, 1H, H^{3'}), 4.46 (br dd, *J* = 6.4, 4.1 Hz, 1H, H^{4'}), 3.91-3.84 (m, 2H, H^{5'a}, H^{5'b}), 3.29 (ddq, *J* = 20.3, 13.6, 6.9 Hz, 2H, CH₂^a), 1.57 (s, 3H, C(CH₃)₂), 1.56-1.49 (m, 2H, CH₂^b), 1.35 (s, 3H, C(CH₃)₂), 1.31-1.08 (m, 10H, CH₂^c, CH₂^d, CH₂^e, CH₂^f, CH₂^g), 0.73 (br t, *J* = 6.7 Hz, 3H, CH₃^h).

¹³C NMR (D₂O, 100 MHz): δ (ppm) 158.9 (C⁶), 152.7 (C²), 151.4 (C⁴), 137.2 (C⁸), 115.3 (C⁵), 113.8 (C(CH₃)₂), 89.2 (C^{1'}), 85.3 (C^{4'}), 84.4 (C^{2'}), 81.5 (C^{3'}), 64.4 (C^{5'}), 41.1 (C^a), 31.7 (C^b), 26.7, 24.7 (C(CH₃)₂), 29.2, 28.9, 26.9 (C^c, C^d, C^e, C^f), 22.4 (C^g), 13.7 (C^h).

³¹P NMR (D₂O, 161 MHz): δ (ppm) 3.33.

MS (ESI⁺): *m/z* calcd for [C₂₁H₃₄N₅O₈P]⁺: 515.21; found: 538.55 [M+Na]⁺, 1053.38 [2M+Na]⁺.

MS (ESI⁻): *m/z* calcd for [C₂₁H₃₄N₅O₈P]⁻: 515.21; found: 514.24 [M-H]⁻, 1051.07 [2M-2H+Na]⁻.

7.2.6.10. General procedure for the synthesis of *N*²-acyl-2',3'-*O*-isopropylidene-guanosines (**105** and **106**)

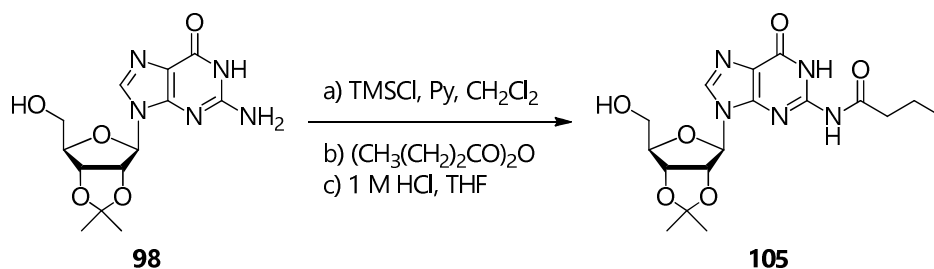
TMSCl (2.70 mL, 21.27 mmol) was added dropwise to a suspension of **98** (969 mg, 3.00 mmol) in a dry 5:1 CH₂Cl₂/pyridine mixture (90.0 mL) under inert atmosphere at 0°C. The resulting mixture was stirred at RT for 4 h, becoming more transparent, and the appropriate acylating agent (3.30 mmol) was added dropwise over 2' at 0°C. The reaction was stirred at RT and monitored by TLC (CH₂Cl₂ saturated with NH₃-MeOH, 9:1) until complete consumption of the starting material.

The solution was washed with 1 M HCl (2x60 mL) and saturated aqueous NaHCO₃ (2x60 mL) and dried over Na₂SO₄. The solvent was evaporated under reduced pressure, removing residual pyridine by co-evaporation with toluene.

The resulting yellow foam was dissolved in a 1:1 1 M HCl/THF mixture (30 mL) and stirred at RT for 2 h. CH₂Cl₂ (150 mL) was added, the solution was washed with H₂O (90 mL) and dried over Na₂SO₄. After removing the solvent under reduced pressure, the resulting crude was purified by flash column chromatography (CH₂Cl₂-MeOH, 20:1 for **105** and 25:1 for **106**).

7.2.6.10.1. *N*²-Butyryl-2',3'-*O*-isopropylidene-guanosine (**105**)

C₁₇H₂₃N₅O₆; MW 393.39



White powder (740 mg, 1.88 mmol).

Yield: **63%**

*R*_f: 0.29 (CH₂Cl₂-MeOH, 20:1)

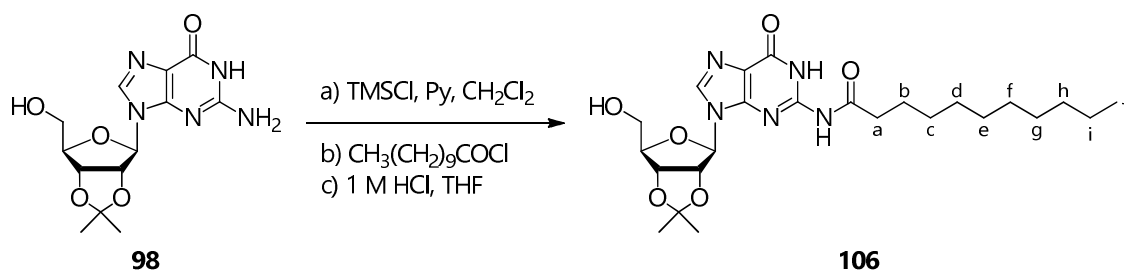
¹H NMR (CDCl₃, 400 MHz): δ (ppm) 12.28 (br s, 1H, N¹H), 9.82 (br s, 1H, N²H), 8.14 (s, 1H, H⁸), 5.93 (d, *J* = 3.0 Hz, 1H, H^{1'}), 5.19 (dd, *J* = 6.0, 3.0 Hz, 1H, H^{2'}), 5.15 (dd, *J* = 6.2, 1.7 Hz, 1H, H^{3'}), 4.39 (q, *J* = 2.7 Hz, 1H, H^{4'}), 4.38-4.24 (br s, 1H, OH^{5'}), 4.00 (dd, *J* = 12.2, 3.0 Hz, 1H, H^{5'a}), 3.82 (dd, *J* = 12.2, 2.6 Hz, 1H, H^{5'b}), 2.57 (t, *J* = 7.4 Hz, 2H, COCH₂), 1.76 (hex, *J* = 7.4 Hz, 2H, CH₂CH₃), 1.60 (s, 3H, C(CH₃)₂), 1.37 (s, 3H, C(CH₃)₂), 1.01 (t, *J* = 7.4 Hz, 3H, CH₃).

^{13}C NMR (CDCl_3 , 100 MHz): δ (ppm) 175.2 (COCH_2), 155.1 (C^6), 147.6 (C^2), 147.2 (C^4), 138.4 (C^8), 121.3 (C^5), 114.0 ($\text{C}(\text{CH}_3)_2$), 91.8 ($\text{C}^{1'}$), 86.3 ($\text{C}^{4'}$), 83.7 ($\text{C}^{2'}$), 81.0 ($\text{C}^{3'}$), 62.3 ($\text{C}^{5'}$), 38.7 (COCH_2), 27.1 ($\text{C}(\text{CH}_3)_2$), 25.0 ($\text{C}(\text{CH}_3)_2$), 18.0 (CH_2CH_3), 13.3 (CH_3).

MS (ESI⁺): m/z calcd for $[\text{C}_{17}\text{H}_{23}\text{N}_5\text{O}_6]^+$: 393.16; found: 394.52 $[\text{M}+\text{H}]^+$, 416.71 $[\text{M}+\text{Na}]^+$, 787.38 $[2\text{M}+\text{H}]^+$, 809.46 $[2\text{M}+\text{Na}]^+$.

7.2.6.10.2. *N*²-Undecanoyl-2',3'-*O*-isopropylidene-*g*uanosine (106)

$\text{C}_{24}\text{H}_{37}\text{N}_5\text{O}_6$; MW 491.58



Light yellow powder (914 mg, 1.86 mmol).

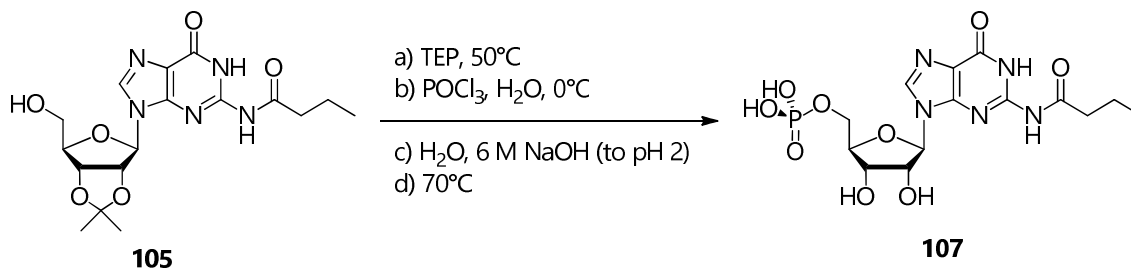
Yield: **62%**

R_f : 0.37 (CH_2Cl_2 -MeOH, 20:1)

^1H NMR (CDCl_3 , 400 MHz): δ (ppm) 12.27 (br s, 1H, N^1H), 9.81 (br s, 1H, N^2H), 8.07 (s, 1H, H^8), 5.91 (d, $J = 3.2$ Hz, 1H, $\text{H}^{1'}$), 5.19 (dd, $J = 6.0, 3.3$ Hz, 1H, $\text{H}^{2'}$), 5.09 (dd, $J = 6.0, 1.8$ Hz, 1H, $\text{H}^{3'}$), 4.39 (br dd, $J = 5.1, 3.0$ Hz, 1H, $\text{H}^{4'}$), 3.96 (dd, $J = 12.0, 2.6$ Hz, 1H, $\text{H}^{5'a}$), 3.80 (dd, $J = 12.1, 2.6$ Hz, 1H, $\text{H}^{5'b}$), 2.56 (t, $J = 7.5$ Hz, 2H, CH_2^a), 1.76-1.64 (m, 2H, CH_2^b), 1.59 (s, 3H, $\text{C}(\text{CH}_3)_2$), 1.40-1.21 (m, 17H, $\text{CH}_2^c, \text{CH}_2^d, \text{CH}_2^e, \text{CH}_2^f, \text{CH}_2^g, \text{CH}_2^h, \text{CH}_2^i, \text{C}(\text{CH}_3)_2$), 0.89 (t, $J = 6.8$ Hz, 3H, CH_3^j).

^{13}C NMR (CDCl_3 , 100 MHz): δ (ppm) 174.9 (COCH_2), 154.0 (C^6), 147.1 (C^2), 146.4 (C^4), 139.0 (C^8), 119.6 (C^5), 113.2 ($\text{C}(\text{CH}_3)_2$), 91.2 ($\text{C}^{1'}$), 85.9 ($\text{C}^{4'}$), 83.0 ($\text{C}^{2'}$), 80.4 ($\text{C}^{3'}$), 61.4 ($\text{C}^{5'}$), 36.1 (C^a), 30.9, 28.5, 28.4, 28.3, 28.2, 28.0 ($\text{C}^c, \text{C}^d, \text{C}^e, \text{C}^f, \text{C}^g, \text{C}^h$), 26.2 ($\text{C}(\text{CH}_3)_2$), 24.2 ($\text{C}(\text{CH}_3)_2$), 23.7 (C^b), 21.6 (C^i), 13.1 (C^j).

MS (ESI⁺): m/z calcd for $[\text{C}_{24}\text{H}_{37}\text{N}_5\text{O}_6]^+$: 491.27; found: 514.59 $[\text{M}+\text{Na}]^+$, 1005.38 $[2\text{M}+\text{Na}]^+$.

7.2.6.11. *N*²-Butyrylguanylic acid (**107**)C₁₄H₂₀N₅O₉P; MW 433.31

A suspension of **105** (54 mg, 137 μmol) in TEP (460 μL) was stirred at 50°C for 30' under inert atmosphere. POCl₃ (78 μL, 837 μmol) and H₂O (2.8 μL, 156 μmol) were added at 0°C and the resulting mixture was stirred at 0°C for 6 h. The disappearance of the substrate was monitored by TLC (EtOH-H₂O, 7:3; *R_f* = 0.84). After adding H₂O (688 μL), pH was adjusted to 2 with 6 M NaOH and the resulting colourless solution was stirred at 70-80°C for 2 h.

The mixture was neutralized with 6 M NaOH, diluted with H₂O (150 mL) and freeze-dried. The resulting crude was purified by semi-preparative HPLC to get **107** as a white powder (44 mg, 102 μmol).

Yield: 75%

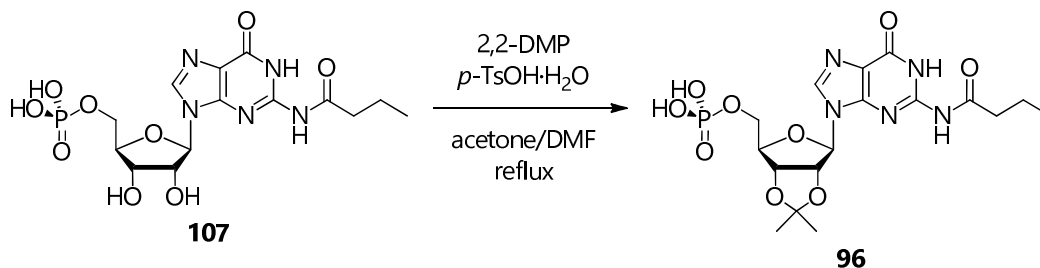
Time (min)	Column volumes	% A (H ₂ O/0.1% TFA)	% B ((H ₂ O/0.1% TFA)-CH ₃ CN, 4:1)
0 - 2	0.5	100	0
2 - 50	12	60 → 0	40 → 100

R_f: 0.72 (EtOH-H₂O, 7:3)HPLC *t_R*: 16.4' (52.6% B)

¹H NMR (D₂O, 400 MHz): δ (ppm) 8.30 (s, 1H, H⁸), 6.04 (d, *J* = 6.0 Hz, 1H, H^{1'}), 4.88 (t, *J* = 5.6 Hz, 1H, H^{2'}), 4.55 (t, *J* = 4.0 Hz, 1H, H^{3'}), 4.44-4.39 (dt, *J* = 5.2, 3.1 Hz, 1H, H^{4'}), 4.23-4.13 (m, 2H, H^{5'a}, H^{5'b}), 2.57 (t, *J* = 7.2 Hz, 2H, COCH₂), 1.76 (hex, *J* = 7.6 Hz, 2H, CH₂CH₃), 1.03 (t, *J* = 7.2 Hz, 3H, CH₃).

¹³C NMR (D₂O, 100 MHz): δ (ppm) 178.2 (COCH₂), 157.2 (C⁶), 149.4 (C²), 147.6 (C⁴), 139.8 (C⁸), 120.0 (C⁵), 87.7 (C^{1'}), 84.1 (d, ³*J*_{CP} = 8.4 Hz, C^{4'}), 73.7 (C^{2'}), 70.5 (C^{3'}), 64.5 (br d, ²*J*_{CP} = 4.3 Hz, C^{5'}), 38.3 (COCH₂), 18.0 (CH₂CH₃), 12.7 (CH₃).

³¹P NMR (D₂O, 161 MHz): δ (ppm) 1.64.MS (ESI): *m/z* calcd for [C₁₄H₂₀N₅O₉P]⁻: 433.10; found: 433.61 [M]⁻, 455.88 [2M+Na]⁻.

7.2.6.12. *N*²-Butyryl-2',3'-*O*-isopropylidene-guanilylic acid (**96**)C₁₇H₂₄N₅O₉P; MW 473.37

2,2-DMP (2.95 mL, 23.99 mmol) and *p*-TsOH·H₂O (23 mg, 121 μmol) were added to a suspension of **107** (50 mg, 115 μmol) in a dry 4:1 acetone-DMF mixture (1.70 mL) under inert atmosphere and the resulting mixture was refluxed for 6 h.

The suspension was neutralized with 3 M NaOH and freeze-dried. The crude was purified by semi-preparative HPLC to obtain **96** as a white solid (16 mg, 34 μmol).

Yield: 30%

Time (min)	Column volumes	% A (H ₂ O)	% B (H ₂ O-CH ₃ CN, 4:1)
0 - 4	1	95	5
4 - 48	10	95 → 0	5 → 100

*R*_f: 0.26 (*n*-BuOH-AcOH-H₂O, 4:1:1)

HPLC *t*_R: 51.6' (23.1% B)

¹H NMR (D₂O, 400 MHz): δ (ppm) 8.16 (s, 1H, H⁸), 6.10 (d, *J* = 2.8 Hz, 1H, H¹), 5.33 (dd, *J* = 6.1, 2.8 Hz, 1H, H²), 5.18 (dd, *J* = 6.1, 2.1 Hz, 1H, H³), 4.55 (dd, *J* = 5.7, 4.4 Hz, 1H, H⁴), 3.96 (dt, *J* = 11.3, 4.6 Hz, 1H, H^{5a}), 3.88 (dd, *J* = 11.3, 5.0 Hz, 1H, H^{5b}), 2.47 (t, *J* = 7.4 Hz, 2H, COCH₂), 1.64 (hex, *J* = 7.4 Hz, 2H, CH₂CH₃), 1.58 (s, 3H, C(CH₃)₂), 1.37 (s, 3H, C(CH₃)₂), 0.90 (t, *J* = 7.4 Hz, 3H, CH₃).

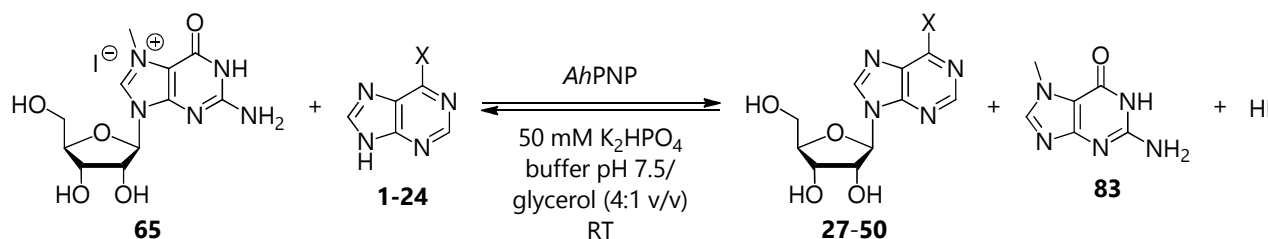
¹³C NMR (D₂O, 100 MHz): δ (ppm) 178.2 (COCH₂), 157.4 (C⁶), 151.7 (C²), 147.7 (C⁴), 142.4 (C⁸), 114.6 (C⁵, C(CH₃)₂), 90.9 (C¹), 85.7 (C⁴), 84.1 (C²), 81.6 (C³), 64.1 (C⁵), 38.4 (C^a), 26.1, 24.3 (C(CH₃)₂), 18.1 (C^b), 12.7 (C^c).

³¹P NMR (D₂O, 161 MHz): δ (ppm) 2.03.

MS (ESI): *m/z* calcd for [C₁₇H₂₄N₅O₉P]⁻: 473.13; found: 473.47 [M]⁻, 495.36 [M-H+Na]⁻, 946.56 [2M]⁻, 967.52 [2M-2H+Na]⁻, 1418.19 [3M-H]⁻.

7.2.7. Batch and flow synthesis of ribonucleosides

7.2.7.1. General procedure for the batch synthesis of 6-substituted purine ribonucleosides catalyzed by AhPNP



AhPNP (1.15 IU) was added at 25°C to a solution of **65** (1.0 mM) and **1-24** (1.0 mM) in a 4:1 (v/v) 50 mM K₂HPO₄ buffer pH 7.5/glycerol mixture (20 mL). At fixed times (10', 30', 1 h, 3 h, 6 h and 24 h), aliquots (200 μL) of the reaction mixture were withdrawn, centrifuged on 10 kDa MWCO centrifugal filter devices (12000 rpm, 25°C) for 2' and the solution was analyzed by analytical HPLC.

The formed nucleosides **27-50** were identified by comparison of their retention times in analytical HPLC with those of pure samples.

HPLC method 1:

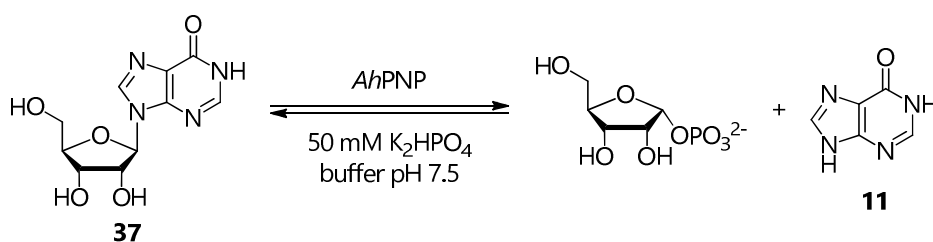
Time (min)	% A (10 mM K ₂ HPO ₄ buffer pH 3.2 or 4.5)	% B (MeOH)
0 - 20	97 → 35	3 → 65
20 - 30	35	65

HPLC method 2:

Time (min)	% A (10 mM K ₂ HPO ₄ buffer pH 3.2 or 4.5)	% B (MeOH)
0 - 25	97 → 30	3 → 70

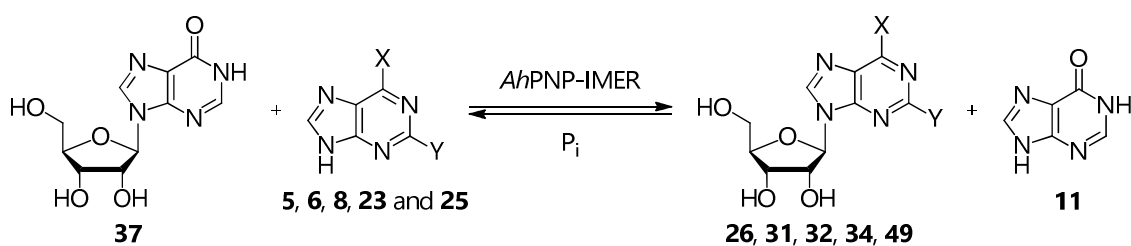
HPLC method 3:

Time (min)	% A (10 mM K ₂ HPO ₄ buffer pH 3.2 or 4.5)	% B (MeOH)
0 - 15	97	3
15 - 25	97 → 50	3 → 50

7.2.7.2. *Ah*PNP-IMER activity assay

A solution of **37** (40 mM) in 0.1 M K_2HPO_4 buffer pH 7.5 (5 mL) was pumped once through the *Ah*PNP-IMER at 37°C, collected, diluted with the analytical HPLC mobile phase (1:10) and analyzed on-line.

Time (min)	% A (H_2O)	% B (MeOH)
0 - 15	90	10

7.2.7.3. General procedure for the flow synthesis of 6-substituted purine ribonucleosides catalyzed by *Ah*PNP-IMER

A solution of **5**, **6**, **8**, **23**, or **25** (2.5 mM for **5** and **6** and 5 mM for **8**, **23** and **25**) and **37** (2:1 *donor/acceptor* ratio) in 10 mM K_2HPO_4 buffer pH 7.5 (10 mL for **5** and **6** and 5 mL for **8**, **23** and **25**) with DMSO as co-solvent (5.0 mL for **8** and **23** and 7.5 mL for **5**) was recirculated through the *Ah*PNP-IMER at 0.5 mL·min⁻¹ and 37°C. Each reaction was performed in duplicate and monitored on-line by the analytical HPLC set to assess the time necessary to reach the equilibrium (10' for **8** and **25**, 20' for **5** and **6** and 30' for **23**).

In all cases, a third reaction was carried out and purified on-line by the semi-preparative HPLC apparatus.

Analytical scale

For **27**:

Time (min)	% A (H_2O)	% B (MeOH)
0 - 15	90	10

For **31** and **32**:

Time (min)	% A (10 mM NH_4OAc buffer pH 5.5)	% B (MeOH)
0 - 6	90	10
6 - 15	90 → 60	10 → 40

For **34** and **49**:

Time (min)	% A (10 mM NH ₄ OAc buffer pH 5.5)	% B (MeOH)
0 - 6	90	10
6 - 15	90 → 85	10 → 15

For **58**:

Time (min)	% A (10 mM NH ₄ OAc buffer pH 5.5)	% B (MeOH)
0 - 6	90	10
6 - 15	90 → 80	10 → 20

Semi-preparative scale

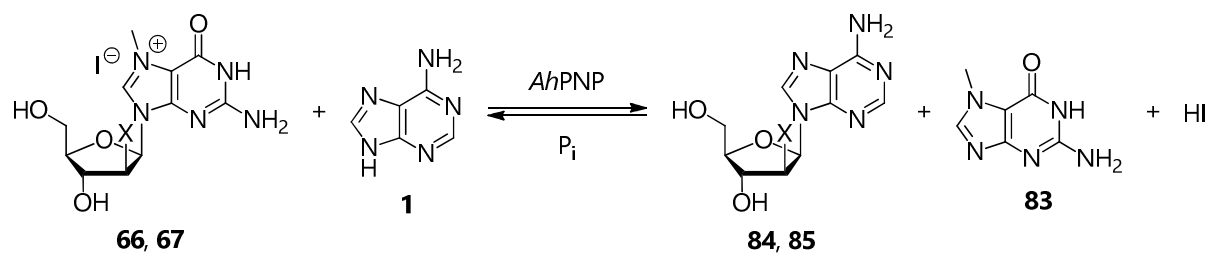
For **31** and **32**:

Time (min)	% A (10 mM NH ₄ OAc buffer pH 5.5)	% B (MeOH)
0 - 30	50	50

For **34**, **49** and **58**:

Time (min)	% A (10 mM NH ₄ OAc buffer pH 5.5)	% B (MeOH)
0 - 60	90	10

7.2.7.4. General procedure for the batch synthesis of 2'-deoxyadenosine (**84**) and arabinosyladenine (**85**) catalyzed by *AhpNP*



AhpNP (0.20 IU for **66** and 2.00 IU for **67**) was added at 25°C to a solution of **66** or **67** (1.0 mM) and **1** (1.0 mM) in a 4:1 (v/v) 50 mM K_2HPO_4 buffer pH 7.5/glycerol mixture (20 mL). At fixed times (10', 30', 1 h, 3 h, 6 h and 24 h), aliquots (200 μ L) of the reaction mixture were withdrawn, centrifuged on 10 kDa MWCO centrifugal filter devices (12000 rpm, 25°C) for 2' and the solution was analyzed by analytical HPLC.

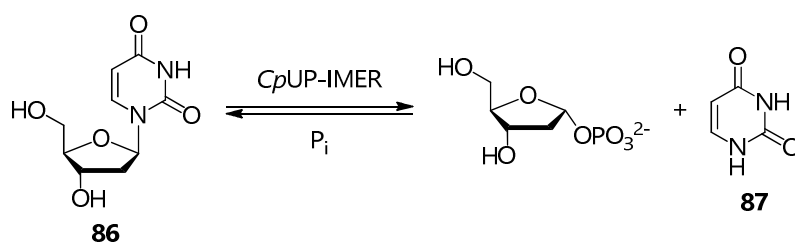
The formed nucleoside **84** was identified by comparison of its retention time in analytical HPLC with those of pure samples. The formation of **85** was not detected.

For **84**:

Time (min)	% A (10 mM K_2HPO_4 buffer pH 4.5)	% B (MeOH)
0 - 15	97	3
15 - 35	97 \rightarrow 50	3 \rightarrow 50

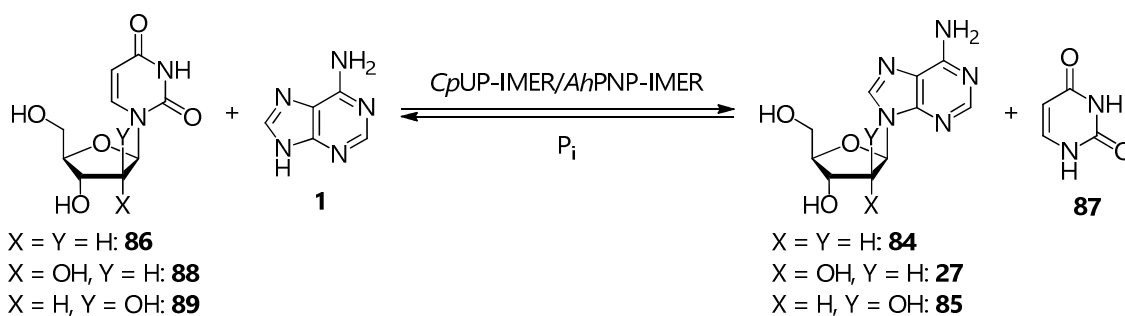
For **85**:

Time (min)	% A (10 mM K_2HPO_4 buffer pH 4.5)	% B (MeOH)
0 - 20	95	5

7.2.7.5. *CpUP-IMER* activity assay

A solution of **86** (40 mM) in 0.1 M K_2HPO_4 buffer pH 7.5 (5 mL) was pumped once through the *CpPNP-IMER* at 37°C, collected, diluted with the analytical HPLC mobile phase (1:10) and analyzed on-line.

Time (min)	% A (H_2O)	% B (MeOH)
0 - 15	90	10

7.2.7.6. General procedure for the flow synthesis of 2'-deoxyadenosine (**84**), adenosine (**27**) and arabinosyladenine (**85**) catalyzed by *CpUP-IMER/AhpPNP-IMER*

A solution of **1** (5 mM for **86** and **88** and 1 mM for **89**) and **86**, **88** or **89** (2:1 donor/acceptor ratio) in 10 mM K_2HPO_4 buffer pH 7.25 (10 mM for **86** and **88** or 2 mM for **89**, 10 mL) was recirculated through the combined *CpUP-IMER* and *AhpPNP-IMER* system at $0.5 \text{ mL} \cdot \text{min}^{-1}$ and 37°C. Each reaction was performed in duplicate and monitored on-line by the analytical HPLC set to assess the time necessary to reach the equilibrium.

For **84** and **27**:

Time (min)	% A (10 mM K_2HPO_4 buffer pH 5.5)	% B (MeOH)
0 - 15	95 → 85	5 → 15

For **85**:

Time (min)	% A (10 mM K_2HPO_4 buffer pH 4.5)	% B (MeOH)
0 - 15	95 → 80	5 → 20

Collaborations and acknowledgements

This PhD Thesis is the result of a joint cooperation among four research groups which fruitfully shared goals, ideas, expertise, facilities and people:

- the Laboratory of Organic Chemistry (**Prof. Giovanna Speranza, Dr. Carlo F. Morelli and Dr. Carla D. Serra**) at the Department of Chemistry of the University of Milan;
- the Laboratory of Pharmaceutical Biocatalysis (**Dr. Daniela Ubiali, Dr. Giulia Cattaneo, Dr. Teodora Bavaro and Dr. Immacolata Serra**) and the Laboratory of Pharmaceutical Analysis (**Prof. Enrica Calleri and Prof. Gabriella Massolini**) at the Department of Drug Sciences of the University of Pavia;
- the Laboratory of Molecular and Cellular Pharmacology of Purinergic Transmission (**Dr. Stefania Ceruti and Dr. Chiara Parravicini**) at the Department of Pharmacological and Biomolecular Sciences of the University of Milan;
- the Center for Drug Research (**Dr. Georg Höfner and Prof. Klaus T. Wanner**) at the Faculty of Chemistry and Pharmacy of the Ludwig Maximilian University of Munich (Munich, Germany).

Special thanks are due to **Dr. Giulia Cattaneo** (PhD) for the development of the LC-ESI-MS/MS method which was carried out during her stay in Munich under the supervision of **Prof. Klaus Wanner**.

The enzymes (*HsPNP* and *MtPNP*) used to perform the LC-ESI-MS/MS assay were kindly supplied by **Dr. Marcela C. De Moraes** at the Federal University of São Paulo (Department of Chemistry, São Paulo, Brazil).

Molecular modeling studies on the human GPR17 receptor were performed by **Dr. Chiara Parravicini** at the University of Milan (Department of Pharmacological and Biomolecular Sciences).

Sincere thanks are due to **Prof. Igor A. Mikhailopulo** (National Academy of Sciences of Belarus, Institute of Bioorganic Chemistry, Minsk, Belarus) and **Prof. Gennaro Piccialli** (University of Naples Federico II, Department of Pharmacy, Naples) for their careful, thoughtful and extensive review of this PhD Thesis, as well as for their constructive suggestions.

References

- [1] L. P. Jordheim, D. Durantel, F. Zoulim, C. Dumontet *C. Nat. Rev. Drug Discov.* **2013**, *12*, 447-464.
- [2] a) D. M. Huryn, M. Okabe *Chem. Rev.* **1992**, *92*, 1745-1768; b) E. De Clercq *J. Clin. Virol.* **2004**, *30*, 115-133.
- [3] C. M. Galmarini *Electron. J. Oncol.* **2002**, 22-32.
- [4] a) M. Lemke, D. A. Williams *Foye's principles of medicinal chemistry*, Wolters Kluwer Health, Lippincot Williams and Wilkins, Balimora, USA; b) H. P. Rang, M. M. Dale, J. M. Ritter, R. J. Flower, *Pharmacology 6TH Ed.*, Elsevier Maison, **2006**; c) E. De Clercq, J. Neyts *Handb. Exp. Pharmacol.* **2009**, *189*, 53-84; d) O. O. Adetokunboh, A. Schoonees, T. A. Balogun, C. S. Wiysonge *BMC Infect. Dis.* **2015**, *15*, 469/1-469/13.
- [5] a) E. Beutler, L. D. Piro, A. Saven, A. C. Kay, R. McMillan, R. Longmir, C. J. Carrera, P. Morin, D. A. Carson *Leuk. Lymphoma* **1991**, *5*, 1-8; b) F. E. Parkinson, K. A. Rudolphi, B. B. Fredholm *Gen. Pharmacol.* **1994**, *25*, 1053-1058; c) C. B. Yoo, P. A. Jones *Nat. Rev. Drug Discov.* **2006**, *5*, 37-50.
- [6] a) P. Cairolì, S. Pieraccini, M. Sironi, C. F. Morelli, G. Speranza, P. Manitto *J. Agric. Food Chem.* **2008**, *56*, 1043-1050; b) C. F. Morelli, G. Speranza, P. Manitto *Flavor Fragr. J.* **2011**, *26*, 279-281.
- [7] L. C. Jimmerson, C. W. Clayton, S. MaWhinney, E. G. Meissner, Z. Sims, S. Kottlilil, J. J. Kiser *Antiviral Res.* **2016**, *138*, 79-85.
- [8] a) L. Childs-Kean *Clin. Ther.* **2015**, *37*, 243-267; b) A. Perez-Pitarch, B. Guglieri-Lopez, R. Ferriols-Lisart, M. Merino-Sanjuan *Int. J. Antimicrob. Agents*, **2016**, *47*, 184-194.
- [9] A. H. Yau, E. M. Yshida *Can. J. Gastroenterol. Hepatol.* **2014**, *28*, 445-451.
- [10] a) J.-F. Wang, L. R. Zhang, Z.-J. Yang, L.-H. Zhang *Bioorg. Med. Chem. Lett.* **2004**, *12*, 1425-1429; b) P. Šilhár, M. Hocek, R. Pohl, I. Votruba, I. Shih, E. Mabery, R. Mackman *Bioorg. Med. Chem.* **2008**, *16*, 2329-2366; c) I. Serra, S. Daly, A. R. Alcantara, D. Bianchi, M. Terreni, D. Ubiali *RSC Adv.* **2015**, *5*, 23569-23577.
- [11] M. Hocek, P. Šilhár, I. Shih, E. Mabery, R. Mackman *Bioorg. Med. Chem. Lett.* **2006**, *16*, 5290-5293.
- [12] a) A. Bzowska, E. Kulikowska, D. Shugar *Pharmacol. Ther.* **2000**, *88*, 349-425; b) J. A. Secrist III, W. B. Parker, P. W. Allan, L. L. Bennett, W. R. Waud, J. W. Truss, A. T. Fowler, J. A. Montgomery, S. E. Ealick, A. H. Wells, G. Y. Gillespie, V. K. Gadi, E. J. Sorscher *Nucleos. Nucleot.* **1999**, *18*, 745-757; c) S. A. Kaliberov, D. J. Buchsbaum *Expert Opin. Drug Deliv.* **2006**, *3*, 37-51; d) Y. Zhang, W. B. Parker, E. J. Sorscher, S. E. Ealick *Curr. Top. Med. Chem.* **2005**, *5*, 1259-1274.
- [13] a) M. J. Pugmire, S. E. Ealick *Biochem. J.* **2002**, *361*, 1-25; b) V. Nair, B. Bera, E. R. Kern *Nucleos. Nucleot. Nucl.* **2003**, *22*, 115-127; c) S. A. Kaliberov, D. J. Buchsbaum *Expert Opin. Drug Deliv.* **2006**, *3*, 37-51.
- [14] a) L. B. Townsend *Chemistry of nucleosides and nucleotides, vol. 1*, Plenum Press, New York and London, **1988** and references within; b) H. Vorbruggen, C. Ruh-Pohlenz *Handbook in nucleosides synthesis*, Wiley, New York, **2001**.
- [15] A. Yamazaki, I. Kumashiro, T. Takenishi *J. Org. Chem.* **1967**, *32*, 3258-3260.
- [16] M. Okutsu, A. Yamazaki *Nucleic Acids Res.* **1976**, *3*, 231-235.
- [17] a) K. Imai, R. Marumoto, K. Kobayashi, Y. Yoshioka, J. Toda, M. Honjo *Chem. Pharm. Bull.* **1971**, *19*, 576-786; b) K. Omura, R. Marumoto, Y. Furukawa *Chem. Pharm. Bull.* **1981**, *29*, 1870-1875.
- [18] R. J. Rousseau, R. K. Robins, L. B. Townsend *J. Am. Chem. Soc.* **1968**, *90*, 2661-2668.
- [19] G. Shaw, R. N. Warrener, M. H. Maguire, R. K. Ralph *J. Chem. Soc.* **1958**, 2294-2299.
- [20] N. J. Cusack, B. J. Hildick, D. H. Robinson, P. W. Rugg, G. Shaw *J. Chem. Soc., Perkin Trans.* **1973**, *16*, 1720-1731.
- [21] M. Sano *Chem. Pharm. Bull.* **1962**, *10*, 308-313.

- [22] S. D'Errico, G. Oliviero, N. Borbone, V. Piccialli, V. D'Atri, L. Mayol, G. Piccialli *Eur. J. Org. Chem.* **2013**, 30, 6948-6954.
- [23] S. D'Errico, G. Oliviero, N. Borbone, F. Nici, V. Piccialli, B. Pinto, D. D'Alonzo, L. Mayol, G. Piccialli *Eur. J. Org. Chem.* **2015**, 2015(10), 2244-2249.
- [24] S. D'Errico, G. Oliviero, J. Amato, N. Borbone, V. Cerullo, A. Hemminki, V. Piccialli, S. Zaccaria, L. Mayola, G. Piccialli *Chem. Commun.* **2012**, 48, 9310-9312.
- [25] a) M. Hoffer *Chem. Ber.* **1960**, 93, 2777-2781; b) M. J. Robins, R. K. Robins *J. Am. Chem. Soc.* **1965**, 87, 4934-4940; c) C. C. Bhat *Synthetic procedures in nucleic acid chemistry*, W. W. Zorbach and R. S. Tipson Ed., **1968**, 521; d) M. J. Robins, R. K. Robins *J. Org. Chem.* **1969**, 34, 2160-2163; e) F. F. Christensen, A. D. Broom, M. J. Robins, A. Bloch *J. Med. Chem.* **1972**, 15, 735-739;
- [26] a) E. Fischer, B. Felferich *Chem. Ber.* **1914**, 47, 210-233; b) H. J. Leonard, R. A. Laursen *Biochemistry* **1965**, 4, 354-365; c) Z. Kazimierczuk, H. B. Cottam, G. R. Revankar, R. K. Robins *J. Am. Chem. Soc.* **1984**, 106, 6379-6382; d) H. Vorbrüggen, C. Ruh-Pohlentz *Synthesis of nucleosides in organic reactions*, Wiley, New York, **2000**.
- [27] J. A. Montgomery, K. Hewson *J. Heterocyclic Chem.* **1964**, 1, 213-214.
- [28] M. Prystaš, J. Farkaš, F. Šorm *Collect. Czech. Chem. Commun.* **1965**, 30, 3123-3133.
- [29] a) U. Niedballa, H. Vorbrüggen *Angew. Chem. Int. Ed.* **1970**, 9, 461-462; b) U. Niedballa, H. Vorbrüggen *Angew. Chem.* **1970**, 82, 449-450; c) U. Niedballa, H. A. Vorbrüggen *J. Org. Chem.* **1974**, 39, 3654-3660; d) U. Niedballa, H. Vorbrüggen *J. Org. Chem.* **1974**, 39, 3660-3663; e) U. Niedballa, H. Vorbrüggen *J. Org. Chem.* **1974**, 39, 3664-3667; f) U. Niedballa, H. Vorbrüggen *J. Org. Chem.* **1974**, 39, 3668-3671; g) H. Vorbrüggen, K. Krolkiewicz, B. Bennua *Chem. Ber.* **1981**, 114, 1234-1255.
- [30] B. C. Bookser, N. B. Raffaele *J. Org. Chem.* **2007**, 72, 173-179.
- [31] F. W. Lichtenthaler, K. Kitahara *Angew. Chem. Int. Ed.* **1975**, 14, 815-816.
- [32] a) C.-H. Wong, G. M. Whitesides *Enzymes in synthetic organic chemistry*, Pergamon, Oxford, **1994**; b) A. K. Prasad, S. Trikha, V. S. Parmar *Bioorg. Chem.* **1999**, 27, 135-154; c) E. S. Lewkowicz, A. M. Iribarren *Curr. Org. Chem.* **2006**, 10, 1197-1215; d) I. A. Mikhailopulo *Curr. Org. Chem.* **2007**, 11, 317-335; e) I. A. Mikhailopulo, A. I. Miroshnikov *Mendeleev Commun.* **2011**, 21, 57-68; f) L. E. Iglesias, E. S. Lewkowicz, R. Medici, P. Bianchi, A. M. Iribarren *Biotechnol. Adv.* **2015**, 33, 412-434.
- [33] a) W.-D. Fessner *Biocatalysis from discovery to application*, Springer Desktop Edition in Chemistry, **2000**; b) K. Faber *Biotransformations*, Springer Desktop Edition in Chemistry, **2000**.
- [34] a) T. Utagawa *J. Mol. Cat. B*, **1999**, 6, 215-222; b) G. Cotticelli, P. Magri, M. Grisa, G. Orsini, G. Tonon, G. Zuffi *Nucleos. Nucleot.* **1999**, 18, 1135-1136; c) K. Yokozeki, T. Tsuji *J. Mol. Cat. B* **2000**, 10, 207-213.
- [35] J. M. Guisán *Immobilization of Enzymes and Cells*, Springer International Publishing AG., **2006**.
- [36] K. Drauz, H. Gröger, O. May *Enzyme catalysis in organic synthesis: a comprehensive handbook*, VCH, Weinheim, **2002**.
- [37] T. A. Krenitsky *J. Biol. Chem.* **1968**, 243, 2871-2875.
- [38] M. Friedkin *J. Biol. Chem.* **1950**, 184, 449-459.
- [39] A. Konrad, J. Piškur, D. A. Liberles *Gene* **2012**, 510, 154-161.
- [40] R. A. Caceres, L. F. S. M. Timmers, R. G. Ducati, D. O. N. da Silva, L. A. Basso, W. F. de Azevedo Jr., D. S. Santos *Biochimie* **2012**, 94, 155-165.
- [41] R. A. Caceres, L. F. Timmers, I. Pauli, L. M. Gava, R. G. Ducati, L. A. Basso, D. S. Santos, W. F. de Azevedo *J. Struct. Biol.* **2010**, 169, 379-388.
- [42] G. Mikleusevic, Z. Stefanic, M. Narczyk, B. Wielgus-Kutrowska, A. Bzowska, M. Luic, PDB DOI: 10.2210/pdb3ooh/pdb, ID: 3OOH.

- [43] a) S. E. Ealick, S. A. Rule, D. C. Carter, T. J. Greenhough, Y. S. Babu, W. J. Cook, J. Habash, J. R. Helliwell, J.D. Stoeckler, R. E. Parks *J. Biol. Chem.* **1990**, *265*, 1812-1820; b) S. V. L. Narayana, C. E. Bugg, S. E. Ealick *Acta Cryst.* **1997**, *D53*, 131-142.
- [44] A. A. Edwards, J. D. Tipton, M. D. Brenowitz, M. R. Emmett, A. G. Marshall, G. B. Evans, P. C. Tyler, V. L. Schramm *Biochemistry* **2010**, *49*, 2058-2067.
- [45] C. Mao, W. J. Cook, M. Zhou, G. W. Koszalka, T. A. Krenitsky, S.E. Ealick *Structure* **1997**, *5*, 1373-1383.
- [46] Z. Štefanić, G. Mikleušević, M. Narczyk, B. Wielgus-Kutrowska, A. Bzowska, M. Luić *Croat. Chem. Acta* **2013**, *86*, 117-127.
- [47] F. Canduri, V. Fadel, L. A. Basso, M. S. Palma, D. S. Santos, W. Filgueira de Azevedo Jr *Biochem. Biophys. Res. Commun.* **2005**, *327*, 646-649.
- [48] E. M. Bennett, C. Li, P. W. Allan, W. B. Parker, S. E. Ealick *J. Biol. Chem.* **2003**, *278*, 47110-47118.
- [49] G. Koellner, A. Bzowska, B. Wielgus-Kutrowska, M. Luić, T. Steiner, W. Saenger, J. Stepieński *J. Mol. Biol.* **2002**, *315*, 351-371.
- [50] C. Mao, W. J. Cook, M. Zhou, A. A. Federov, S. C. Almo, S. E. Ealick *Biochemistry*, **1998**, *37*, 7135-7146.
- [51] C. B. Barnett, K. J. Naidoo *J. Phys. Chem. B*, **2013**, *117*, 6019-6026.
- [52] G. B. Evans, V. L. Schramm, P. C. Tyler *Curr. Med. Chem.* **2015**, *22*, 3897-3909.
- [53] a) P. C. Kline, V. L. Schramm *Biochemistry*, **1993**, *32*, 13212-13219; b) P. C. Kline, V. L. Schramm *Biochemistry*, **1995**, *34*, 1153-1162.
- [54] M.-C. Ho, W. Shi, A. Rinaldo-Matthis, P. C. Tyler, G. B. Evans, K. Clinch, S. C. Almo, V. L. Schramm *Proc. Natl. Acad. Sci. U. S. A.* **2010**, *107*, 4805-4812.
- [55] A. Lewandowicz, V. L. Schramm *Biochemistry* **2004**, *43*, 1458-1468.
- [56] T. A. Krenitsky, G. W. Koszalka, J. V. Tuttle *Biochemistry* **1981**, *20*, 3615-3621.
- [57] W. J. Hennen, C. H. Wong *J. Org. Chem.* **1989**, *54*, 4692-4695.
- [58] W. Shen, J.-S. Kim, P. E. Kish, J. Zhang, S. Mitchell, B. G. Gentry, J. M. Breitenbach, J. C. Drach, J. Hilfinger *Bioorg. Med. Chem. Lett.* **2009**, *19*, 792-796.
- [59] a) H. Ghanem, E. Jabbour, S. Faderl, V. Gandhi, W. Plunkett, H. Kantarjian *Expert Rev. Hematol.* **2010**, *3*, 15-22; b) I. V. Fateev, K. V. Antonov, I. D. Konstantinova, T. I. Muravyova, F. Seela, R. S. Esipov, A. I. Miroshnikov, I. A. Mikhailopulo *Beilstein J. Org. Chem.* **2014**, *10*, 1657-1669.
- [60] a) X. Zhou, K. Szeker, L.-Y. Jiao, M. Oestreich, I. A. Mikhailopulo, P. Neubauer *Adv. Synth. Catal.* **2015**, *357*, 1237-1244; b) X. Zhou, I. A. Mikhailopulo, M. N. Cruz Bournazou, P. Neubauer *J. Mol. Catal. B* **2015**, *115*, 119-127.
- [61] I. D. Konstantinova, K. V. Antonov, I. V. Fateev, A. I. Miroshnikov, V. A. Stepchenko, A. V. Baranovsky, I. A. Mikhailopulo *Synthesis* **2011**, *10*, 1555-1560.
- [62] J. A. Trelles, A. L. Valino, V. Runza, E. S. Lewkowicz, A. M. Iribarren *Biotechnol. Lett.* **2005**, *27*, 759-763.
- [63] a) C. D. Serra *Developing enzymes for synthetic applications. A study of nucleoside phosphorylases as biocatalysts in transglycosylation reactions*, **2009**; b) D. Ubiali, C. D. Serra, I. Serra, C.F. Morelli, M. Terreni, A. M. Albertini, P. Manitto, G. Speranza *Adv. Synth. Catal.* **2012**, *354*, 96-104.
- [64] A. A. Lashkov, N. E. Zhukhlistova, T. A. Seregina, A. G. Gabdulkhakov, and A. M. Mikhailov *Crystallogr. Rep.* **2011**, *56*, 560-589.
- [65] *Global tuberculosis report 2016*, World Health Organization (http://www.who.int/tb/publications/global_report/en/).
- [66] a) D. G. Russell, C. E. Barry III, J. L. Flynn *Science* **2010**, *328*, 852-856; b) Z. Ma, C. Lienhardt, H. McIlleron, A. J. Nunn, X. Wang *Lancet* **2010**, *375*, 2100-2109.

- [67] a) R. C. Goldman, K. V. Plumley, B. E. Laughon *Infect. Disord. Drug Targets* **2007**, *7*, 73-91; b) C. Dye *Nat. Rev. Microbiol.* **2009**, *7*, 81-87; c) A. A. Velayati, M. R. Masjedi, P. Farnia, P. Tabarsi, J. Ghanavi, A. H. Ziazarifi, S. E. Hoffner *Chest.* **2009**, *136*, 420-425.
- [68] G. Riccardi, S. T. Cole *Science* **2009**, *8*, 801-804.
- [69] G. Manina, M. Bellinzoni, M. R. Pasca, J. Neres, A. Milano A, A. L. de Jesus Lopes Ribeiro, S. Buroni, H. Škovlerová, P. Dianišková, K. Mokušová, J. Maráv, V. Makarov, D. Giganti, G. Degiacomi, G. Riccardi *Mol. Microbiol.* **2010**, *77*, 1172-1185.
- [70] R. G. Ducati, A. Breda, L. A. Basso, D. S. Santos *Curr. Med. Chem.* **2011**, *18*, 1258-1275.
- [71] a) E. A. T. Ringia, V. L. Schramm *Curr. Top. Med. Chem.* **2005**, *5*, 1237-1258; b) D. C. Madrid, L.-M. Ting, K. L. Waller, V. L. Schramm, K. Kim *J. Biol. Chem.* **2008**, *283*, 35899-35907; c) T. Donaldson, K. Kim *Infect. Disord. Drug Targets* **2010**, *10*, 191-199.
- [72] a) L. F. Timmers, R. A. Caceres, A. L. Vivian, L. M. Gava, R. Dias, R. G. Ducati, L. A. Basso, D. S. Santos, W. F. de Azevedo *Arch. Biochem. Biophys.* **2008**, *479*, 28-38; b) R. G. Ducati, L. A. Basso, D. S. Santos, W. F. de Azevedo *Bioorg. Med. Chem.* **2010**, *18*, 4769-4774.
- [73] A. Lewandowicz, W. Shi, G. B. Evans, P. C. Tyler, R. H. Furneaux, L. A. Basso, D. S. Santos, S. C. Almo, V. L. Schramm *Biochemistry* **2003**, *42*, 6057-6066.
- [74] a) W. Shi, L. A. Basso, D. S. Santos, P. C. Tyler, R. H. Furneaux, J. S. Blanchard, S. C. Almo, V. L. Schramm *Biochemistry* **2001**, *40*, 8204-8215; b) W. F. de Azevedo Jr., R. A. Caceres, L. F. S. M. Timmers, R. G. Ducati, L. A. Rosado, L. A. Basso, D. S. Santos, PDB DOI: 10.2210/pdb3scz/pdb, ID: 3SCZ.
- [75] a) E. A. Taylor Ringia, P. C. Tyler, G. B. Evans, R. H. Furneaux, A. S. Murkin, V. L. Schramm *J. Am. Chem. Soc.* **2006**, *128*, 7126-7127; b) R. G. Ducati, D. S. Santos, L. A. Basso *Arch. Biochem. Biophys.* **2009**, *486*, 155-164.
- [76] I. S. Kazmers, B. S. Mitchell, P. E. Dadonna, L. L. Wotring, L. B. Townsend, W. N. Kelley *Science* **1981**, *214*, 1137-1139.
- [77] a) S. Saen-Oon, S. Quaytman-Machleder, V. L. Schramm, S. D. Schwartz *Proc. Natl. Acad. Sci. U. S. A.* **2008**, *105*, 16543-16548; b) S. Saen-Oon, M. Ghanem, V. L. Schramm, S. D. Schwartz *Biophys. J.* **2008**, *94*, 4078-4088.
- [78] C. M. Blackburn, M. J. Gait *Nucleic acids in chemistry and biology*, Oxford University Press **1996**.
- [79] J. Donohue, K. N. Trueblood *J. Mol. Biol.* **1960**, *2*, 363-371.
- [80] C. Moreau, G. A. Ashamu, V. C. Bailey, A. Galione, A. H. Guse, B. V. L. Potter *Org. Biomol. Chem.* **2011**, *9*, 278-290.
- [81] a) R. Stolarski, C. E. Hlagberg, D. Shugar *Eur. J. Biochem.* **1984**, *138*, 187-192; b) S. S. Tavale, H. M. J. Sobell *Mol. Biol.* **1970**, *48*, 109-123.
- [82] a) M. Orozco, C. Lluís, J. Mallol, E. I. Canela, R. Franco *Quant. Struct. Act. Relat.* **1989**, *8*, 109-114; b) M. Orozco, E. I. Canela, R. Franco *Mol. Pharmacol.* **1989**, *35*, 257-264.
- [83] a) M. Ikehara, S. Uesugi, K. Yoshida *Biochemistry* **1972**, *11*, 830-836; b) R. H. Sarma, C.-H. Lee, F. E. Evans, N. Yathindra, M. Sundaralingam *J. Am. Chem. Soc.* **1974**, *96*, 7337-7348.
- [84] S. Uesugi, M. Ikehara *J. Am. Chem. Soc.* **1977**, *99*, 3250-3253.
- [85] V. Nair, D. A. Young *Magn. Reson. Chem.* **1987**, *25*, 937-940.
- [86] F. Jordan, H. Niv *Biochim. Biophys. Acta* **1977**, *476*, 265-271.
- [87] a) M. Bartolini, V. Cavrini, V. Andrisano *J. Chromatogr. A* **2004**, *1031*, 27-34; b) E. Calleri, C. Temporini, E. Perani, C. Stella, S. Rudaz, D. Lubda, G. Mellerio, J. Veuthey, G. Caccialanza, G. Massolini *J. Chromatogr. A* **2004**, *1045*, 99-109; c) E. M. Forsberg, J. R. Green, J. D. Brennan *Anal. Chem.* **2011**, *83*, 5230-5236; d) E. Calleri, C. Temporini, G. Massolini *J. Pharm. Biomed. Anal.* **2011**, *54*, 911-925; e) M. C.

- de Moraes, R. G. Ducati, A. J. Donato, L. A. Basso, D. S. Santos, C. L. Cardoso, Q. B. Cass *J. Chromatogr. A* **2012**, *1232*, 110-115.
- [88] A. M. Girelli, E. Mattei *J. Chrom. B* **2005**, *819*, 3-16.
- [89] a) D. M. Roberge, B. Zimmermann, F. Rainone, M. Gottsponer, M. Eyholzer, N. Kockmann *Org. Process Res. Dev.* **2008**, *12*, 905-910; b) M. D. Hopkin, I. R. Baxendale, S. V. Ley *Chem. Commun.* **2010**, *46*, 2450-2452.
- [90] a) L. Tamborini, D. Romano, A. Pinto, M. Contente, M. C. Iannuzzi, P. Conti, F. Molinari *Tetrahedron Lett.* **2013**, *54*, 6090-6093; b) J. Lawrence, B. O'Sullivan, G. J. Lye, R. Wohlgemuth, N. Szita *J. Mol. Catal. B: Enzym.* **2013**, *95*, 111-117.
- [91] V. Sotolongo, D. V. Johnson, D. Wahnou, I. W. Wainer *Chirality*, **1999**, *11*, 39-45.
- [92] a) J. J. Roy, T. E. Abraham *Chem. Rev.* **2004**, *104*, 3705-3721; b) R. A. Sheldon *Adv. Synth. Catal.* **2007**, *349*, 1289-1307.
- [93] A. Illanes *Comprehensive biotechnology*, Elsevier B. V. **2011**, 25-39.
- [94] a) P. Bonomi, T. Bavaro, I. Serra, A. Tagliani, M. Terreni, D. Ubiali *Molecules* **2013**, *18*, 14349-14365; b) D. N. Tran, K. J. Balkus *ACS Catalysis* **2011**, *1*, 956-968.
- [95] a) L. Cao *Carrier-bound immobilized enzymes. Principles, application and design*, Wiley-VCH, Weinheim, **2005**; b) I. Serra, C. D. Serra, S. Rocchietti, D. Ubiali, M. Terreni *Enzyme Microb. Technol.* **2011**, *49*, 52-58.
- [96] a) J. Mehta, N. Bhardwaj, S. K. Bhardwaj, K.-H. Kim, A. Deep *Coord. Chem. Rev.* **2016**, *322*, 30-40; b) J. Campos-Teran, I. Inarritu, J. Aburto, E. Torres, Eduardo *Proteins in Solution and at Interfaces*, 335-351, John Wiley & Sons, **2013**; c) D. I. Fried, F. J. Brieler, M. Froeba *ChemCatChem* **2013**, *5*, 862-884.
- [97] a) N. Vasylieva, S. Marinesco *Neuromethods* **2013**, *80*, 95-114; b) A. S. Drozdov, O. E. Shapovalova, V. Ivanovski, D. Avnir, V. V. Vinogradov *Chem. Mater.* **2016**, *28*, 2248-2253; c) S. Chuanoi, Y. Anraku, M. Hori, A. Kishimura, K. Kataoka *Biomacromolecules* **2014**, *15*, 2389-2397; d) M. Cantarella, F. Alfani, L. Cantarella, A. Gallifuoco *Methods in Biotechnology*, 67-76, Springer International Publishing AG., **1997**.
- [98] M. C. de Moraes, C. L. Cardoso, Q.B. Cass *Anal. Bioanal. Chem.* **2013**, *405*, 4871-4878.
- [99] a) S. Rocchietti, D. Ubiali, M. Terreni, A. M. Albertini, R. Fernández-Lafuente, J. M. Guisán, M. Pregnotato *Biomacromolecules* **2004**, *5*, 2195-2200; b) D. Ubiali, S. Rocchietti, F. Scaramozzino, M. Terreni, A. M. Albertini, R. Fernández-Lafuente, J. M. Guisán, M. Pregnotato *Adv. Synth. Catal.* **2004**, *346*, 1361-1366.
- [100] I. Serra, T. Bavaro, D. A. Cecchini, S. Dalyc, A. M. Albertini, M. Terreni, D. Ubiali *J. Mol. Cat. B* **2013**, *95*, 16-22.
- [101] I. Serra, D. Ubiali, J. Piškur, S. Christoffersen, E. S. Lewkowicz, A. M. Iribarren, A. M. Albertini, M. Terreni *ChemPlusChem* **2013**, *78*, 157-165.
- [102] E. Calleri, D. Ubiali, I. Serra, C. Temporini, G. Cattaneo, G. Speranza, C. F. Morelli, G. Massolini *J. Chromatogr. B* **2014**, *968*, 79-86.
- [103] R. Appel *Angew Chem. Int. Ed.* **1975**, *14*, 801-811.
- [104] I. Serra, S. Conti, J. Piškur, A. R. Clausen, B. Munch-Petersen, M. Terreni, D. Ubiali *Adv. Synth. Catal.* **2014**, *356*, 563-570.
- [105] F. Hansske, D. Madej, M. J. Robins *Tetrahedron*, **1984**, *40*, 125-135.
- [106] A. P. Mehta, S. H. Abdelwahed, H. Xu, T. P. Begley *J. Am. Chem. Soc.* **2014**, *136*, 10609-10614.
- [107] M. Gruen, C. Becker, A. Beste, C. Siethoff, A. J., R. S. Goody *Nucleos. Nucleot.* **1999**, *18*, 137-151.
- [108] J. J. Voegel, M. M. Altolfer, S. A. Benner *Helv. Chim. Acta* **1993**, *76*, 2061-2069.

- [109] D. Ubiali, C. F. Morelli, M. Rabuffetti, G. Cattaneo, I. Serra, T. Bavaro, A. M. Albertini, G. Speranza *Curr. Org. Chem.* **2015**, *19*, 2220-2225.
- [110] E. Calleri, G. Cattaneo, M. Rabuffetti, I. Serra, T. Bavaro, G. Massolini, G. Speranza, D. Ubiali *Adv. Synth. Catal.* **2015**, *357*, 2520-2528.
- [111] S. Yamato, N. Kawakami, K. Shimada, M. Ono, N. Idei, Y. Itoh *J. Chromatogr. A* **2000**, *896*, 171-181; b) M. Ono, N. Idei, T. Nakajima, Y. Itoh, N. Kawakami, K. Shimada, S. Yamato *J. Pharm. Biomed. Anal.* **2002**, *29*, 325-334; c) S. Yamato, N. Kawakami, K. Shimada, M. Ono, N. Idei, Y. Itoh, E. Tachikawa *Biol. Pharm. Bull.* **2004**, *27*, 210-215.
- [112] M. M. Bradford *Anal. Biochem.* **1976**, *72*, 248-254.
- [113] T. M. Kadia, V. Gandhi *Exp. Rev. Hematol.* **2017**, *10*, 1-8.
- [114] a) G. Massolini, E. Calleri, A. Lavecchia, F. Loiodice, D. Lubda, C. Temporini, G. Fracchiolla, P. Tortorella, E. Novellino, G. Caccialanza *Anal. Chem.* **2003**, *75*, 535-542; b) C. Temporini, E. Perani, F. Mancini, M. Bartolini, E. Calleri, D. Lubda, G. Felix, V. Andrisano, G. Massolini *J. Chromatogr. A* **2006**, *1120*, 121-131.
- [115] G. Cattaneo, D. Ubiali, E. Calleri, M. Rabuffetti, G. C. Hofner, K. T. Wanner, M. C. De Moraes, L. K. B. Martinelli, D. S. Santos, G. Speranza *Anal. Chim. Acta* **2016**, *943*, 89-97.
- [116] a) Y. Yang, Y. Chen, H. Aloysius, D. Inoyama, L. Hu *Enzyme Technologies*, 165-235, John Wiley & Sons, **2010**; b) F. Angelucci, A. E. Miele, G. Boumis, M. Brunori, D. Dimastrogiovanni, A. Bellelli *Curr. Top. Med. Chem.* **2011**, *11*, 2012-2028; c) X. Xie, J. Guo, Y. Kong, G. X. Xie, L. Li, N. Lv, X. Xiao, J. Tang, X. Wang, P. Liu *J. Gene Med.* **2011**, *13*, 680-691; d) J. J. Kraus, O. De Crescenzo, R. G. Harrison *PLoS One*, **2013**, *8*, e76403; e) K. P. Guillen, C. Kurkjian, R. G. Harrison *J. Biomed. Sci.* **2014**, *21*, 65/1-65/8.
- [117] J. V. Tuttle, T. A. Krenitsky *J. Biol. Chem.* **1984**, *259*, 4065-4069.
- [118] D. Gonsalvez, A. H. Ferner, H. Peckham, S. S. Murray, J. Xiao *Neuropharm.* **2016**, *110*, 586-593.
- [119] a) N. Baumann, D. Pham-Dinh *Physiol. Rev.* **2001**, *81*, 871-927; b) N. G. Bauer, C. Richter-Landsberg, C. Ffrench-Constant *Glia* **2009**, *57*, 1691-1705; c) F. Biname, D. Sakry, L. Dimou, V. Jolivel, J. Trotter *J. Neurosci.* **2013**, *33*, 10858-10874; d) J. T. Ahrendsen, W. Macklin *Neurosci. Bull.* **2013**, *29*, 199-215; e) S. Mitew, C. M. Hay, H. Peckham, J. Xiao, M. Koenning, B. Emery *Neuroscience* **2014**, *276*, 29-47.
- [120] a) R. S. Fields, B. Stevens *Trends Neurosci.* **2000**, *23*, 625-633.; b) R. D. Fields, G. Burnstock *Nat. Rev. Neurosci.* **2006**, *7*, 423-436; c) A. Verkhratsky, O. A. Krishtal, G. Burnstock *Mol. Neurobiol.* **2009**, *39*, 190-208; d) M. Fumagalli, S. Daniele, D. Lecca, P. R. Lee, C. Parravicini, R. D. Fields, P. Rosa, F. Antonucci, C. Verderio, M. L. Trincavelli, P. Bramanti, C. Martini, M. P. Abbracchio *J. Biol. Chem.* **2011**, *286*, 10593-10604; e) G. Burnstock *BJU Int.* **2011**, *107*, 192-204; f) G. Burnstock *Neuropharm.* **2015**, *104*, 4-17.
- [121] M. Congreve, C. J. Langmead, J. S. Mason, F. H. Marshall *J. Med. Chem.* **2011**, *54*, 4283-4311.
- [122] B. K. Kobilka *Biochim. Biophys. Acta* **2007**, *1768*, 794-807.
- [123] M. C. Lagerstrom, H. B. Schioth *Nat. Rev. Drug Discovery* **2008**, *7*, 339-357.
- [124] a) H. Ren, I. J. Orozco, Y. Su, S. Suyama, R. Gutierrez-Juarez, T. L. Horvath, S. L. Wardlaw, L. Plum, O. Arancio, D. Accili *Cell* **2012**, *149*, 1314-1326; b) B. Zhao, C. Z. Zhao, X. Y. Zhang, X. Q. Huang, W. Z. Shi, S. H. Fang, Y. B. Lu, W. P. Zhang, Q. Xia, E. Q. Wei *Neuroscience* **2012**, *202*, 42-57; c) A.-D. Qi, T. K. Harden, R. A. Nicholas *J. Pharm. Exp. Ther.* **2013**, *347*, 38-46; d) T. Kendall Harden *Sci. Signal.* **2013**, *6*, pe34/1-pe34/4; e) S. Hennen, H. Wang, L. Peters, N. Merten, K. Simon, A. Spinrath, S. Blaettermann, R. Akkari, R. Schrage, R. Schroeder, D. Schulz, C. Vermeiren, K. Zimmermann, S. Kehraus, C. Drewke, A. Pfeifer, G. M. Koenig, K. Mohr, M. Gillard, C. E. Mueller, Q. R. Lu, J. Gomez, E. Kostenis *Sci. Signal.* **2013**, *6*, ra93/1-ra93/17; f) S. Cosentino, L. Castiglioni, F. Colazzo, E. Nobili, E.

- Tremoli, R. Rosa, M. P. Abbracchio, L. Sironi, M. Pesce *J. Cell. Mol. Med.* **2014**, *18*, 1785-1796; g) E. Zappelli, S. Daniele, M. P. Abbracchio, C. Martini, M. L. Trincavelli *Int. J. Mol. Sci.* **2014**, *15*, 6252-6264; h) Y. L. Xing, P. T. Roth, J. A. S. Stratton, B. H. A. Chuang, J. Danne, S. L. Ellis, S. W. Ng, T. J. Kilpatrick, T. D. Merson *J. Neurosci.* **2014**, *34*, 14128-14146; j) K. Simon, S. Hennen, N. Merten, S. Blaettermann, M. Gillard, E. Kostenis, J. Gomeza *J. Biol. Chem.* **2016**, *291*, 705-718; i) H. Ren, J. R. Cook, N. Kon, D. Accili *Diabetes* **2015**, *64*, 3670-3679; k) C. Parravicini, S. Daniele, L. Palazzolo, M. L. Trincavelli, C. Martini, P. Zaratini, R. Primi, G. Coppolino, E. Gianazza, M. P. Abbracchio, I. Eberini *Cell. Signal.* **2016**, *28*, 631-642; l) M. Boccazzi, D. Lecca, D. Marangon, F. Guagnini, M. P. Abbracchio, S. Ceruti *Purinergic Signal.* **2016**, *12*, 661-672; m) G. Marucci, D. Dal Ben, C. Lambertucci, C. Santinelli, A. Spinaci, A. Thomas, R. Volpini, M. Buccioni *ChemMedChem* **2016**, *11*, 2567-2574; n) Z. Ou, Y. Sun, L. Lin, N. You, X. Liu, H. Li, Y. Ma, L. Cao, Y. Han, M. Liu *J. Neurosci.* **2016**, *36*, 10560-10573; o) A. R. Mendelsohn, J. W. Larrick *Rejuvenation Res.* **2016**, *19*, 521-524.
- [125] a) M.P. Abbracchio, G. Burnstock, J. M. Boeynaems, E. A. Barnard, J. L. Boyer, C. Kennedy, G. E. Knight, M. Fumagalli, C. Gachet, K. A. Jacobson, G. A. Weisman, G.A. *Pharmacol. Rev.* **2006**, *58*, 281-341; b) D. Lecca, M. L. Trincavelli, P. Gelosa, L. Sironi, P. Ciana, M. Fumagalli, G. Villa, C. Verderio, C. Grumelli, U. Guerrini, E. Tremoli, P. Rosa, S. Cuboni, C. Martini, A. Buffo, M. Cimino, M. P. Abbracchio *PLoS One* **2008**, *3*, e3579.
- [126] a) C. Parravicini, G. Ranghino, M. P. Abbracchio, P. Fantucci *BMC Bioinformatics* **2008**, *9*, 263; b) C. Parravicini, M. P. Abbracchio, P. Fantucci, G. Ranghino *BMC Struct. Biol.* **2010**, *10*, 8; c) E. Calleri, S. Ceruti, G. Cristalli, C. Martini, C. Temporini, C. Parravicini, R. Volpini, S. Daniele, G. Caccialanza, D. Lecca, C. Lambertucci, M. L. Trincavelli, G. Marucci, I. W. Wainer, G. Ranghino, P. Fantucci, M. P. Abbracchio, G. Massolini *J. Med. Chem.* **2010**, *53*, 3489-3501.
- [127] a) L. Mamedova, V. Capra, M. R. Accomazzo, Z. G. Gao, S. Ferrario, M. Fumagalli, M. P. Abbracchio, G. E. Rovati, K. A. Jacobson *Biochem. Pharmacol.* **2005**, *71*, 115-125; b) P. Ciana, M. Fumagalli, M. L. Trincavelli, C. Verderio, P. Rosa, D. Lecca, S. Ferrario, C. Parravicini, V. Capra, P. Gelosa, U. Guerrini, S. Belcredito, M. Cimino, L. Sironi, E. Tremoli, G. E. Rovati, C. Martini, M. P. Abbracchio *EMBO J.* **2006**, *25*, 4615.4627; c) S. Paruchuri, H. Tashimo, C. Feng, A. Maekawa, W. Xing, Y. Jiang, Y. Kanaoka, P. Conley, J. A. Boyce *J. Exp. Med.* **2009**, *206*, 2543-2555; d) T. Benned-Jensen, M. M. Rosenkilde *Br. J. Pharmacol.* **2010**, *159*, 1092-1105; d) I. Eberini, S. Daniele, C. Parravicini, C. Sensi, M. L. Trincavelli, C. Martini, M. P. Abbracchio *J. Comput. Aided Mol. Des.* **2011**, *25*, 743-752; e) S. Daniele, M. L. Trincavelli, M. Fumagalli, E. Zappelli, D. Lecca, E. Bonfanti, P. Campiglia, M. P. Abbracchio, C. Martini *Cell Signal* **2014**, *26*, 1310-1325; f) C. Sensi, S. Daniele, C. Parravicini, E. Zappelli, V. Russo, M. L. Trincavelli, C. Martini, M. P. Abbracchio, I. Eberini *Cell Signal* **2014**, *26*, 2614-2620.
- [128] A. Maekawa, B. Balestrieri, K. F. Austen, Y. Kanaoka *Proc. Natl. Acad. Sci. U. S. A.* **2009**, *106*, 11685-11690.
- [129] a) E. Boda, F. Vigano, P. Rosa, M. Fumagalli, V. Labat-Gest, F. Tempia, M. P. Abbracchio, L. Dimou, A. Buffo *Glia* **2011**, *59*, 1958-1973; b) P. Crociara, R. Parolisi, D. Conte, M. Fumagalli, L. Bonfanti *PLoS One* **2013**, *8*, e63258; c) H. Nakatani, E. Martin, H. Hassani, A. Clavairoly, C. L. Maire, A. Viadieu, C. Kerninon, A. Delmasure, M. Frah, M. Weber, M. Nakafuku, B. Zalc, J. L. Thomas, F. Guillemot, B. Nait-Oumesmar, C. Parras *J. Neurosci.* **2013**, *33*, 9752-9768.
- [130] R. J. Franklin, C. Ffrench-Constant *Nat. Rev. Neurosci.* **2008**, *9*, 839-855.
- [131] a) D. Zhang, Z. G. Gao, K. Zhang, E. Kiselev, S. Crane, J. Wang, S. Paoletta, C. Yi, L. Ma, W. Zhang, G. W. Han, H. Liu, V. Cherezov, V. Katritch, H. Jiang, R. C. Stevens, K. A. Jacobson, Q. Zhao, B. Wu *Nature* **2015**, *520*, 317-321; b) PDB DOI: 10.2210/pdb4xnw/pdb, ID: 4XNW.

- [132] a) P. Cairoli, S. Pieraccini, M. Sironi, C. F. Morelli, G. Speranza, P. Manitto *J. Agric. Food Chem.* **2008**, *56*, 1043-1050; b) C. F. Morelli, P. Manitto, G. Speranza *Flavour Frag. J.* **2011**, *26*, 279-281; c) D. Ubiali, C. D. Serra, I. Serra, C. F. Morelli, M. Terreni, A. M. Albertini, P. Manitto, G. Speranza *Adv. Synth. Catal.* **2012**, *354*, 96-104; d) E. Calleri, D. Ubiali, I. Serra, C. Temporini, G. Cattaneo, G. Speranza, C. F. Morelli, G. Massolini *J. Chromatogr. B* **2014**, *968*, 79-86; e) D. Ubiali, C. F. Morelli, M. Rabuffetti, G. Cattaneo, I. Serra, T. Bavaro, A. M. Albertini, G. Speranza, Giovanna *Curr. Org. Chem.* **2015**, *19*, 2220-2225; f) E. Calleri, G. Cattaneo, M. Rabuffetti, I. Serra, T. Bavaro, G. Massolini, G. Speranza, D. Ubiali *Adv. Synth. Catal.* **2015**, *357*, 2520-2528; g) G. Cattaneo, D. Ubiali, E. Calleri, M. Rabuffetti, G. C. Höfner, K. T. Wanner, M. C. De Moraes, L. K. B. Martinelli, D. S. Santos, G. Speranza *Anal. Chim. Acta* **2016**, *943*, 89-97.
- [133] A. Kuninaka *J. Agric. Chem. Soc. Jpn.* **1960**, *34*, 489-493.
- [134] Paola Cairoli *Sintesi di composti con potenziale sapore umami e studi di correlazione struttura-attività*, **2006** (PhD Thesis).
- [135] N. Bodor, M. J. S. Dewar, A. J. Harget *J. Am. Chem. Soc.* **1970**, *92*, 2929-2936.
- [136] <http://ndbserver.rutgers.edu/archives/proj/valence/bases8.html>.
- [137] K. Guille, W. Clegg *Acta Cryst. C* **2006**, *62*, 515-517.
- [138] F. Taddei *Il legame chimico*, UTET, **1976**.
- [139] O. Kemal, C. B. Reese *J. Chem. Soc., Perkin Trans. 1* **1981**, 1569-1573.
- [140] Y. Fan, B. L. Gaffney, R. A. Jones *Org. Lett.* **2004**, *6*, 2555-2557.
- [141] a) Valeria Pappalardo *Studies on umami taste. Preparation of hydrolyzed vegetable proteins (HVPs) and glutamate-ribonucleotide hybrids*, **2014** (PhD Thesis); b) Ivan Franzoni *Chemoenzymatic synthesis of nucleosides*, **2011** (Master Thesis); c) Sofia Vailati Facchini *Studies on umami taste. Synthesis of N2-alkyl derivatives of guanosine 5'-monophosphate*, **2013** (Master Thesis); d) Marco Nicola Iannone *Studies on umami taste. Preparation of glutamate-ribonucleotide hybrids*, **2014** (Master Thesis); e) Veronica Lucchini *Synthesis of guanosine derivatives as potential tools to investigate umami taste*, **2015** (Master Thesis);
- [142] M. Ohno, Z.-G. Gao, P. Van Rompaey, S. Tchilibon, S.-K. Kim, B. A. Harris, A. S. Gross, H. T. Duong, S. Van Calenbergh, K. A. Jacobson *Bioorg. Med. Chem.* **2004**, *12*, 2995-3007.
- [143] V. Nair, X. Ma, Q. Shu, F. Zhang, V. Uchil, G. R. Cherukupalli, R. Govardhan *Nucleos. Nucleot. Nucl.* **2007**, *26*, 651-654.
- [144] M. Qian, R. Glaser *J. Am. Chem. Soc.* **2005**, *127*, 880-887.
- [145] P. Francom, M. J. Robins *J. Org. Chem.* **2003**, *68*, 666-669.
- [146] T. Ikemoto, A. Haze, H. Hatano, Y. Kitamoto, M. Ishida, K. Nara *Chem. Pharm. Bull.* **1995**, *2*, 210-215
- [147] a) A. R. Kore, M. Shanmugasundaram, A. V. Vlassov *Bioorg. Med. Chem. Lett.* **2008**, *18*, 4828-4832; b) M. Warminski, J. Kowalska, J. Buck, J. Zuberek, M. Lukaszewicz *Bioorg. Med. Chem. Lett.* **2013**, *23*, 3753-3758.
- [148] A. Sakakura, M. Katsukawa K. Ishihara *Org. Lett.* **2005**, *7*, 1999-2002.
- [149] W. Zhe Z. Yu-Fen *Phosphorus, Sulfur Silicon Relat. Elem.* **2008**, *183*, 735-736.
- [150] a) P. Englebienne, A. Van Hoonacker, M. Verhas *Spectroscopy* **2003**, *17*, 255-273; b) L. Jason-Moller, M. Murphy, J. Bruno *Current Protocols in Protein Science*, 19.13.1-19.13.14, John Wiley & Sons, Inc., **2006**; c) Y. Kuroda, M. Saito, H. Sakai, T. Yamaoka *Drug Metab. Pharmacokinet.* **2008**, *23*, 120-127; d) K. Vuignier, J. Schappler, J.-L. Veuthey P.-A. Carrupt, S. Martel *Anal. Bioanal. Chem.* **2010**, *398*, 53-66; e) J. Trevino, C. Bayon, A. Arda, F. Marinelli, R. Gandolfi, F. Molinari, J. Jimenez-Barbero, M. J. Hernaiz *Chem. Eur. J.* **2014**, *20*, 7363-7372; f) A. Olaru, C. Bala, N. Jaffrezic-Renault, H. Y. Aboul-Enein *Crit.*

- Rev. Anal. Chem.* **2015**, *45*, 97-105; g) R. Antiochia, P. Bollella, G. Favero, F. Mazzei *Int. J. Anal. Chem.* **2016**, *2016*, 2981931; h) D.-S. Wang, S.-K. Fan *Sensors* **2016**, *16*, 1175-1192.
- [151] T. Ozturk, E. Ertas, O. Mert *Chem. Rev.* **2010**, *110*, 3419-3478.
- [152] Z. Wang *Comprehensive Organic name reactions and reagents*, John Wiley & Sons, Inc., **2010**.
- [153] L. Legnani, L. Toma, P. Caramella, M. A. Chiacchio, S. Giofre, I. Delso, T. Tejero, P. Merino *J. Org. Chem.* **2016**, *81*, 7733-7740.
- [154] a) J. A. Landgrebe *J. Org. Chem.* **1965**, *30*, 2997-3000; b) E. Iglesias *J. Org. Chem.* **2000**, *65*, 6583-6594.
- [155] A. O. King, N. Okukado, E. Negishi *J. Chem. Soc., Chem. Commun.* **1977**, *19*, 683-684.
- [156] J. A. Casares, P. Espinet, B. Fuentes, G. Salas *J. Am. Chem. Soc.* **2007**, *129*, 3508-3509.
- [157] B. Fuentes, M. García-Melchor, J. A. Casares, G. Ujaque, A. Lledós, F. Maseras, P. Espinet *Chem. Eur. J.* **2010**, *16*, 8596-8599.
- [158] W. A. Waters *J. Chem. Soc.* **1942**, 266-270.
- [159] a) R.G. Silva, L.P. Carvalho, J.S. Oliveira, C.A. Pinto, M.A. Mendes, M.S. Palma, L.A. Basso, D.S. Santos *Protein Expr. Purif.* **2003**, *27*, 158-164.